Investigating neural structures and behavioural biases in perceptual decision-making

Imogen Large

Merton College

University of Oxford

A thesis submitted for the degree of

Doctor of Philosophy in Physiology, Anatomy and Genetics

Trinity 2015

Acknowledgements

First and foremost, I would like to express gratitude to my supervisor Prof. Kristine Krug, not only for her inspiration, guidance, and seemingly unending knowledge of physiology, but also her trust in allowing me great levels of freedom and independence while pursuing this thesis. Had she not seen something in me when I was a Biology undergraduate taking my first steps in the field of neuroscience, I would never have attempted a PhD in such a fascinating topic.

I am likewise forever indebted to Prof. Sarah Randolph, my undergraduate tutor, who first inspired me to take the path of scientific research - and who always had great faith in me. My sincere thanks also go to Dr. Liz Pellicano and Prof. Holly Bridge, for supporting my work in both developmental behavioural neuroscience and magnetic resonance imaging - and where necessary, for providing encouragement and insight into their fields. Their expertise and support were invaluable throughout this PhD. Dr. Stuart Clare also supported the development of MRI sequences for this study, and served as an examiner in both my transfer and confirmation of status - providing me with challenging questions and undoubtedly improving the quality of work as a whole.

I would also like to thank my fellow lab mates, with whom I share memories of outdoor frisbee, jazz music departmental escapes, and the occasional times that the FMRIB servers went down (along with all hopes of being able to complete any analysis on that day). In particular, I would like to thank Sarah Finnegan, who has provided me with countless cups of tea, chocolate digestive biscuits, and a yearly cake-off challenge - and without whom I would not have enjoyed my time at Oxford half as much. A special mention also has to go to Kimmy, who really, really, really believes that he is capable of coming out best in a fight against 2 wolves (or 1000 rats). We shared many deeply DPhil-irrelevant discussions about the nature of love, music, and how long he could stare out of the window in existential despair.

All those who participated in my studies were incredibly generous with their time, and I can only hope that this thesis provides some scientific repayment for that debt.

I am most thankful for the unending love and patience of my mother, Christine Elliott, who has been with me for my entire academic journey - no matter what the circumstance - and I can only hope that I give even the smallest proportion of that emotional support back. I would also like to express appreciation for Steve, who has had to endure listening to theories about my work (among other things) as I have written up, and my sister Sofy, who sent me many irrelevant .gifs to look at. One of my dearest friends, Harriet, was always to hand with a glass of wine when needed.

Finally, I would like to thank Avignon, who provided precisely no support - though did on occasion deign to sit in the same room as me while I was writing up. For a cat, that's pretty good going.

Abstract

Why do we behave as we do? The general mechanisms underlying visual perception and decision-making within a social context have been under scientific scrutiny for over half a century (Sherif, 1945; Asch, 1951; Berns et al, 2005). In spite of this, neither a definitive mechanism for how perceptual biases arise, nor a robust neural basis have emerged. In the first part of my thesis, I use a combination of visual behavioural testing and computational modelling to investigate the development of perceptual biases under social advice in children, and explore their potential mechanisms. In the second part, I use structural and functional magnetic resonance imaging in adults to examine the organisation of a cortical region that has been implicated in such visual perceptual decisions.

First, I use a two-alternative forced choice visual task to probe the extent to which typically-developing children (between 6 and 14 years) conform to social advice, when making judgments about ambiguous and unambiguous structure-from-motion stimuli. Perceptual bias reported by typically-developing children with a single advisor was largely absent in the youngest children, but increases with age. When reaction time data were analysed with a drift diffusion model, the results suggested that the conforming bias of the older children was likely the product of a perceptual, not simply a decision, bias. The typically-developing children were then compared with age and IQ-matched children with autism. The autistic group showed a small conforming bias in decisions for the youngest children, while the effect of social advice decreased with age. Drift diffusion modelling showed no evidence of a perceptual bias, but rather a potential bias at later stages of processing, in the formation of the judgment.

Second, I investigate how well visual area hMT+ can be mapped and characterised in individual human subjects. Visual cortical area hMT+ in humans is homologous to a macaque monkey region associated with perceptual decisions about the stimuli used in our visual psychophysics experiment with children (Krug 2004; Krug, 2013). By comparing two types of structural MRI scan sensitive to myelination (MP2RAGE at 7T and T1w/T2w at 3T) with functional localisers for hMT+, I found a consistent association of MRI contrasts indicating dense myelin with the functional localisers for group averaged datasets. However, regional patterns of myelination, and their association with functional hMT+, varied considerably between individual subjects. I went on to examine the internal functional organisation of area hMT+ with a high-resolution 7T fMRI scan. These scans provided evidence that in humans as in the monkey, cortical clusters respond selectively to specific stimulus aspects, such as specific directions of motion, or 3D depth.

These behavioural experiments in conjunction with computational modelling suggest that advice given by others can bias perceptual decisions about visual stimuli. High field MRI of a cortical region implicated in these perceptual processes, visual area hMT+, indicate a columnar architecture that can be revealed using current technology. Combining the two approaches should allow us directly to probe the neural basis of perceptual changes under social influence in humans.

Contents

List of Figures

List of Tables

Chapter 1

Introduction

"Humans see what they want to see."

- Rick Riordan, The Lightning Thief

Neuroscience traditionally focuses on four strands - cognition, perception, sensation, and behaviour. Experimental approaches have varied from behavioural to electrophysiological, imaging to histology, though an interdisciplinary approach offers the best opportunity for exploring how underlying mechanisms in the brain give rise to perception. By using techniques from developmental, imaging, and cognitive neuroscience, I have explored the mechanisms by which social information can affect perceptual decisions. First, I have used behavioural psychophysics and computational modelling to explore the effect of social advice on perception and behaviour across human development. Second, I have used structural and functional magnetic resonance imaging to investigate cortical areas which are thought to underlie neural processes involved in perceptual decision-making in the adult human.

1.1 Visual Perception

How do I know that what I see as blue is what you see as blue?

The question of perception has long been of interest in neuroscience and philosophical fields. In 1858, philosopher and later British Prime Minister William Gladstone noted the odd usage of colour adjectives in Homeric text. Rather than describe the sea as a deep blue, as modern literature might, Homer instead used an ambiguous word that translates to "wine-dark", "black", "brown" - or indeed a host of other colours. The absence of 'blue' from descriptive ancient vernacular extends to ancient China, the Qur'an, Hindu Vedic hymns, and the ancient Hebrew version of the Bible (Geiger, 1880). While Gladstone interpreted this as a mass colour blindness of the ancient peoples of the world, more recent research suggests that this was a question of linguistic effects on perception; a Roberson et al (2012) study on the Himba tribe revealed that they could not readily distinguish 'blue' from 'green' - an obvious distinction for modern Western cultures that linguistically categorise these two wavelengths of light (see Figure 1.1 for the stimulus used in the study, see also Berlin & Kay, 1969). This classic philosophical question of colour perception addresses the vexed question of subjective perceptual experience; even though we tend to assume our experience of the world is based on the objective processing of sensory information, the context and culture in which we experience such information clearly affects our perception and reporting of it.

The disjoint between the assumption of objectivity in ourselves, despite an acknowledgment of subjective experience in others, forms the basis of many perceptual psychophysics experiments, as it creates the opportunity to present ambiguous sensory

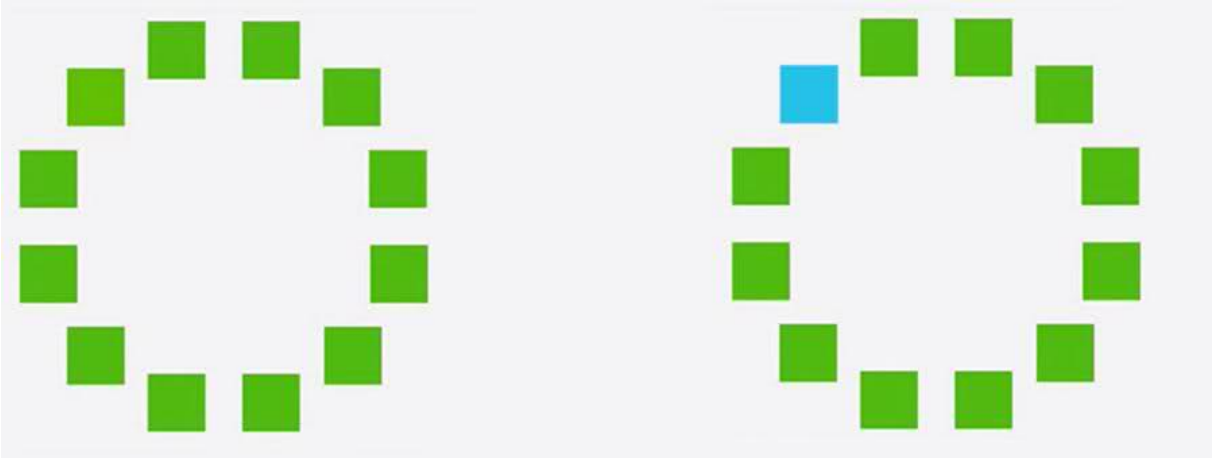

Figure 1.1: **Two examples of stimuli used in the Himba-English colour study (from Roberson et al, 2012)**
People of the Himba tribe, who do not differentiate linguistically between green and blue, were much slower than English speakers to point out the 'odd colour out' in the right hand stimulus. Correspondingly, English speakers were very slow to point out the 'odd colour out' in the left hand stimulus (the 'odd colour out' in the left stimulus is in the same place as in the right hand stimulus, with an RGB values of 97 192 4, while the other squares have RGB values of 80 186 15), while the Himba people were easily able to see the difference.

information to subjects who believe there to be a singular, robust sensory interpretation of that data. Ambiguous figures provide the most accessible example of the divide between sensory information and our perception of that information. An ambiguous stimulus has multiple, alternating, mutually exclusive perceptual interpretations, while the sensory information remains the same. They can be static (Figure 1.2) or moving (such as the 'spinning ballerina illusion' created by Nobuyuki Kayahara in 2003). Figures can be presented within a context, such as in a group of multiple figures, with the promise of a reward for a response, with social advice, or without a context. The transient stability of their various perceptual interpretations for the observer allows us to probe the mechanisms by which such interpretations are reached.

A key question in the presentation of ambiguous figures is what causes a subject to reach one perceptual interpretation - stimulus-driven 'bottom-up' processing (in

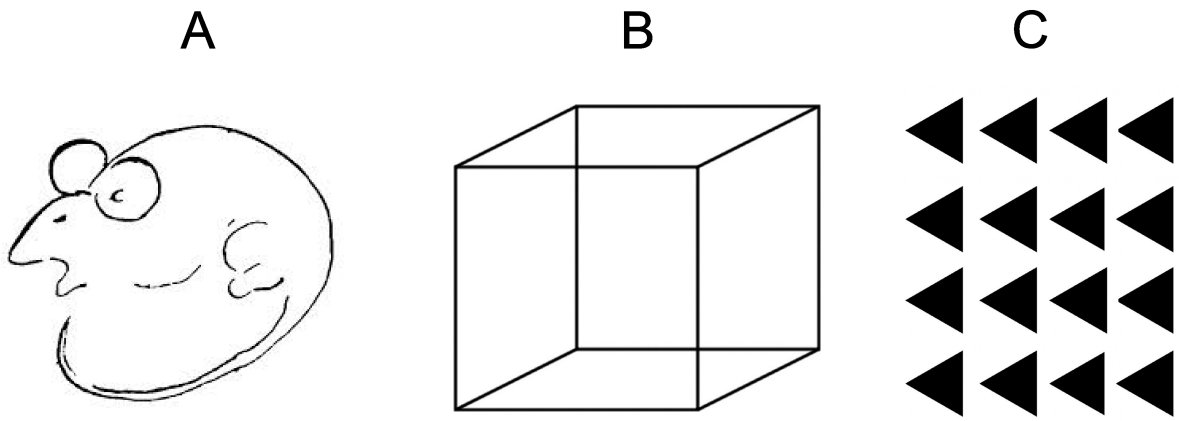

Figure 1.2: **Examples of static ambiguous figures**
Bugelski and Alampay's (1961) 'rat-man', which switches between the percept of a rat and of an old man's face. B. The classic 'Necker cube' (Necker, 1832) which switches between one square forming the front or back surface of the cube. C. A field of equilateral triangles switches perceived pointing directions as a whole field, rather than as individual figures.

particular the effect of noise), an experience/context-driven 'top-down' signal, or a combination of the two. From an evolutionary perspective, stimulus-driven sensory processing and interpretation are important to ensure that an animal accurately perceives and can appropriately respond to the present environment. However, experience and expectation have been shown to influence perception. The top-down processing model provides a context for visual data, and posits that it is things such as expectation, experience and attention that determine what is perceived. An example of this type of processing was demonstrated by Bugelski and Alampay in 1961 with their 'rat-man' ambiguous figure (Figure 1.2A). When participants were exposed to images of animals followed by an ambiguous figure, they were far more likely to perceive a rat than a man. This suggests that they processed the ambiguous image in the light of previously experienced information. Further studies have shown that when presented with an ambiguous stimulus such as the Necker cube (Necker, 1832; Figure 1.2B), subjects can to some extent switch perceptual interpretations voluntarily (Kornmeier

& Bach, 2004; 2005), implying the action of a top-down control mechanism. Though this does not rule out the possibility of bottom-up control of perceptual switching (the percept of the cube also 'switches' without deliberate intent), it certainly implicates a role for top-down processing. Klink et al. (2012) have summarised the evidence for context-driven perception as ranging from temporal context (Brascamp et al, 2008) to spatial context (Palmer, 1980, see also Figure 1.2C), while other studies have shown a role for socially induced expectation (Lee et al, 2006) and experience (Girgus et al, 1977), highlighting the range of potential contextual effects on perceptual processing and decisions.

It is clear that the context in which sensory information is received can affect the perception of it - the question then becomes, which contextual factors can affect how we perceive the world, and to what extent?

1.2 Social Influences on Perception

By the time we reach adulthood, it is sometimes thought that we have grown beyond the need to conform to peer pressure, and that we operate as independent units; this is supported by evidence showing that the effect of peer opinions on risk perception decreases with age (Knoll & Blakemore, 2015). That said, people have repeatedly carried out heinous crimes on the back of mass conformity to what is perceived as popular opinion. In the light of the Nazi atrocities carried out during the Second World War, Solomon Asch conducted the now famous Asch conformity experiments on male college students (Asch, 1951), with the aim of understanding the underlying reasons for conformity to judgments or views that appear so clearly wrong. The basis

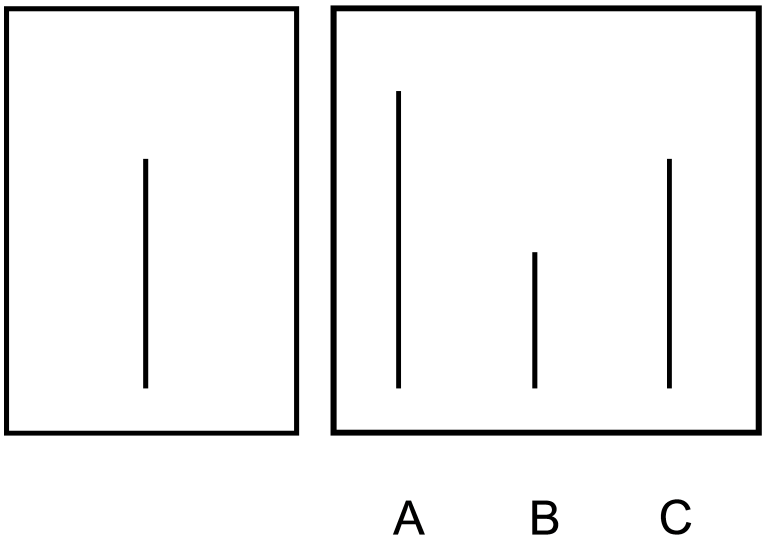

Figure 1.3: **A set up similar to the Asch Experiments (1951)** Participants would be asked to indicate which of the three lines on the right matches the line on the left in length.

of the experiment was a simple, non-ambiguous visual decision task, requiring the participant to match visually a single line in length to one of a set of three lines of different length (Figure 1.3).

In a control condition, with no contextual additions, participants had an error rate of 1%. However, when confederates were introduced, providing publicly announced incorrect responses to the task, participant error raised to 33%, with 75% of participants conforming at least once to an incorrect majority response.

Interestingly, in the Asch experiment, it was anecdotally reported that participants who exhibited the most conforming behaviour also reported perceptual distortion - they were unaware that confederates were providing incorrect responses, and believed that they themselves were responding correctly. This suggests that social context could be capable of affecting not only behaviour, but also the perception of unambiguous visual information. Richard Crutchfield built upon these experiments in 1955 by showing that the physical presence of a confederate was not necessary to induce conformity; approx-

imately the same percentage of conformity (30%) was found when the Asch paradigm was conducted using a panel of lights to indicate the responses of 'other participants'. Further to this, both Berns (2005) and Edelson et al (2011) have shown using fMRI that socially associated written information (opinions written in text appearing with a person's photograph) can affect the neuronal representation of long-term memory. It is therefore clear that social information can influence decisions even when removed from a more naturalistic 'face to face' paradigm.

The evolutionary precedent for socially-induced bias is clear - many minds may make light work of a complex decision. The ability to act coherently as a group has allowed humans to work collaboratively towards goals that would be unobtainable by one individual (the building of CERN, for example, required the collaboration of scientists across many nations). Collaboration and cohesion is clearly one effect of social conformity - one example of this is the autokinetic social experiments conducted by Sherif in 1935. Initially, Sherif asked individual participants to state how far they believed an ambiguous movement by a point of light to have travelled. Each participant had a typical 'norm' reported distance, consistent over 100 trials. When individuals with differing norms were then asked to perform the experiment in groups of 3, their responses steadily converged until they reached a group 'norm', that differed from their own individual 'norm'. More recent research by Bahrami (Mahmoodi & Bahrami, 2013; Hertz & Bahrami, 2016) has shown that collective decision-making can improve our own decisions (rather than impeding or 'misleading' them) by reducing individual bias, supporting the idea of an evolutionary advantage to integrating social information with sensory data.

The question is therefore raised as to the mechanism by which social information

is integrated into the decision process. Psychologists have traditionally divided social influence into either 'normative' (peer pressure conformity) or 'informational' (altering an opinion based on advice given by a confederate) (see Deutsch & Gerard, 1955 for an application of these two models to the Asch experiment). Conforming publicly to an incorrect opinion would be an example of normative social influence. Changing one's opinion on the quality of a painting after hearing another person's opinion would be an example of informational social influence. In essence, there is no pressure to conform to informational social influence as the information is treated as additional sensory data, while the pressure is strong in a normative situation. Behavioural experiments can reveal to some extent whether normative or informational social influences are affecting decision-making. However, up to this point they have not shown whether the social information can alter visual processing of a visual stimulus, or whether it just adds a judgmental bias.

It follows logically that the more ambiguous the sensory information, the more readily the context in which that information is processed should affect perceptual decisions about these stimuli. Experiments using ambiguous figures date back to the 1930s, with both Sherif (1935, autokinetic stimulus) and Jenness (1932, glass bottle filled with a number of beans) showing that participants tended to conform to social advice in ambiguous situations. This effect has also been shown in children, with Hamm & Hoving (1969) demonstrating that greater levels of ambiguity in an autokinetic stimulus lead to an increase in conforming responses. Though little research has been done examining conformity while using a spectrum of ambiguous stimuli, these experiments suggest that the more 'difficult' the ambiguity, the greater the levels of conformity.

It is clear that adults and children conform to social advice in some situations when

judging the appearance of both ambiguous and unambiguous visual stimuli. Both normative and informational processes have been implicated, which might act through perceptual changes or biases in judgments. In order to understand better the mechanisms at play, it follows to look at how social conformity develops for both ambiguous and non-ambiguous stimulus types.

1.3 The development of social perception

Humans are a naturally gregarious species - even from infancy, we preferentially attend face and face-like stimuli (Gliga et al, 2009). Social development is so consistent between typically-developing individuals that it is used to mark infant developmental milestones - facial recognition, positive response to touch, self-recognition, smiling, attentiveness to being called, and enjoyment of human company are all traits that should develop within the first 6 months of life (Murray & Andres, 2005). Previous research has made it clear that social influence has some effect from an early age. At a similar time to the Asch experiments, Berenda et al (1950) demonstrated evidence for behavioural conformity to socially-derived information in children between 7 and 10 years of age. More recently, Corriveau and Harris (2010) have shown that children as young as 4 show an effect of social influence in response to an adult majority opinion. Haun & Tomasello (2011) extended this finding to social conformity with an age-matched peer group in 4-year-olds - though it is important to note that this change was in public expression of opinion only, and not in private response. This highlights the importance of being able to separate peer pressure induced behavioural conformity (normative social pressure) from genuine perceptual change (informational

social influence).

It is also clear from previous data that the way in which social influence affects decision-making changes across the course of development. Younger children (6 years of age) demonstrate more caution about peer cooperation in a Prisoner's Dilemma task than older children (10 years of age) (Sally & Hill, 2006), supporting the idea that they may be less inclined to trust the opinion of a peer, and more likely to express this in non-public contexts. In line with this, Steinberg & Monahan (2009) showed that susceptibility to peer pressure increases throughout development up to the age of 14 years, while Hamm & Hoving (1969) showed that conformity to a peer increases beyond the age of 7, and Iscoe et al (1963) showed that when a task was ambiguous, conformity increased as a linear function of age between 3 and 10. With a greater age span tested, Blakemore et al (2015) have shown that between the ages of 8 and 59 there is a consistent social influence on risk perception - though it decreases with age, particularly beyond 14. That peer pressure effects are present in humans of many ages is not novel; the data above also suggest that the effect of social influence changes through child development. What remains unclear is how social influence changes in its effects across development from childhood to adolescence, and whether the underlying mechanisms of social influence integration are changed by development.

None of these previous studies have used a stimulus that can be disambiguated and ambiguated without it being evident to the participant. This has made it difficult to assess a quantifiable measure of either conformity or perceptual bias: when a solely ambiguous stimulus is used, the participant may realise that the ambiguous stimuli are difficult to categorise, or may switch between alternate perceptual states within a trial, while for an unambiguous stimulus, it may become immediately apparent that

the provided social information is incorrect or otherwise fabricated. The majority of these studies also rely on public reporting of response, increasing the normative social pressure and stress of the task. This makes it difficult to judge whether the behavioural response is an accurate perceptual report on the part of the participant.

In this thesis, I will examine further how social influence develops in childhood, and in particular what mechanisms might underlie changes in perceptual decision-making under advice. I investigate the developmental time course of social influence on perceptual decision-making, focusing on informational influence through using only one advisor rather than a majority decision. I use a perceptual task that allows me to fluidly control stimulus ambiguity, without the need to alternate between different types of stimuli and changing task difficulty. Previous research indicates that we might expect stronger conformity for ambiguous visual stimuli, and an increase in conformity up to the age of 14, while younger children will demonstrate less conformity.

1.4 Mechanisms for social influence on perceptual decisions

The question remains as to the level at which decision-processing is affected by social influence - in particular whether sensory or perceptual processes can be affected by the social advice, such that participants might see or remember a stimulus differently. The alternative is that participants perceive the stimulus correctly and are biased in their behavioural judgment. It is difficult to investigate this question without measuring neural activity in relevant brain regions.

One method of analysing the way in which social information affects decision-

making processes on a computational level - and thus making inferences about potential neural substrates - is by collecting reaction time (RT) data during behavioural tasks and applying a drift diffusion model to those reaction times (Figure 1.4).

The drift diffusion model is based on the theory of Brownian motion, theorised to represent patterns of neuronal activity (Ratcliff, 1978). A decision variable drifts from a given starting bound at random, and sensory evidence affects its drift rate to different decision criteria or bounds. If forced to make a choice between options 'A' or 'B' (as in classic 2 alternatives forced choice experiments (2AFC)), the brain accumulates supporting and opposing sensory evidence over time until the decision variable drifts over a decision bound, resulting in the behavioural choice of either 'A' or 'B'. This computational process has been linked to specific neural computations in the primate cerebral cortex (see Gold & Shadlen 2007 for a review). The integration of various pieces of information before and after stimulus onset into this decision-making process not only affects the decision, but also the reaction time of the participant. The drift diffusion model (Ratcliff & McKoon, 2008) is capable of analysing these factors by predicting choice, mean RT (reaction time), and RT distributions as a function of stimulus strength or contextual conditions (Ratcliff & Tuerlinckx, 2002).

Specific parameters can then be estimated from the input data, and give insight into the nature of the decision process. Two important parameters in explaining behavioural changes in the context of the model are changes in the drift rate of the decision variable (v - the rate at which evidence accumulates), and the location of the starting bound (z - the point from which the decision variable drifts). When multiple decisions are made under specified conditions (such as correct or incorrect social advice), they produce a distribution of reaction times (RTs). The two parameters of drift rate and starting

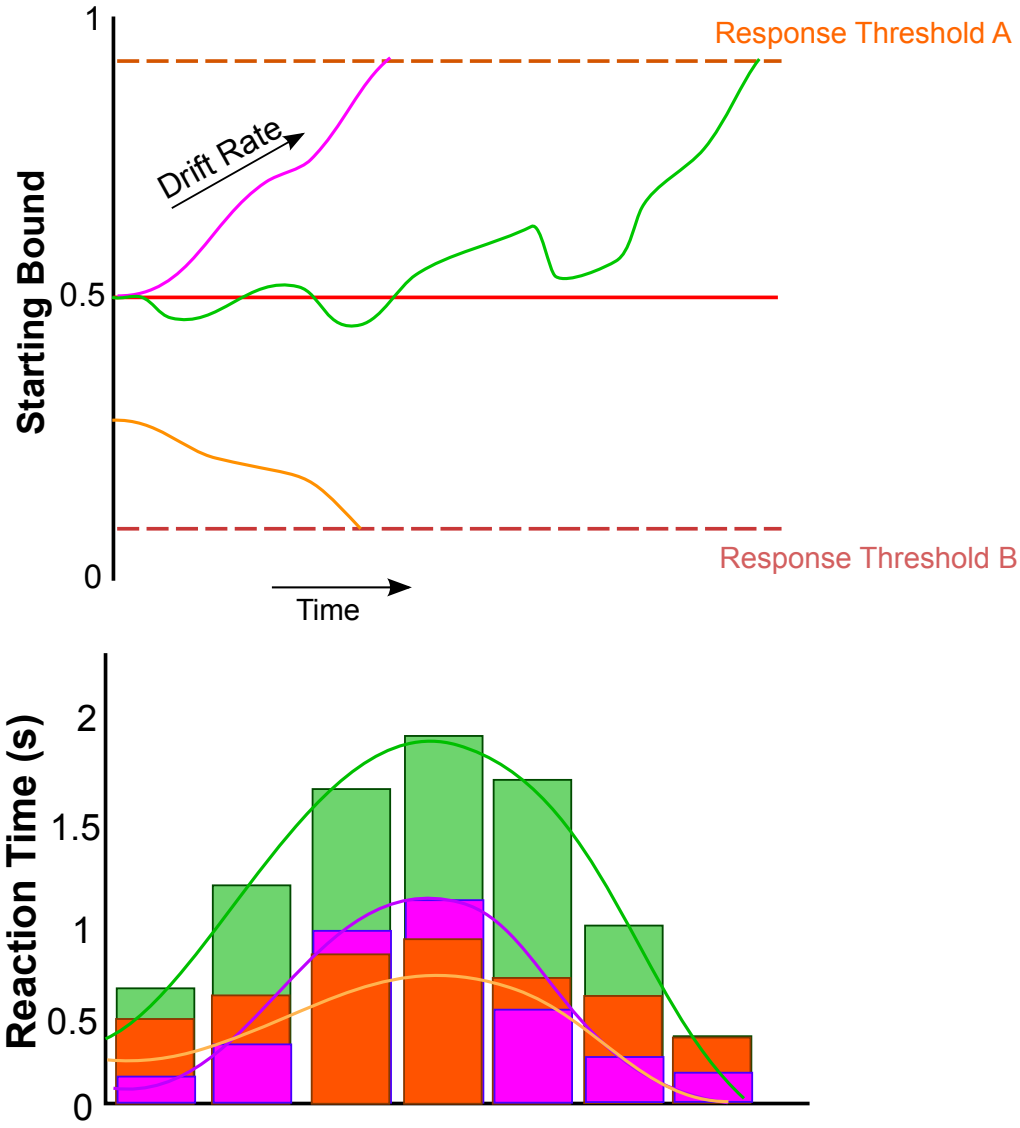

Figure 1.4: **A diagram of a simple drift diffusion model**
A) The decision variable meanders around in a Brownian fashion until it reaches a response threshold (the decision bound), resulting in a behavioural decision (either A or B). If the starting bound for a decision differs significantly from 0.5 (the midpoint between two potential choices) this suggests that there was an initial judgmental bias, potentially caused by normative pressure to conform. The drift rate (v) is affected by the sensory evidence available, and under certain conditions (such as social context or reward) can indicate whether a decision was perceptually biased. Drift rate and starting bound can be extracted from reaction time. The orange, green, and pink lines in the top figure show potential evidence accumulation paths. The starting bound is indicative of initial judgmental bias, prior to stimulus onset. Each line indicates an example accumulation path for different decision types. The green line indicates a path in which there is no normative or informational bias (i.e. a decision made without external context). Sensory evidence gradually accumulates until a response threshold is reached. The orange line indicates a normatively-influenced evidence accumulation path - the starting bound differs significantly from the midpoint. Finally, the pink line indicates an informationally-influenced accumulation path (a change in drift rate relative to the context-free green line, but no change in starting bound).
B) Shows the different reaction time distributions for the evidence accumulation pathways shown in the top figure, demonstrating how different distributions arise from different overall evidence accumulation paths. For example, although the orange and pink pathways meet their respective response thresholds at approximately the same time, their RT distribution differs, with the pink distribution appearing more peaked. This difference results in the calculation of different drift rate and starting bound.

bound make different predictions about the RT distribution. Drift rate changes predict a ratio of roughly 4:1 in the leading and tail edges of the RT distribution, while starting bound changes predict a ratio of approximately 2:1 (Ratcliff & McKoon, 2008). As such, by modelling the RT distributions under different conditions, we can extract predictions of drift rate and starting bound values - and so make inferences about the potential mechanisms underlying decisions. Figure 1.4B gives some examples of different RT distributions, and how they relate to the drift of a decision variable.

Significant changes in these variables have been taken to indicate whether the participant was perceptually biased during the decision making process, or had a judgmental bias. If the drift rate varies significantly between different decisions or under different contexts (such as social advice or reward), this suggests a perceptual bias may have affected the decision - a shift or bias in sensory processing as a result of the integration of this additional information. The greater the drift rate deviates from 0, the stronger the perceptual bias in the direction of the decision being made. However, if the starting bound for the decision variable varies significantly from 0.5 (the midpoint between the two potential decisions) this indicates that the decision was biased prior to viewing the stimulus, and that any pre-stimulus information was treated as orthogonal to the stimulus information. This would suggest that any conformity was purely normative in nature. This is the general framework in which this type of behavioural data has been interpreted with the help of the drift diffusion model.

Various neuroimaging and electrophysiological studies (Mazurek et al, 2003; Voss et al 2004; Huk & Shadlen, 2005; Hanks et al 2006; Summerfield & Koechlin, 2010; Zhang, 2012) have supported a link between the drift rate of a decision variable and representation of sensory evidence in the cortex. As such, the parameters of the drift diffusion

model have been linked with real discrete brain processes, particularly in occipital area V5/MT and parietal area LIP as well as others (Gold & Shadlen review, 2007), making the model suitable not only for the analysis of behavioural results, but also as a way of linking them to the underlying neurophysiological processes. The drift diffusion model is most effective for decisions made within a few seconds, with full attention to the stimulus - and assumes that evidence is steadily accumulated until a decision bound is reached. As such, for certain types of decision-making it is not appropriate - Hanks, Kiani, and Shadlen (2014) demonstrated that speed-accuracy decisions in the macaque were not well-predicted by the drift diffusion model, as neuronal readings indicated most of the evidence required to make a decision occured at the start of decision formation. Other types of computational model exist for explaining 2AFC experiments - such as the 'Race Model' (Pike et al, 1966), in which evidence is acquired for the two decisions simultaneously and it is a 'race' to the response threshold, or the 'Mutual Inhbition Model' (Usher & McClelland, 2001) in which evidence is also acquired for the two decisions simultaneously, but each accumulator inhibits the other until evidence in one direction is effectively decayed. Each model is suitable for describing a subset of 2AFC experiments, depending on stimulus and decision type.

Given that the drift diffusion model has been used effectively to describe previous experiments with the type of basic task I intend to use (Cicmil et al, 2015), I will investigate perceptual decisions in children under social influence using a drift diffusion model, in order to make inferences about the processes underlying the behavioural decisions made.

1.5 Autism Spectrum Disorder and social influence

Autism Spectrum Disorder (ASD) is viewed as a clinically heterogeneous group of developmental disabilities, most characteristically defined as a series of social/communication impairments coupled with restricted and repetitive interests and behaviours (Diagnostic and Statistical Manual of Mental Disorders, Fifth Edition - DSM-V). As such, it posits an interesting foil to the behaviour of typically-developing adults and children presented with social information. The underlying assumption is that neural mechanisms underlying social interactions might develop differently, and so might be impaired. Despite their heterogeneity, diagnosable symptoms tend to present themselves by the time a child reaches 2 years of age (Myers and Johnson, 2007). As of 2011, Autism Spectrum Disorder (ASD) is estimated to affect 1.1% of children aged 4-16 in the UK (2011 UK Census data).

Despite autism's prevalence, a clear understanding of both the etiology and heritability of ASD is still lacking in the scientific and medical community. A multitude of genetic components have been linked to ASD (Sykes & Lamb, 2007; Aldinger et al 2011), but their contribution to the development of ASD is still unclear - candidate gene CASPR2, for example, is involved in dendritic arborisation and tends to localise to highly myelinated regions (Anderson et al, 2012). Other implicated genes include SLC25A12 (which affects myelination), transcription regulator MeCP2, and OXTR, a receptor for oxytocin. Autism has a high rate of co-morbidity with other disorders at a genetic level - genes linked to ADHD, Schizophrenia, Joubert syndrome, and numerous others, are also linked to the incidence of autism (Aldinger et al 2011). Schizophrenia, a disorder associated with neural demyelination (Davis et al 2003; Valeiras et al 2014),

is sometimes co-morbid with autism - which is interesting, as some genes linked to ASD work in heavily-myelinated regions (e.g. CASPR2, SLC25A12). This suggests that there may be some a link between regional myelination and ASD. In support of this idea, Deonie et al (2015) claimed to show with structural MRI that young autistic adults have less overall myelination than matched typically-developing controls. That said, the quantitative nature of these results have been called into question, and other studies with much larger sample sizes (such as Haar et al, 2014, with around 1000 autistic participants between 6 and 65 years of age) have suggested that anatomical measures of difference measured with MRI are of limited use insofar as diagnosing autism. As such, though it is possible that lower levels of myelination could contribute to the development of autism (as well as other neural disorders), it is far from definitive, and requires further investigation.

Cerebellar damage increases the risk of a child developing ASD by 36 times (Wang et al, 2014). Vargas et al (2005) have also demonstrated from tissue studies that autistic patients had significant levels of neuroinflammation in the cerebral cortex, white matter, and cerebellum. As some regions of the cerebellum affect the development of putative neocortical substrates for social interaction, this points to an underlying neural basis for the social/communication deficits observed in some people with autism.

A more systems-based approach implicates the orbitofrontal-striatal-amygdala circuit as dysfunctional in individuals with ASD (Bachevalier & Loveland, 2006) - a region implicated in social response to faces and approval (Schultz, 2000). The amygdala was also one region that was activated during the social conformity task conducted by Berns et al (2005), further supporting its role in interpreting and processing social context. Dakin & Frith (2005) have proposed that abnormalities in the superior temporal sul-

cus (STS) may explain some of the motion processing deficits in ASD individuals, and electrophysiological studies in monkeys suggest that the visual cues that activate the STS are also involved in social perception (Allison et al, 2000).

Environmental factors have also been implicated as increasing the likelihood of a child being diagnosed with ASD. Maternal diabetes has been shown to increase the risk of ASD twofold (Gardener et al, 2009), as has more advanced parental age in either partner (Shelton et al, 2010; Parner et al, 2012). Prenatal stress has also been retrospectively associated with ASD (Ward et al, 1990), supported by a study in the rhesus macaque, which demonstrated that juvenile monkeys whose mothers were exposed to stress prenatally showed significantly less appropriate social behaviours than controls (Clarke et al, 1996).

It is clear that autism has widespread and numerous potential causes and predispositions - genetic, structural, and environmental (see Chaste & Leboyer, 2012, for a review). Many of the potential causes are directly linked to social interaction and communication, an integral part of functioning effectively in the majority of typical structured environments, such as school and work. Given the naturally gregarious nature of typically developing humans, a greater understanding of how autistic individuals process social information is not only vital to deepening our understanding of the condition's complexities, but also in developing interventions to improve integration into typical social and educational working environments - or even altering them altogether.

Unlike typically developing children, those who register on the autism spectrum show little to no natural predisposition towards social interaction. During the first year of development, they do not orientate towards name calls, and display diminished

or otherwise abnormal eye contact, as well as showing "social aloofness" (Osterling et al, 2002). Children with ASD between the ages of 2 and 5 are less likely to spontaneously offer help, or to attempt social re-engagement after interaction has ceased (Liebal et al, 2009), while those between the age of 4 and 6 show no or even reduced preference for the sound of their mother's voice when compared to non-socially salient noises (Klin, 1991). At the age of 13, children with ASD tend to look at the background, rather than at socially interacting characters in the foreground, of static photographs (Riby & Hancock, 2008). By the time they reach 15, they have not developed the concept of social flattery - in contrast to typically-developing children, who improve drawing ratings in the presence of the purported artist between the ages of 4 and 6 (Fu & Lee, 2007), children with ASD between the ages of 12 and 15 show no such upward alteration of reported rating in front of the self-proclaimed artist (Chevallier, Molesworth & Happé (2012). This suggests that, unlike the altered behaviour of typically developing adults and children under social influence, those with ASD should be less affected - in effect, their responses should reflect the sensory information provided, regardless of social context. Further to this, the potential effect of perceptual bias induced by social information should not occur in children or adults with ASD.

Research has suggested that adults with autism may be less susceptible to social information (Bowler & Worley 1994) and reputation (Izuma et al, 2011) than typical adults, but no research has compared such responses in age-matched children with ASD. That said, Sally & Hill (2006) did demonstrate that younger autistic children (6 years old) were more likely to co-operate with their peers than age-matched typically developing children in a Prisoner's Dilemma task - however, unlike their peers, their level of cooperativeness did not increase with age. This suggests that there is a sig-

nificant divergence in neural development for autistic relative to typically-developing children, which affects not only their desire to socially interact, but their ability to process and integrate social information. Pertinently, Pellicano & Burr (2012) suggested that people with autism tended to perceive the world "more accurately" as a result of reduced bias by prior expectation - which implies social information is unlikely to affect perceptual decisions made by people with ASD. In this thesis, I will investigate the effect of social advice from a single age- and gender-matched advisor on perceptual decisions made by children with ASD across a developmental range. I will compare this data to age- and IQ-matched typical controls, and apply a drift diffusion model to the data in order to examine the mechanisms of perceptual decision-making underlying social behaviour in autism spectrum disorders.

1.6 The neural basis of visual perception

The primate visual cortex is responsible for visual information processing, and comprises of over 30 areas (Felleman & Van Essen, 1991) including the striate cortex, or primary visual cortex V1, and the extrastriate cortex, formed of areas V2, V3, V4, V5/MT, and V6, among others. One predominant thesis is that the visual cortex is primarily organised according to functional modularity, with specific regions performing specific functions (Calabretta et al, 2005), such as processing colour, motion, and form - although evidence has been found for multiple areas responding to the same type of stimulation (for example, areas V2 and V4 both show colour wavelength sensitivity (DeYoe et al, 1985). The visual cortex has a retinotopic organisation, such that in primary visual cortex, the spatial organisation of neurons corresponds to the spatial

location of stimulation on the retina (Tootell et al, 1998). Extrastriate regions of the visual cortex can also be defined in terms of their differing retinotopic maps, such as differentiating area V5/MT from neighbouring MST (Huk & Heeger, 2002).

Perhaps due to the evolutionary significance of vision in the primate, there appears to be reasonable homology between human and non-human primate visual cortex (Van Essen, 2002). Functional homology in major areas such as V1 (DeValois et al, 1974), V4 (Gallant et al, 2000) and V5/MT (Rees et al, 2000) between macaque and human has been shown via electrophysiology and fMRI respectively (see a review by Orban et al, 2004, for more detail). This homology posits the macaque as a model species for carrying out studies on the human visual system. The link between sensory stimulation and brain activation has been well characterised for the primate visual cortex - retinotopy and population receptive field maps remain gold standard methods for functionally segregating many early visual regions in humans (Engel, Glover & Wandell, 1996). However, the neural basis of perception continues to be a more complex issue.

Electrophysiology in non-human primates has been one way to explore the link between sensory input, behaviour, and perception (see review by Parker & Newsome, 1998). By directly associating the activity of neurons with behavioural responses, and by modulating that activity, we can explore how brain activity affects and is connected to behavioural output. Macaque visual area V5/MT has been particularly well-characterised physiologically (Dubner & Zeki, 1971; Zeki, 1974; Maunsell & Van Essen, 1983; Allman & Kaas, 1976), and as such serves as a good model to test perceptual hypotheses - more so as it has a human homologue in area V5/MT (part of the hMT+ complex). Macaque V5/MT has a distinct internal organisation based on visual topography and functional columns. Albright et al (1984) characterised the

motion selectively of this area, demonstrating that it has sensitivity to 360 degrees of motion over 1mm of surface area. Deangelis and Newsome built on this by delineating the disparity selectivity of area MT, showing that it tended to be sensitive to near and far disparities in distinct patches of neurons, intersected by non-disparity sensitive regions (Deangelis & Newsome, 1999). As such, our current conception of macaque area V5/MT is as a region with columns sensitive to specific directions of motion, overlaid with regions of disparity sensitivity. This work laid the foundation of a sensory model upon which perceptual experiments could be conducted by examining the link between neuronal activation and behaviour.

Correlational experiments on responses from single neurons to visual stimulation have given us significant insight into the fine-grain workings of area V5/MT with regard to the link between behaviour and perception. Such work has been pioneered by neuroscientists such as Newsome and colleagues, who have shown a relationship between behavioural choice and visual responses of neurons in area V5/MT (Britten, Newsome, Shadlen & Movshon, 1996), and Dodd, who showed that firing of V5/MT neurons correlates with reported perception of a rotating structure-from-motion figure (Dodd, Krug et al, 2001). The columnar structure of V5/MT has also facilitated causal microstimulation experiments, in which the activity of small neural clusters is manipulated, allowing researchers to directly probe the relationship between activity in clusters of neurons and perceptual report. Using this technique, Salzmann et al (1990) showed that microstimulation in area V5/MT affects perceptual judgments of motion direction, which is supported by DeAngelis et al (1998), who showed that microstimulation of V5/MT neurons can bias perception, while Krug et al (2013) have used this technique to show a role for area V5/MT in resolving perceptual ambiguity. Britten

& van Wezel also showed in 2002 that neighbouring region MST can be stimulated to bias perceptual judgments in optic flow tasks. As such, it seems clear that this visual region of the macaque brain is involved not only in processing sensory information, but in making perceptual decisions.

Conducting experiments on human homologue area V5/MT proves more difficult, as the spatial and temporal resolution of methods outside single cell electrophysiology make it harder to localise specific signals, and therefore associate them with behavioural response. However, using imaging to delineate selectively responsive regions in area V5/MT to sensory stimulation, and then imaging these known regions while a human engages in perceptual tasks, could provide some insight into its contribution to human behavioural decisions - as well as an insight into human visual perception. Positron emission tomography (PET), magnetic resonance imaging (MRI), and magnetoencephalography (MEG), are all imaging methods that have been used to examine human brain activity. The good temporal resolution of PET scans has been used to demonstrate that visual signals can reach area V5/MT before they activate area V1 (Barbur et al 1993). However, PET scans lack the spatial resolution of MRI, and while they (and other imaging methods such as MEG) may be useful for analysing temporal responses, they lack the spatial resolution to map the fine sensory maps of visual regions. MRI has a far higher spatial resolution than PET or MEG (more recently, sub-milimetre), and with high field imaging at 7T becoming accessible, MRI presents a viable alternative for human brain mapping.

Large-scale projects such as the Human Connectome Project (see Van Essen et al 2013 for an overview) have brought to light the value of big dataset MRI for the functional mapping of cortical regions. However, using MRI to create detailed func-

tional maps of visual areas has had limited success - in 2007, Yacoub et al functionally localised ocular dominance columns in V1 with some measure of repeatability, but this experiment is yet to be replicated in another lab. Further to this, Zimmerman et al (2011) attempted to map motion sensitivity across area hMT+ as a whole (at 0.8mm isotropic voxel size), but found limited results indicative of orientation selectivity - potentially due to the use of combined opposite motion direction contrasts during analysis. That said, as high resolution imaging at 7T becomes more widely available, reliable and replicable, it presents an opportunity for conducting perceptual experiments in humans that can tease out the link between sensory information and perception. This is because imaging at high resolution may allow us to capture activation in clusters of neurons (such as columns). If this can be achieved, changes in activation among these clusters, coupled with behaviourally reported percepts of stimuli (such as ambiguous figures), could link the participant's perceptual experience to sensory activation in the cortex. If the same stimuli were then presented within a context that could alter behavioural response (such as social advice or reward), we could assess the degree to which behavioural report matches sensory activation. By doing so, we would gain insight into how and why behavioural responses change when the basic stimulus remains the same.

Examining the neural basis of social perception, rather than just visual perception, again proves more complex. A number of networks are implicated in social behaviour - the size of the orbital prefrontal cortex in humans is an accurate predictor of social network size (Powell et al, 2012) and social competence (Powell et al, 2010), changes in activity in the occipital-parietal network and amygdala have been associated with social conformity (Berns et al, 2005), and the superior temporal sulcus (STS) has

also been shown to have a role in social perception in both macaques and humans (Allison & McCarthy, 2000). Bachevalier & Loveland (2006) have claimed that deficits in the orbitofrontal-amygdala network are a primary factor in the social difficulties that develop in people with autism, while Schultz (2000; 2005) has suggested that they are the product of developmental problems in the fusiform face area and amygdala. Further to this evidence, a number of studies have shown that abnormalities in the STS are present in those with autism (Zilbovicius et al., 2000; Meresse et al. 2005; Hadjikhani et al. 2007) and are associated with visual and auditory social deficits (Castelli et al., 2002; Gervais et al., 2004; Pelphrey et al., 2005).

It is clear that a number of networks and regions are associated with the complex act of social perception, presenting multiple potential pathways for integration with sensory information. The regions implicated certainly share connections with the visual cortex (such as the STS) and extrastriate region hMT+ (Yeo et al, 2011), and as such are suggestive of a social network involving specific social regions of the brain, early sensory visual regions, and sensory-perceptual area V5/MT.

1.7 The identification and organisation of visual perceptual areas

In order to carry out non-invasive experiments in humans that can relate equivalent information about the link between sensory information and perception, as electrophysiology has for the macaque, fine-grain functional maps of visual cortical areas are essential - as is the ability to reliably localise regions of interest. As area hMT+ has a clear homology with the macaque V5/MT and MST complex (Rees et al, 2000), has

been well-characterised in the macaque (Dubner & Zeki, 1971; Zeki, 1974; Allman & Kaas, 1976; Maunsell & Van Essen, 1983), and is implicated in perceptual as well as sensory processing (Salzmann et al, 1990; Krug et al, 2013), it is positioned as a region of exceptional interest in this regard.

In humans, extrastriate visual area hMT+ has been identified and divided into V5/MT and MST based on selectivity for direction of motion and retinotopy (Huk et al., 2002; Amano et al., 2009; Cottereau et al., 2011), but its anatomical location relative to the sulcal pattern is variable (Wang et al., 2014). The reason for this variability is unclear, but could be attributed to the well-known sulcal variance between individual humans. Ono, Kubick & Abernathy (1990) and Thompson (1996) have attempted to quantify the level of sulcal variability between individual human brains. Although major sulci, such as the central sulcus, tend to be consistent across all individuals, there is a significant degree of variability in other sulci, particularly in the occipital lobe. Indeed some minor sulci and gyri may be altogether absent. The sulcus commonly associated with area hMT+ (the posterior limb of the inferior temporal sulcus) is present in all typically developed human adults, although its position is highly variable (Thompson, 1996). Sulci in the parieto-occipital region vary both anterior-posteriorly and vertically by up to 19mm between individuals (Thompson, 1996). This structural variance, combined with the variable position of functional hMT+ relative to the sulcus, can mean that it is found across a sulcus, wholly on a gyrus, or entirely in a sulcus.

Cytoarchitectonics has been of interest as a method of anatomically dividing up the brain by examining the differential distribution of cells for over a century (Brodmann, 1909). Within the cortical grey matter are varying degrees of myelination (a fatty

sheath surrounding axons), the pattern of which is known as brain myeloarchitecture. Particular regions of the cortex have distinctive myelin markers, such as the Stria of Gennari (Gennari, 1782) and the heavy myelination of the central sulcus (Naidich, Blum & Firestone, 2001). In non-human primates, histology has identified distinct myelination of the V5/MT-MST complex (Ungerleider et al., 1986). In line with this, computer-aided histological analysis of *post mortem* human cortex has posited a likely homologous region of myelination around the sulcal definition of hMT+ in humans (Annese et al., 2004).

As various high-resolution structural magnetic resonance imaging (MRI) protocols are developed, resolving differences in myeloarchitecture *in vivo* across the cortex has become a possibility (Bock et al., 2011; De Martino et al. 2014; Eikhoff et al. 2005). Using MRI, it has been possible to identify known myelinated regions, such as the Stria of Gennari (Barbier et al. 2002; Bridge et al., 2005), previously unknown myelinated regions such as the auditory cortex (Dick et al., 2012), as well as more broad cross-cortex myelination maps (Glasser et al., 2011; Ganzetti et al., 2014). As such, the possibility of a non-anatomical definition of V5/MT that remains tied to the underlying cytoarchitecture of the cortex has become plausible.

The ability to detect myelination accurately across the human cortex is not only important for the localisation of functional regions, but also for clinical purposes. Autism, for example, is associated with thinner insulating myelin around axons (Deoni et al. 2014) as well as deficiencies in proteins that tend to gather in highly myelinated regions (Anderson et al, 2012). There are numerous other neural disorders that correlate with abnormal levels of myelin (e.g. multiple sclerosis, Genain et al 1999; schizophrenia, Davis et al 2003). As such, developing accurate methods for myelin detection not only

allows us to better localise regions of the brain, but potentially could form part of a diagnostic toolset. Furthermore, with disorders known to alter over the course of development, such as autism, accurate detection of myelination levels over time could help us to understand its role in progressing visible symptoms.

Several structural MRI scan types have emerged for detecting patterns of myelination across the cortex. First are magnetisation transfer ratio (MTR) protocols, which have been shown to detect demyelination in grey matter (Schmierer et al, 2004; Fjaer et al, 2014). Second are T2* MRI protocols, which are sensitive to the differences in magnetic susceptibility of neighbouring tissues, and as such are good for visualising myelin patterns as they detect the ferritin and iron that tends to associate with myelin. T2* contrasts have revealed qualitative patterns of myelination across area V1 (Sanchez-Panchuelo et al, 2012). Third are T1-weighted/T2-weighted ratios, which have low contrasts shown to equate to 'myelin maps' across the cortex (Yoshiura et al, 2000; Glasser & Van Essen, 2011). Finally there are T1-weighted MP2RAGE sequences, which combine two inversion times within the scan protocol (Marques et al, 2010). High intensities in MP2RAGE contrasts are known to correlate with regions of high myelin density (Sanchez-Panchuelo et al, 2012; Dinse et al, 2013).

Both T1w/T2w and MP2RAGE protocols produce T1-weighted images without the image intensity bias created by inhomogenous transmit and receive RF profiles. As the existence of cortical myelin shortens T1 relaxation times, imaging protocols sensitive to T1 should allow the assessment of local myelin density (Barbier, 2002; Yoshiura et al, 2000; Marques et al 2010). While all of these structural scans have shown some degree of association with myelination, the correlation of MTR scans with myelin content has recently been called into question (Fjaer et al, 2015), and the

nature of T2*-weighted imaging means that image intensity is dependent on cortical location - the image contrast depends on the angle of tissue boundaries relative to the static magnetic field, meaning that the images are not quantitative measures as the intensity can vary independently of iron content. As T1w/T2w and MP2RAGE protocols produce images that are less dependent on tissue angle (and may therefore be more quantitative measures), and have a good body of recent evidence supporting intensities that correlate with cortical myelination in grey matter (T1w/T2w: Glasser & Van Essen, 2011, 2013, 2014; Abdollahi et al 2014; Ganzetti et al 2014; MP2RAGE: Sanchez-Panchuelo et al 2012; Dinse et al 2013, 2015; Lutti et al 2014), they present a good prospect for comparing with functional localisers of visual cortical areas as a way of assessing myelination of these areas.

Although both approaches have been previously employed to identify regions of greater myelination, including a putative hMT+ complex (Glasser and van Essen 2011, Sanchez-Panchuelo et al., 2012; Dinse et al. 2013), these methods have yet to be systematically compared to functional and retinotopic definitions in individual brains, instead having been displayed on average surfaces and compared to resting state, atlas, and anatomical definitions. As such, previous research has lacked both a comparison of structural localisation of areas to specific functional localisers for these regions, and an examination of how well localisation of areas holds in an individual participant - something critical should these techniques move into the clinical field. In addition, scan protocols for T1w/T2w images have been developed at 3T, while for MP2RAGE they have been developed at 7T. As such, these two scans also provide an interesting chance to compare structural localisation of regions based on myelin density at two different field strengths.

By assessing *in vivo* MRI detection of myelin levels on an individual basis, and comparing these definitions to individual functional maps, it should be possible to comment upon the reliability of such measures and their potential application within clinical circumstances. Reliable localisation of area V5/MT in the individual should also open avenues for mapping the specific, intrinsic functional organisation of this region, because at the scale of columns, averaging across individuals is likely to blur specific signals. Electrophysiological evidence from the macaque has shown homologous V5/MT is organised both into columns of neurons sensitive to specific directions of motion (Albright et al, 1984) and patches sensitive to near and far disparity (DeAngelis & Newsome, 1999). By using the greater signal-to-noise ratio of 7T scan data (Triantafyllou et al, 2005) to capture high resolution isotropic voxels of 1mm, it should be possible to functionally map area V5/MT - opening the door to perceptual experiments on humans that can approach the resolution of macaque electrophysiology.

In this thesis, I will investigate structural and functional measures of localising human visual area hMT+, and the functional organisation of this area. First I will examine the concurrence of current functional and structural methods of localising area hMT+, by comparing standard functional localisers with two structural methods of detecting myelination. Second, I will use a high-resolution functional scan to explore the functional organisation of area hMT+ with respect to motion and disparity selectivity, and compare this organisation to that previously found with electrophysiology in the macaque.

Chapter 2

The development of social influence on perception at the start of adolescence in typically-developing children

2.1 Introduction

"A man can be himself only so long as he is alone."

- Arthur Schopenhauer, Counsels and Maxims

Although most humans are familiar with the notion that peers can affect their decision-making processes, the scientific exploration of this idea rose to prominence with the Asch experiments in the 1950s. This seminal work demonstrated that in certain circumstances, adults would conform to a clearly incorrect majority opinion. Anecdotal reports from participants in the experiments suggested that in some cases, social information could bias the perceptual interpretation of sensory information - that when conforming to sensorially incorrect decisions, the participant could believe that they were answering correctly due to their erroneous perceptual interpretation, biased by social context. This could be an example of 'informational social influence' -

the psychological model of social influence wherein data obtained from a confederate in a social context alters both behaviour and perception in a situation. The companion model is 'normative social influence', in which only behaviour is altered, leading to conformity rather than a change in perception (see Deutsch & Gerard, 1955 for an application of these two models to the Asch experiment). The nature of the Asch experiment makes it impossible to differentiate between the two types of influence. However, the idea that perception can be biased by social influence has been supported by evidence from other studies across the decades suggesting that, in adults, simple visual perceptual decisions are affected by the social context in which they are made (Asch, 1951, 1956; Moscovici & Personnaz, 1980; Berns et al. 2005; Germar et al, 2013). It is this model of informational social influence, leading to a bias in perceptual report rather than to behavioural conformity, which I will investigate in this chapter.

Research with children (Hamm & Hoving 1969; Corriveau & Harris 2012) has demonstrated that children as young as 7 years of age already integrate social information into public and private perceptual responses - but to a lesser extent than their older peers of 10 and 13 years, or adults. This raises two key questions: firstly, what the developmental course of social influence integration is, and secondly, whether these results were the product of peer-pressured behavioural conformity (normative social influence), or the integration of social received advice with sensory evidence (informational social influence), potentially resulting in the alteration of stimulus perception. There is little research on the transitional developmental stage at which susceptibility to social information increases to the point of affecting judgments.

Prior research has already suggested that children conform to a lesser extent than adults, but has not explored at what point in development this switch occurs - and in-

deed whether it is a switch, or a gradual progression of increasing conformity. Although children as young as 3 can attribute value judgments to socially-delivered information by indicating the more accurate advisor (Corriveau & Harris 2011), suggesting that they understand the task and information at hand, they do not tend to agree with an obviously incorrect majority consensus. Notably, Haun & Tomasello (2011) have shown that children are more influenced by social information if they are in a situation that requires a public declaration of response - although they do not conform to social information to the same extent as adults.

Typically, social influence experiments in children have used a normative influence structure (e.g. public reports of response, such as in Hamm & Hoving, 1969), rather than the judge-advisor system (JAS) that has gained traction with adults (i.e. Sniezek & Buckley, 1995; Yaniv & Kleinberger, 2000; Sniezek & Van Swol, 2001). Judge-advisor systems allow for more in-depth probing of the decision-making process, as both the strategies for advice (correct, incorrect, neutral, recommendation; Dalal & Bonaccio, 2010) and judgment (conformity, dependence, rejection, rational; Scott & Bruce, 1995) can vary, and the way in which they do can provide information about the perceptual experience of the participant. A recent study by Rakoczy et al (2015) has demonstrated that children between 3 and 6 years old will retrospectively modify their previous judgments when provided with advice as a function of advisor expertise - suggesting that they attend to the quality of information given when choosing to integrate it with their reported decision. As such, we could expect to acquire interesting and informative results using an advice model with children.

In this chapter, I will explore the effect informational influence has on decision-making by only providing children with the judgment of a single advisor. The so-

cial context in which decisions are made affects behavioural judgments in many ways. Though there is limited research on the comparison of advisor type and how this affects conformity levels, Knoll & Blakemore (2015) have shown that younger adolescents tend to conform more to a 'teen advice' group, while older groups preferentially conform to an adult group. I will also investigate the effect of different types of advisor, peer and adult, on children's perceptual decisions.

Extracting information on how social influence affects neural computations of decision-making in the brain can be difficult without implementing invasive procedures. Single-unit recordings in monkey cortex (such as Mauzurek et al, 2003; Bland & Schaefer, 2011) have provided insight into decision-making on a physiological level, helping us to build a putative model upon which to base the mechanisms for decision-making in humans. Though imaging techniques such as MEG (gambling and emotions study, Giorgetta et al 2013), EEG (image discrimination study, Ratcliff, Philiastides & Sajda, 2009), and fMRI (social influence paradigm, Berns et al 2005) have been used while humans have undertaken various decision-making tasks, they lack either the spatial or the temporal acuity to provide evidence akin to electrophysiology. While fMRI is rapidly gaining the spatial resolution required to detect small clusters of neurons responsive to stimulus elements (see Chapter 5), the technology remains limited.

It is also often difficult to discern gradations of social influence and develop quantitative models of decision-making for the type of stimuli that are typically used in social influence studies. Explicitly "right" or "wrong" images and puzzles shift the focus away from the integration of social information and onto how reliable a participant perceives an advisor to be. Furthermore, the use of unambiguous stimuli means that rather than biasing information processing, socially provided information has to override sensory

processing. This may cause subjects to grow suspicious of the advisor's accuracy and cause them to disregard the information provided, weakening the experiment.

Structure-from-motion cylinder stimuli (SFM, Appendix B) overcome this issue, as they can have either unambiguous or ambiguous rotational direction, whilst the visual percept remains constant to the observer (Treue et al 1991; Nawrot & Blake 1989, 1991). SFM stimuli are formed of two planes of dots, moving in opposite directions. For a vertical cylinder, as employed in this study, these directions would be left and right. 3D anaglyph information can be applied to the rightward and leftward moving dots to provide a sensory rotational direction, or removed to render the direction ambiguous. So long as the stimulus is presented at a time shorter than the typical perceptual switch rate, and the disparity applied to unambiguous stimuli is sufficiently small, the participant will be unaware of the difference between ambiguous and unambiguous stimuli (Nawrot & Blake, 1993). The participant should therefore be unaware that their responses can be neither correct nor incorrect in some cases. This makes it possible for social information to bias ambiguous percept response without the subject being aware of stimulus ambiguity, thus allowing us to explore how social context affects decisions when it is correct, incorrect, or neither.

By fitting behavioural response data with a psychometric function, we are able to quantify the extent to which social context affects the perceptual decision. A relative shift in the fitted curve of data collected within different social conditions, such as different advice about the appearance of the visual stimulus, suggests a perceptual bias induced by that social context. Contrastingly, a relative decline in the gradient of the psychometric function without a shift can indicate an increase in error rate as a product of social context. Based on previous data, younger age groups should

conform less than older age groups with social advice, and older age groups should be consistently biased by social context. The effects of social context should be greatest when the sensory evidence is ambiguous, as was suggested by Hamm & Hoving (1969).

I will investigate how social influence affects perceptual decision-making for a range of ambiguous to unambiguous stimuli through child development from the age of 6 to 14. I will also investigate whether the confederacy of an advisor affects the extent of social influence at different ages, by using both peer and adult advisors. In order to make inferences about the processing level at which a behavioural decision is affected (or otherwise) by social advice, I will also investigate the perceptual decisions in children under social influence by fitting a drift diffusion model to reaction time data. As discussed in Chapter 1.4, particular parameter values estimated by the model when fitted to reaction time data can give some insight into whether a decision was the product of perceptual or judgmental bias. From this, one can make inferences about whether behaviour under social influence was the product of purely normative conformity, or perceptual bias. The computational model predicts different reaction time distributions dependent on the relative contribution of drift rate (v) and starting bound (z) to behavioural decisions. These values can be extracted and statistically compared for different conditions (such as the direction of social advice). A significant effect of drift rate would suggest that perceptual bias affected the decision, while a significant deviation of starting bound from the midpoint between two decisions potentially implicates judgmental bias.

2.2 Methods

Experiment 1 refers to experiments in which the social advice was provided by an age and gender-matched peer. Experiment 2 refers to experiments in which the social advice was provided by a gender-matched adult. All research was conducted in accordance with the British Psychological Society and Society of Research in Child Development guidelines, and ethical permission was gained from the Institute of Education, University of London. Participant's guardians gave informed written consent after obtaining the verbal consent of their child, and were free to leave the study at any time, and procedures were conducted in accordance with the declaration of Helsinki.

2.2.1 Participants

Participants who were tested were children aged between 6 and 14 years, divided into 3 groups (Experiment 1: 6-8 year olds (n = 34, 14 female), 9-11 year olds (n = 20, 11 female), 12-14 year olds (n = 19, 10 female)); Experiment 2: 6-8 year olds (n= 20, 11 female), 9-11 year olds (n = 18, 12 female), 12-14 year olds (n = 26, 20 female).

Data were collected either at participants' schools or at a Brain Detectives event organised by the Institute of Education (IoE) in London. For all participants, the experiment was conducted in a room separate from other people with a door that excluded external noise. During visual tasks, the lights were turned off and curtains closed. Where possible, participants also underwent measures of cognitive (Second Edition Weschler Abbreviated Scale of Intelligence, WASI-II (Weschler, 1999)) and social (Social Communication Questionnaire, SCQ (Rutter, Bailey & Lord, 2003)) abilities. All were tested for normal visual acuity using a Snellen chart (minimum

acuity 6/9 with correction), and for stereovision with a random dot stereogram TNO test (minimum threshold 240 seconds of arc).

Prior to the main social experiment, participants engaged in a short disparity threshold experiment with the SFM cylinder but without social advice. Establishing the individual 3D threshold allowed the application of appropriate peri-threshold disparities for the main experiment (those close to threshold and exceeding threshold performance to ensure a smooth psychophysical function), as well as ensuring that the participant understood the experiment. 22 participants in Experiment 1 (n = 11 at 6-8 years, n = 6 at 9-11 years, n = 5 at 12-14 years) did not have threshold data collected due to the constraints of the event at which data was collected.

For participants without a cylinder threshold disparity measure, the first two blocks of social data were discarded to account for learning effects (e.g. Brascamp et al 2008; Fuller et al 2009), and all data for these participants were discounted from group analysis if data plotted regardless of direction of social advice indicated an error rate greater than 20% at the largest disparities used (1 participant was excluded). For participants with a cylinder disparity threshold measure, those who failed to get 85% correct responses at the largest disparity, or showed a bias of more than 80% in either direction at zero disparity, were discounted from group analyses (2 excluded at 12-14, 5 at 9-11, and 5 at 6-8 years old). As such, participants included in the analyses were, for Experiment 1: 6-8 year olds (n = 29, 12 female), 9-11 year olds (n = 15, 9 female), 12-14 year olds (n = 17, 10 female), and for Experiment 2: 6-8 year olds (n= 20, 11 female), 9-11 year olds (n = 18, 12 female), 12-14 year olds (n = 26, 20 female).

If a participant took longer than 8 seconds to respond, that trial was excluded from further analysis. 8 seconds was chosen as the cut off point as it allowed for the

inclusion of decisions in which the child might struggle with a conflict between sensory information and social influence (thus taking longer to decide), while excluding trials in which the child failed to perform accurately due to distraction or attempting to engage with the experimenter (the mean of excluded trials across age groups was 14.67 seconds, n = 24).

Though we might expect to see sex differences between boys and girls involved in the study, no significant differences in behaviour were observed when age groups were divided by sex. As such, for analysis, groups were not divided along gender lines.

2.2.2 Set-up

Visual stimuli were projected from an Apple MacBook Pro (2.7GHz Intel Core i7, Intel HD Graphics 4000 1024MB) to an ELO surface capacitive touchscreen (model E653173, screen size 22") at a resolution of 1280 x 1024 pixels with a frame rate of 60Hz. They were viewed at a distance of 40cm through red-cyan glasses in a dark room.

2.2.3 Stimuli

The stimulus was a structure-from-motion (SFM, See Appendix B) cylinder composed of two transparent planes of black and white random dots on a mid-grey background, moving in opposite directions, with a sinusoidal velocity profile. The cylinder rotated through 90° of 360° over a period of 1 second (0.25 turns per second). Stimulus size was 6x6° of visual angle, with 125 black and 125 white dots, each subtending 0.2° randomly plotted per cylinder. 1% of dots randomly died and were replotted on each frame. Disparity could be applied to the dots via anaglyph red-green stereo. There was a central white fixation point subtending 0.1° visual angle.

Participants were told that they were taking part in a spaceship pilot training course, and would be judging the direction of spin of black holes in order to navigate a spaceship around them. This story type was chosen and designed as it had to potential to be entertaining for a broad spectrum of child ages (6 to 14 years) - while also remaining a plausible explanation of the task stimulus (a spinning SFM cylinder). Prior to the experiment, they were shown a Microsoft PowerPoint presentation introducing them to the story behind the task. Subsequently, before the social experiment, they were introduced to their advisor via a separate PowerPoint presentation (presentations are shown in Appendix A).

In the social conditions, a video clip (length 3000ms) of an advisor was shown before each stimulus. When a social stimulus was used for Experiment 1, the advisor was both age and gender matched to the participant. For Experiment 2 the advisor gender-matched to the participant, but an adult. The video was presented such that the advisor was facing the participant and looking into the camera. They delivered the same line within a 3 second video - 'The black hole is spinning [left/right]' - presented just before the SFM stimulus. There were 10-14 unique videos per condition (i.e. 20-28 videos of each advisor in total). At the end of a trial block, participants were shown a randomised end screen providing neutral congratulations on finishing the task. The stimuli were coded in MATLAB using the Psychtoolbox extension (Brainard DH, 1997).

There was no specific control for attention, but the participant was observed throughout the task in order to ensure that they were attending to the stimulus. Long reaction times (>8s) were removed from analysis, as this typically indicated a trial in which the participant had ceased to attend the stimulus.

2.2.4 Experimental tasks

Stereoacuity Thresholding

Figure 2.1 shows a schematic of the trial structures, which were identical for Experiment 1 and 2, save for the age of the advisor. Before engaging in the main experiment, the participants took a threshold test using the SFM stimulus presented in the main experiment (see also Participants). This consisted of 2 blocks of 42 trials evenly distributed across 7 disparities (3 positive, 3 negative, one ambiguous; typically +0.03°, +0.02°, +0.01°, 0°, -0.01°, -0.02°, -0.03°), pseudo-randomly interleaved, The participant would fixate on a central point for 500ms, and then be presented with an SFM cylinder for up to 2000ms. They could give a response at any point from cylinder onset. Participants responded by pressing either on the left or right side of the stimulus on the touchscreen (where the words 'left' and 'right' showed the respective sides), in order to indicate which direction the dots of the front surface of the cylinder were moving.

Left-Right Control

A subgroup of children from both experiments (78 children total, 29 aged 6-8 years, 30 aged 9-11 years, 17 aged 12-14 years) also took part in a brief control experiment prior to the presentation of a threshold stimulus. Pseudorandomly interleaved, they were requested to either touch the left or the right side of the screen (10 times left, 10 times right) with the textual instruction: 'Please touch the left/right side of the screen'. This was to establish that they could accurately differentiate between left and right. All children in both experiments were also asked to demonstrate with their finger to the researcher which direction was 'spinning left', and which direction was 'spinning right',

prior to engaging in the experiment.

Social task

The social stimulus had the same trial structure as the threshold stimulus but with an additional 3000ms social information 'advice' video preceding the stimulus. Participants undertook 10 blocks of 21 trials across 7 disparities and two types of social advice ('left' and 'right'; 210 trials total). For unambiguous stimuli, advice was correct in 2/3 of trials. Different advice trials were pseudo-randomly interleaved and advice videos for a particular direction randomly chosen from the pool of 20-28 videos. For ambiguous stimuli, direction advice was randomly 50%:50% right:left across trials. Direction of response and reaction time data were collected. Sequence of instruction and experimental screens for the social task is in Appendix A.

2.2.5 Analysis

Psychometric Functions

Data were grouped by age (6-8, 9-11, and 12-14 years of age) for analysis. Psychometric functions were plotted both for each individual participant, and for average behavioural responses at each stimulus disparity within the three age groups. Data were divided by the type of advice received ('left' or 'right') and plotted as proportion leftwards responses (y-axis) over binocular disparity in degrees of visual angle for individuals (x-axis, shown in Appendix C), or for the group average, over normalised disparity strength (x-axis).

A cumulative Gaussian function was fitted to each psychometric dataset, using custom MATLAB scripts based on the MATLAB *cdfplot* function. To test how well the

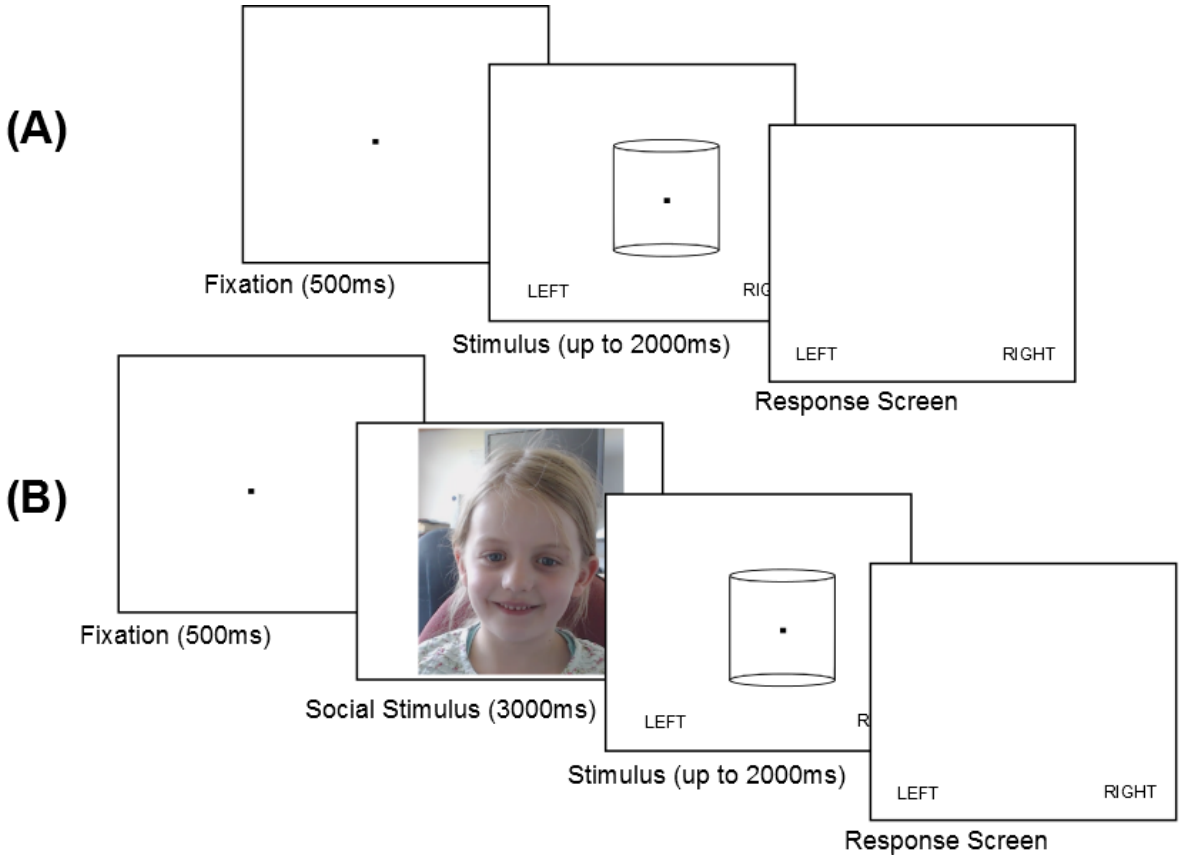

Figure 2.1: **Schematic Trial structures for (A) threshold stimulus and (B) social information stimulus**

model fit the data, an adjusted R-square was calculated with an f-test to establish significance for fitting the datasets with two separate functions versus one single function. The effect of social advice across disparities was tested in paired fashion using a non-parametric Wilcoxon Rank Sum test conducted in MATLAB (*ranksum* function) as data distribution were not normal (tested with the Kolgorov-Smirnov). P-values for multiple comparisons were corrected with the Bonferroni correction. An N-way ANOVA was also conducted in MATLAB to test for the overall effect of advice and disparity on behavioural responses.

Reaction Times

Reaction time data were investigated using an analysis of median response times under different conditions via a Wilcoxon Rank Sum (Bonferroni-corrected for multiple comparisons), and a drift diffusion model applied using the Diffusion Model Analysis Toolbox (DMAT, KU Leuven; Vandekerckhove & Tuerlinckx, 2008), both conducted in MATLAB. Median values were used as the data were not normally distributed. The drift diffusion model was run under several conditions to assess how advice direction and stimulus disparity strength affected model parameters.

Drift Diffusion Model fitting

In order to assess model fit, the Bayesian Information Criterion (BIC) was used (Gideon & Shwarz, 1978). The BIC for each of these models was compared across conditions and age groups: a lower value corresponds to a better fit. It should be noted that the BIC tends to give worse fits with increasing model complexity (Bhat & Kumar, 2010; Neath et al, 2012) - and as such penalises unrestricted models with a large number of

varying parameters. A comparison of BIC scores between models with a 2-way paired t-test (significant at a Bonferroni-corrected p-value of <0.05) revealed which was the best fit for each case.

To investigate the effect of social advice on model parameters, 5 models were tested. These models were chosen in order to investigate two factors implicated affecting perceptual decision-making - drift rate and starting bound. Given our interest in separating out whether changes in behaviour were the result of actual shifts in perception or, simply behavioural bias, it made sense to focus on the two parameters most strongly (but separately) linked to each of these potential causes.

In all cases, parameters were allowed to vary with stimulus disparity.

Model 1) No effect of social advice allowed on any parameter.

Model 2) All parameters may vary with advice other than drift rate (v).

Model 3) All parameters may vary with advice other than starting bound (z).

Model 4) Only drift rate and starting bound may vary with advice.

Model 5) Unrestricted model - all parameters may vary with advice.

To investigate the effect of SFM stimulus disparity (strength of the stimulus) on model parameters, 5 models were tested.

Model 1) No effect of stimulus disparity allowed on any parameter.

Model 2) All parameters may vary with stimulus disparity other than drift rate.

Model 3) All parameters may vary with stimulus disparity other than starting bound.

Model 4) Only drift rate and starting bound may vary with stimulus disparity.

Model 5) Unrestricted model - all parameters may vary with stimulus disparity.

When allowed the vary with advice under the model, the starting bound under different advice conditions was calculated by dividing the relative starting bound parameter by the bound separation. The starting bound is a value that indicates the starting point of evidence accumulation towards a decision bound. A starting bound value close to 0.5 suggests that there was no evidence of a judgmental bias (and as such that bias towards the advisor's judgment could be a product of biasing sensory information processing during the trial), while a bound significantly deviating from 0.5 could indicate judgmental bias, such that in cases where there is conformity with the advice, the decision might have been biased towards conformity prior to stimulus presentation. When allowed to vary under the model, the significance of drift rate was also assessed under different advice conditions (e.g. conforming, non-conforming, incorrect conformity, correct conformity) - larger drift rate values may indicate that sensory processing was biased when viewing the stimulus.

As the data were not normally distributed, a non-parametric Wilcoxon Rank Sum ($p<0.05$) was used to compare conditions (e.g. conforming vs. non-conforming responses), and the median value was plotted in graphs.

2.3 Results

I have investigated the perceptual judgments of children in response to a moving SFM stimulus across childhood, from ages 6 to 14 years. I explored the effect of social advice and different types of advisors quantitatively, in order to make inferences about the nature of their behaviour and its underlying causes. In experiment 1, social advice was provided by an age- and gender-matched peer. In experiment 2, advice was provided

by a gender-matched adult advisor.

2.3.1 Median stereoacuity thresholds across child development

In order to assess how well the participants could carry out the basic visual task, I formally determined binocular disparity thresholds for most participants before they entered the task. I excluded 12 children because they did not have good stereo vision or failed for other reasons to carry out the task accurately (2 excluded at 12-14 years, 5 at 9-11 years, and 5 at 6-8 years old; see Methods for criteria). Among the children included in the analysis, there was no significant difference in the measured median stereo thresholds across or between the different age groups (Wilcoxon Rank Sum, $p<0.05$; Table 2.1, Figure 2.2, Figure 2.3). As such, the children in the youngest age group tested (6-8 years), in the middle age group (9-11 years), and the oldest age group (12-14 years) were all equally capable of carrying out the visual task. Stereothresholds are comparable with those of adults and appear mature (e.g. Coutant et al, 1993; Heron et al 1985).

Accurately assessing the stereoacuity of each individual participant is particularly important in this type of perceptual experiment. In order to minimise the chance of the participant suspecting that the advisor is clearly incorrect in a significant proportion of cases the visual task should not be too easy and therefore carried out near threshold. Furthermore, the measurement of stereoacuity and threshold psychometric function can be used as a control for task performance for each individual and across different experiments. Measurements of stereoacuity collected prior to the two experiments with different advisors indicate typical stereo performance for both experimental groups (see Coutant et al, 1993 for a study of typical stereo performance in young adults). There

Age Group	Peer Advisor	Adult Advisor	Overall
6 - 8 years	0.0198° ±STD 0.010 (n=18)	0.0117° ±STD 0.017 (n=20)	0.0154° ±STD 0.008 (n=38)
9 - 11 years	0.0163° ±STD 0.016 (n=9)	0.0125° ±STD 0.015 (n=18)	0.0139° ±STD 0.012 (n=27)
12 -14 years	0.0145° ±STD 0.014 (n=12)	0.0178° ±STD 0.014 (n=26)	0.0149° ±STD 0.011 (n=38)

Table 2.1: **Median stereoacuity thresholds for each age group**
The behavioural data from all included participants who participated in the threshold experiment without social advice. Data were fitted individually with cumulative Gaussian functions. Psychometric thresholds were determined by taking the standard deviation of a fitted curve. They are expressed in degrees of visual angle. There were no significant differences between age groups, and also no systematic difference within each age group between the children entering Experiment 1 and those entering Experiment 2 (Wilcoxon Rank Sum, $p > 0.05$). An ANOVA showed no significant effect of age group on threshold ($p = 0.5951$, $F = 0.5925$, $df = 2$).

was no significant difference in stereoacuity between the two advisor groups at any age, and all fall within a normal range. As an additional check, an N-way ANOVA run on the data shows that disparity has a significant effect on response (Table 2.1, $p<0.0001$) for all ages regardless of advisor. This demonstrates that any differing results between age groups or advisor groups are not a product of capacity to perform well at the visual task.

2.3.2 The effect of social advice on perceptual judgments

Psychometric functions are a well-tested method of assessing sensory performance quantitatively. Behavioural data are fitted with a model of behavioural performance. The slope of the fitted function indicates sensitivity to stimulus strength as well as accuracy, while a shift in location can indicate biases in perceptual decision-making (see a review by Gold & Ding, 2013). A cumulative Gaussian function was fitted to the normalised, pooled behavioural responses for each age group tested, and statistical tests were carried out to determine the goodness of fit and the strength of effect by social context.

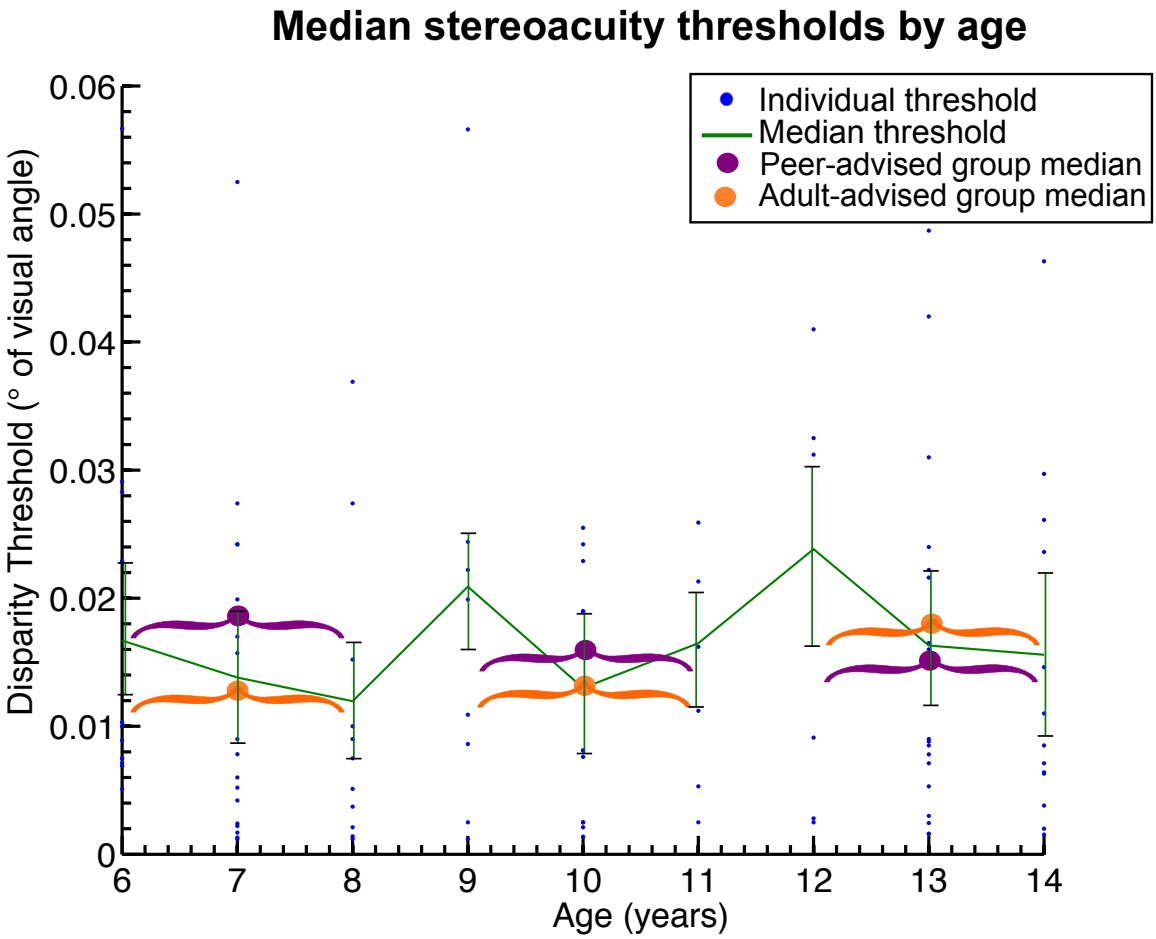

Figure 2.2: **Stereoacuity thresholds across all ages for typically developing children**

Median stereoacuity values at each age are show in green. Error bars show confidence intervals. There is no systematic change in stereoacuity between the ages 6 and 14 years. The purple circles indicate median stereoacuity values for the peer-advised group, while the orange circles indicate median stereoacuity values for the adult-advised group. Brackets indicate the ages included within a group (6-8, 9-11, 12-14 years). These are shown separately in Figure 2.3.

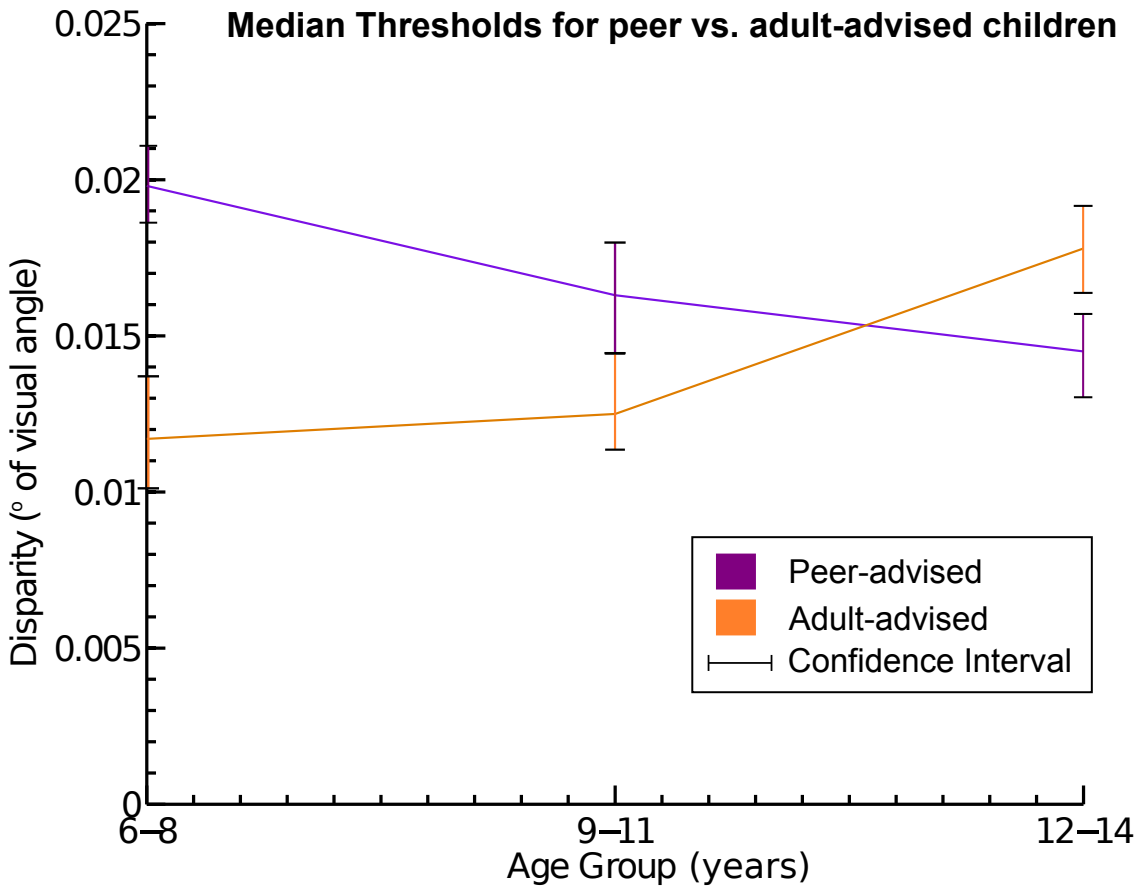

Figure 2.3: **Median stereoacuity thresholds for typically developing children, split by advice group**

The purple line indicates peer-advised median stereoacuity values, the orange line adult-advised. Error bars show the confidence intervals. There is no significant difference in stereoacuity between peer and adult-advised groups overall, or between any age group.

The perceptual judgments of the youngest age group (6-8 years) seemed to be affected very little by social advice. Data for the youngest age group was equally well fit with a single cumulative Gaussian function as with two functions that were allowed to vary by their mean, for both peer and adult-advised groups (adjusted r-square = 0.9991 versus 0.9992, p = 0.70, n= 29; adjusted r-square = 0.9996 versus 0.999, p = 0.89, n= 20; Figure 2.4, top). The same is true of the middle age groups (adjusted r-square = 0.9992 versus 0.9980, p = 0.89, n= 15; 9-11 years, adjusted r-square = 0.9990 versus 0.9970, p = 0.99, n= 18; Figure 2.4, middle). However, for both types of advisor, the behavioural responses for older children (12-14 years) were better described by fitting two curves that were allowed to differ in their mean (adjusted r-square value of 0.9999 for two curves versus = 0.5948 for one, p = $<$0.0001, n=17; adjusted r-square value of 0.9999 for two curves versus = 0.7998 for one, p = $<$0.0001, n=26; Figure 24, bottom). For the 12-14 year olds, regardless of the advisor type, social influence consistently shifted perceptual judgments in the direction indicated by the advisor. Significant social effects were seen across different stimulus strength ($p<0.0001$, Wilcoxon Rank Sum) but appeared strongest for the ambiguous zero disparity stimuli.

Overall the psychometric function for the youngest age group (6-8 years) showed no consistent bias with peer advice. However, when the responses at each binocular were tested separately, these children are more likely to respond with the opposite of what they were advised than conform to advice when stimulus information was ambiguous (i.e. at a binocular disparity of 0 (Figure 2.4, top). This effect was significant ($p<0.0001$, Wilcoxon Rank Sum). There was no significant effect of social advice at any other binocular disparity. An N-way ANOVA showed that advice had a significant effect on behavioural response (Table 2.2, p = 0.02528), likely primarily driven

by this contrarian response for ambiguous stimuli. There was no effect of advice on peer-advised behaviour at ages 9-11 years (Figure 2.4, middle) - at no point was there a significant difference between responses to left or right advice relative to disparity. This suggests that children of this age do not integrate peer social information into their decision. Correspondingly, an N-way ANOVA showed no significant effect of advice on behavioural response (Table 2.2, $p = 0.8713$). Finally, the oldest peer-advised group (12-14 years of age) demonstrate the expected effect of advice - both psychometric functions were shifted relative to one another in the direction conforming to the social advice (leftwards when advice given was 'left' and vice versa for 'right'). This effect is significant at almost every binocular disparity ($p<0.0001$, Wilcoxon Rank Sum), and suggests that this age group was integrating social advice exhibiting a behavioural bias in the direction of advice. This is confirmed by an N-way ANOVA, which showed that advice overall had a significant effect on behavioural response (Table 2.2, $p<0.0007$).

Adult-advised participants broadly show the same results (Figure 2.4 B), with a couple of small differences. The contrarian behaviour to social advice for ambiguous stimuli was still significant for the youngest age group, but appears reduced when compared with the effect of peer-advised 6-8 year olds ($p<0.005$, Wilcoxon Rank Sum) - and an N-way ANOVA reveals no significant overall effect of advice on behavioural responses (Table 2.2, $p = 0.0771$). A significant contrarian response to advice when the stimulus was ambiguous can also now be demonstrated for the middle age group when advised by an adult ($p<0.0001$, Wilcoxon Rank Sum) - an effect not present in the peer-advised middle group. But, like the middle peer-advised group, advice had no significant overall effect on behavioural responses (N-way ANOVA, Table 2.2, $p = 0.1692$). Finally, the oldest group (12-14 years old) showed much stronger conformity

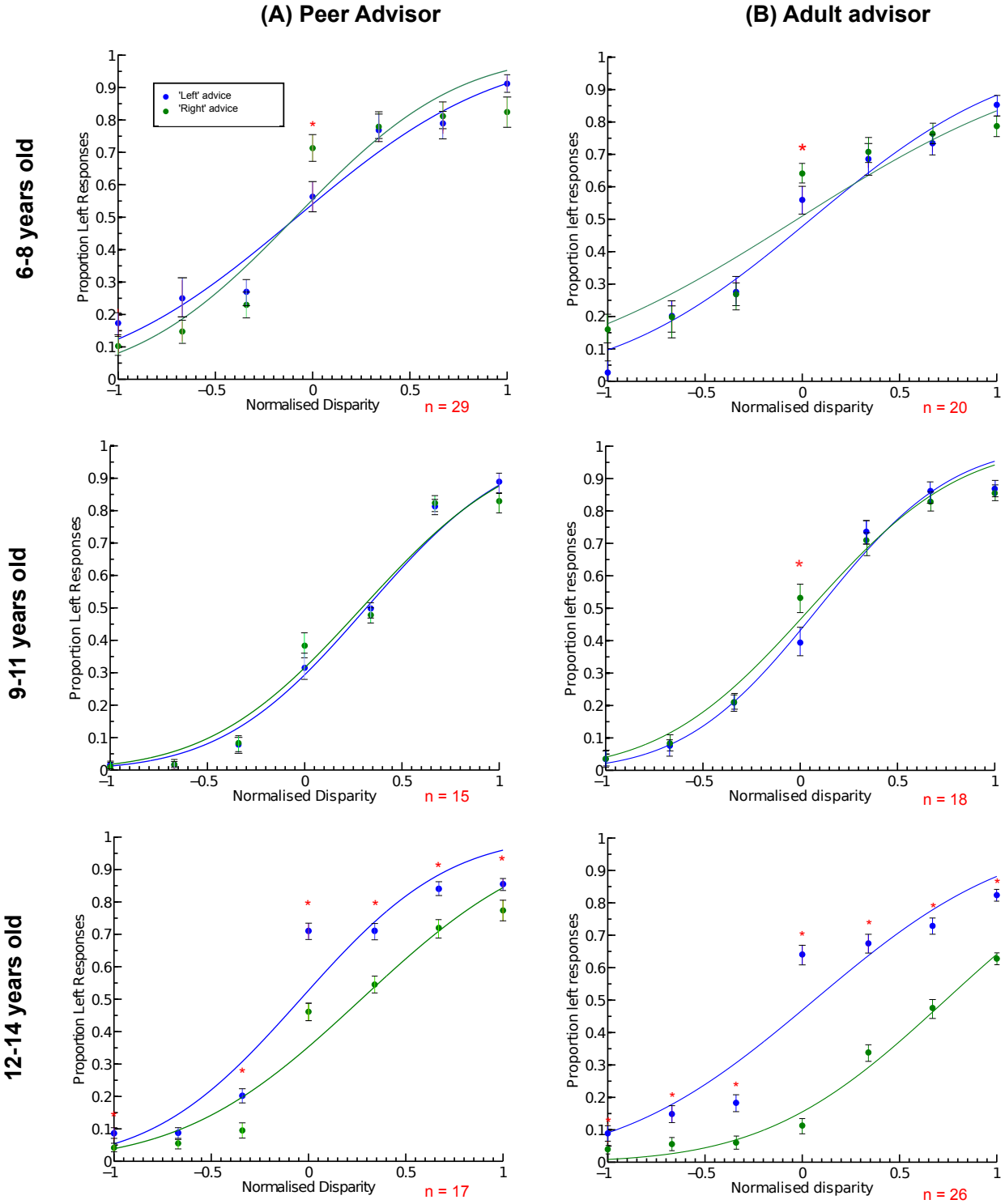

Figure 2.4: **The effect of social advice on perceptual decisions**
A. Graphs show the average psychometric functions of children in different age groups with social advice from an age-matched peer. Behavioural responses were plotted against normalised binocular disparities, and were fitted with two cumulative Gaussians, separately for advice 'left' (blue) and advice 'right' (green). Error bars = standard error of the mean (SEM). * indicates a significant difference between responses for 'leftwards' versus 'rightwards' advice (Wilcoxon Rank Sum, $p<0.05$, Bonferroni corrected). B. Behavioural results with an adult as advisor. Same conventions as in A.

	Peer Advice									
Age	**Advice**			**Disparity**			**Interaction**	**Age**		
(years)	F	p	df	F	p	df	p	F	p	df
6 to 8	72.92	0.02528*	1	96.61	<0.0001*	6	0.0193*	291.54	<0.0005*	2
9 to 11	0.03	0.8713	1	491.43	<0.0001*	6	0.0327*			
12 to 14	240.32	<0.0007*	1	560.13	<0.0001*	6	<0.0001*			
	Adult advice									
Age	**Advice**			**Disparity**			**Interaction**	**Age**		
(years)	F	p	df	F	p	df	p	F	p	df
6 to 8	3.13	0.0771	1	121.54	<0.0001*	6	<0.0001*	319.15	<0.0005*	2
9 to 11	1.89	0.1692	1	151.24	<0.0001*	6	0.0062*			
12 to 14	344.44	<0.0002*	1	77.35	<0.0001*	6	<0.0001*			

Table 2.2: **N-way ANOVA results for effect of advice, disparity, and age group on overall response for peer-advised and adult-advised children**
An asterisk indicates a significant p-value (<0.05). For all participants, disparity had a significant effect on behavioural response, as we would expect for a participant correctly performing the visual task. For the oldest age group, regardless of advisor, social advice had a significant effect on response. For the youngest peer-advised group, advice had a weaker significant effect on response. For neither advisor group did advice have a significant effect on the responses of the middle age group. In all cases, advice and disparity interacted significantly, indicating differential effects at different disparities. Age group also clearly had a significant effect on responses, as can be seen in the psychometric functions of the behavioural data.

at each disparity when advised by an adult than by a peer. As hypothesised, this effect was strongest when stimulus information is ambiguous ($p<0.00001$, Wilcoxon Rank Sum). The N-way ANOVA corroborates this with a highly significant effect of advice on overall behavioural responses for adult-advised 12-14 year olds ($p<0.0002$, Table 2.2).

Given the general comparability of the effect of social advice on behavioural response within each age group, this suggests that the nature of the advisor (peer or adult) did not qualitatively affect the way in which social information was integrated into the decision process - at least between unknown peer versus unknown adult. To ensure that the results in the youngest age groups were not the product of children not understanding the left:right advice structure and potentially mixing up these two sides of the screen, we included in a sup-group of experiments (78 children total, 29 aged 6-8 years, 30 aged 9-11 years, 17 aged 12-14 years) in a brief control test asking children to either press left or right on the screen, without an SFM stimulus (10 trials 'left', 10 trials 'right'). In all cases, across all age groups, children performed this task with 100% accuracy. Furthermore, throughout all experiments 'LEFT' or 'RIGHT' was prominently displayed on the appropriate screen side (see Appendix A), and prior to the experiment children were requested to read aloud the astronaut story constructed around the computer task (see also Appendix A), which established that they were of a suitable reading age to understand these words.

The plotted data demonstrates that for both peer-advised and adult-advised participants, the youngest age group were (depending on stimulus strength) either not affected by social context, or tended to adopt a contrarian approach wherein they rejected the validity of the social advice. The middle age group appears to disregard or

ignore social advice when peer-advised, but display a more similar behavioural pattern to the youngest age group when adult-advised. The oldest age group, however, appear to integrate the social information to a larger extent and are biased in favour of the social advice.

2.3.3 Effect of social advice on accuracy of response

If participants were integrating advisor information with their perceptual decision, we would expect that accuracy rates would decrease when incorrect advice was given, and increase with correct advice. Figure 2.5 bears this out for the oldest age group (regardless of advisor) - accuracy of judgments was significantly lower when advice was incorrect. For the youngest peer-advised group, and middle adult-advised group, there was no significant effect of social advice (Figure 2.5). If anything, accuracy tended to be slightly higher when the advice was incorrect. This matches with what one might refer to as their more 'suspicious' approach to social advice, taking a contrarian approach behaviourally when stimuli are ambiguous. This could indicate a of distrust social advice within these groups.

2.3.4 Social Advice and reaction times

As participants were asked to respond as quickly and accurately as possible (starting at stimulus onset), we were able to collect reaction time data. Reaction time data can be used in their own right, as well as part of a drift diffusion model, to further analyse behavioural responses. If a participant took longer than 8 seconds to respond, that trial was excluded from analysis.

Overall, the oldest age group (regardless of advisor) had significantly faster re-

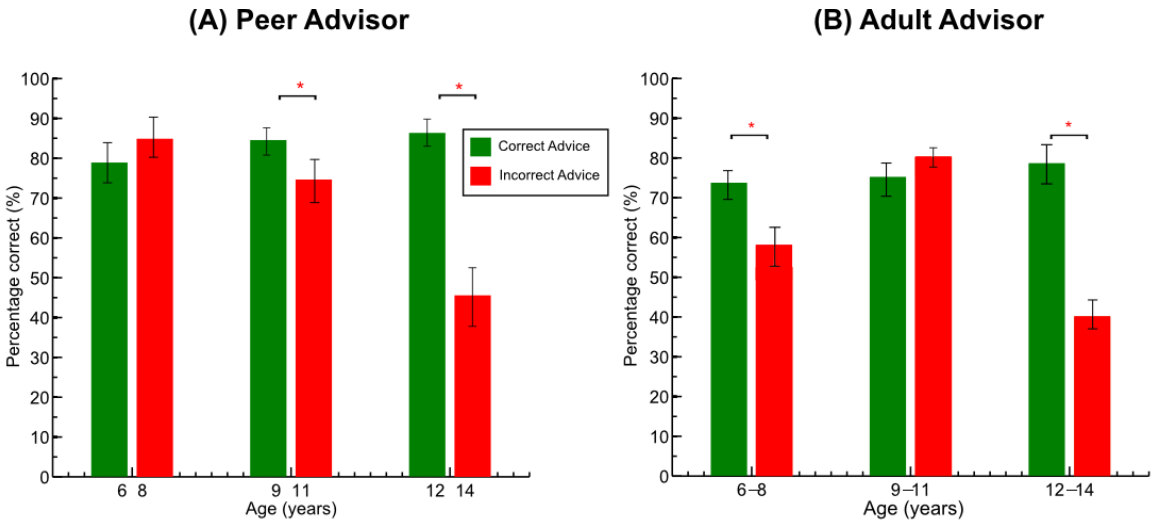

Figure 2.5: **Percentage correct responses when advice was correct or incorrect, for peer-advised and adult-advised children, divided by age group**
For both peer and adult-advised children, the oldest age group performed significantly worse when advice was incorrect (Wilcoxon Rank Sum, $p<0.05$ Bonferroni corrected, indicated by a red asterisk). This is expected, as they showed conformity with social advice. An ANOVA across groups indicated that age group had a significant effect on percentage correct ($p = 0.025$, $F = 70.45$, $df = 2$) but advisor type did not ($p = 0.8837$, $F = 0.0243$, $df = 2$).
Notably, in the peer advised group, the youngest children did not perform significantly better with correct advice. The same was true for the middle age group of adult-advised participants. This correlates with the behavioural data, which suggested that for ambiguous sensory information, peer-advised 6-8 year olds and adult-advised 9-11 year olds were more likely to adopt a contrarian response to the social advice. This approach could have extended to responses when stimuli were non-ambiguous (responses to ambiguous data are not included here as advice was neutral).

action times than the youngest group (mean = 1.778 versus 2.381s, $p<0.0001$ by Wilcoxon Rank Sum), although median thresholds for binocular disparity were comparable (0.0154° and 0.0149° for younger and older respectively). Therefore, although behavioural performance on the visual task was comparable across age groups, the youngest children took longer to reach a decision. This may have been a product of the older children being more accustomed to computer-based activities, or it could indicate an underlying change in the speed of sensory decision-making or behavioural responses with age. This is in line with other developmental data (see Kiselev, Espy & Sheffield, 2008 for a recent study comparing reaction times of 4-6 year olds with adults). Error rate, regardless of advice, did not have a significant effect on reaction time, though there was a slight trend for correct responses to be slightly faster (median across age groups of 1.948 versus 2.104s, $p = 0.201$, Wilcoxon Rank Sum). This suggests that the reaction time effects seen were at least partly the product of social advice, rather than error rate.

Across the age groups (regardless of advisor), social advice had a significant effect on reaction times: incorrect social advice increased reaction times and correct social advice decreased reaction times (median across age groups of 2.419 versus 2.057s, $p<0.0001$, Wilcoxon Rank Sum). All peer-advised typical age groups were significantly slower to conform to incorrect social advice than correct advice (Figure 2.6A), as were the youngest and oldest adult-advised groups. Although the middle age group of adult-advised participants does not show this effect significantly, a trend in this direction is still present (Figure 2.6B). This is a fairly intuitive result - when two pieces of information oppose one another, the decision-making process takes longer than when they correspond.

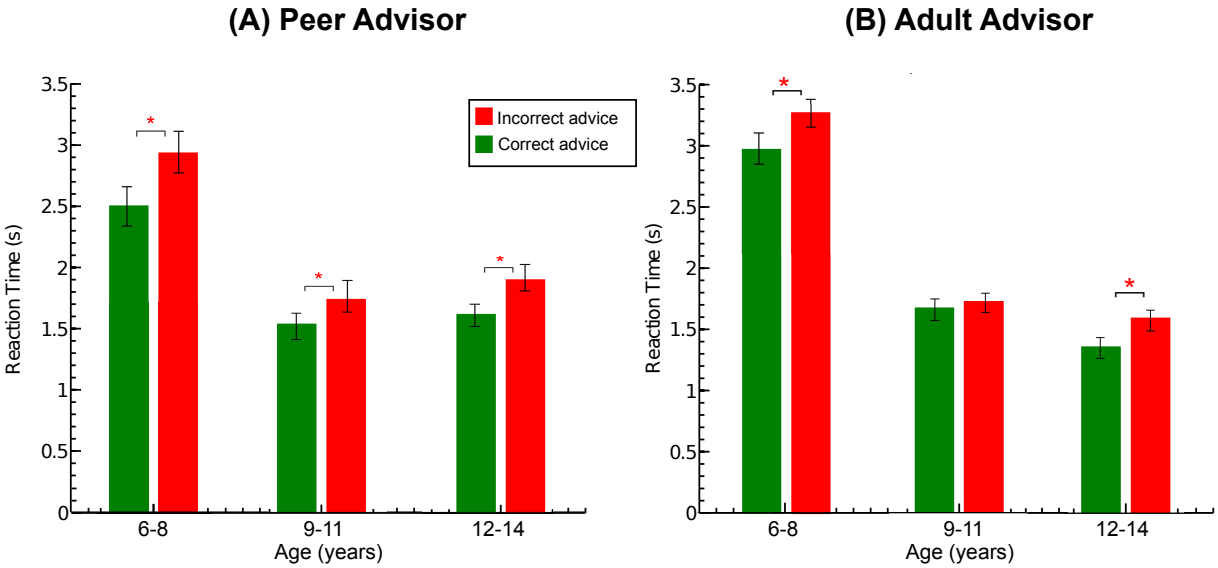

Figure 2.6: **Median reaction times when conforming correctly or incorrectly, for peer-advised and adult-advised children, divided by age group**

When peer-advised children incorrectly conform, they have a significantly longer reaction times (Wilcoxon Rank Sum, p <0.05 Bonferroni corrected) - as expected. For adult-advised children, the same trend exists, but only the youngest and oldest age groups take significantly longer to incorrectly conform (Wilcoxon Rank Sum, p <0.05 Bonferroni corrected). An ANOVA across groups indicated that age group had a significant effect on response ($p = 0.005$, $F = 153.76$, $df = 2$) but advisor type did not ($p = 0.9851$, $F = 0.0139$, $df = 2$). Red asterisks indicate a significant difference between correctly and incorrectly conforming within age groups, while vertical lines show confidence intervals.

Interestingly, the youngest peer-advised age group and the middle adult-advised age group were the only groups to take significantly longer overall to agree with the social advice than to disagree, regardless of whether it was correct or not, and including 'neutral' advice ($p<0.0001$, Wilcoxon Rank Sum). There was no significant effect for any other age group ($p = 1$, Wilcoxon Rank Sum). This may well be reflected in the youngest peer- and middle adult-advised more contrarian approach apparent for the ambiguous stimuli - they were quicker to disagree than agree.

2.3.5 Modelling behavioural responses under social advice with the drift diffusion model

In order to get deeper insight into the underlying decision processes at work when children make judgments under social advice, I analysed the behavioural data from the experiments described above with a drift diffusion model (DMAT Toolbox, Vandekerckhove & Tuerlinckx (2007, 2008); based on Ratcliff & McKoon (2002, 2008)). The two main parameters modelled that reflect changes in the decision process are starting bound and drift rate, which can provide some insight into judgmental and perceptual bias. Other parameters include 'non-decision time' (a sum period of all other processes involved in enacting a decision, such as motor reaction time), inter-trial range (the variation in non-decision time), and boundary separation (the 'distance' between the two decisions). A change in drift rate between conditions indicates a perceptual bias, whereas a change in the starting bound suggests a judgmental bias. In order to test for a significant effect of drift rate and starting bound prior to conducting statistical analysis, the Bayseian Information Criterion (BIC) was compared across models where either drift rate and/or 'starting bound were allowed to vary, and where they were not (see Methods for more detail). A lower BIC indicates a better model fit. It should be noted once again that the BIC tends to give worse fits with increasing model complexity (Bhat & Kumar, 2010; Neath et al, 2012) - and as such penalises unrestricted models with a large number of varying parameters. If the model fits better when drift rate is allowed to vary than not, we take there to be a significant effect of drift rate on behaviour, likewise for starting bound.

The following models for explaining the data were tested, as outlined in the methods:

1) No parameter allowed to vary with advice (no effects).

2) Drift rate not allowed to vary with advice (no v), other parameters free.

3) Starting bound not allowed to vary with advice (no z), other parameters free.

4) Only drift rate and starting bound allowed to vary with advice (only v and z).

5) All parameters allowed to vary with advice.

These models were selected in order to test whether advice was an important factor in decisions (if not, we would expect Model 1 to provide an adequate fit to the data), to explore the relative importance of drift rate versus starting bound (Models 2 and 3), to examine how well drift rate and starting bound explain variance in behaviour produced by advice (Model 4), and to check that starting bound and advice provided a better fit than simply allowing every parameter to vary (Model 5). In choosing which models to test, we hypothesised that Model 4 would provide the best fit, as we would expect starting bound and drift rate to best explain the decision-making behaviour of participants.

Where both drift rate and starting bound were allowed to vary with advice condition (Model 4), the model provided the best fit (Table 2.3). As such, this model was used to provide the starting bound and drift rate values for analysis. As drift rate and starting bound are the parameters of the model associated with decision making, it should be expected that this model would provide the best fit, as it reflects the decision-making process. Wilcoxon Rank Sum statistical tests were then applied to determine significant differences in drift rate or starting bound between conditions.

Interestingly, there was consistent variation in the second best model fit. For the groups that showed no behavioural evidence for conformity (6-8 and 9-11 year olds), the model that allowed all factors to vary with advice *but* the drift rate had the second

best fit (Model 2), while for the groups that showed evidence of behavioural conformity (12-14 years old) the model allowing all factors but the starting bound to vary with advice provided the second best fit (Model 3, Table 2.3). This means that allowing the starting bound to vary with advice for the younger two groups improved the fit of the model more than allowing the drift rate to vary, while for the oldest group, allowing the drift rate to vary with advice improved the model fit more than allowing the starting bound to vary. These results support the idea that perceptual bias may have played a role in the behaviour of the oldest age group (who showed evidence of conformity), while judgmental bias may have had more effect on the younger two groups (who did not show evidence of conformity).

The worst fits were apparent for the the 'no effects' model (Model 1), and the unrestricted model (Model 5). This is to be expected; as advice affected behaviour, a model that does not allow decision parameters to vary with advice cannot adequately explain variation in reaction times, and the unrestricted model had larger numbers of varying parameters, known to produce worse fits as judged by the BIC (Bhat & Kumar, 2010; Neath et al, 2012).

Starting bound (relative starting bound divided by bound separation, indicating the separation of two choices), when significantly different from the exact midpoint between two choices, can suggest a judgmental bias. When the drift diffusion model fitted to the behavioural data allowed both starting bound and drift rate to vary with advice, both the youngest and middle age groups peer-advised showed significant deviation from 0.5 when not conforming to social advice in either direction (Figure 2.7 (A)). The middle age group also showed a small, but significant deviation when conforming to leftward advice. This indicates that judgmental bias was a significant factor in

Model	6-8 (1)	9-11 (1)	12-14 (1)	6-8 (2)	9-11 (2)	12-14 (2)
1 (no effects)	12238.33	13481.52	12485.31	11393.63	11156.15	11574.45
2 (no v)	3534.5*	4258.14*	7841.21	4298.81*	3915.92*	8174.66
3 (no z)	6131.11	6927.81	4291.11*	7143.67	6148.95	4914.11*
4 (only v and z)	*2984.53*	*3148.14*	*2918.18*	*3041.95*	*3194.46*	*2724.65*
5 (unrestricted)	11172.03	10029.23	10991.1	11190.54	10285.87	11002.09

Table 2.3: **BIC values for different drift diffusion parameter models** '1' indicates Experiment 1, where the advisor was a peer. '2' indicates Experiment 2, where the advisor was an adult. 'v' = drift rate, 'z' = starting bound. A lower BIC value indicates a better model fit. In all cases, parameters were allowed to vary with stimulus disparity. For model 1, no parameter was allowed to vary with advice condition. For models 2 and 3, either 'v' or 'z' were not allowed to vary with advice. For model 4, only 'v' and 'z' were allowed to vary with advice, while other parameters were not. Model 5 was unrestricted. For all groups, model 4 showed the best fit (red italicised text). Notably, the second best fit (indicated by an asterisk) for 6-8 and 9-11 year olds was given when drift rate was restricted, and for the oldest age group when starting bound was restricted. This compliments the idea that drift rate was most important for the oldest age group, while starting bound had more of an effect for the middle and youngest groups.

informing the decisions of these children, and affected reaction times. It could suggest that they were treating social information as independent from stimulus information, and consciously choosing whether or not to conform to the advisor. Importantly, the oldest age group (who showed behaviourally the strongest and most consistent conformity with social advice) showed no significant deviation from 0.5 under any condition, indicating they were perceptually rather than judgmentally biased. This pattern is repeated for those with an adult advisor (Figure 2.7 (B)): the youngest and middle age groups showed a significant bias of starting bound from 0.5 for all responses (in the direction of behavioural response given), while the oldest group showed no significant deviation at all.

When the drift diffusion model allowed drift rate to vary in an unrestricted manner with stimulus disparity (the strength of rotation either left (positive disparity) or right (negative disparity)), drift rate was found to have a clear relationship with stimulus

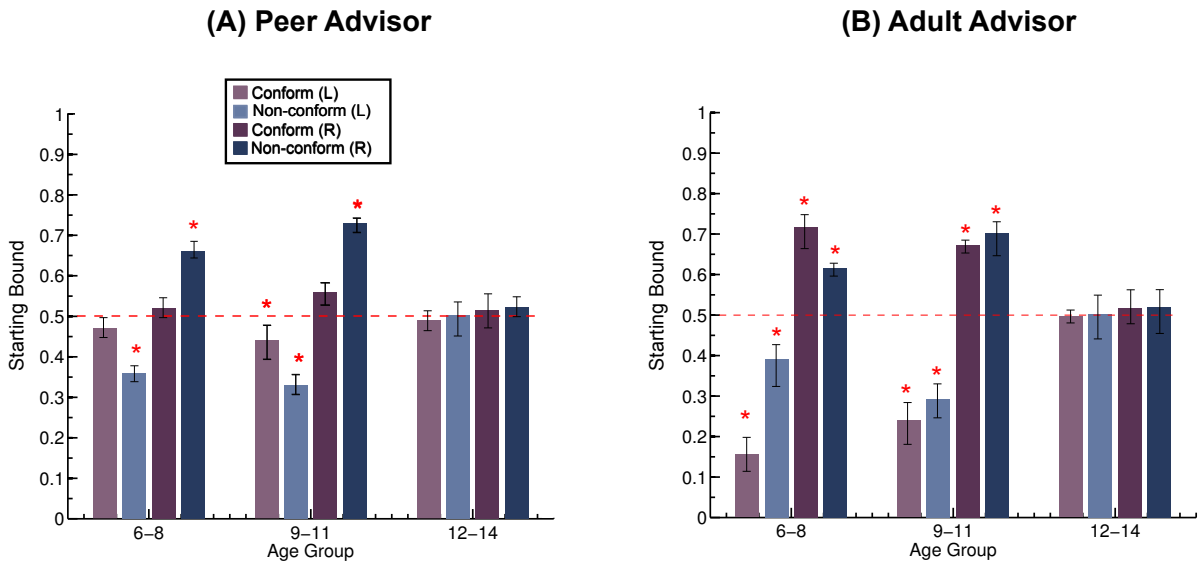

Figure 2.7: **Starting Bounds for peer-advised and adult-advised children, divided by direction of advice and age group**

* indicates that the starting bound deviates significantly from 0.5 midpoint between the two decision bounds (Wilcoxon Rank Sum, $p<0.05$, Bonferroni corrected). '0' represents the 'left' decision bound, and 1 represents the 'right' decision bound. Error bars show confidence limits. A significant deviation from 0.5 suggests a directional effect of judgmental bias. For the oldest children (in both advice groups), starting bound for the diffusion modelling does not deviate significantly from the mid-point across conformity conditions. This suggests little influence of judgmental bias on the perceptual decision.

disparity. This was such that a positive disparity resulted in a positive drift rate estimate, and vice versa, across all age groups. When split by advice (Figure 2.8), there was a trend for drift rate to diverge in the direction of advice for the oldest age groups (12-14 years), regardless of advisor type. Drift rates diverged significantly in the direction of advice at ambiguous disparities. This supports the idea that some decisions made by this group were driven by changes in drift rate, and as such may have been the product of perceptual bias in the direction of social advice.

When the drift diffusion model allowed both drift rate and starting bound to vary with advice, only the oldest age groups showed significant drift rate values, regardless of advisor type. In addition, these were the only group to show drift rates significantly differing from 0 (Figure 2.9, (A) and (B)). This suggests that they were perceptually biased when conforming to the social advice, and that social information was potentially affecting stimulus processing. The youngest and middle age groups showed no significant difference in drift rate between conforming and non-conforming, but tended to significantly deviate from the centre point of the starting bound (Figure 2.7).

An N-way ANOVA was conducted on the drift rate data, with age, advisor type, and condition as factors. For the youngest two groups, regardless of advisor, condition did not have a significant effect on drift rate ($p > 0.2$ in all cases) - though it did for the oldest typical group ($p < 0.05$). Age had a significant effect on drift rate ($p < 0.01$), driven by the significant drift rates seen in the oldest typical group. Advisor type did not have a significant effect between age groups ($p > 0.1$). This supports the idea that, regardless of advisor, drift rate was only a significant factor in the decision-making process for the oldest age group.

This further supports the hypothesis that while the oldest age group was perceptu-

ally biased by social information, the younger two groups tended to either disregard the information, or selectively and more intentionally conform at the behavioural decision stage.

2.3.6 Summary

Overall, the data indicate that the way the oldest group responded to social context in their decision-making was profoundly different to that of the youngest and middle groups. The oldest group, whether advised by peers or adults, tended to conform to the social advice, such that their perceptual decisions were overall biased across all levels of sensory stimulus information - but more so perhaps when sensory information was ambiguous. The drift diffusion data indicates a perceptual bias. The youngest age group showed little effect of social advice on perceptual judgments, but they tended to oppose social advice when sensory information was ambiguous. Any behavioural bias should be a judgmental rather than a perceptual bias. When sensory information was ambiguous, they tended to oppose the social context, presumably in favour of their own interpretation. It is tempting to suggest that they were less trusting of the advisor, and therefore were more likely to adopt the opposite position when sensory information was ambiguous. When advised by a peer, the middle group appears to disregard social advice entirely, with no effect being seen at any point. Those in the middle group advised by adults showed a similar trend to the youngest group, opposing advice when sensory information was ambiguous.

It is worth noting that in spite of these general results on conformity, there were also some weaker trends in the data: there was some evidence for the effect of conforming with social advice at the level of accuracy of judgments. Conforming to correct social

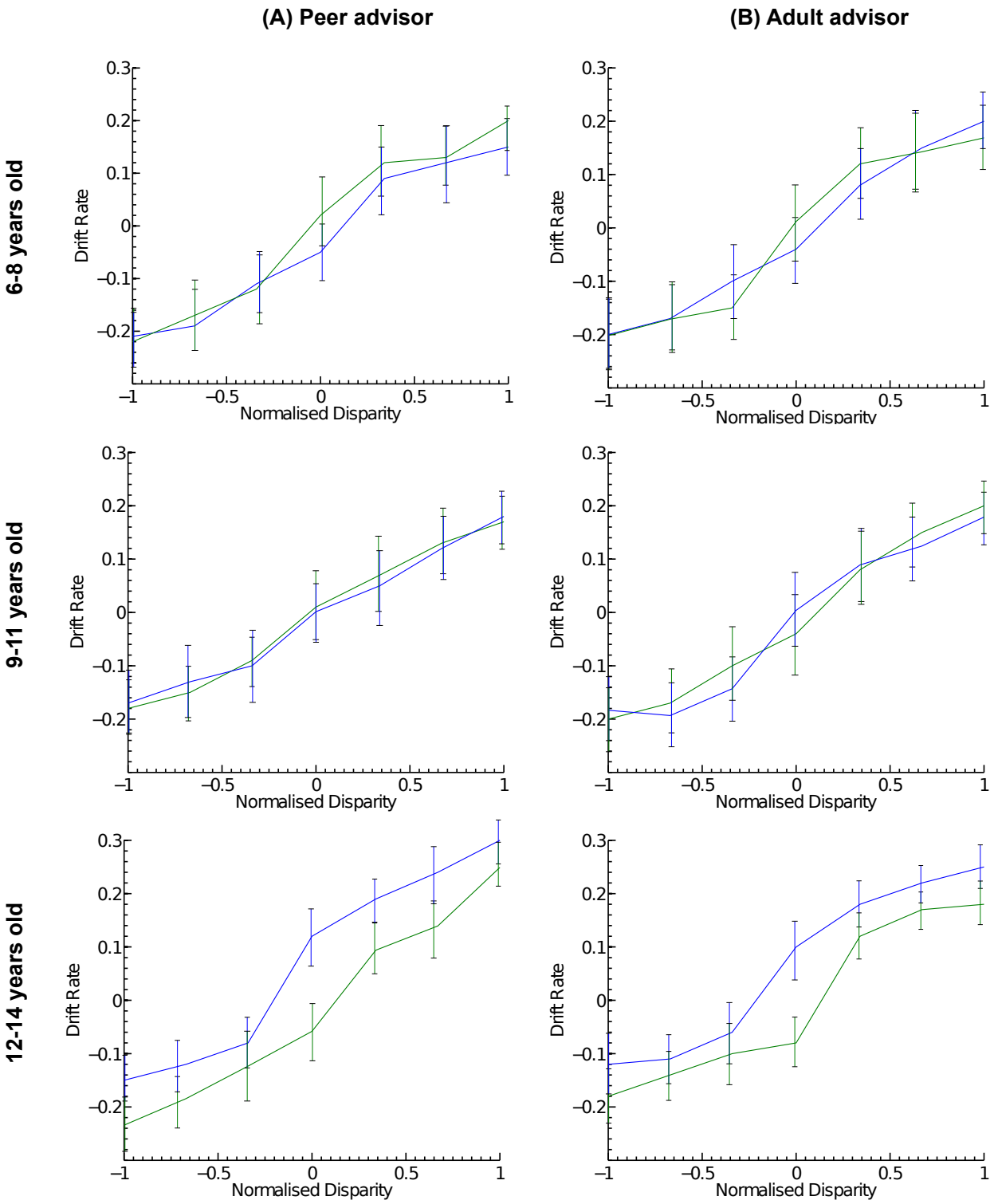

Figure 2.8: **Drift rate estimates plotted against stimulus disparity, split by advice type**

The green lines indicate parameter estimates when advice was 'right', the blue when advice was 'left'. The 'left' decision bound was positive, while the 'right' decision bound was negative. As such, a positive drift rate indicates drift in the leftward direction. (A) shows responses from the peer-advised group, (B) shows responses from the adult-advised group. Rows show responses by age group. Drift rate estimates vary in the direction of stimulus disparity, with the oldest age group showing clear deviation of drift rates in the direction of advice. Error bars show confidence intervals.

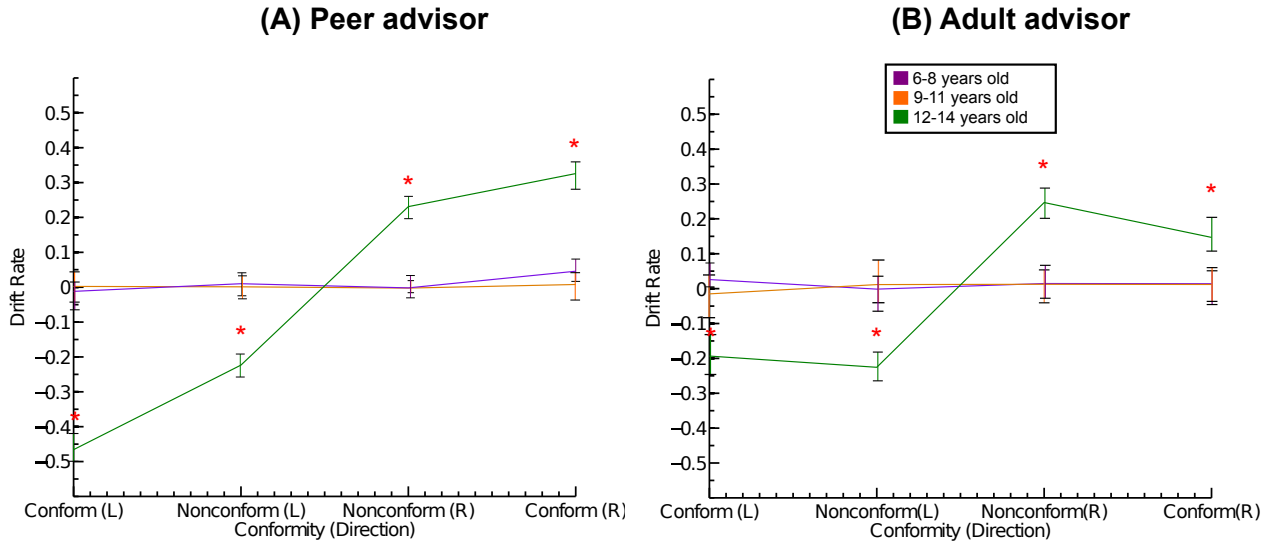

Figure 2.9: **Drift rates with advice for peer-advised and adult-advised children, divided by age group**

The purple line represents 6-8 year olds, the orange 9-11 year olds, and the green 12-14 year olds. * indicates a significant difference of the data point from 0. The oldest age groups for both peer and adult-advised participants showed significant drift rates that followed the direction of response given (Wilcoxon Rank Sum, $p<0.001$). Error bars show confidence intervals.

advice not only significantly increased accuracy for the oldest age groups but also for the middle age group (Figure 2.5) when peer-advised, and for the youngest and oldest groups when adult-advised. In the youngest peer-advised group, there was a trend to be more incorrect when social advice had actually been correct. This corroborates with the fact that there was a tendency for this group to oppose social advice. This same trend is seen in the more contrarian middle adult-advised age group. In general, the social influence of advice on perceptual decisions increases with age: as children enter adolescence, they transition from weaker judgmental effects to a stronger perceptual bias.

2.4 Discussion

2.4.1 The effect of age on behavioural response to social advice

The data show clearly that regardless of advisor type, conformity to social advice increases in development with the age of participants. The main transition appears to happen between the ages of 9-11 and 12-14 years old. Further to this, the effect social information has on decision-making is most apparent when sensory information was ambiguous, with the contrarian response by the youngest group (peer and adult advised) and middle group (adult-advised) showing a significant effect of advice only at this point, and the conforming oldest group of teenagers (peer and adult advised) showing the strongest significant effect when the stimulus is ambiguous. This follows with predictions from other research that suggest people are most likely to show an effect of social information in situations where stimulus information is ambiguous (Hamm & Hoving, 1969).

The most significant behavioural result is the conformity observed exclusively in the oldest age group, which extends beyond ambiguous stimuli and into those that are non-ambiguous, regardless of advisor type. Combined with the drift diffusion results, this compellingly suggests that the oldest age group may have been perceptually biased by social information. It is worth noting that the age at which we detect significant conformity (12-14 years) in this dataset tends to be greater than other papers studying social influence across development - Allen et al (1972) found that social influence had a decreasing effect between the age of 8 and 12 years, Cohen et al (1973) found greatest conformity under the age of 11 years, while Hamm & Hoving (1969) found the greatest effect starting from age 10 years. However, Strassberg & Wiggen (1972)

found that conformity increased between ages 11 and 13 years in an Asch-type task. The common thread shared by all of these studies is that their tasks are based on normative social influence, or peer pressure, the effect of which can be substantially changed by the environment, the nature of giving a response, and group composition (Asch, 1955; Asch, 1956; Cohen et al, 1973; Aronson et al, 2013), which could account for the variety of results.

The stimuli used are also often unambiguous in nature. Research indicates that normative conformity to unambiguous stimuli decreases between the ages of 3 and 10 (Hamm & Hoving, 1969; Bishop & Beckman, 1971) while across the same period conformity to ambiguous stimuli increases (Hamm & Hoving, 1969; Isoe et al, 1963). The data presented here explore informational social influence provided by one confederate about a series of ambiguous and unambiguous stimuli, in which there was little pressure to conform to the advice given. In a normative task, we might expect behavioural conformity to occur at a slightly younger age, with a general increase in conformity (most pronounced at the ambiguous level) starting in the middle age group of 9-11 years. Our result of greater conformity in the oldest age group (12-14) but not the younger two suggests that informational social influence may work by a slightly different mechanism, and become more prominent later in development. This could be due to the increasing levels of independence that come with adolescence - at which point it could become less important to simply conform regardless of internal thought processes, and more important to integrate confederate information into the decision-making process.

Previous research has tended to focus on the level of conformity to the information, and has not shown the contrarian response we observe in several groups. This may be due to the preference for investigating normative (peer pressure) rather than

informational (socially-given advice) social influence - of which I was testing only the latter. One potential explanation for the contrarian behaviour could be taken from Sally & Hill (2006), who showed that children under the age of 10 were less likely to co-operate with their peers. This effect might be seen in the youngest age groups, who show a stronger contrarian response when advised by a peer than an adult. However, it does not explain the middle adult-advised group, who show a much stronger contrarian effect than the peer-advised equivalent age group (who had a non-significant trend towards contrarian responses at the ambiguous stimulus level). That said, statistically, many of these effects and differences are weak. This may or may not be a part of the developmental process of integrating social advice; as children approach the age of 11, they enter a transitional stage in their education (from primary to secondary school). It may well be that while the role of their peer group remains the same at this age, the role of their teachers and other adults changes. Children are encouraged to become more independent, taking control of their school journey, homework, and chores around the house. This could result in an inclination towards both assertiveness and questioning authority - at least when information is unclear.

2.4.2 The effect of advisor type on behavioural response to social advice

As might be expected, the age of the advisor relative to participant appears to have an effect on the degree of conformity to advice. The oldest group conformed significantly more when advised by an adult than a peer, in line with results found by Knoll & Blakemore (2015) who found that older adolescents preferentially conform to adult rather than 'teen' advisors. Young adolescents were found to prefer the 'teen' advisors

- which could account for the greater levels of contrarian responses seen in the middle age group when advised by adults on ambiguous stimuli. However, the youngest age group of our study displayed slightly less of a contrarian response to adult advisors, suggesting that they might have preferred adult to peer advice. This is also supported by Knoll & Blakemore, who showed that all age groups other than young adolescents preferred adult advice to that of teenagers.

Starting bound data suggest that any bias related to social advice for the younger two groups may have been due to judgmental bias, with a greater effect for adult advisors, as starting bounds tended to deviate to a greater extent from the midpoint than when they were advised by peers. This, coupled with the behavioural data, might suggest that the middle and younger groups were treating advisors as providing information distinct in nature from the perceptual task information, and were perhaps intentionally choosing whether or not to follow advice - potentially prior to even seeing the stimulus. For the oldest group, starting bounds did not significantly change with advice in both peer and adult-advised groups - underscoring that perceptual bias was likely the underlying cause of any conforming behaviour in both cases. In both peer and adult advised groups, drift rates followed the same trend: greater perceptual bias with increasing age regardless of advisor, though more emphasised when the advisor is an adult.

2.4.3 The transition from judgmental to perceptual bias

The drift diffusion model renders it possible to make inferences about the underlying cause of behavioural conformity. The way in which participants make decisions appears to change over the developmental range tested. Regardless of advisor, trends for start-

ing bound and drift rate remain consistent between age groups; there is little effect of drift rate for the youngest and middle groups, while there is a highly significant effect for the oldest (Figure 2.8), with drift rates significantly increasing. Similarly, the oldest age group rarely deviates from the midpoint of the starting bound, compounding the evidence that their conforming may be the product of perceptual bias (integrating social information with the sensory stimulus information) - while the younger two groups tend to deviate from the midpoint, suggesting that when their decisions are influenced by that of the advisor, it was the product of judgmental bias ('intentional' behavioural conformity without an effect on sensory perception, as discussed in Edwards et al, 1965; Link & Heath, 1975; Ratcliff & McKoon 2008).

This might suggest that over the course of development, children become genuinely perceptually biased by social information - typically around the age of 12. This may be the product of neural development, potentially forging links between social regions such as the STS and orbito-frontal cortex, or visual perceptual regions of the occipital lobe (as discussed in Chapter 1). Though it may be tempting to suggest that this indicates younger children report sensory observations more reliably than older children (or indeed adults), the starting bound results (Figure 2.7) suggest that when they report in line with social advice, they may at times reach a decision prior to observing the stimulus itself. As such, though they are not perceptually biased by social advice, not every behavioural decision they make is based on their perceptual experience. While it could be that they perceive more accurately, their behavioural report may not be a reliable measure of that experience.

2.4.4 Potential neural mechanisms for the developmental change in conformity

As children develop through adolescence, the connectivity between different brain regions changes, and there are significant steps in brain development (increases in cerebral white matter and CSF between ages 7 and 16, Giedd et al 1999; increases in cortical grey matter and white matter between the ages of 4 and 20, peaking at 12 years old for the frontal and parietal lobes, Sowell et al 2002), often attributed to hormonal factors (Geidd et al, 1999; Sowell et al, 2002). Puberty has been attributed as having a hand in changes in both brain structure and function (Patton & Viner, 2007; Casey et al, 2008; see Blakemore et al 2013 for a review). Changes particularly relevant to this research include the reorganisation of visual cortex (Nunez et al, 2003) and reward-related regions such as the dopaminergic pathways running to prefrontal cortex. These changes happen at around the same time for which I have found evidence of changes in the mechanisms for integrating social information into visual perceptual decisions. Thus, the question is whether we can link changes in neural mechanisms and circuits to these changes in perceptual decision-making under social influence.

Thomas et al (2004) showed using functional magnetic resonance imaging that as age increases (from 7 to 11 years, compared with adults), cortical regions are progressively favoured over subcortical for reaction-time learning tasks. Cortical regions contribute to what we consider as 'higher cognitive functions' - such as the processing of social information (see Amodio & Frith, 2006, for a review of the role of medial frontal cortex; see Allison et al 2000 and Rushworth et al (2013) for a review of the role of the superior temporal sulcus). Mars et al (2013) showed that between the macaque and hu-

man there are similar connectivity relationships around the social cognition-associated temporoparietal cortex, and Rushworth, Mars & Sallet (2013) discussed the association of socially-motivated and influenced behavioural changes with activity changes in these regions. As such increasing reliance on cortical regions in human development could favour the development of networks across these areas that promote the integration of social advice with sensory evidence.

Stevens et al (2009) used resting-state data to examine inter-regional functional connectivity between the ages of 12 and 30 years. They found that mutual connectivity tended to decrease with age, and postulated that this was the product of stronger connections within established networks (while less established networks have their connectivity pruned), with an improvement in inter-network efficiency over time. Serletis et al (2011) have shown that the amount of interconnectivity a neuron has, and its level of isotropy, is linked to greater levels of noise (and vice versa). Though there is not much experimental data available on network efficiency, noise, and behaviour, a recent electrophysiology study by Chen et al (2015) has demonstrated that network aniosotropy improves object encoding in the inferior temporal cortex of the macaque, while noise covariation did not. As such, it could be that in younger age groups, inefficient networks lead to greater intrinsic noise levels. When social advice is provided in conjunction with sensory stimuli evidence, the higher intrinsic noise may make the information overall less salient, and lead younger children to not conform (or indeed contradict the advice) - particularly when sensory information is already ambiguous and noisy. It thus follows that in older children with greater network efficiency, overall noise levels decrease and could cause additional information to appear useful, rather than buried as extra noise around the stimulus. Further to this idea, Sowell et al (2003)

showed that grey matter density in the posterior temporal regions (near to the social network of the superior temporal sulcus (Allison et al, 2000), and posited perceptual area V5/MT) increases from 7 until the age of 30 years, while declining elsewhere - while Olesen et al (2003) demonstrated joint maturation of both white and grey matter in the fronto-parietal networks (also associated with social processing (Xin & Lei, 2015)). This could be indicative of an increase in connectivity between social networks in the brain, and visual areas responsible for perceptual processing.

2.4.5 Conclusions

Overall, it appears that regardless of advisor, children move from not being biased by informational social advice to showing bias in perceptual decisions by social information around the ages of 11 and 12 years. A drift diffusion analysis suggests that this bias in older children might affect sensory processing of visual stimuli, and therefore that perceptual experience might be directly affected by social information. These developmental changes may be the product of network maturation in the posterior temporal and fronto-parietal networks of the brain at this age. These results suggest that older children (and by extension, adults) might genuinely believe that they are providing a correct response when biased by a social informant.

Although this particular research has demonstrated no significant difference between the responses of boys and girls under social influence, other research has found different results. Hamm & Hoving (1969) found that female children between 7 and 13 years of age tended to conform more in a normative situation, as did Carrigan & Julian (1966) for children at the age of 11 years. Furthermore Mock & Tuddenham (1971) showed that female children between the ages of 9 and 11 years showed greater

normative conformity to same-sex peer judgments. That said, for all of these studies the conformity was normative - in this study, the social influence is informational. This could account for the difference - LeFurgy and Woloshin (1969) found no gender difference in conformity for children when the task required the assessment of ambiguous moral judgments, and Dodge & Muench (1969) found no difference in 11 year old children when the task was to make perceptual judgments under social influence. It could be that female children are more susceptible to normative social influence - but not informational social influence. This may be the product of the social norms that encourage female children to be quiet, co-operative and compliant - of which children as young as 3 years are aware (JEO Blakemore, 2003) - which them lead them to normatively conform in public situations.

Chapter 3

The development of social influence on perceptual decisions in children with ASD

3.1 Introduction

"It does not matter what sixty-six percent of people do in any particular situation. All that matters is what you do."

- John Elder Robison, Be Different: Adventures of a Free-Range Aspergian

Over the past couple of decades, the incidence of Autism Spectrum Disorder (ASD) diagnosis has increased dramatically (Filipek et al., 1999), from approximately 0.5 per 1000 to an estimated 2 per 1000 (Newschaffer et al., 2007) people worldwide. In the United States, CDC statistics place its prevalence at 14.7 children per 1000. In spite of ASD representing a wide range of complex neurodevelopmental disorders, with variable origins and symptoms, one of the primary ways in which typically-developing people experience the autism of others is in its typified social and communication impairment (Gray, 1993).

There is no doubt that the social behaviour of autistic children differs from that

of typically-developing - favouring objects rather than people with attention, not responding to being addressed by name, non-reciprocal conversation, and atypical eye contact are all deficits have been associated with the disorder for a long time (Kanner, 1943). Impairments in intellectual capacity are common, and it is estimated that around 26% of autistic people function within 'normal' intellectual parameters (Noeterdaeme & Wriedt, 2010). The divide between 'higher' and 'lower' functioning people with a diagnosis of autism extends towards adaptive capacity for social behaviour - Downs & Smith (2004) showed that high-functioning children with ASD were capable of displaying cooperative social behaviour with other children, and to some extent Theory of Mind (the ability to attribute mental states and beliefs to others). However, they remained impaired in expression of emotions and most socially appropriate behaviour. Happé also observed in a meta-analysis (2005) that children with ASD required a higher verbal ability to pass simple Theory of Mind tasks - in essence, they can use their intellectual abilities to "hack out" solutions. These studies suggest that autism itself (rather than a co-morbid disorder) affects social ability at a fundamental level.

Visual perception is also altered in children with autism. Perhaps most prominently, there is a strong tendency towards local (rather than global) perception of stimuli (Frith et al., 1989; Shah & Frith 1993; Joliffe & Baron-Cohen, 1997). In perceptual terms, this translates to a preference for identifying the individual components of an image, rather than its overall appearance or 'global gestalt'. From this, we might expect that the local components of visual stimuli (such as second order motion - movement defined by contrast, texture, flicker; Sperling, 1988) would be favoured over the global components. It has been suggested that children on the autism spectrum are less able

to recognise biological motion (Blake et al 2003), and have reduced sensitivity to complex motion-texture stimuli relative to typically-developing matched peers. However, they fare better in discriminating second-order motion stimuli (Bertone et al., 2003), most prominently before the age of 6 (Bertone et al., 2008). In addition, in optic flow experiments, children with ASD have been shown to have a higher threshold for detecting motion coherence (Spencer et al., 2000). Further to this, Happé at al (2011) engaged 89 adolescents with ASD in motion coherence, biological motion, and form-from-motion tasks, and found no performance differences when compared to age and IQ matched typical controls. There has been extensive research into the developmental course of motion coherence detection and discrimination in children with ASD between childhood and adolescence - which tends to decrease with age for both ASD and typical groups, though more prominently in those with ASD (Del Viva et al., 2006). It is clear that there is some conflict in the literature as to whether there consistently exist motion processing deficits in autism spectrum disorders.

Both first and second order motion detection have been strongly associated with activity in hMT+ subregion area V5/MT (Smith et al, 1998), while optic flow experiments are associated with hMT+ subregion MST (Smith et al., 2006). Previous experiments with typically-developing participants have demonstrated that the perception of motion coherence is directly related to increased activity within hMT+ and specifically not earlier visual areas (Rees et al., 2000) - though these experiments have not been carried out in children or adults with an ASD diagnosis. As such, these data might suggest that some specific difference in area hMT+ between typically developing and autistic children could have contributed to what may be their differing abilities in motion discrimination.

Such comprehensive research has not been conducted with regards to stereoacuity and 3D perception. A study by Kaplan et al (1999) has suggested that strabismus, which can lead to stereoblindness or otherwise reduced stereoacuity, is more prevalent in autistic populations. It may be that the co-occurence of strabismus with autism is accounts for the varying results of previous research on the abilities of children with ASD to discriminate motion, given the association of stereo discrimination and motion detection within area hMT+; in the macaque, the columnar structures responsible for direction of motion discrimination are directly associated with those responsible for stereodiscrimination (DeAgnelis & Newsome, 1999). As such, it is important to study the development of stereoacuity across development in populations with ASD, particularly given that area hMT+ is also associated with visual perception (Krug et al, 2013).

I conducted the same peer-matched social advice study as the previous chapter for typical development in a group of children with autism diagnoses, in order to investigate the mechanisms underlying the perceptual decisions of autistic children in social situations. I investigated the developmental time course from 6 to 14 years and compared the results directly to those obtained during typical development. The stimuli involved are formed of a combination of 3D stereo and motion, and therefore presented the opportunity to examine the development of 3D perception in children with ASD.

3.2 Methods

All research was conducted in accordance with the British Psychological Society and Society of Research in Child Development guidelines, and ethical permission was gained from the Institute of Education, University of London. Participant's guardians gave informed written consent after obtaining the verbal consent of their child, and were free to leave the study at any time, and procedures were conducted in accordance with the declaration of Helsinki.

3.2.1 Participants

Participants who were tested were children with a prior diagnosis of autism spectrum disorder, aged between 6 and 14 years, divided into 3 groups (6-8 years: n = 12, 2 female, 9-11 years: n = 13, 3 female, 12-14 years: n = 12, 3 female).

Data were collected either at participants' schools, homes, or at a Brain Detectives event organised by the IoE in London. Participants also underwent measures of cognitive (Second Edition Weschler Abbreviated Scale of Intelligence, WASI-II (Weschler, 1999)) and social (Social Communication Questionnaire, SCQ (Rutter, Bailey & Lord, 2003)) abilities. All were tested for normal visual acuity using a Snellen chart (minimum acuity 6/9 with correction), and for stereovision with a random dot stereogram TNO test (minimum threshold 240 seconds of arc). In all cases, the participants had previously received a formal diagnosis of autism.

The participants were matched by age to a typical control group controlled for mean IQ (see Table 3.1 for summary). These control participants were the same as in Experiment 1 of Chapter 2. As we did not observe a gender effect on the behavioural

ASD					Typical			
Age range (years)	**n**	**WASI-II mean**	**SCQ range**	**ADOS range**	**Age range (years)**	**n**	**WASI-II mean**	**SCQ range**
7.2-8.5	9	103.4	14 to 23	5 to 17	6.5-8.6	29	104.1	0 to 12
9.1-11.3	11	109.5	8 to 38	5 to 27	9.2-11.7	15	108.3	2 to 3
12.6-14.4	10	102.3	13 to 31	9 to 12	12.1-14.5	17	105.8	1 to 6

Table 3.1: **ASD and typical control participants included in the analysis**

results in Chapter 2, the group was not controlled for gender.

Prior to the main social experiment, participants engaged in a short stereothreshold experiment without a social stimulus (see Chapter 2 Methods). Establishing a 3D threshold allowed the application of appropriate peri-threshold disparities for the main experiment (those close to threshold and exceeding threshold performance) to obtain a smooth psychometric function, as well as ensuring that the participant understood the task. 22 participants in the typical control group (n = 11 at 6-8 years, n = 6 at 9-11 years, n = 5 at 12-14 years) did not have threshold data collected due to the constraints of the event at which data was collected. Those participants who failed to obtain 85% correct responses at the largest disparity, or showed a bias of more than 80% in either direction for zero disparity stimuli, were excluded from group analyses (3 excluded at 6-8 years, 2 excluded at 9-11 years, 2 excluded at 12-14 years). As such, participants included in the analyses were at 6-8 years: n = 9, (1 female), at 9-11 years: n = 11 (2 female), and at 12-14 years: n = 10, (3 female).

If a participant took longer than 8 seconds to respond on a trial, that trial was excluded from analysis, as this typically indicated a trial in which the participant had ceased to attend the stimulus.

3.2.2 Set-up

The set-up was matched to that discussed in Chapter 2 on typical development.

3.2.3 Stimulus

The stimuli used were matched to those used in Chapter 2 on typical development.

3.2.4 Experimental tasks

The experimental tasks were matched to those used in Chapter 2 on typical development. The sole difference was that every child who participated (rather than a subgroup) took part in the brief control experiment on understanding the left/right instructions prior to the presentation of a threshold stimulus. Pseudorandomly interleaved, they were requested to touch either the left or the right side of the screen (10 times left, 10 times right) with the textual instruction 'Please touch the left/right side of the screen'. This was to establish that they could accurately differentiate between left and right. All children were also asked to demonstrate with their finger to the researcher which direction was 'spinning left', and which direction was 'spinning right', prior to engaging in the experiment.

3.2.5 Analysis

Analysis methods were matched to those discussed in Chapter 2 on typical development.

3.3 Results

I have investigated the effect of social advice of an age-matched peer on perceptual decisions made by children with a diagnosis of autism spectrum disorder, in response to a moving SFM stimulus, across the developmental course from 6 to 14 years of age. As part of this, I examined the development of stereoacuity thresholds over this age range.

3.3.1 Stereoacuity thresholds across child development with autism spectrum disorder

Aside from the importance of assessing stereoacuity for experimental efficacy as laid out in the previous chapter, establishing that the children with ASD are able to accurately see and respond to the experimental stimulus is important. Visual deficits are relatively common in autism, ranging from a lack of eye contact and increase in peripheral glances, to a difficulty in maintaining visual attendance and in integrating central and peripheral visual field information (Townsend et al, 1996; Yoshida et al, 2011). Visual deficits have also been linked to the social impairments apparent in autism: recognition of biological motion is specifically impaired in children with autism (Blake et al 2003), and visual fixation patterns serve as a good predictor of social competence for those diagnosed with autism (Klin et al, 2002). Some have even claimed that ASD social impairments may in fact derive from atypical visual representation in children with autism (Frey et al, 2013), leading to a preference for peripheral visual stimulation rather than central. Given that the visual stimulus used in this study was centrally located, I tested first whether the children with ASD participating in this study could accurately assess 3D

Age Group	ASD	Typical
6 to 8	0.0126° ±STD0.015(n=9)	0.0198° ±STD 0.010(n=18)
9 to 11	0.0156° ±STD0.016(n=11)	0.0163° ±STD 0.016(n=9)
12 to 14	0.0206° ±STD0.015(n=10)	0.0145° ±STD 0.014(n=12)

Table 3.2: **Median Stereoacuity Thresholds for children with ASD and typically developing children**
Thresholds were taken as the standard deviation of a fitted curve to behavioural data collected during the 'threshold' experiment. They are expressed in degrees of visual angle. For typical children, thresholds tend to improve with age, while the reverse trend is seen in the autistic children. The difference in thresholds is significant for the oldest age group (Wilcoxon Rank Sum $p<0.05$, Bonferroni corrected for multiple comparisons). An ANOVA showed no significant effect of age group on threshold within either group (Typical: $p = 0.5951$, $F = 0.5925$, $df = 2$; ASD: $p = 0.3690$, $F = 1.0232$, $df = 2$), and no significant effect of diagnosis on threshold between groups ($p = 0.68837$, $F = 0.243$, $df = 1$).

depth with suitable stereo threshold comparable to the typically-developing group of age-matched children.

The autistic group showed stereo thresholds comparable to their counterpart typically-developing group (Table 3.2, Figure 3.2). There was no significant difference in thresholds for the youngest and middle age groups - though the oldest autistic age group had a significantly higher stereo threshold (Wilcoxon Rank Sum, $p<0.05$, Bonferroni-corrected) it was still within reasonable bounds of 3D performance (Coutant et al, 1993). This corresponds well to previous literature suggesting central visual acuity may degrade with age due to the preferential treatment of peripheral visual information in children with autism (Frey et al, 2013). When divided by age rather than analysis group, there was overall a very mild trend towards decreasing stereoacuity with age for the group with ASD (Figure 3.1, Figure 3.2), though this was not significant. As an additional check on task performance, an N-way ANOVA run on the data shows that disparity has a significant effect on response (Table 4, $p<0.0001$) for all ages regardless of autism diagnosis.

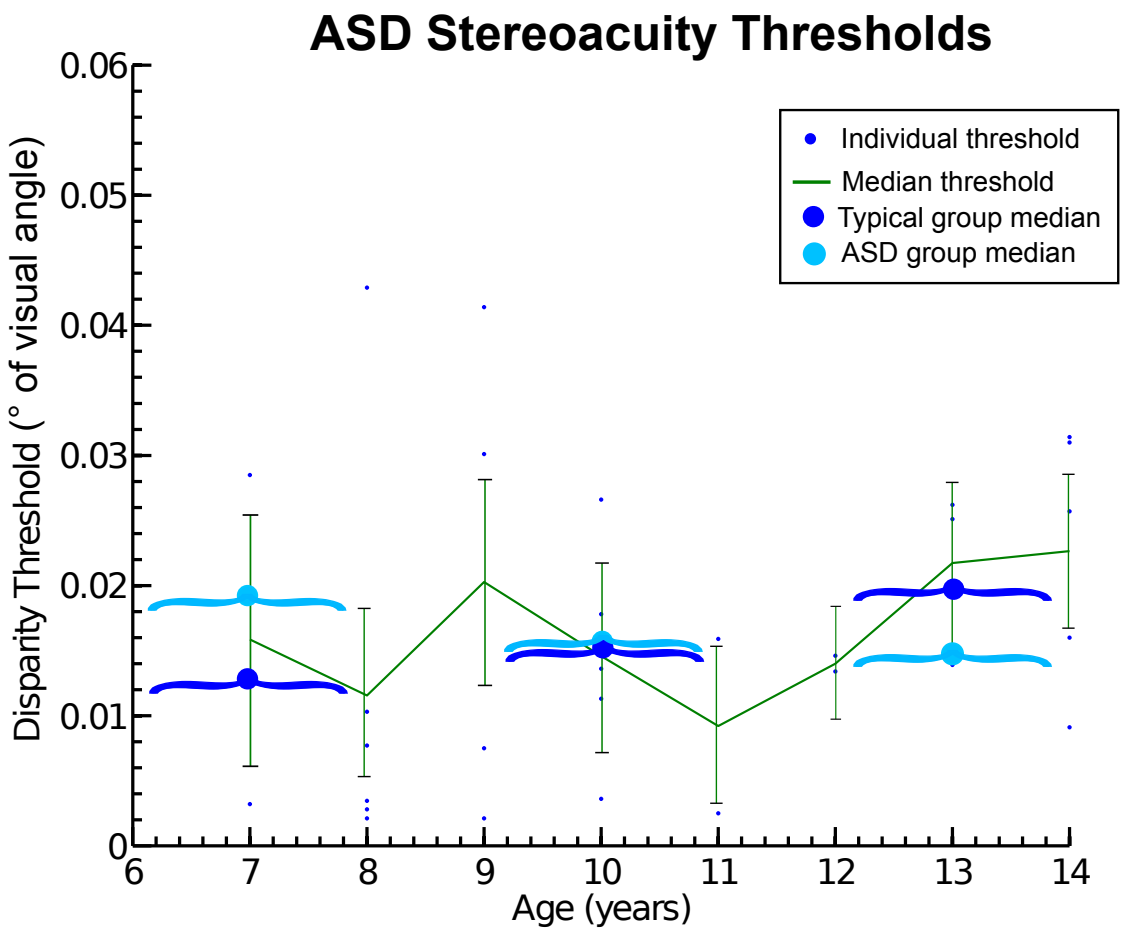

Figure 3.1: **Stereoacuity Thresholds between 6 and 14 years for children with ASD**

Median stereoacuity values at each age are show in green. Error bars show confidence intervals. There is no significant change in stereoacuity between the ages 6 and 14 years. The light circles indicate median stereoacuity values for the typical groups, while the dark blue circles indicate median stereoacuity values for the ASD groups. Brackets indicate the ages included within a group (6-8, 9-11, 12-14 years). These are shown separately in Figure 3.2.

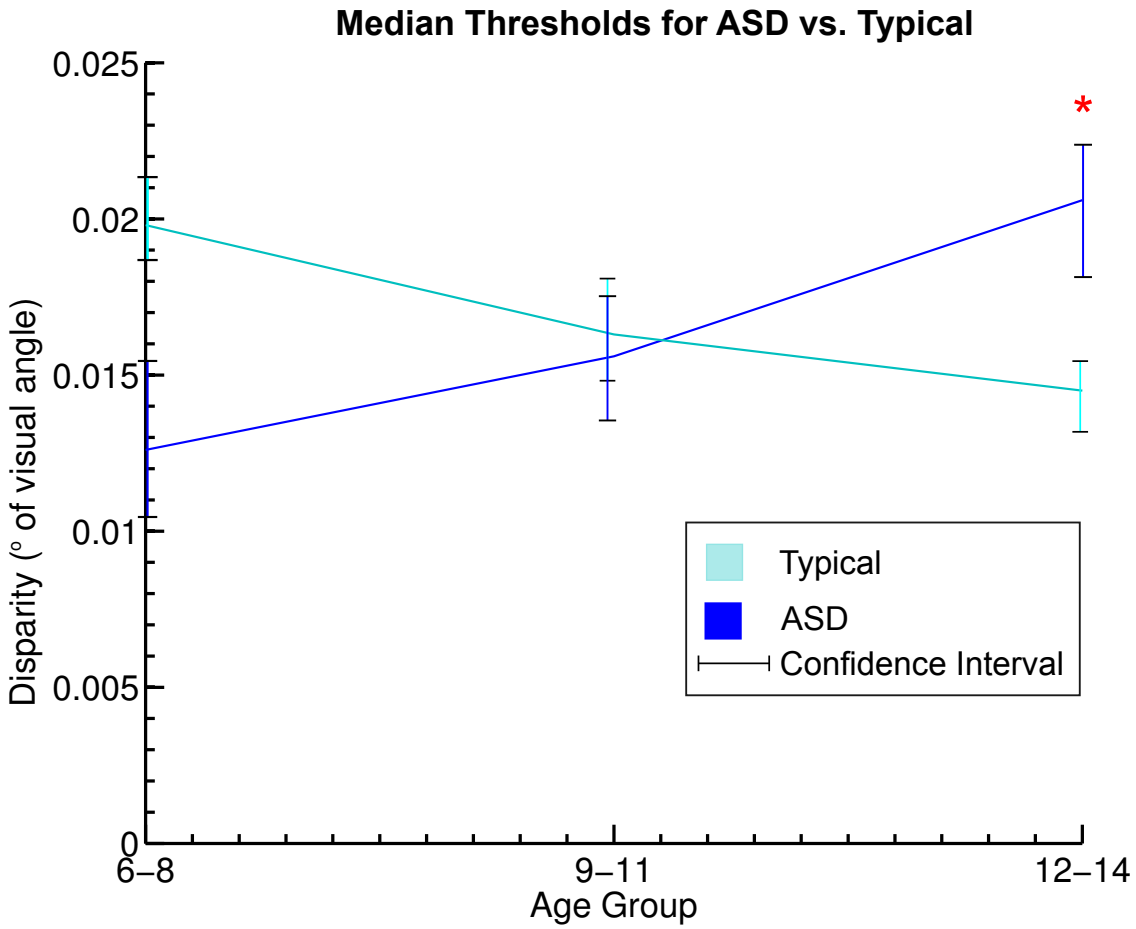

Figure 3.2: **Median Stereoacuity Thresholds for ASD and typically developing children**

Data from Table 3.2 presented in graph form. The dark blue line indicates autistic children, the pale blue line typically-developing children. The error bars indicate confidence intervals. A red asterisk indicates a significant difference between groups (Wilcoxon Rank Sum, $p < 0.05$, Bonferroni corrected).

Given that all mean stereo thresholds fell within reasonable bounds of visual performance, there is no reason to think that any results are the product of one group having a visual deficit, or lower overall performance. Only participants with adequate 3D performance were included (see Methods). Equivalent task difficulty was ensured by matching stimuli to individual thresholds: participants who displayed lower stereoacuity viewed proportionally larger disparities than those who showed greater stereoacuity.

3.3.2 The effect of social advice from a peer on perceptual judgments in ASD

I tested the effect of informational social advice from one age-matched peer advisor on the behavioural responses of children with ASD, and compared them with age and IQ-matched groups of typically developing children when viewing the same stimulus. Three age groups were compared - 6-8, 9-11, and 12-14 years of age.

One of the primary diagnostic criteria of ASD is impairment in social interaction and communication. As such, we might expect children with ASD to entirely disregard social advice in favour of accurate perceptual interpretation. In contrast to the results from typical controls, we see a weak but consistent bias in the direction of advice in all age groups (Figure 3.3).

The overall perceptual judgments of the two youngest age groups with ASD (6-8 and 9-11 years old) showed a small bias in line with social advice, unlike the typically-developing equivalent age groups. When data were split by 'left' and 'right' advice, and fitted cumulative Gaussian functions, the data were better fit with two functions that were allowed to vary by their mean than a single function (6-8 years old: adjusted r-square = 0.9998 versus 0.821, $p < 0.05$, $n = 9$; 9-11 years old: adjusted r-square =

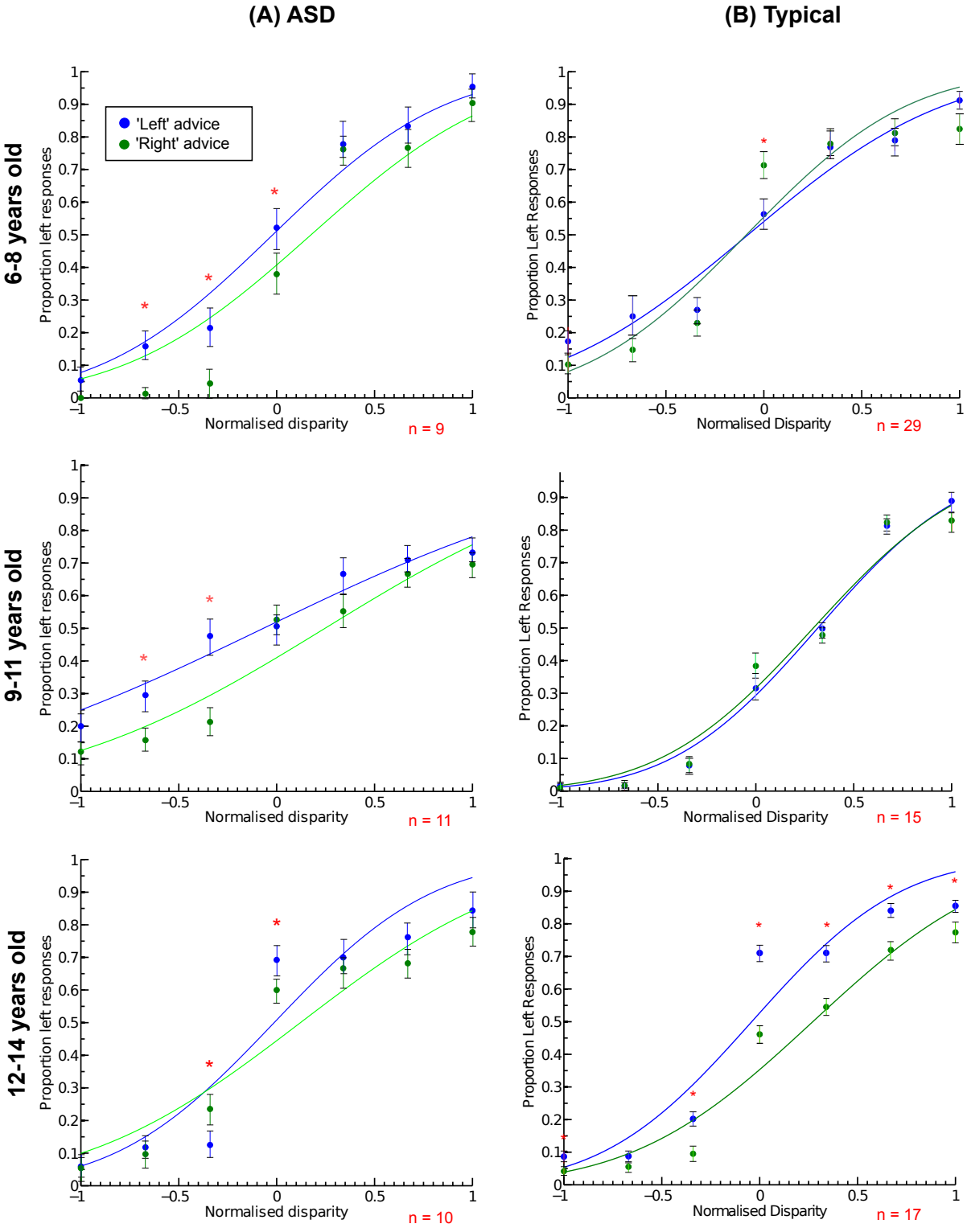

Figure 3.3: **The effect of social advice on perceptual decisions**

A. Responses from children with ASD, divided by age group. Average behavioural responses to stimuli of differing binocular disparity were fitted with cumulative Gaussians, separately for advice 'left' (blue) and advice 'right' (green). Error bars = standard error of the mean (SEM). * indicates significant difference between responses for 'left' versus 'right' advice (Wilcoxon Rank Sum, $p<0.05$, Bonferroni corrected). B. Behavioural responses from typically developing children. Same convention as A.The social bias effect demonstrated by the oldest typical children is not present in the oldest autistic children. However, the youngest children with ASD show a weak influence of social advice, unlike the youngest typical children.

0.980 versus 0.832, p = 0.05, n= 11). This suggests that children with ASD in these age groups were slightly biased by social advice in the direction advised - a pattern not seen in equivalent age groups of typical children (see Chapter 2 for more detail). However, the oldest age group with ASD (12-14 years) showed no bias in the direction of social advice. Unlike the oldest typical group, and the younger two groups with ASD, the psychometric data were as well fitted with one function as with two functions that were allowed to vary by their mean (adjusted r-square = 0.9994 versus 0.9998, p = 0.9904, n= 10).

When the effect of advice at each binocular disparity was tested separately, the youngest children with a diagnosis of autism showed responses that significantly diverge in favour of social advice when the stimulus was ambiguous, and for two of the negative disparities (Wilcoxon Rank Sum, $p<0.0001$, Figure 3.3A, top). An N-way ANOVA also showed an overall significant effect of advice on behavioural response (Table 3.3, p = 0.0025). Though the N-way ANOVA also showed a significant effect of advice on the equivalent typical 6-8 year old group, this was likely driven by the contrarian response observed when the stimulus was ambiguous (Figure 3.3B, top), rather than the weak conform shown by the youngest group with ASD. Similar to the youngest ASD age group, the responses of middle group of children with ASD diverged significantly in favour of social advice for two negative disparities (Figure 3.3A, middle, $p<0.0001$), though not at the ambiguous level. This effect was strong enough to drive a significant effect of advice on behavioural response under an N-way ANOVA (Table 3.3, p = 0.0021), an effect not seen in the equivalent typical 9-11 year old group. Although the data were better fit with one function than two split by advice, the oldest group with ASD (12-14 years) showed a significant divergence of behaviour in favour of social advice

at the ambiguous disparity (Figure 3.3A, bottom, Wilcoxon Rank Sum, $p<0.005$), and a significant affect against advice at one negative disparity (Wilcoxon Rank Sum, $p<0.0001$). However, the N-way ANOVA showed no significant effect of advice on behavioural response at this age (Table 3.3, $p = 0.627$). This again contrasts with the 12-14 year old typical group, who did show a significant effect of advice on behavioural response.

A potential explanation for the weak effect advice had on behavioural response for the younger ASD groups is that the social information introduced a confusing element for these children. Some children in the younger two ASD groups verbally responded to the social advisor with a range of commentary - from suggesting that they were deliberately attempting to confuse the participant ('Oh no! They tricked me again!', 'Are they trying to trick me?', 'They are being very confusing.') to questioning the reliability of the advisor ('They aren't very good at this.', 'It's just as well I'm here to help them out!', 'The spaceship would have crashed if it was just them driving'). This is in contrast to the oldest ASD group, who did not offer any verbal response to the advisor. It may be that the younger two ASD groups were more attentive to the social stimulus.

The data suggest a divergence in the effect of social advice from a peer as children with ASD reach adolescence. Overall, in the ASD group, a weak susceptibility to social advice in younger children disappears with age (Figure 3.3A, Table 3.3), while in typically-developing children a strong bias due to social advice develops in the oldest group (Figure 3.3B).

	ASD							
	Advice		**Disparity**		**Interaction**	**Age Group**		
	F-value	p-value	F-value	p-value	p-value	F-value	p=value	df
6 to 8	9.21	0.0025*	123.68	<0.0001*	0.0017*	65.1	0.031*	2
9 to 11	9.5	0.0021*	29.6	<0.0001*	0.0566			
12 to 14	0.24	0.627	28.32	<0.0001*	0.0061*			
	Typical							
	Advice		**Disparity**		**Interaction**	**Age Group**		
	F-value	p-value	F-value	p-value	p-value	F-value	p=value	df
6 to 8	72.92	0.02528*	96.61	<0.0001*	0.0193*	291.54	<0.0005*	2
9 to 11	0.03	0.8713	491.43	<0.0001*	0.0327*			
12 to 14	240.32	<0.0007*	560.13	<0.0001*	0.0724			

Table 3.3: **N-way ANOVA results for effect of advice, disparity, and age group on overall response for autistic and typically-developing children** An asterisk indicates a significant p-value (<0.05). For the groups with ASD, advice had a significant effect on the choices of the younger two age groups, but was non-significant for the oldest group. For the typically-developing group, advice had a significant effect on the youngest group, although the direction of influence was reversed, and a large significant effect on the oldest group in the direction of advice. In all cases, disparity has a significant effect on response, indicating that participants were appropriately responding to the task. Interaction effects between advice and disparity are due to the differential effects of advice at different disparities (such as a strong effect at the ambiguous level in the oldest typical group). Age group also clearly had a significant effect on responses, as can be seen in the psychometric functions of the behavioural data.

3.3.3 The effect of social advice on accuracy of response

At no point in any ASD group is there a significant difference between the effect of correct and incorrect advice (Wilcoxon Rank Sum p >0.2, Bonferroni-corrected, Figure 3.4A), though there is a very slight trend towards improved accuracy as a product of correct advice in the youngest ASD age group (Figure 3.4A), which contrasts with the slight opposite trend found in the equivalent age typical group (Figure 3.4B). In the oldest group with ASD, there is very little difference in accuracy whether advice is correct or incorrect, whereas the oldest typical group shows a strong significant effect of decreased accuracy when advice is incorrect (Figure 3.4B).

These results could support the conjectures from the psychometric functions that social advice becomes less influential during development in the group with ASD, as there is a trend (though not significant) for the effect of advice on accuracy to decrease with age. This contrasts with an increasingly significant effect of advice on accuracy with age in the typically-developing groups.

3.3.4 Social Advice and Reaction Times

When advice and sensory information are in conflict, we would expect it to take longer to reach a perceptual decision (provided that the information is taken into account).The typically developing age groups all took significantly longer to respond when conforming to incorrect social advice (Figure 3.5B). However, the children with a diagnosis of ASD show no such pattern at any age tested (Figure 3.5A). In all cases was there no significant difference between reaction times when conforming correctly versus incorrectly (Wilcoxon Rank Sum, p =0.704/0.341/0.194 respectively). The youngest group with ASD appear faster than their equivalent typical peers, while the older two age

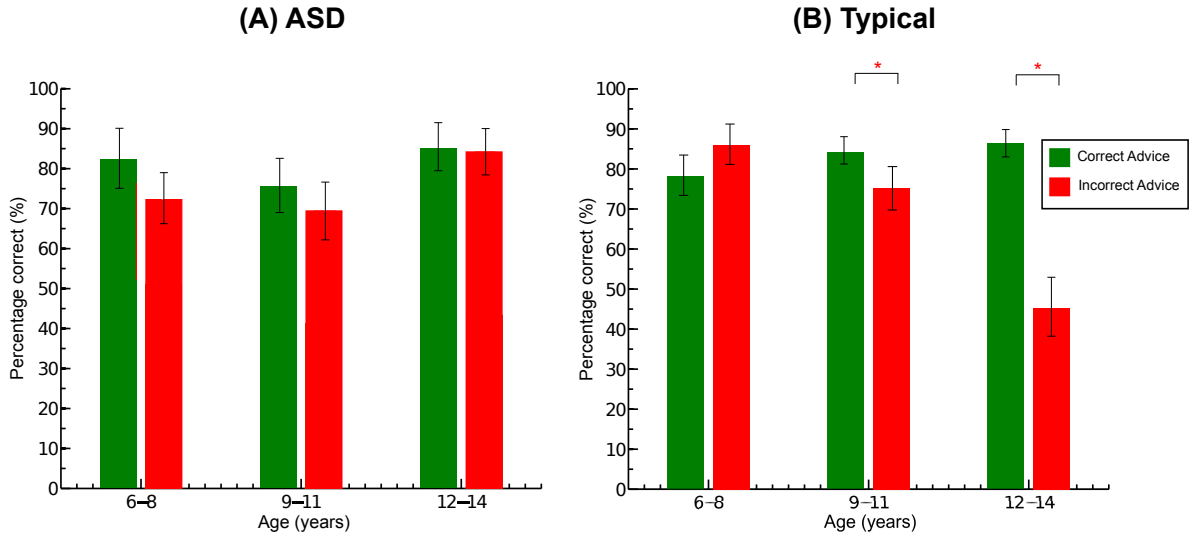

Figure 3.4: **Percentage correct responses when advice was correct or incorrect, for autistic and typical children, divided by age group**
Unlike the typical group, in the group with an autism diagnosis, there is no significant improvement in accuracy when advice is correct for any age group. An ANOVA across groups indicated that age group had a significant effect on percentage correct for the typically developing children ($p = 0.025$, $F = 70.45$, $df = 2$), as did diagnosis between groups ($p = 0.031$, $F = 64.56$, $df = 1$). Red asterisks indicate a significant difference between correct and incorrect advice within age groups (Wilcoxon Rank Sum, $p < 0.05$, Bonferroni-corrected). Error bars show confidence limits.

groups of children with ASD took slightly longer than the equivalent typical groups to respond, and there was no trend for an decrease in reaction time with age (as observed in the typical group). Given that the age groups all had similar mean IQs, it seems unlikely that this was an artefact of requiring more time to complete the task.

An N-way ANOVA, with the factors of age, incorrect/correct advice, and autism diagnosis, was conducted on the data. For the ASD group, age was not a significant factor in reaction time ($p=0.773$), while it was for the typical group ($p<0.01$). Likewise, advice had no significant effect on reaction times in the ASD group ($p=0.519$), while it did for the typical group ($p<0.01$). ASD diagnosis had a significant effect on reaction times between typical and ASD groups at all ages ($p<0.05$). This suggests that while the reaction times of typically developing children significantly improved over time,

those of children with ASD remained more consistent. Advice accuracy also did not significantly affect reaction times for children with ASD, which supports the idea that they may have attended to social information less than their typically developing peers. Error rate, regardless of advice, did not have a significant effect on reaction time, though there was a trend for correct responses to be faster in the group with ASD (median RT for the ASD group of 1.877 versus 2.133, $p = 0.1$, Wilcoxon Rank Sum), and a weaker trend in the same direction for the typical group (median RT for the typical group of 2.003 versus 2.199s, $p = 0.314$, Wilcoxon Rank Sum. This suggests that any reaction time differences seen were at least partly the product of social advice, rather than error rate.

This result suggests that the autistic children may not incorporate the social advice into their perceptual decision, and confirms the result from the Gaussian fit to the behavioural data at the oldest age group with an ASD diagnosis.

3.3.5 Modelling behavioural responses under social advice with the drift diffusion model

As in Chapter 2, I fit a drift diffusion model (DMAT Toolbox, Vandekerckhove & Tuerlinckx (2007, 2008); based on Ratcliff & McKoon (2002, 2008)) to the reaction times and choices from the behavioural data in order to make inferences about the underlying decision processes at work. Drift rate ('v) and starting bound ('z') are two parameters fitted in the model that can provide insight into perceptual and judgmental bias, with a shift in drift rate between conditions suggesting a perceptual bias, while a shift in starting bound from the midpoint between two decisions indicates a judgmental bias.

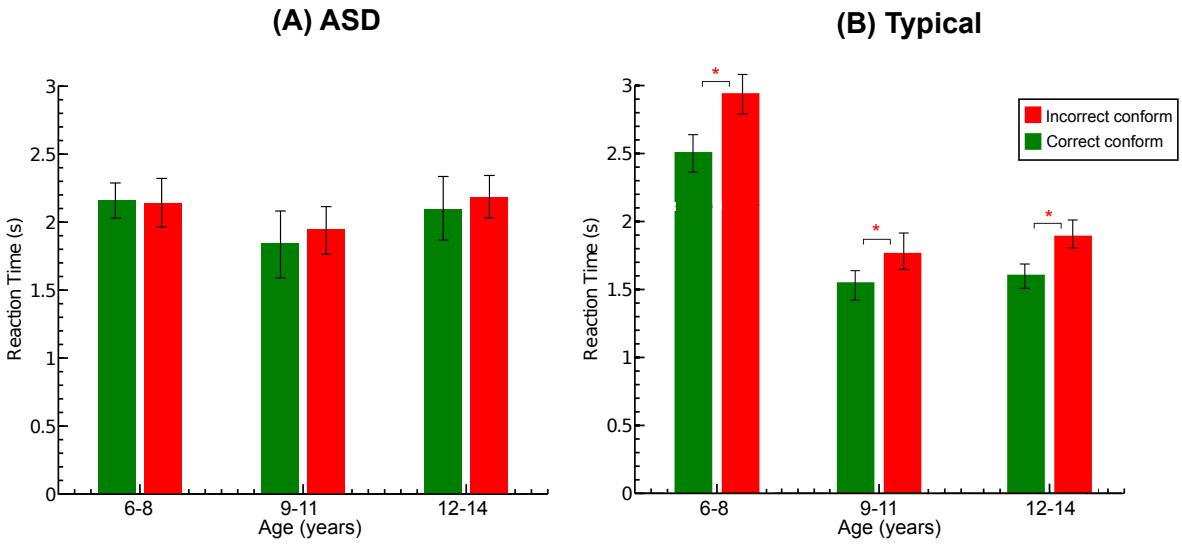

Figure 3.5: **Reaction times when conforming correctly and incorrectly with social advice, for children with ASD and typical children, divided by age group**

For children with ASD, there was no significant difference in reaction time for correct and incorrect conforms. For typical children, incorrect conforms always have a significantly longer reaction time (Wilcoxon Rank Sum, $p < 0.05$ Bonferroni corrected). An ANOVA across groups indicated that age group had a significant effect response for typically developing children ($p = 0.005$, $F = 153.76$, $df = 2$), as did diagnosis between groups ($p = 0.05$, $F = 53.70$, $df = 1$). Red asterisks indicate a significant difference between correctly and incorrectly conforming within age groups. Error bars show confidence limits.

Following the methods of Chapter 2, I first tested for a significant effect of both these parameters using a comparison of BIC values across models where different parameters were allowed to vary (see Methods in Chapter 2 for more detail). A lower BIC indicates that the model provides a better fit. All models allowed parameters to vary with disparity. The model allowing only starting bound and drift rate to vary with advice conditions (Model 4, Table 3.4) provided the best fit. As such, this model was used to test for parameter values under different conditions. Wilcoxon Rank Sum statistical tests were then applied to determine significant differences in drift rate or starting bound between conditions.

Interestingly, the second best fitting model for all autistic age groups was Model 2, which allowed all parameters to vary with advice conditions other than drift rate. This matches results for the two younger typically-developing groups, who also showed no evidence of behavioural conformity or perceptual bias under the drift diffusion model (see Chapter 2 Results for a more in-depth discussion). The oldest typical group, who did show evidence for behavioural conformity and perceptual bias, had a worse fit using this model, and a second best fit with Model 3, which allowed all parameters to vary other than starting bound with advice (Table 3.4). This suggests that starting bound was a more important factor than drift rate in decisions made by all the children with ASD.

For all 3 autistic age groups, starting bound values significantly deviated from the mid-point between the two decisions (0.5), regardless of whether they conformed to the social advice or not (Figure 3.6A); the direction of deviation was always in the direction of advice provided. In contrast, for the youngest two typically developing age groups, the starting bound was more weakly (though still significantly) deviated from

Model	6-8 (1)	9-11 (1)	12-14 (1)	6-8 (2)	9-11 (2)	12-14 (2)
1 (no effects)	12093.95	11452.89	11946.77	12238.33	13481.52	12485.31
2 (no v)	4411.13*	3948.38*	4194.82*	3534.5*	4258.14*	7841.21
3 (no z)	8474.41	7819.93	8733.9	6131.11	6927.81	4291.11*
4 (only v and z)	*2983.84*	*2751.88*	*3145.11*	*2984.53*	*3148.14*	*2918.18*
5 (unrestricted)	10938.52	10088.03	10947.82	11172.03	10029.23	10991.1

Table 3.4: **BIC values for age groups with ASD, and typically developing groups**

'1' denotes the group with ASD, '2' the typically-developing control group. 'v' = drift rate, 'z' = starting bound. A lower BIC value indicates a better fit. For model 1, no parameter was allowed to vary with advice condition. For models 2 and 3, either 'v' or 'z' were not allowed to vary. For model 4, only 'v' and 'z' were allowed to vary, while other parameters were not. Model 5 was unrestricted. For all groups, model 4 showed the best fit (red italicised text). Notably, the second best fit model (indicated by an asterisk) for all ASD groups was given when drift rate was restricted (Model 2). This model also gave the best fit for the two younger typically-developing groups, while for the oldest age group the second best fit was given by model 3, when starting bound was restricted.

the midpoint, when they were non-conforming (Figure 3.6B). For the oldest typically-developing group, who showed the most conformity in behaviour, the starting bound never significantly deviated from the midpoint. While the pattern of starting bound biases disappeared with age for the typically developing group, it remained consistent across autistic age groups. Such changes in the starting bound (with the direction of social advice) suggest a judgmental bias at the level of sensorimotor rather than sensory processing.

When the drift diffusion model allowed drift rate to vary in an unrestricted manner with stimulus disparity (the strength of rotation either left (positive disparity) or right (negative disparity)), drift rate was found to have a clear relationship with stimulus disparity. This was such that a positive disparity resulted in a positive drift rate estimate, and vice versa, across all age groups and diagnoses. When split by advice (Figure 3.7), there was no significant divergence of drift rate in the direction of advice given for any age group with ASD. This is in contrast to the typically-developing oldest

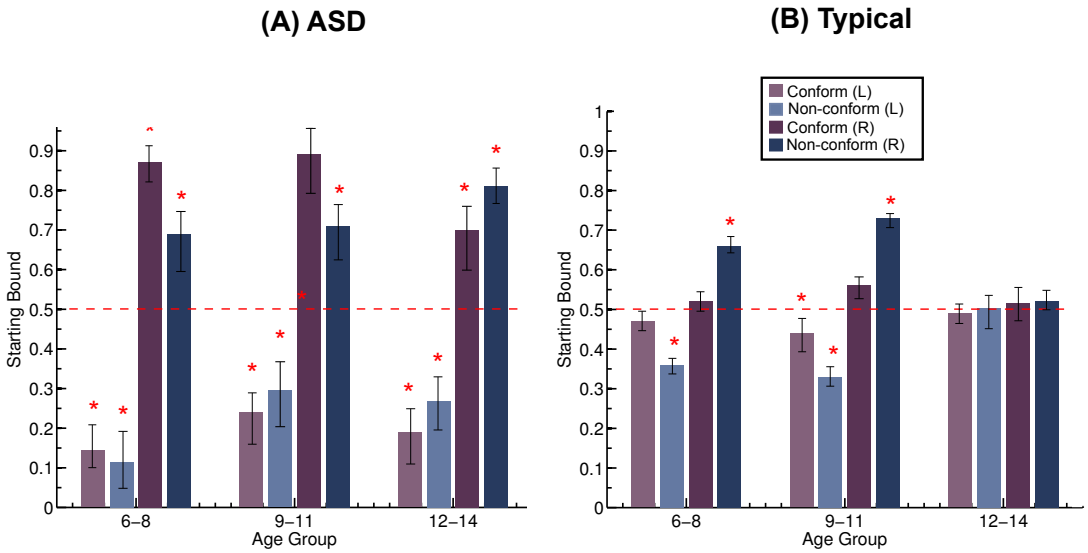

Figure 3.6: **Starting Bounds for children with ASD and typical children, divided by direction of advice and age group**

* indicates that the starting bound deviates significantly from 0.5 midpoint between the two decision bounds (Wilcoxon Rank Sum, $p<0.05$, Bonferroni corrected). '0' represents the 'left' decision bound, and 1 represents the 'right' decision bound. Error bars show confidence limits. A significant deviation from 0.5 suggests a directional effect of judgmental bias. For the oldest typical children, starting bound for the diffusion modelling did not deviate much from the mid-point across conformity condition. This suggests little influence of judgmental bias on the perceptual decision. In contrast, for the oldest autistic group (and indeed all age groups for autistic children), the starting bound shifts consistently in the direction of response given, indicating strong judgmental rather than perceptual bias when advice was considered.

group, who show some effect on drift rate in favour of advice direction. This supports the idea that decisions made by the group with ASD were not driven by changes in drift rate, and as such were unlikely to be the product of perceptual bias.

For the typically-developing groups, the best fitting model required a change in drift rate for the oldest age group - with drift rate increasing both in the direction of advice, and with conformity (Figure 3.8). This suggests that in adolescence, typically-developing children integrate social advice with sensory information to make a perceptual decision. However, the children with a diagnosis of ASD showed no significant change in drift rate when it was allowed to vary (Table 3.4) with advice or conformity. Notably, a model allowing only starting bound and not drift rate to vary showed a better fit to the data than one allowing only drift rate to vary (Table 3.4). Furthermore, their drift rates were more comparable to those of a typically-developing child between the ages of 6 and 11 years (Figure 3.8B). As such, it follows that drift rate was not an important parameter in determining behavioural response for children with ASD.

An N-way ANOVA was conducted on the drift rate data, with age and condition as factors. Neither age nor condition had a significant effect on drift rate for the ASD group ($p > 0.2$ in all cases). Similarly, for the youngest two typical groups, condition did not have a significant effect on drift rate ($p > 0.2$ in all cases) - though it did for the oldest typical group ($p < 0.05$). Age also had a significant effect on drift rate ($p < 0.01$), driven by the significant drift rates seen in the oldest typical group. This further supports the idea that drift rate was not a significant factor in the decision-making process under social conditions for children with ASD, but was for the oldest typically developing group. This suggests that children with ASD (and the youngest two typically-developing groups) were not perceptually biased by social information.

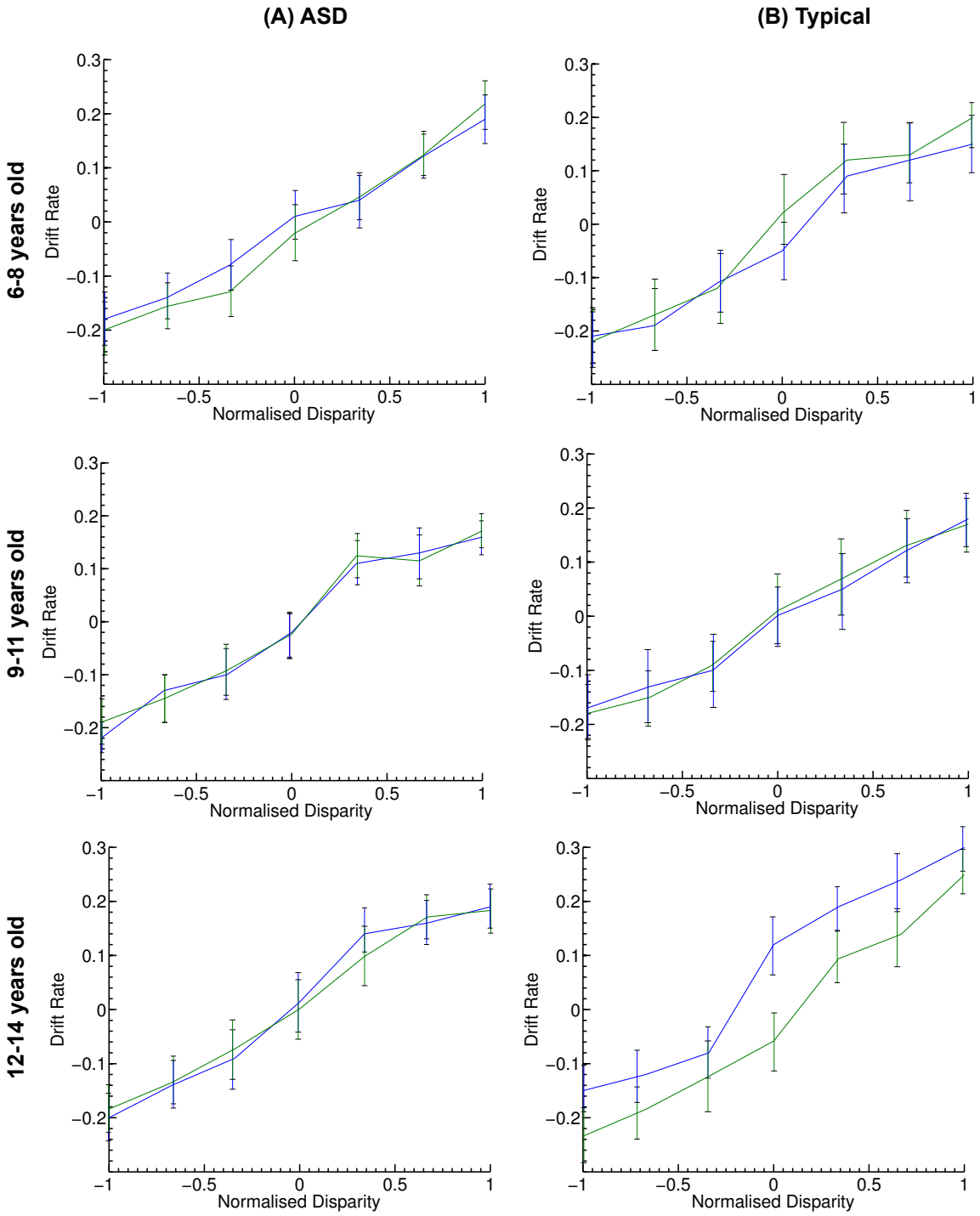

Figure 3.7: **Drift rate estimates plotted against stimulus disparity, split by advice type**

The green lines indicate parameter estimates when advice was 'right', the blue when advice was 'left'. The 'left' decision bound was positive, while the 'right' decision bound was negative. As such, a positive drift rate indicates drift in the leftward direction. (A) shows responses from the ASD group, (B) shows responses from the typically-developing group. Rows show responses by age group. Drift rate estimates vary in the direction of stimulus disparity, showing sensory processing of the stimulus, with the oldest typical age group showing deviation of drift rates in the direction of advice. Error bars show confidence intervals.

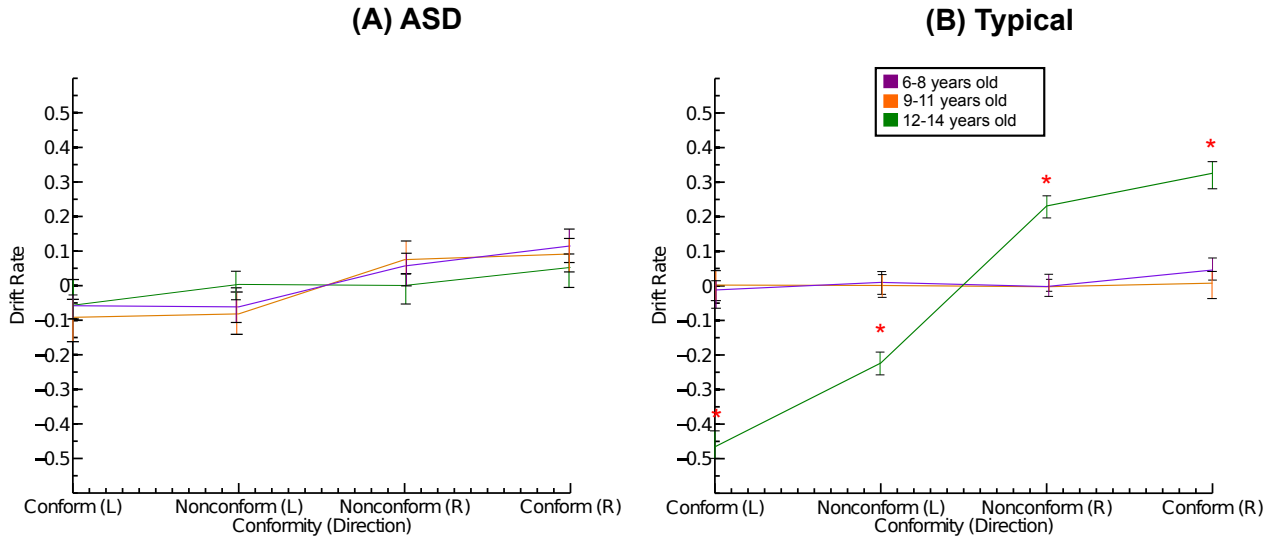

Figure 3.8: **Drift rates with advice for children with ASD and typical children, divided by age group**

The purple line represents 6-8 year olds, the orange 9-11 year olds, and the green 12-14 year olds. * indicates a significant difference of the data point from the data point of the other two groups. Error bars show confidence intervals. The oldest age groups for both typical participants demonstrate a drift rate that follows the direction of response given (Wilcoxon Rank Sum, $p<0.001$, Bonferroni-corrected). Drift rates do not significantly differ between autistic age groups, nor significantly follow the direction of the decision made.

3.3.6 Summary

Overall, behavioural results, and those from the drift diffusion model, suggest that the fundamental process of decision-making under social influence did not change for children with ASD between the ages of 6 and 14 years. This contrasts with a clear developmental change for typically developing children across the same developmental range. That starting bound and drift rate data show similar results for children with autism overall, and typical children between the ages of 6 and 11 years, suggests an underlying developmental difference with an onset approximating adolescence.

Although they have shown they are capable of understanding and performing the task without social advice (Table 3.2), it is clear from behavioural data, reaction times, and the drift diffusion model, that the changes in the development of decision-making

under social influence seen from 6 to 14 years in typically developing children are not present in children with ASD. The weak evidence for behavioural conformity (Figure 3.2, Table 3.3) disappears for the oldest age group with ASD, and the accuracy of the social advice had no significant effects on reaction time or participant accuracy at any age. Further to this, results from the drift diffusion model suggest that starting bound, rather than drift rate, was the more salient parameter in explaining behavioural responses (Table 3.4, Figure 3.4, 3.5), indicating that judgmental rather than perceptual bias is a better explanatory factor of any conforming behaviour present in the children with ASD.

3.4 Discussion

Previous research has suggested that both children and adults with ASD do not attend to socially salient aspects of visual information (Klin et al, 1991; Riby & Hancock, 2008), and are not responsive to notions of reputation (Izuma et al, 2011) or flattery (Chevallier et al 2012). From this, one would predict that social advice from a peer would have little effect on a visual task for people with ASD, regardless of age. This is not what was observed in this study - the youngest groups with ASD showed some behavioural conformity in line with advice, with the effect disappearing in the oldest group. A typical comparison group show the opposite effect, with little behavioural effect of social advice for the youngest groups, and a strong bias in the oldest. Computational modelling on the behavioural data suggests that there is a different underlying mechanism for this change in conformity between the two groups.

3.4.1 The effect of age on social conformity in children with ASD

The effect of age on behavioural responses to social advice was less apparent in the ASD group than in the typically developing group. The youngest two age groups showed some weakly conforming behaviour in line with social advice, but this effect disappeared in the oldest group - the opposite to what happened across development in the typically developing groups. The most significant difference between autistic age groups comes from the N-way ANOVA - which shows that advice has a significant effect on the ASD group responses from the age of 6 to 11 years, and ceases to be significant in the oldest group (the point at which it becomes significant for typically developing children). This could suggest that on certain trials, the younger children with ASD were choosing to conform to social information - supported by the starting bound data suggesting judgmental rather than perceptual bias. This could be explained by the onset interventionist treatment; by the age of 9, children who have been formally diagnosed with autism usually have begun treatments to facilitate social integration (Kasari et al, 2012) in common interaction situations. The youngest two age groups may therefore have recently been exposed to treatment suggesting that they co-operate in social situations, and attend to what other peers say. As such, it may be that the youngest children say the same as others simply because it is a general rule that they have been taught to follow. However, without a detailed background on the treatment (or otherwise) of the children with ASD involved in this study, it is hard to empirically support this conclusion.

There is very little previous research specifically on social conformity in children

with ASD, but a normative social influence study showed that children with ASD between the ages of 9 and 11 years conformed less in an Asch paradigm than their typically developing peers (Yafai et al, 2013). The behavioural data from this informational social influence study do not support that result, as the typically developing 9-11 year old group showed no effect of social advice on behaviour, while the equivalent children with ASD showed a small effect in the direction of social advice. This suggests that informational social influence may affect children with ASD in a different manner to normative social influence. It is possible that the youngest two age groups did not consider the social stimulus to be 'social'. As informational social influence acts as an additional piece of sensory information, while normative influence acts as a pressure to conform, it could be that the latter has no effect on behaviour, while the former is considered as additional information outside the bounds of a social context. This effect of social influence on behaviour is not present in the oldest ASD group - it could be that the children in this group treated the informational social advice as a 'social', rather than as asocial information, and as such attended to it less than the younger ASD groups. Overall, this is supported by the paradigm for autistic perception proposed by Pellicano & Burr (2012) which suggested that people with autism have a reduced bias by prior expectation - and so as an innate part of autism are less likely to exhibit bias towards stimulus-preceding information.

Together, the behavioural analysis and drift diffusion results suggest that children with ASD were differently affected by social advice, with the effect largely vanishing with at the onset of adolescence. It is worth noting that general task performance was lower in the middle age group of children with ASD, though their mean threshold without advice is comparable to that of the age-matched typically developing group -

so it is unlikely that these results are a product of poor performance on the task in general. Decreased task performance suggests that advice may have been confusing for this age group, which is supported by the quantity of verbal interactions directed at the advisor by this group during the task (see Results 3.3.2 for details).

3.4.2 Are autistic children perceptually biased by social context?

The drift diffusion model provides clear evidence that children with ASD are not integrating contextual social information with sensory about the stimulus, in spite of the younger two groups weakly altering their behaviour in the favour of social advice. Notably, drift rates and starting bounds in children with ASD at all ages are comparable to drift rates in typically developing children below the age of 12 - the age before we observe any indication of a perceptual bias in typical children.

This is supported by starting bound evidence (Figure 3.6) that suggests that younger children with ASD are inclined towards the decision bound in line with social advice direction, likely prior to viewing the stimulus. As such, they are more likely to respond in line with what the advisor suggests, due to being judgmentally rather than perceptually biased. This could imply that children with ASD are adopting a strategic attitude towards their behavioural responses, potentially answering what they believe is supposed to be correct, rather than what they actually perceive. However, this is counteracted by evidence that suggests both adults and children with ASD are essentially unaffected by the concept of reputation (Izuma et al, 2011) or flattering and pleasing others (Fu & Lee, 2007). As such, it is surprising that they would respond with anything other than the information from the stimulus. It may be that for the

younger two groups with ASD, social advice was a confusing element that overall increased error rates in the task: these two groups did have the highest overall error rates, in spite of equitable stereothresholds and performance in control tasks without social advice. As a result, they may have been less confident in their judgments, and so more ready to attend to advice.

Overall, children with ASD appeared to show similar behaviour across all age groups, though with increasing age any weak behavioural biases lessened. In contrast, for the oldest typically-developing group, the behavioural bias increased significantly. Though there is clearly some behavioural conformity in the younger two age groups with ASD, there is no evidence from the drift diffusion model that the underlying processes at work fundamentally differ from those in the oldest group with ASD - both drift rates and starting bounds were very similar. The drift diffusion model parameter values for drift rate and starting bound were also similar to the younger typical groups, who showed no behavioural conformity. While the behavioural changes seen in typically developing groups across development correlate with an increased drift rate and a decline in starting bound values, those across development for the ASD groups do not. As such, any behavioural changes in the ASD group do not indicate a change in the underlying decision-making process.

3.4.3 Neural basis for the difference between children with ASD and typically-developing children

A difference in development of social conformity between children with ASD and typically developing children is very clear from the behavioural and model data. This suggests that there may be an underlying mechanism or pathway that does not de-

velop in the group with ASD. As previously discussed, certain pathways and structures mature throughout adolescence in typically-developing children, including the fronto-parietal circuit and posterior temporal lobe (Sowell et al, 2003; Olesen et al, 2003).

In children with ASD, white matter volumes are greatly decreased relative to neurotypical controls in the temporoparietal junctions and superior temporal sulcus (Barnea-Goraly et al, 2004), and grey matter volumes are decreased in the posterior superior temporal sulcus (Greimel et al, 2013). The superior temporal sulcus is posited as a social network node (Allison et al, 2000), as such, decreases in both the grey and white matter in this region could indicate reduced connectivity with sensory perceptual regions, such as area V5/MT. This could account for the lack of integration of social information into perceptual processing for the structure-from-motion task on the part of children with ASD, given that this type of task is specifically linked to sensory and perceptual signals in homologous macaque area V5/MT (Krug et al, 2013). The reduction in brain matter volume in social-specific regions of the brain relative to typically-developing children could be linked to the lack of social information integration development in children with ASD.

It seems that while children with ASD may attend to informational social influence in decision-making before adolescence, they do not integrate this information with other sensory data, which would result in a perceptually biased decision. Unlike typically-developing children, beyond the age of 11 years it appears that children with ASD are not behaviourally biased by social information when making a perceptual choice. This could be the product of the differing grey and white matter development in typically-developing and adolescents with ASD, suggesting that certain networks for integrating social and sensory information may develop differently in the brains of children with

ASD.

3.4.4 Limitations and Conclusions

One clear limitation of this particular thesis chapter is the difference in sample size between the typical control group, and the group with ASD. This is particularly pronounced for the youngest group (29 typical versus 9 with ASD), though apparent for the middle (15 typical versus 11 with ASD) and oldest (17 versus 10 with ASD) groups. The sample size difference was partly the product of the difficulty in recruiting children with ASD who were capable of performing the task - 16 potential participants were screened out prior to engaging in the study due to issues with stereovision.

Though the differences between typical and ASD groups are intriguing, they certainly merit and require further research with expanded group sizes - particularly given the heterogeneity of how ASD manifests at an individual level.

With that in mind, we can draw some conclusions from the data. Overall, it seems that though behaviour changes over the course of development in children with ASD, the underlying mechanisms of perceptual decision making do not. While computational modelling demonstrates that typically developing children undergo a 'switch' between 11 and 12 in the factors that underlie their decision-making under social influence (from a judgmental bias to a perceptual bias), the same model suggests that there is no change in decision-making mechanisms for children with ASD across the same developmental period. Instead, the decision-making mechanisms remain consistent across development, and bear a remarkable similarity to those of the youngest two typically developing groups.

3.4.5 Future Directions

In order to better examine the neural substrate for the decisions made in this task, high-resolution neuroimaging provides one route. With the potential to examine clusters of neurons that respond to specific aspects of a stimulus, we may be able to robustly observe a participant's sensory and perceptual experience throughout the task - and compare it to their behavioural responses. This type of experiment could provide insight into whether a participant's behaviour matches their perceptual experience when agreeing with social advice (thus demonstrating a perceptual bias), or whether they are simply normatively conforming.

By exploring the location, structure, and function of area hMT+ (putatively the area responsible for the sensory and perceptual decisions made in Chapters 2 and 3) in adults, the next two chapters lay the groundwork for a future developmental imaging study that would take the advice task of the previous two chapters into an MRI scanner. Ideally this thesis itself would have explored the advice task in the scanner, but this was not practical within the time limitations of a PhD.

Although the first chapters of this thesis have been concerned with the behaviour of children, adults were chosen over children as participants due to practical limitations. It is necessary to establish a functional homology with macaque area MT in order to make inferences about the perceptual function of hMT+. As no developmental study has been conducted in the macaque on the development of MT organisation, it may well have been that a developmental study in humans would have found no homology purely due to the area not being fully developed. Adults are also better able to tolerate the multiple scanning sessions required to accrue robust evidence of a functional and structural organisation within area hMT+. Given that high resolution imaging requires

a great degree of participant co-operation and stillness, it was deemed that an adult population would be most suitable for the experiments conducted in the next two chapters.

Chapter 4

Localisation of visual cortical region hMT+, and subregions V5/MT and MST using patterns of myelination

4.1 Introduction

"The specific histological differentiation of the cortical areas proves irrefutably their specific functional differentiation..."

- Korbinian Brodmann (1909, translated by von Bonin, 1960)

The segmentation of the primate brain into areas with distinct structure and functions serves as a cornerstone in our understanding of anatomy, and the brain more generally. The visual system in primates is formed of over 30 areas (Felleman & Van Essen, 1991), defined by a combination of different functions, structures, and connections. For over a century, neuroscientists have attempted to reliably map functional regions of the cortex through a variety of different criteria (Brodmann, 1909; see Turner & Geyer, 2014 for a review). Structural methods have included examining the differential distribution of cell bodies (cytoarchitecture; Brodmann, 1909) or determining myeli-

nation patterns within the cortical ribbon (known as myeloarchitecture), using both histology (Gennari, 1792; Flechsig, 1920; Annese et al, 2005) and structural magnetic resonance imaging (e.g. Sanchez-Panchuelo, 2012; Bridge et al 2014). Functionally, the organisation of individual visual areas has also been investigated both through neurophysiological recordings (Hubel & Wiesel 1968; Zeki 1974) and functional magnetic resonance imaging (fMRI) (Sereno et al 1995; Engel et al. 1997; Wandell et al 2011).

The human primary visual cortex, V1, has been examined with a variety of magnetic resonance imaging (MRI) techniques - including sulcal location (Dale and Sereno, 1993; Dale et al., 1999; Fischl and Dale, 2000; Benson et al., 2014), myeloarchitecture (Clark et al., 1992; Barbier et al., 2002; Bridge et al., 2005; Clare and Bridge, 2005; Eickhoff et al., 2005) and retinotopic organisation (Engel et al., 1997). Several of these techniques have also successfully been used to define other early visual areas, such as V2 and V3 (Benson et al. 2014). However, subsequent visual areas have proved more challenging to localise. Furthermore, aligning different techniques within individual human brains can prove difficult, leading to inconsistencies in cortical area definitions between methods.

One example of such an area is well-studied extrastriate visual area hMT+, which has been localised and further divided into V5/MT and MST based on selectivity for direction of motion and retinotopy (Huk & Heeger, 2002; Amano & Wandell 2009; Cottereau, 2011), but lacks a precise anatomically identified location across human brains. This is not the case for the functionally homologous macaque V5/MT-MST complex, which has been localised using its functional selectivity, determined both with neurophysiology and with fMRI (Zeki, 1971; Allman & Kaas, 1976; Maunsell and Van Essen, 1983; Albright, 1984; DeAngelis & Newsome, 1999; Kolster et al., 2010) and its anatomical location on the posterior bank of the superior temporal sulcus (Dubner and

Zeki, 1971; Van Essen et al., 2012). While the sulcal anatomical markers of V5/MT are sufficient in the macaque to delineate its anatomical location (Sincich, Adams & Horton, 2003), the pattern of sulci and gyri in the cortex is far more complex and variable in humans (Thompson et al, 1996). As such, there is no consistent anatomical location for hMT+, though it usually lies somewhere around the lateral surface of the occipital lobe within the posterior limb of the inferior temporal sulcus (Dumoulin et al, 2000). An alternative anatomically-based definition of hMT+ that remains tied to the underlying cytoarchitecture could allow us to confirm functional definitions of visual areas in humans, as is possible in the macaque.

Using cytoarchitecture to anatomically segregate the brain into distinct regions was most famously conducted by Korbinian Brodmann in 1909. The differing myeloarchitecture across cortical grey matter is one trait by which this can be done. In mammals, myelination of axons in the cerebral cortex begins during the second postnatal month of life (Flechsig, 1876), with the somatosensory and motor regions being amongst the first to become myelinated (see From et al, 2014, for a review). Particular regions of the human cortex are known from histology to have denser myelination, such as the Stria of Gennari (Gennari, 1782) and the heavy myelination of the central sulcus (Naidich, Blum & Firestone, 2001).

In non-human primates, visual motion area V5/MT of the Rhesus macaque is well defined in terms of both anatomical location and its distinct myeloarchitecture (Ungerleider et al., 1986; Lewis & Van Essen 2000). The putative dense myelination of this region is likely linked to its role in motion processing, requiring quick neuronal signalling for faster response times. Computer-aided histological analysis of post-mortem human cortex has posited a likely region of myelination around the sulcal definition

of functionally homologous hMT+ in humans (Annese et al, 2004). Given that the distinct myeloarchitecture associated with area V5/MT in the macaque may be linked to its function in motion processing, it is plausible that functionally homologous area hMT+ may also have a pattern of myelination - which would allow a consistent identification of this extrastriate visual area in humans. However, comparing functional definitions with histological delineations of myeloarchitecture within humans poses a difficult question, as one of the available techniques used is *in vivo*, while the other is traditionally applied *post mortem*.

High-resolution structural MRI scans could provide the '*in vivo* histology' required to directly compare myeloarchitecture with functional definitions of cortical regions (Bridge et al, 2006; Deistung et al, 2013). Glasser & Van Essen (2011) have shown associations of areas of dense myelination with parts of the occipital lobe and putative (non-functionally defined) hMT+, while Dick et al (2012) demonstrated associations of dense myelin with areas of functionally localised auditory cortex for average datasets. Similarly, probabilistic maps of retinotopically defined hMT+ show correspondence with average myelin maps (Abdollahi et al. 2014). However, as discussed in Chapter 1.7, previous research has lacked both a direct comparison with specific functional localisers for cortical areas in the occipital lobe, and a comparison of these methods within individual subjects. Though consistent association of dense myelination with functionally defined regions of extrastriate cortex has not been shown at an individual level, current technology is sufficient to assess the level of myelin density across human cortex and compare these maps to individual functional localisers that specifically target area hMT+ and subdivisions. Matching individual myelin density maps to specific functional localisers for hMT+ and its subdivisions will give us a measure

of congruence between different mapping techniques - important both in clinical and research settings.

As discussed in Chapter 1.7, T1w/T2w and MP2RAGE protocols represent two types of structural scan well-positioned to assess myelin density across the cortex. They have been extensively used in previous research, including assessing myelination around a putative hMT+ (Glasser et al 2011,2013; Abdollahi et al 2014; Dinse et al 2013,2015; Sanchez-Panchuelo et al 2012), and have contrasts that are less dependent on tissue angle, meaning that the maps of intensities across the cortex represent less qualitative measurements than some other scan protocols used to visualise myelination patterns, such as T2*. T1w/T2w and MP2RAGE protocols have been developed at 3T and 7T respectively, and as such also represent an interesting opportunity to investigate and compare myelin mapping techniques between different field strengths.

By comparing multiple structural and functional methods of defining hMT+, MST and V5/MT within the same individual human subjects, a comparison of reliability for both individual and average maps of the visual cortex should be possible. Reliable localisation of visual areas lays the foundation for future behavioural experiments using fMRI. Furthermore, by comparing two scan protocols sensitive to myelin (MP2RAGE and T1w/T2w) against standard functional methods, it should be possible to assess how accurately myelin-related signals can be measured with MRI *in vivo*.

4.2 Methods

4.2.1 Subjects

A total of 10 subjects (6 male, 4 female), age range 24-36 years (mean age 27.8 years) participated in one or more of the scans detailed below. See Appendix E for a summary of which participants took part in which scans. All had normal or corrected-to-normal vision and no previous history of psychiatric disorder. All research was conducted in accordance with the Oxford University Central University Research Ethics Committee (CUREC/IDREC) guidelines, from whom ethical permission for this study was gained (MSD-IDREC-C1-2012-033). Participants gave informed consent and were free to leave the study at any time, and procedures were conducted in accordance with the declaration of Helsinki.

4.2.2 Set-up

Visual stimuli were generated in the Psychophysics Toolbox (Brainard, 1997; Pelli, 1997) extension of MATLAB. Visual stimuli were projected from an Apple MacBook Pro (2.7GHz Intel Core i7, Intel HD Graphics 4000 1024MB) to CRT screen via a VGA cable, with a resolution of 1600 x 1200 pixels. The image was projected from the CRT via an Eiki LC-XL 100 projector (with custom throw lens) to a back projection acrylic screen in the bore of the scanner. The peak luminances (cd/mm^2) were 552.6 (white), 161.6 (red), and 452.1 (blue). Participants viewed this screen through a series of mirrors. The display width was 30cm, and the distance of the display from the participant was 49.5cm.

4.2.3 Structural scan protocols

During structural scans, participants were requested to remain still, and watched a nature documentary of their choice.

7T MP2RAGE protocol

All 10 subjects were scanned at 7T (Siemens) using a 32-channel receive, 1-channel transmit coil. An MP2RAGE scan was acquired at 0.7x0.7x0.7mm (TE = 3 ms; TR = 5000 ms). The TI 1 contrast was 900 ms and the TI 2 contrast was 3200ms and flip angles were 4^{o} and 5^{o} respectively.

Three participants underwent the MP2RAGE scan a second time on separate days.

T1w/T2w protocol

Three of the subjects were also scanned at 3T (Siemens Verio) using a 32-channel head coil. Two T1-weighted MPRAGE scans (1 x 1 x 1 mm isotropic voxel size; TE = 3.77ms; TR = 2400ms; Flip angle = 8^{o}) and 3 T2-SPACE scans (1 x 1 x 1 mm isotropic; TE=449ms; TR=3200m) were collected within the same session. Scans of the same type were averaged; the mean image of the MPRAGE scans was then divided by the mean image of the T2-SPACE scans to create a T1w/T2w image, after the methods of Glasser and Van Essen (Glasser and Van Essen, 2011).

4.2.4 Functional scan protocol

In order to localise the regions of interest (hMT+, V5/MT, and MST), subjects participated in two functional scans - a motion localiser, and retinotopy. All subjects were scanned at 7T (Siemens) using a 32-channel receive, 1-channel transmit coil. 10

subjects participated in the first motion localiser scan session, in which 3 echo planar imaging (EPI) BOLD runs (1x1x1mm isotropic voxel size), 38 slices (TE = 26 ms; TR = 3000 ms; flip angle = 90^{o}) were acquired. These scans were acquired in the same session as the MP2RAGE scan. 8 subjects participated in a second retinotopy scan session, in which 10 EPI BOLD scans following the same protocol were acquired.

4.2.5 Visual Stimuli

Motion Localiser

In the first scan, subjects were instructed to fixate centrally on a white dot subtending 0.1° of visual angle, while the visual stimulus of an incoherently moving dot field (dot density of ~7/°) was presented. The percept of motion incoherence was produced by having the dots randomly replotted on each frame, with a dot lifetime of 1s. The background was mid-grey, and half the dots were black, half white, each subtending 0.2° of visual angle. Each run consisted of three different stimulus types, presented for 15 seconds, each of which was presented 5 times: 1) a full field moving dot stimulus (40° x 34°), 2) a moving dot stimulus limited to a single hemifield, with the edge located 10° from the central fixation cross (arranged to cover at least 10° x 34° of one hemifield), 3) a baseline condition of full field static dots. A rest condition was also included, in which only the fixation point was displayed. There were 3 runs in the scan session, such that each stimulus was presented 15 times in total. The duration of one run was 375 seconds. hMT+ was localised with the full field moving dot stimulus (40° x 34° of visual angle) while MST was localised from ipsilateral activation to the hemifield only moving dot stimulus (10° x 34° of visual angle) placed 10° of visual angle either to the left or right of the central fixation point (Huk & Heeger, 2002). See Appendix D.1 for

a figure of this stimulus.

Retinotopy

In a second scan, area V5/MT was localised retinotopically with a rotating wedge aperture (subtending 10° visual angle) over a moving black and white checkerboard (after Amano, Wandell & Dumoulin, 2009), with a central white fixation point subtending 0.1° visual angle. Each spoke of the checkerboard moved smoothly in opposite directions, such that one wedge of black/white squares moved inward, while its neighbour moved outward. Motion direction changed randomly every 2-3 seconds. The contrast pattern motion had a 2Hz temporal frequency. A full rotation took 36 seconds, and there were 6 stimulus cycles per scan. The position of the wedge aperture moved in synchrony with fMRI volume acquisition (every 3 seconds). At regular intervals (after a stimulus cycle), the stimulus was removed from the screen, and the subject viewed only the mid-grey background for 18 seconds. There were 4 stimulus free periods (72s), relative to 6 stimulus cycles (216s) - as such each stimulus free period replaced a different position of the wedge aperture. These rest periods have been shown to evoke greater activation in area hMT+ (Amano et al, 2009). See Appendix D.2 for a figure of this stimulus.

4.2.6 Analysis

4.2.6.1 Structural scan analysis

For each individual scanned at 7T, the structural MP2RAGE scan was brain extracted using FSL-BET (Smith, 2002), after which any remaining non-brain structures were removed by hand in Freeview. The resulting scan was then reconstructed using the

Freesurfer recon-all pipeline to extract the cortical surface.The same MP2RAGE scan for each participant was brain extracted using FSL-BET (Smith, 2002), after which any remaining non-brain structures were removed by hand in Freeview, then overlaid onto the individual inflated hemispheric surface using Freesurfer's *mri_ vol2surf* command (Reuter et al., 2012; Dale, A. M., B. Fischl, et al., 1999).

Each hemisphere overlay was thresholded at a signal intensity of +1SEM above the mean to produce a map of intensities related to myelin across the unfolded cortical surface. In order to test the reliability of the intensities detected by the MP2RAGE protocol, 3 subjects underwent a second 7T structural scan session on a different day. For statistical comparison of maps from individuals who took part in two structural scan sessions at 7T (n = 3), both MP2RAGE scans were segmented separately in native space using FSL-FAST (Zhang et al., 2001) and then imported into MATLAB for analysis of intensity correspondence across the cortex and within the functionally defined ROI for hMT+ using custom scripts.

To calculate percentage correspondence (whole cortex correspondence) between two scans across the cortex, 'myelin maps' were first established by thresholding the two scans to be compared at +1SEM (as above), then binarised to create a mask. The number of overlapping voxels above threshold between the two scans were then divided by the total number of voxels above threshold (excluding the overlapping voxels from one scan).

Correspondence between two scans within a specific ROI was similarly calculated: first, voxels in the ROI above threshold signal intensity were identified. The number of these voxels activated in *both* scans was divided by the total number of voxels activated in both ROIs (excluding the overlapping voxels from one scan).

For the analysis of 'myelin maps' based on MP2RAGE images, the temporal lobe of each hemisphere was masked out due to a known artefact resulting in falsely high intensities in this area at 7T (Vaughan et al, 2001), which could otherwise bias the intensity threshold.

In order to establish 'myelin maps' from the 3T data, the same procedure was employed (without temporal lobe masking), but the inflation generated in Freesurfer was based on one structural T1-weighted MPRAGE scan, and the myelination surface map was generated from the averaged T1w/T2w scans. To facilitate direct comparisons, the T1w/T2w surface map was also aligned to the individual's 7T structural scan via FSL-FLIRT with 7 DOF. The registration was applied within Freesurfer in order to produce a T1w/T2w 'myelin surface map' in the space of the 7T scan - this meant that it could be overlaid onto the individual's inflated 7T MP2RAGE cortical surface.

To compare the correspondence between both T1-weighted MP2RAGE and T1w/T2w scans, whole-cortex-correspondence and within-ROI-correspondence analyses were carried out as above within MATLAB.

4.2.6.2 Functional scan analysis

All functional images were corrected for head motion in pre-processing using MCFLIRT (Jenkinson et al, 2002), and to preserve the spatial resolution, no smoothing was applied.

Motion localiser To localise area hMT+ and subdivision MST, a motion localiser was used. Data from functional motion localiser scans (obtained at 7T) were analysed in FSL-FEAT and aligned to the structural scans using FSL-FLIRT (Jenkinson et al.,

2001). Data were linearly registered to a whole-head EPI with the same slice prescription (3 DOF translation only), then to the high resolution structural MP2RAGE (BBR algorithm).

For each of the three functional scan runs, a general linear model was used to model the activation for each of the moving stimulus types compared to the static dots. For individual scans, data were thresholded at $z > 2.3$, with a cluster threshold of $p = 0.05$. This allowed the assessment of data quality and registrations, and examination of the level of subject movement prior to combining runs in a higher-level analysis. The unthresholded data for the three individual runs were then combined using a Fixed Effects model, with a z-threshold of >2.3 and cluster threshold of $p = 0.05$. A continuous area of activation in response to the full-field dot stimulus near the putative anatomical location of area hMT+ was taken as area hMT+. Ipsilateral activity within hMT+ was assigned as area MST. This activation sometimes formed a single cluster that extended outside of hMT+, in which case the entire cluster was included.

Processed data were imported into Freesurfer, then registered and overlaid onto the cortical surface. The quality of registration was assessed by eye via the Freesurfer tkmedit tool, and found in all cases to be very well matched.

To determine group responses, a higher-level analysis was conducted for full-field and ipsilateral data across all subjects with a Mixed Effects (FLAME 1+2) model within FSL-FEAT. The output of this analysis was overlaid onto an inflated averaged structural scan within Freesurfer, using the same procedure as for the individual data.

Separate group average functional maps were created by the same procedure for the three subjects who underwent the MP2RAGE and T2-SPACE structural scans, for specific comparison with the T1w/T2w data.

Retinotopy To localise hMT+ subdivision V5/MT, polar retinotopic mapping was used (Huk & Heeger, 2002; Amano & Wandell, 2009). Polar and eccentric retinotopy were analysed within the Freesurfer retinotopy pipeline. Phase-encoded data generated by activation in response to the moving checkerboard wedge stimulus were analysed via Fourier analysis, which results in a phase and amplitude value at each voxel for the stimulus that generated the strongest activation. These were averaged over multiple within-individual repeat scans to provide a polar retinotopic map.

Activity within area hMT+ that showed a contralateral retinotopic map was assigned to be area V5/MT. For two subjects (004 & 007), ipsilateral activity also showed within the retinotopically active region - this activity was excluded from the definition of V5/MT. A group average location of retinotopic area V5/MT was generated by binarising the V5/MT mask from each individual, summing these 8 masks and then thresholding by 4, giving an area in which $\geq$50% of individuals showed overlapping activation. Throughout this process, the thresholds were blinded to ensure that subjective opinion did not affect the results. This thresholded group definition was overlaid onto the average structural surface within Freesurfer.

Separate group average functional locations for V5/MT were created by the same procedure for the three subjects who underwent the MP2RAGE and T2-SPACE structural scans, for specific comparison with the T1w/T2w data.

4.2.6.3 Functional and anatomical correspondence

Quantitative assessment of the correspondence of regions anatomically defined as densely myelinated ('myelin voxels') with the functionally defined regions was achieved by importing the functional and structural data into MATLAB for further analysis. The

percentage of voxels with myelin-related signals above threshold, present within functionally defined area hMT+, area MST, and area V5/MT, provided an estimate of ROI correspondence.

4.2.6.4 Comparison of Thresholds

To compare both functional and myelin definitions, and ensure that results were not a product of threshold selection, the thresholds for three subjects were also systematically varied within each hemisphere. Structural images in this study were thresholded at mean +1SEM. To assess myelin thresholds, three thresholds were selected in addition to the standard mean +1 SEM. These were 'very low threshold' - thresholded at the mean signal, 'low threshold' - thesholded at the mean +0.5 SEM, and 'high threshold' at mean +1.5 SEM. These thresholds were compared with the original functional definitions (z>2.3). Functional definitions were also varied systematically, with three thresholds in addition to the original z-threshold of >2.3. These were 'very low threshold' - thresholded at >1.3, 'low threshold' - thesholded at >1.8, and 'high threshold' - thresholded at >2.8. These thresholds were then compared with the original myelin definitions (mean signal +1SEM).

4.3 Results

4.3.1 Functional localisation

In order to provide a reliable functional measure against which to compare structural scans, a standard localisation of hMT+ was performed using activation to full field moving dots relative to stationary dots (Tootell et al 1995; Huk & Heeger, 2002).

Area MST was identified as a sub-region of this motion-sensitive area using a moving dot stimulus restricted to the ipsilateral hemifield. Retinotopic activation for motion stimuli in the contralateral visual hemifield was used to map V5/MT functionally. The respective areas activated and their definitions are shown on the inflated cortical surface for one example subject and the group average (Figure 4.1).

The functional locations for V5/MT, MST and hMT+ correspond well with the results of Huk et al. (2002), whose hMT+ and MST localisation these methods were based upon. Like Huk and colleagues, MST was often found anterior to V5/MT, and V5/MT had a consistent retinotopic map that differentiated it from the surrounding area. Functional MST would sometimes extend outside of the region localised as hMT+, also consistent with prior results; in these cases, the contiguous region of activation was defined as functional MST. Four out of 16 hemispheres also showed some degree of overlap between functional definitions of V5/MT and MST, as previously seen in data collected by Huk and colleagues (2002, 4/20 hemispheres). In these cases, ipsilateral activation defined as MST was excluded from the definition of V5/MT (see Methods).

4.3.2 Structural MP2RAGE and T1w/T2w comparison

When MP2RAGE and T1w/T2w structural scan data were compared for the same three individual subjects directly on the cortical surface, some consistent regions of high signal intensity were located where predicted from known patterns of dense myelination across human cortex. These regions included the central sulcus and the occipital lobe around V1 and hMT+ (Figure 4.2).

Correspondence across the cortex between the two types of MRI scans for individu-

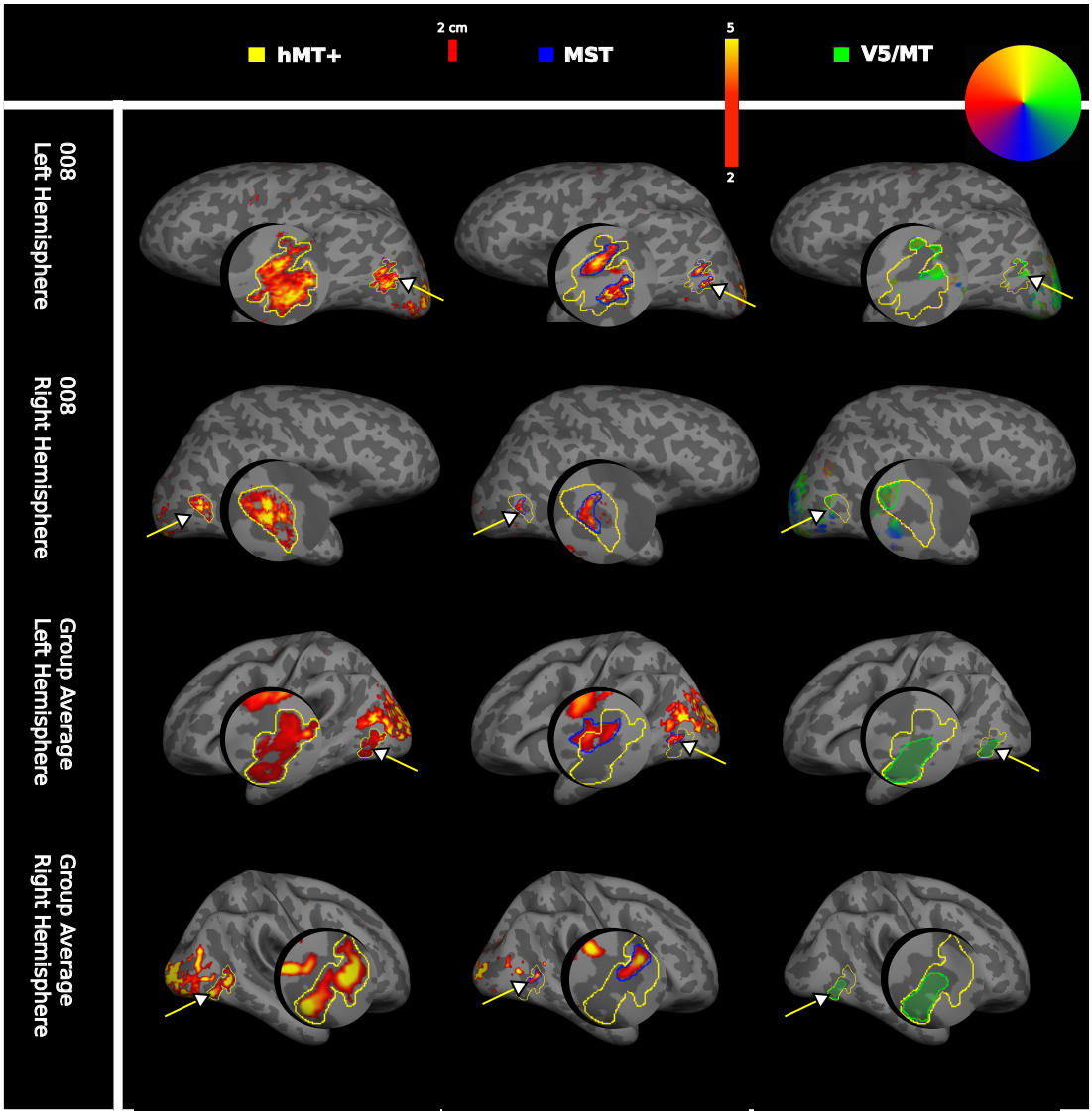

Figure 4.1: **Individual and average functional activation for visual areas hMT+, MST and V5/MT**

Functional activation for visual areas hMT+, MST and V5/MT are shown on the inflated cortex, including a magnified cut-out of the area of interest. The first column shows the functional activations for area hMT+ to a full field moving dot stimulus (yellow outline), the second column the ipsilateral activation for area MST (blue outline) and the third column the contralateral retinotopic activation for area V5/MT (green outline). Activation patterns are presented for the left and right hemispheres, for one example subject (008 first and second row) and for the group average (n= 10 subjects for hMT and for MST; n = 8 subjects for V5/MT; third and fourth row).

als ranged from 38.2-87.5% (Table 4.1). However, there were clear regional differences in sensitivity between the two scanning protocols. MP2RAGE scans tended to generate stronger signals around the central sulcus, while T1w/T2w showed greater intensities around the occipital pole. But since areas known to be densely myelinated remained consistent between the two scan types, signal intensities are still likely associated with myelination.

In order to provide an appropriate chance level of correspondence against which to compare these values, the data from these scans were spatially shuffled in MATLAB to produce images of randomly placed intensities. Correspondence between these two shuffled images was then calculated. Whole cortex correspondence between the spatially shuffled images ranged from 2-6%. As such, it is reasonable to say that the actual correspondence between the types of scan was significantly better than chance.

Inter-scan correspondence for the left hemisphere ROI for hMT+ was generally high, and for the group average was 68.07% (Table 4.1) with an individual range of 13.5-79.91%. As with whole cortex correspondence above, spatially shuffling data within the ROI for area hMT+ produced a correspondence range of 1-8%, again indicating that the correspondence between scan types was better than chance. In all individuals, inter-scan correspondence was generally higher for left hMT+ than for right hMT+, and less myelin-related signal was detected in the right hemispheres overall. As each hemisphere was thresholded with reference to mean signal separately, this result is unlikely to be the product of incorrect threshold reference points, and may represent an actual difference in hemispheric myelination.

In order to assess the inter-scan reliability of the signal intensities measured from the MP2RAGE scans, three subjects participated in a repeat scan at a later date. For

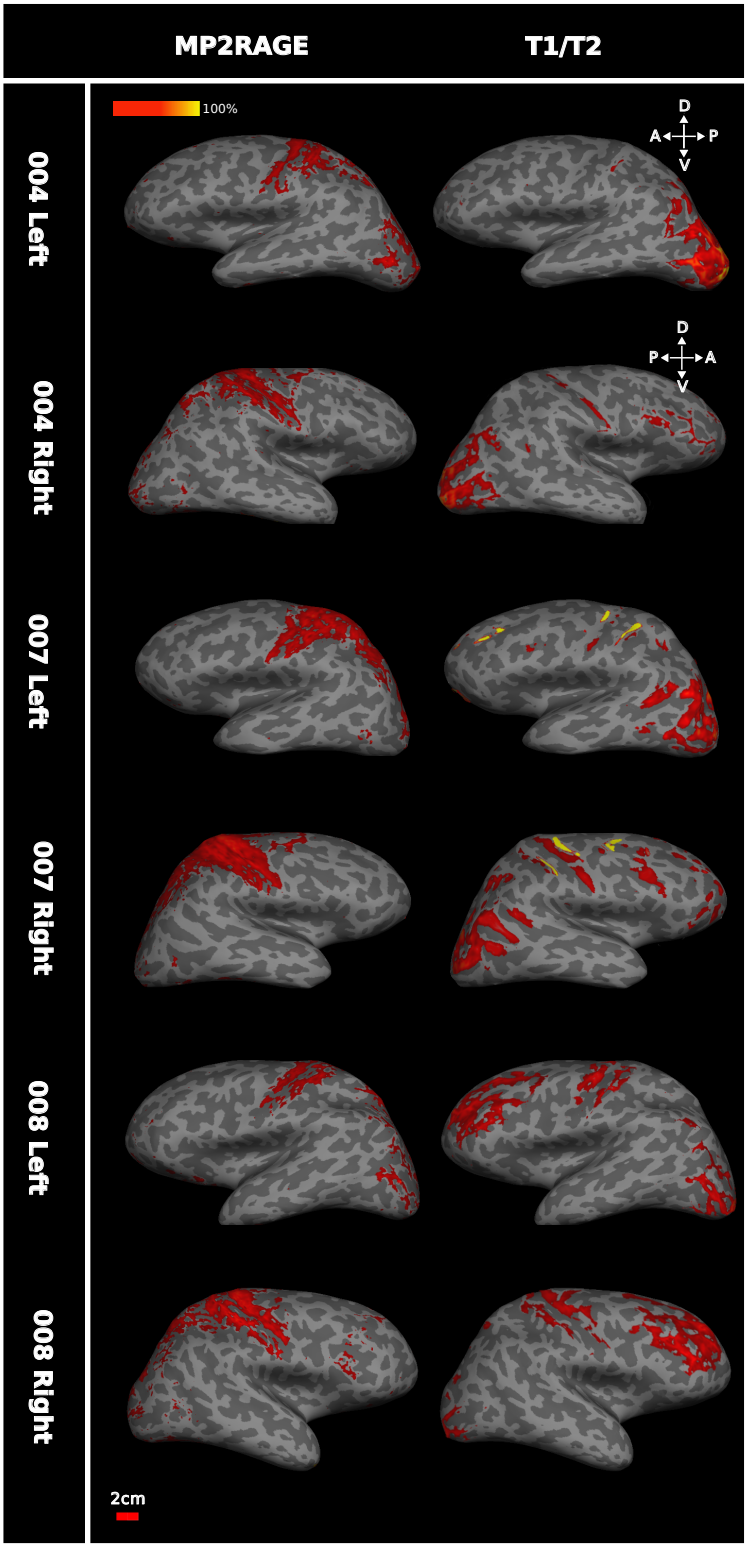

Figure 4.2: **Comparing MP2RAGE and T1w/T2w scans for myelin**
The pair of brains in each row shows the 'myelin maps' obtained for one hemisphere of the same individual subject based on MP2RAGE images at 7T (left) or from T1w/T2w at 3T (right). While MP2RAGE appears more sensitive to central sulcus signals, and T1w/Tw images to occipital signals - and despite some individual variation - the general pattern in these images indicates consistency of high MRI signal in regions associated with dense myelination (central sulcus, V1, hMT+). Data for each hemisphere of the three participants (004, 007, 008) are shown in rows.

Subject	Whole cortex	Whole cortex (shf)	hMT+ lh	hMT+ rh	hMT+ mean (shf)
004	38.2%	2.15%	79.91%	18.8%	1.24%
007	54.0%	5.22%	45.6%	13.5%	3.52%
008	86.9%	6.87%	87.5%	14.2%	7.86%
Group Average	89.2%	3.36%	68.07%	12.6%	4.95%

Table 4.1: **Percentage correspondence between T1/T2 and MP2RAGE images of the same brain**
Values in each column indicate the percentage correspondence between the two scans, either for whole cortex, whole cortex (shuffled, indicated by 'shf'), hMT+ in the left hemisphere, hMT+ in the right hemisphere, and mean correspondence for shuffled datasets in hMT+. It is clear that correspondence between non-shuffled datasets is much higher than that of shuffled datasets, indicating that results were not the product of chance.

Subject	Whole cortex	hMT+ lh	hMT+ rh
007	99.8%	98.1%	98.2%
021	99.2%	99.1%	99.5%
022	99.8%	99.6%	99.1%

Table 4.2: **Percentage correspondence between two MP2RAGE scans performed on different days within the same individual subject**

each individual, the percentage overlap between high intensity regions was calculated within MATLAB. Overlap ranged from 98.2 to 99.8% in each hemisphere (Table 4.2). This suggests that the identified regions of high signal intensity are highly reproducible between scan days, and as such may be measured reliably from scan to scan.

These results suggest that known areas of dense myelination are ratified in structural MRI scans, and correspond between two different scan types and field strengths. It is encouraging that there is a good level of correspondence between different scan types for the desired region of interest (hMT+), at least in the left hemisphere. It is also apparent that there is a good level of reproducibility between high intensity regions when the same scan type is repeated on separate days, suggesting that these intensities are related to the underlying cytoarchitecture.

4.3.3 Comparing the structural definitions of hMT+ obtained with MP2RAGE and T1w/T2w with functional data

When group average 'myelin maps' were directly compared with group average functional definitions obtained from the same subjects on an average surface, a patch indicating heavy myelination was associated with area hMT+ in both hemispheres and for both the MP2RAGE (n = 10) and the T1w/T2w (n = 3) structural scan types (Figures 4.3 and 4.4).

These results are consistent with previous literature (also based on averaged data, such as Glasser and Van Essen, 2011; Abdollahi et al., 2014). However, the group average MP2RAGE data indicated a smaller, more distinct area of dense myelination corresponding almost exclusively to area V5/MT (up to 58% versus up to 2%, Table 4.3) as defined by retinotopy (Figure 4.3). The T1w/T2w data shows a larger area of myelination spreading beyond hMT+, encompassing most of MST (up to 94%) and parts of area V5/MT (up to 41%) (Figure 4.4, Table 4.4).

While the group data shows good correspondence between the functional definition of hMT+ and regions of high myelination, this association is less consistent for individuals, especially for the MP2RAGE images. The T1w/T2w scans (Figure 4.4) usually show a region of high intensity signal associated with the functional location of area hMT+. However, this region is not exclusively aligned with either functional MST or retinotopic V5/MT, though there appears to be a greater degree of overlap with MST and association with the border region between V5/MT and MST across the three subjects (Table 4.4). The individual MP2RAGE scans were also more variable in terms of the strength of the myelin signal detected near hMT+, but generally follow

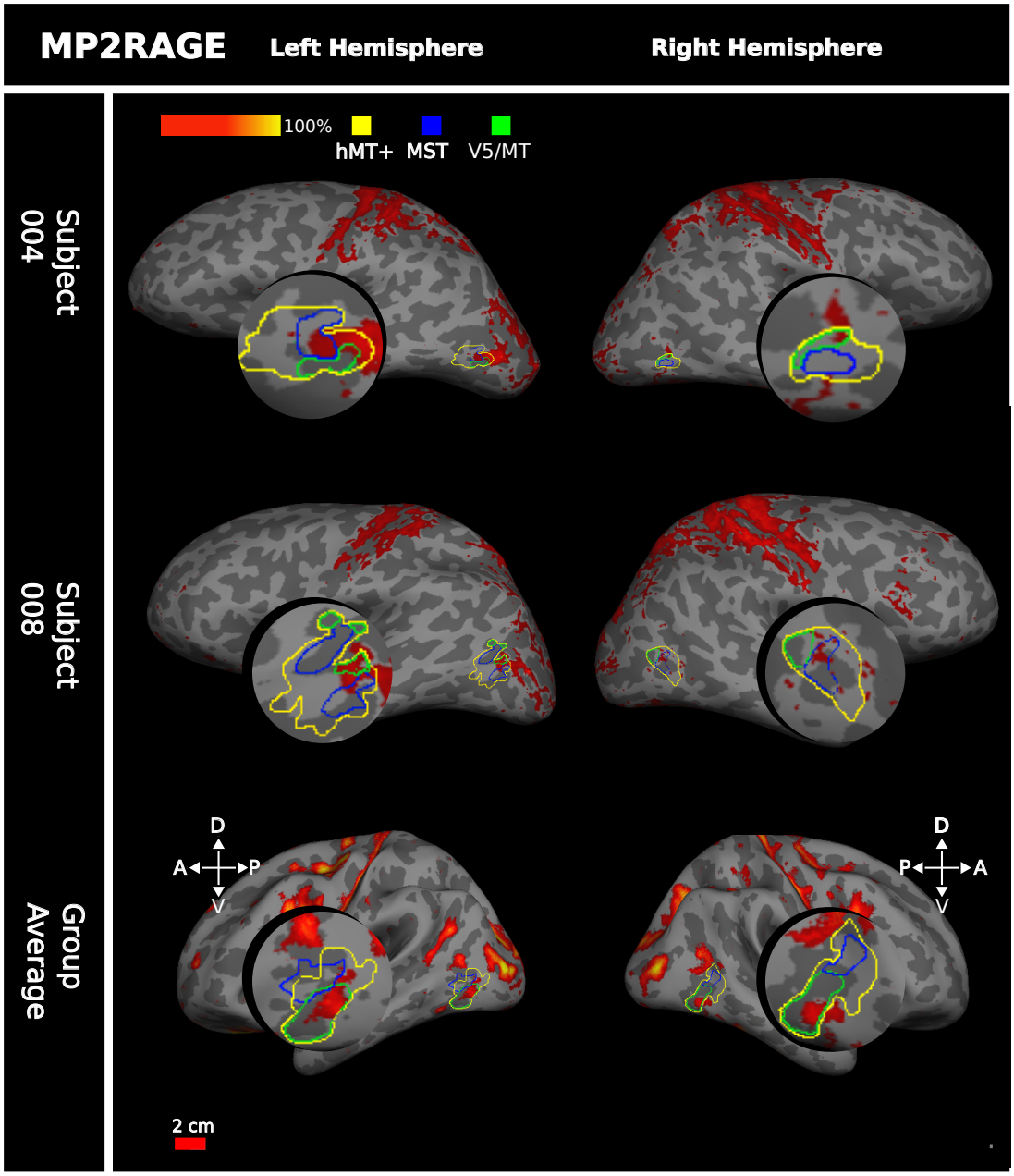

Figure 4.3: **Comparing MP2RAGE myelin intensity with functional hMT+** MP2RAGE 'myelin maps', shown for two example subjects and group average (n=10 subjects). Functional hMT+ is outlined in yellow, functional MST in blue, and retinotopically defined V5/MT in green. Myelin dense areas were defined as 1 SEM above the mean intensity of the MP2RAGE signal for this hemisphere, shown on a red-yellow scale of intensity values. In all hemispheres, a region of dense myelination is associated with area hMT+, MST or V5/MT. However, there is no consistent association with a specific functional subdivision across individuals. Data are presented on the individual subject's inflated cortical surface generated from a 7T structural scan, or the average generated surface (for the average data).

Subject	Hemisphere	% MT+ Overlap	% V5MT overlap	% MST Overlap
001	lh	3.2%	0.0%	6.8%
	rh	0.0%	0.0%	0.0%
002	lh	0.0%	-	0.0%
	rh	3.1%	-	14.9%
003	lh	17.9%	22.0%	0.0%
	rh	1.9%	0.0%	39.7%
004	lh	31.0%	12.1%	50.0%
	rh	4.5%	13.7%	0.2%
007	lh	7.3%	9.9%	12.2%
	rh	14.2%	20.3%	33.2%
008	lh	23.7%	44.5%	6.1%
	rh	11.3%	1.01%	22.3%
011	lh	13.3%	-	2.0%
	rh	1.8%	-	12.6%
021	lh	12.1%	20.6%	2.3%
	rh	18.5%	11.4%	7.6%
022	lh	6.1%	1.4%	0.0%
	rh	12.2%	3.1%	4.1%
038	lh	34.2%	20.0%	7.4%
	rh	15.3%	9.3%	2.2%
Group Avg.	lh	42.3%	58.1%	1.9%
	rh	18.0%	32.2%	0.1%

Table 4.3: **Percentage overlap with myelin detected with the MP2RAGE protocol with functionally localised hMT+, V5/MT, and MST for group average and individual hemispheres**
A dash '-' indicates that no retinotopic data was collected for that individual.

Subject	Hemisphere	% MT+ Overlap	% V5MT overlap	% MST Overlap
004	lh	67.2%	31.9%	67.0%
	rh	50.3%	31.2%	79.2%
007	lh	15.2%	24.2%	28.9%
	rh	9.9%	1.3%	51.0%
008	lh	18.0%	2.1%	16.4%
	rh	1.8%	0.9%	3.4%
Group Avg.	lh	59.8%	27.7%	92.4%
	rh	85.6%	40.8%	94.1%

Table 4.4: **Percentage overlap with myelin detected with the T1w/T2w protocol with functionally localised hMT+,V5/MT, and MST for group average and individual hemispheres**

a similar trend to the T1w/T2w results - showing a smaller myelin region associated with hMT+. There is no consistent alignment with either MST or V5/MT across the individual subjects (Figure 4.3, Table 4.3). The quantitative analysis of the overlap between areas of high intensity in the structural images with functionally defined visual areas supports that parts of the region around hMT+ are highly myelinated in individuals. However, the degree of overlap with hMT+ and the exact location in relation to the functionally defined areas V5/MT and MST appear quite variable. This trend held for both types of structural scan.

Conversely to the individual data, group average MP2RAGE myelin data showed an almost exclusive correspondence with area V5/MT relative to MST, while group average T1w/T2w myelin data showed a large overlap with both V5/MT and MST. To ensure that this difference was not driven by specific structural differences of the three individuals who underwent both scans, a separate group average MP2RAGE consisting of only the three subjects who comprised the T1w/T2w group average was generated. This additional group average MP2RAGE showed the same trend to predominant association of myelin with functional V5/MT as the full group average (not shown), demonstrating that the differences are more likely associated with the two different

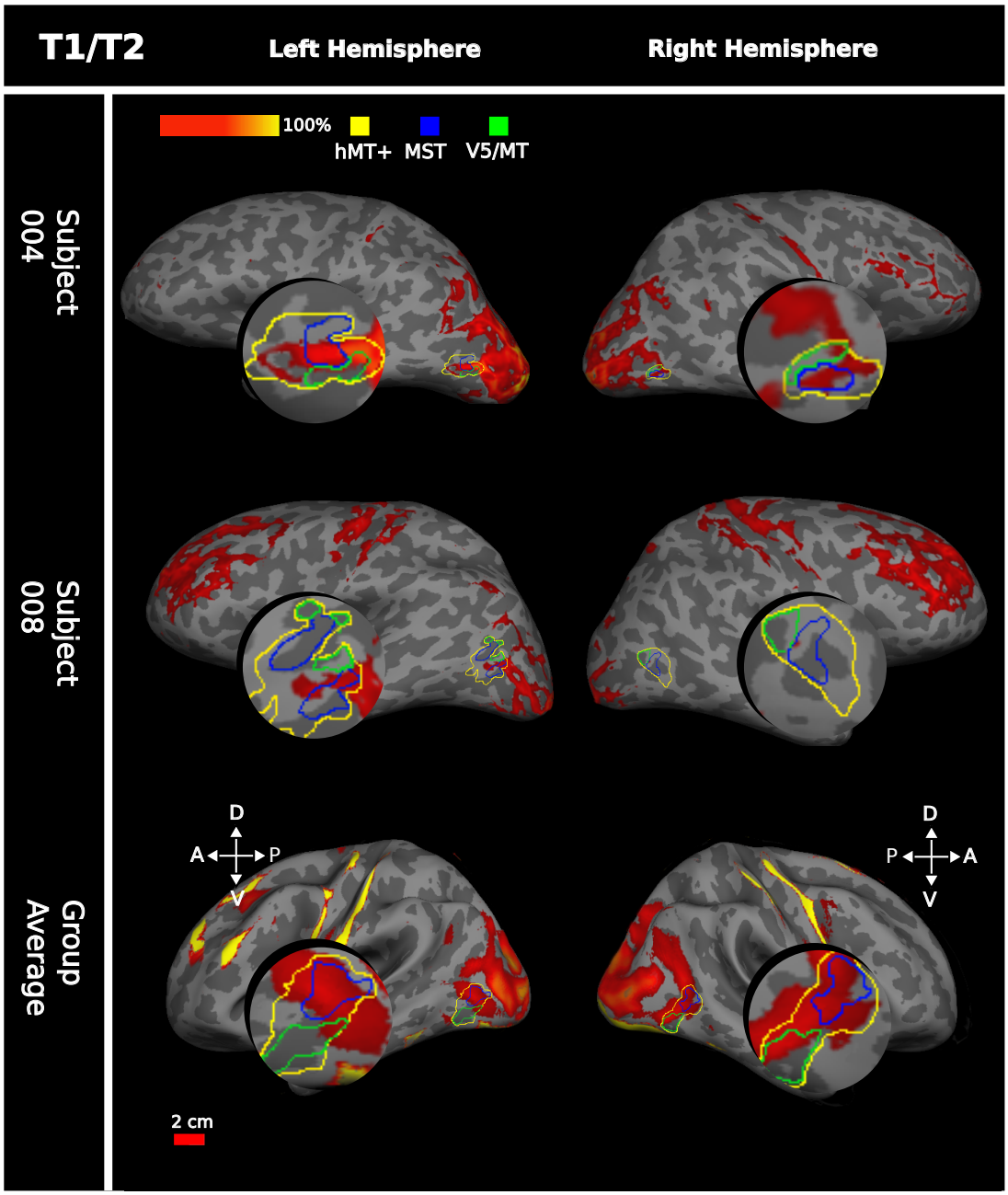

Figure 4.4: **Comparing T1/T2 myelin intensity with functional hMT+** T1w/T2w 'myelin maps', for two example subjects plus group average (n = 3 subjects). Similar measurements and same conventions as in Figure 4.3, but here the 'myelin maps' were generated from the T1w/T2w scan performed at 3T, and group average functional definitions are generated only from the three subjects who participated in these scans.

scanning protocols and not specifically related to these three subjects.

4.3.4 Assessing the propriety of threshold measures

In order to assess the propriety of selected thresholds, and to ensure that individual results were not being obfuscated by incorrect threshold selection, thresholds were also varied systematically around the standard threshold for three subjects, using the MP2RAGE structural data (for one typical example, see Figure 4.5). Varying the threshold for signal intensity associated with myelin does not significantly increase its overlap with the utilised definition of area hMT+, nor change the predominant patterns of dense myelination across the cortex. As we would expect, there is more widespread signal at lower thresholds, indicating that some included values may not be related to dense myelination. Similarly, varying the functional thresholds does not increase the amount of myelin signal encompassed by functionally defined hMT+. This suggests that our results are reliable at the selected threshold, and are not the product of excluding data just above or below threshold.

These overall results suggest that hMT+ in humans is associated with a nearby or overlapping area of increased myelin density, which can be detected with structural MRI methods. The precise location and magnitude of this signal may not be consistent between individuals, but tends to lie at least partly within the boundaries of area hMT+ when assessed with MRI.

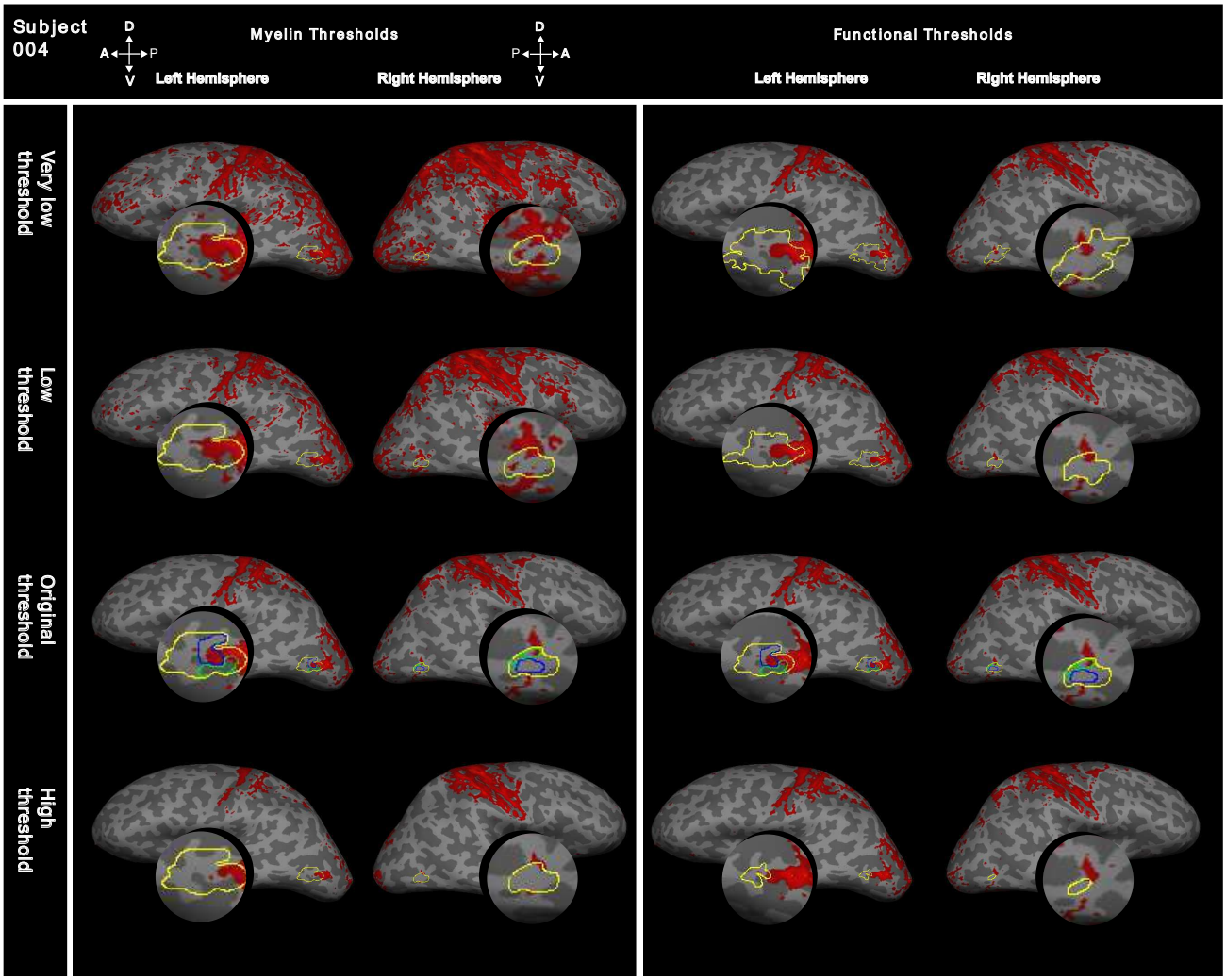

Figure 4.5: **Comparison of thresholds for MP2RAGE myelin and functional definitions for subject 004**

Thresholds were varied systematically at 3 levels for three subjects (data for 004 shown) - 'very low', 'low', and 'high', for both functional definitions and myelin maps (see Methods). Functional definitions of hMT+ are shown in yellow. The third row shows the standard thresholds used for analysis. Over the tested range, the choice of threshold affects myelin overlap with functional definition very little. This pattern was consistent in all 3 subjects tested.

4.4 Discussion

Abnormal levels of myelin have been linked to a number of neurological diseases and disorders, ranging from schizophrenia (Davis et al 2003) to multiple sclerosis (Bruck et al 2005) and autism (Deonie et al, 2015). As such, developing an accurate and reliable way of detecting myelin *in vivo* could prove to have great clinical as well as scientific value.

The association of signals from structural MRI indicating highly myelinated regions with functional maps of hMT+ in humans has a complex relationship. Across the majority of individuals there is a region of high signal suggestive of cortical myelination that overlaps with, or is close to, functional hMT+. There is, however, no consistent association with the subregions V5/MT and MST. Across the group average data, we find a clear overlap with signals indicating dense myelination of either visual area V5/MT (MP2RAGE) or both V5/MT and MST (T1w/T2w). At an individual level, MP2RAGE scans reveal more focused regions of signal intensity, while those in the T1w/T2w and more extensive and spread between the hMT+ subregions and beyond. This suggests that with current technology, the density of myelination cannot be used to distinguish V5/MT from MST consistently in the individual, but could be used as a way of ratifying the location of the hMT+ complex.

4.4.1 Are the detected signals indicative of myelination?

Given the variability in the data at an individual level, it stands to reason that one might question whether the MRI signals detected detected are indicative of myelin. In order to test this it is necessary to show both the reliability of the signal (to show that

the signal pertains to a real underlying structure), and association of the signal with areas known to be heavily myelinated (to show that the signal indicates myelination).

For areas known to be myelinated, such as V1 and the central sulcus, strong signals were detected regardless of scan type. Furthermore, other studies using these scan types have also detected strong signals in these regions (Glasser & Van Essen, 2011; Abdollahi et al 2014; Sanchez-Panchuelo et al, 2012; Dinse et al, 2013) - so along with inter-scan reliability, there is also cross-study consistency. This suggests that the signals are indicative of underlying myelination. The data also show a high level of inter-scan replicability on an individual level. Both across cortex, and restricted to area hMT+, all subjects showed over 98% correspondence in high-intensity regions of signal. This indicates that the high-intensity regions are consistent between subjects, and as such reflect real measured of underlying myeloarchitecture across the cortex. It also suggests that the variance of high-intensity signal location at an individual level could well reflect actual differences in myelination on a case-by-case basis.

However, in order to truly verify the veracity of the signal, and quantitatively show its link to underlying myelination, *post mortem* histology of the same brain would have to be conducted.

4.4.2 Why is there a lack of consistent correspondence at the individual level?

In spite of the multiple measures of replicability for myelin detection in the human (both between and within scan types), it remains that individual human participants did not consistently demonstrate a region of dense myelination overlapping with hMT+, or its subregions - although one was clearly present when the data were averaged across all

participants.

Several factors could account for some of the variance between individual human myleoarchitectural patterns not present for the homologous area V5/MT in the macaque (Ungerleider, 1986): variance generated by incorrect alignment of multiple different MRI images, insensitivity of MRI methods, and effects of actual structural differences in humans. MRI data requires a reasonable amount of processing to move from k-space data to visualised regions of activation. As such, human or computer error has the potential to be introduced, via incorrect alignment or registration. If images were not accurately registered, this could account for the offset clearly visible between regions of dense myelination and our functional definitions. However, all registrations between the functional and structural images were confirmed using Freesurfer tool tkmedit. Further to this, the regions of known myelination such as the central sulcus and V1 corresponded to the correct anatomical regions, while functional definitions of hMT+ were also found to be in the appropriate anatomical location. Moreover, our two scan types demonstrated consistency in areas of dense myelination, in spite of one type requiring multiple registrations and averaging of scans (T1w/T2w).

Functional definitions also have their caveats, such as differences in local vasculature, the effect of attention on haemodynamic response spread, and head orientation relative to the B0 field in the scanner (see Logothetis & Wandell, 2004, for a discussion) - but the relatively consistent anatomical location of the functional activation between individuals suggests that this was not an issue in the dataset. Another potential explanation is the relative level of sulcal complexity in the human cortex. Ono, Kubick & Abathy (1990) and Thompson (1996) have attempted to quantify the level of sulcal variability between individual human brains. Although major sulci, such as the

central sulcus, tend to be consistent across all individuals, there is a significant degree of variability in other sulci, particularly in the occipital lobe. Indeed some minor sulci and gyri may be altogether absent. The sulcus commonly associated with area hMT+ (the posterior limb of the inferior temporal sulcus) is present in all typically developed human adults, although its position is highly variable (Thompson, 1996). Sulci in the parieto-occipital region in particular vary both anterior-posteriorly and vertically by up to 19mm between individuals (Thompson, 1996).

This structural variance, combined with the variable position of functional hMT+ relative to the sulcus (Wang et al, 2014), can mean that it is found across a sulcus, wholly on a gyrus, or entirely in a sulcus. For most of our subjects, functional hMT+ spanned a gyrus and a sulcus, but the sulcal extension varied between individuals. Sulcal location could affect the ability of a structural scan to detect myelinated regions, as the gyrification of the cortex can introduce a variation in the orientation of voxels relative to the cortex, leading to partial volume effects (Clare & Bridge, 2005). As such, different sulcal patterning between individuals may result in differential ability to detect myelin on a case-by-case basis. This said, sulcal patterning could also directly affect the extent of myelination (rather than ability to detect it), as histology has shown lower cortical layers around the fundus of a sulcus tend to appear less dense. This would suggest that the differences in detected myeloarchitecture between individuals are a product of their inter-varying sulcal patterns.

Another potential cause of variation between scans is specific to the type of structural scan used. The two structural scan types detect different aspects of molecules associated with myelin - and it could be that by detecting correlates of myelin, rather than myelin directly (as is possible with histological measures) we slightly offset the

location of myelin signal between individuals.

4.4.3 Is area hMT+, or any of its subregions, reliably associated with dense myelination?

Although the overlap is not always precise, area hMT+ in the majority of hemispheres is associated with signals that indicate a region of dense myelination, that are not dependent on the specific myelin-sensitive scan used. Further to this, repeats of the same structural scan within the individual yields almost identical 'maps' of myelin-associated intensity, indicating the reliability of scan data.

Using an average of the structural images across participants, it is clear that there is a good overall relationship between functional hMT+ and a region of dense myelination. Similar to Glasser et al (2011) and Abdollahi et al (2014), average 'myelin map' data corresponds well with an average functional definition of area hMT+. This consistency is in spite of differing functional localization methods; the previous studies used published anatomical definitions and retinotopy respectively, while specific functional localisers for hMT+, MST and V5/MT were used in this study.

What is less clear is what association myelin has with either major functional subregion of hMT+. The individual human data do not show a consistent relationship with the functionally defined V5/MT or MST. Individuals appear to have an association either with V5/MT, MST, or overall hMT+, depending on subject and scan type. Previous results comparing myelin maps and tonotopic maps in human auditory cortex also noted greater variation in the alignment of anatomical and functional maps in individuals compared with in average datasets (Dick et al., 2012; De Martino et al., 2014) - consistent with our results. Further to this, using a T1w/T2w protocol comprising

the average of 196 Human Connectome Project subjects (compared with retinotopy conducted in 12 participants), Abdollahi et al (2014) found that myelin density tended to focus at the hypothesised border between putative V5/MT and MST - though it is important to note that these areas were not specifically localised. However, the result is similar to the results from the T1w/T2w protocol presented here, which shows an overlap partly with V5/MT, partly with MST in the group average data. It is not clear whether the differences in signal intensity location between the two scan protocols are evidence of differences in underlying myelin - neither of these scans detect myelin directly. It may be that the differing T2 and T2* sensitivities of the two methods also alter sensitivity to local blood oxygenation, tissue iron, or local diffusion, thus changing specific regions of high intensity.

In both scan types the left hemisphere consistently had larger areas of high intensity and more signal in general than the right hemisphere. As each hemisphere was thresholded for peak myelin separately, this result is unlikely the product of incorrect threshold reference points, and may represent an actual difference in hemispheric myelination. Armstrong et al (2004) have previously found significantly higher levels of myelination in the left versus right hemisphere using a different imaging technique (magnetisation transfer imaging), which would support this result.

The consistency of previous average results with our own average data, and the lack of individual consistency found by Dick et al in 2012, suggests that individual variation in myelin density could be being erased by the central tendency of averages. Overall this indicates that human cortical myelination could simply be quite variable between individuals, much as sulcal inter-individual variability is quite extensive (Thompson et a, 1996). As such, structural MRI methods for detecting myelination may not be a good

predictor of functional area location for individual subjects, particularly when it comes to delineating subregions. The ultimate test of the congruence between functional maps and myelination would be to conduct fMRI mapping in conjunction with *post mortem* histology, in the same brain. Though this type of study is difficult, as it requires a longer investment in data collection, it remains a plausible future option.

4.4.4 Conclusions

Overall, the data suggest that the structural MRI protocols tested (MPRAGE and T1w/T2w) are capable of detecting reasonably detailed maps indicating myelin density across the cortex. However, there was substantial variation for individual datasets, both in the overall quantification of myelin and the location of the myelin relative to functional measures. The considerable inter-subject variability requires further investigation in order to determine whether it reflects individual differences in myelination relative to functional areas in humans, or whether it is due to the sensitivity and resolution of the methods used.

The replicability of the overall myelin maps between individuals suggests that these methods could potentially be used to accurately track small structural changes in myeloarchitecture in longitudinal studies, as well as reveal individual differences between subjects. This could prove invaluable for clinical purposes.

Chapter 5

Exploring the functional organisation of area hMT+

5.1 Introduction

"Swiftly the brain becomes an enchanted loom, where millions of flashing shuttles weave a dissolving pattern-always a meaningful pattern-though never an abiding one."

- Charles Sherrington, Man on his nature, 1942

For over 80 years, the macaque has been used as a model species for humans in order to investigate cognitive processes and their underlying neural mechanisms (e.g. Jacobsen, 1936). Where methods are too invasive to use in humans, experiments can be conducted on non-human primates to gain further insight into neural processes activated in response to specific aspects of visual stimuli, producing maps of functional organisation. While research has revealed a great degree of homology between human and macaque, some questions remain as to the direct homology of cognitive processes between monkeys and humans - particularly when applied to the more complex mechanisms of human behaviour.

Single cell electrophysiology has long been the gold standard method of examining

the detailed functional processes involved in sensory perception. While such methods have elucidated the foundations underlying decision-making in non-human primates (see Gold & Shadlen, 2007, for a review), such processes in humans have remained elusive, primarily due to the lack of spatial and temporal resolution available in current non-invasive methodology. Attempts to functionally map the visual cortex using functional magnetic resonance imaging (fMRI) are not novel (e.g. Belliveau et al, 1992) - but have previously only yielded coarse maps of areas (Vanduffel et al, 2004).

As high-field fMRI scanning moves to the fore in probing brain activity potentially at a sub-milimetre level (for example Duong et al, 2000; Heidemann et al, 2012; Zimmerman et al, 2011; Yacoub et al, 2007) the opportunity to functionally map the internal organisation of individual cortical areas has become a possibility. 7T scanners boast a higher signal to noise ratio than at lower fields (Triantafyllou et al, 2005), allowing greater resolutions to be attained. Greater resolutions minimise signal contribution from large veins across the cortex that might obscure the BOLD response from smaller functional structures, while maximizing that from the vasculature feeding into organisational structures such as cortical columns (e.g. Tallantyre, 2009). By harnessing this technology, gaining insight into the functional organisation of visual area hMT+ (and subregions V5/MT and MST) should be possible. Accurate fMRI maps of these areas would not only allow us to compare findings from electrophysiology conducted in the rhesus macaque (Albright et al, 1984; DeAngelis & Newsome, 1999) directly with findings from humans, but could also pave the way for conducting experiments in humans in which somatosensory and visual activations relating to a specific percept can be correlated with behavioural response to better inform researchers about the processes driving behaviour.

Large-scale functional mapping of the cortex has previously been obtained through a variety of imaging means - such as resting state data (Hartrison et al, 2015), retinotopy (Engel et al, 1997), and tonotopy (Cheung et al, 2012). While these provide a robust way of localising larger functional regions of the cortex, they provide little insight into the neural basis leading to such activation, as they lack the resolution to reveal functional structures that relate to specific perceptual interpretations. More recently, 7T MRI has been used as a way to examine much smaller intracortical units - putative columnar structures formed of neuronal clusters selective for specific aspects of a stimulus. The Yacoub group demonstrated exciting proof of functional ocular dominance columns in human visual area V1 (Yacoub et al, 2007) at a resolution of 0.5 x 0.5 x 0.5 mm - though these results have yet to be replicated. Sanchez-Panchuelo et al (2010) have revealed a digitotopic fMRI map of the somatosensory cortex at 7T with a larger (and more attainable) resolution of 1 x 1 x 1mm, as have Stringer et al (2011) using the same resolution. As such, replicability between 1 x 1 x 1 mm voxel resolution scans appears to be more reliable than those conducted at higher resolutions. This may be the product of the larger difference in effective versus nominal resolution at the sub-milimetre level - effective resolution tends to be blurred significantly above nominal resolution for sub-milimetre ranges due to the physiological spread of the haemodynamic response (see Shmuel et al 2007 and Peters et al 2007). In addition, sub-milimetre scans have a lower tolerance for head motion (Qin et al, 2012) and so are more affected by noise. It follows that so long as the functional cluster sizes that one aims to measure are estimated to occupy 1 x 1 x 1mm and upwards of cortical surface area, it should yield better results to scan at this resolution than sub-milimetre.

A detailed map of the columnar organisation of human visual area hMT+, or its

subregions V5/MT and MST, has yet to be achieved through fMRI. However, using invasive methods, macaque area V5/MT has been functionally well characterised. It shows responses to disparity (Maunsell & Van Essen, 1983; DeAngelis & Newsome, 1999), and direction of motion (Zeki, 1974; Albright et al, 1984; Britten et al, 1993), either separably within V5/MT (Smolyanskaya et al, 2013) or in a disparity-dependent manner, as in area MST (Roy et al, 1992). Further to this, signals within macaque area V5/MT correlate with behavioural decisions, and stimulation of this region can lead to a change in behavioural reports of perception, suggesting that it may carry perceptual information as well as sensory (Britten et al, 1996; Salzmann et al 1990; Krug et al, 2004; Krug et al, 2013). fMRI has shown that human area hMT+ is also implicated in the processing of motion (Hess et al, 1989; Kourtzi, 2000) and depth perception (Neri et al, 2004; Rokers et al, 2009; Kim et al, 2015). This similarity in function could indicate that the functional organisation of human hMT+, or its subregions, is similar to that of macaque V5/MT.

In terms of scale, electrophysiological data from Albright et al (1984) and DeAngelis & Newsome (1999) show that macaque V5/MT is selective for 360 degrees of motion across 1mm of cortex, and is organised for disparity with distinct patches of selectivity for near and far, 300-700µm in diameter. A comparison of equivalent cortical structures from macaque to human could be used to infer a scale factor between the two animals, and as such provide a suitable resolution at which to look in the human. Ocular dominance columns are one such structure that have been demonstrated in both the macaque and human - measuring 400-700µm in macaques (Horton et al, 1996) and 800-1400µm in humans (Adams et al, 2007). This suggests a scale factor of 2 between the species. As such, we might expect direction selectivity to be represented with 360

degrees over 2mm of cortical surface, and disparity clusters between 600-1400µm in diameter.

Though fMRI cannot compete with the spatial resolution of electrophysiology, this means that with a reliable isotropic voxel size of 1 x 1 x 1mm, we should be able to capture sufficiently small groups of neurons to be able to investigate to some extent the clusters of disparity and direction-selective responses across hMT+. The ability to detect a rough map of motion axes within area hMT+ has already been demonstrated by Zimmerman et al (2011) - who combined opposite directions of motion to maximise signal and so obtained orientation maps across this area of the cortex. While this work does not confirm Albright et al (1984), who revealed specific columnar selectivity for singular directions of motion rather than stimulus orientation, it does suggest that the signals evoked by motion stimuli within hMT+ will be sufficient to yield high-resolution functional maps of motion and disparity. Further to this, using additional localisers that parcellate hMT+ into its sub-regions could allow a more in-depth comparison with monkey electrophysiology - for example, research demonstrating that within macaque MST, selectivity for direction reverses when changing the disparity sign (Roy et al, 1992).

By showing participants a range of motion and disparity stimuli, it should be possible to reveal the underlying functional organisation of this area with regards to both specific direction of motion, and disparity selectivity.

5.2 Methods

5.2.1 Subjects

A total of 11 subjects participated in the experiment (6 male, 5 female, age range 24-36 years, mean age 28.3), all with normal or corrected-to-normal vision and no previous history of psychiatric disorders. 8 of these subjects were also used for Chapter 4. See Appendix E for a summary of which participants took part in which scans. Normal stereoscopic vision was confirmed with the TNO test prior to scanning (minimum threshold 240 seconds of arc). Subjects were informed as to the nature of the stimulus, but did not undergo any prior training, and were not experienced with stereo-motion tasks. All research was conducted in accordance with the Oxford University Central University Research Ethics Committee (CUREC/IDREC) guidelines, from whom ethical permission for this study was gained (MSD-IDREC-C1-2012-033). Participants gave informed consent and were free to leave the study at any time, and procedures were conducted in accordance with the declaration of Helsinki.

5.2.2 Set-up

Visual stimuli were generated in the Psychophysics Toolbox (Brainard, 1997; Pelli, 1997) extension of MATLAB. Visual stimuli were projected from an Apple MacBook Pro (2.7GHz Intel Core i7, Intel HD Graphics 4000 1024MB) to CRT screen via a VGA cable, with a resolution of 1600 x 1200 pixels. The image was projected from the CRT via an Eiki LC-XL 100 projector (with custom throw lens) to a back projection acrylic screen in the bore of the scanner. The peak luminances (cd/mm^2) were 552.6 (white), 161.6 (red), and 452.1 (blue). Participants viewed this screen through a series

of mirrors. The display width was 30cm, and the distance of the display from the participant was 49.5cm.

5.2.3 Visual Stimuli

In order to localise the regions of interest (hMT+, V5/MT, and MST), subjects participated in two functional scans - a motion localiser and retinotopy. A third functional scan comprised the stimulus intended to examine the functional organisation, with respect to visual motion direction and binocular disparity, of the areas in question.

Motion localiser

In the first scan, subjects were instructed to fixate centrally on a white dot subtending 0.1° of visual angle, while the visual stimulus of an incoherently moving dot field (dot density of ~7/°) was presented. The percept of motion incoherence was produced by having the dots randomly replotted on each frame, with a dot lifetime of 1s. The background was mid-grey, and half the dots were black, half white, each subtending 0.2° of visual angle. Each run consisted of three different stimulus types, presented for 15 seconds, each of which was presented 5 times: 1) a full field moving dot stimulus (40° x 34°), 2) a moving dot stimulus limited to a single hemifield, with the edge located 10° from the central fixation cross (arranged to cover at least 10° x 34° of one hemifield), 3) a baseline condition of full field static dots. A rest condition was also included, in which only the fixation point was displayed. There were 3 runs in the scan session, such that each stimulus was presented 15 times in total. The duration of one run was 375 seconds. hMT+ was localised with the full field moving dot stimulus (40° x 34° of visual angle) while MST was localised from ipsilateral activation to the hemifield

only moving dot stimulus (10° x 34° of visual angle) placed 10° of visual angle either to the left or right of the central fixation point (Huk & Heeger, 2002). See Chapter 4 for detailed results of the localiser stimuli.

Retinotopy

In the second scan, area V5/MT was localised retinotopically with a rotating wedge aperture (subtending 10° visual angle) over a moving black and white checkerboard (after Amano, Wandell & Dumoulin, 2009). Each spoke of the checkerboard moved smoothly in opposite directions, such that one wedge of black/white squares moved inward, while its neighbour moved outward. Motion direction changed randomly every 2-3 seconds. The contrast pattern motion had a 2Hz temporal frequency. A full rotation took 36 seconds, and there were 6 stimulus cycles per scan. The position of the wedge aperture moved in synchrony with fMRI volume acquisition (every 3 seconds). At regular intervals (after a stimulus cycle), the stimulus was removed from the screen, and the subject viewed only the mid-grey background for 18 seconds. There were 4 stimulus free periods (72s), relative to 6 stimulus cycles (216s) - as such each stimulus free period replaced a different position of the wedge aperture. These rest periods have been shown to evoke greater activation in area hMT+ (Amano et al, 2009). See Chapter 4 for detailed mapping results.

Motion-disparity

For the third scan, a moving dot stimulus was used to localise putative columnar structures within the area defined as hMT+ by the motion localiser. The stimulus comprised of two fields of randomly placed black and white dots, each subtending

19x34^{o} of visual angle on a mid-grey background. Each field was placed 1^{o} either side of a white, square, central fixation point which was 0.1^{o} in size, leaving a 2^{o} clear central gap between the two dot fields. Half the dots were black, and half the dots were white, and presented on a mid-grey background. The dots subtended 0.4^{o} to visually distinguish them from the fixation point and to minimise optical illusions such as seeing the fixation point travelling upward when dot field motion was downward. The motion of both dot fields was always the same. The fields either moved up, down, left, right or incoherently. The disparity of the two fields was always opposite, with one field having the equivalent positive (far) disparity to the other field's negative (near) disparity. This was to help subjects converge on the fixation point at zero disparity. As a product of this, the disparity of one field would stimulate the contralateral visual hemifield of one brain hemisphere, while the opposite disparity of the second field would stimulate the contralateral visual hemifield of the other brain hemisphere. Dot disparity was either positive (+0.08^{o}), negative (-0.08^{o}) or uncorrelated. A disparity of +/-0.08 was chosen as it evokes a good response in hMT+ in accordance with several papers on the topic (Cottreau et al 2011 used a range from ±0.0083 - ±0.53^{o}, Bridge & Parker 2007 used ±0.07^{o}, Neri, Bridge & Heeger 2004 used a range between ±0.56^{o} in steps of 0.03^{o}).

A baseline rest stimulus with two static fields of dots with uncorrelated binocular disparity was also included. There were 15 stimuli in one block, and within each block of stimuli, stimulus order was randomised (see Table 9 for a list of all stimuli included in one block).

Each stimulus within a block was presented for 15 seconds, making one block of 15 stimuli 225 seconds long. In one run, three blocks were presented - as such, a single functional run was 675 seconds. There were 3 runs per scan session, such that each

Motion Direction	Field 1 Disparity	Field 2 Disparity
Up	Positive	Negative
Down	Positive	Negative
Left	Positive	Negative
Right	Positive	Negative
Incoherent	Positive	Negative
Up	Negative	Positive
Down	Negative	Positive
Left	Negative	Positive
Right	Negative	Positive
Incoherent	Negative	Positive
Up	Uncorrelated	Uncorrelated
Down	Uncorrelated	Uncorrelated
Left	Uncorrelated	Uncorrelated
Right	Uncorrelated	Uncorrelated
Static	Uncorrelated	Uncorrelated

Table 5.1: **All motion-disparity stimuli presented within a block**
The first column indicates the direction of motion of the two dot fields. The second and third columns describe the disparity applied to each field. In total, 15 stimuli were shown (including one baseline stimulus - static uncorrelated dots) 3 times per run, for a total of 3 runs.

stimulus was shown 9 times.

3 subjects underwent repeat scan sessions on a separate day.

See Appendix D.3 for a figure of this stimulus.

5.2.4 Scan protocols

Functional scans

All subjects were scanned at 7T (Siemens). For all functional scan sessions, echo planar imaging (EPI) BOLD scans with a voxel size of 1 x 1 x 1mm isotropic, TR of 3000ms, TE of 26ms and flip angle of 90^{o} were taken within one session. 38 slices were taken.

Structural scans

A structural scan was also taken for each subject in the first scan session, for presentation and anatomical localization of results. A 0.7x0.7x0.7mm isotropic voxel size MP2RAGE protocol was used. The TR was 5000ms and TE 3ms. The TI 1 contrast was 900ms and the TI 2 contrast 3200ms. Flip angle 1 was 4^{o}, flip angle 2 was 5^{o}.

5.2.5 Analysis

Structural scan analysis

Data from the structural scans were brain extracted using FSL-BET (Smith, 2002), and extraneous structures such as the pial surface were manually removed in Freeview. The cortex was then inflated using the Freesurfer pipeline (Reuter et al., 2012; Dale, Fischl, et al., 1999) as in Chapter 4.

Functional scan analysis

Data from the first and third functional scans were analysed in FSL-FEAT and aligned to the structural scans using FSL-FLIRT (Jenkinson & Smith, 2002), then imported into Freesurfer and overlaid using Freesurfer functions (*overlayfeat2freesurfer*, *mri_vol2surf*). The second set of retinotopy scans were analysed within Freesurfer (see Chapter 4 for details).

In order to explore fully the data from the motion-disparity set of scans (exploring the functional organisation of area hMT+, MST, and V5/MT), the data were analysed in three ways, all using FSL-FEAT. For each analysis, lower-level analyses were run on a per run basis for each individual, then combined into an within-individual averaged

higher-level Fixed Effects analysis, thresholded at $z > 2.3$, using a cluster threshold of $p < 0.05$. These activation data were aligned to the individual's high resolution structural MP2RAGE scan.

As two dot fields were presented on the screen, separated by a thin blank space, one dot field stimulated the contralateral visual hemifield of one brain hemisphere, while the second dot field stimulated the contralateral visual hemifield of the other brain hemisphere. As disparities differed between the dot fields (while direction of motion remained constant), each brain hemifield was stimulated contralaterally by a one disparity, and ipsilaterally stimulated by the opposite disparity. Throughout the analysis, each stimulus was analysed on a hemisphere-by-hemisphere basis, and coded by its contralateral (rather than ipsilateral) activation. For example, a stimulus that combined upward motion with a positive disparity for the right dot field, and a negative disparity for the left, would be coded in the left hemisphere as responses to positive-disparity upward motion, and in the right hemisphere as responses to negative-disparity upward motion. This was because area hMT+ is primarily contralaterally activated, with subdivision V5/MT exclusively contralaterally activated, and subdivision MST both contra- and ipsilaterally activated (Fischer et al, 2012).

Analysis 1: Disparity. For the first analysis, activation was modelled for positive and negative disparities by creating contrasts that combined either contralateral response to all stimuli with a positive disparity, or all stimuli with a negative disparity, versus a baseline of static binocularly uncorrelated dots. This created 2 contrasts: activation in response to positive disparity, and activation in response to negative disparity. This was to explore the general organisation of hMT+ specifically with regards to disparity.

Analysis 2: Motion-disparity. Secondly, activity was modelled for each individual motion-disparity stimulus against a baseline of static binocularly uncorrelated dots, in order to explore the overall functional organisation of hMT+, MST, and V5/MT to motion and disparity. One contrast for each stimulus presented within a block (Table 5.1) was modelled, coded by contralateral disparity, creating 15 contrasts in total.

Analysis 3: Direction of motion selectivity at positive and negative disparities. Finally activation was modelled for rightward & downward motion, and leftward & upward motion, at both contralateral positive and contralateral negative disparities, versus a baseline of static binocularly uncorrelated dots. This activity was modelled by creating contrasts that combined activations to either left or upward, and right or downward stimulation, at either positive or negative disparities in the contralateral visual hemifield (4 contrasts). The purpose of these contrasts was to explore whether it was possible to observe a direction map reversal with disparity reversal in area MST.

In all cases, overlap between clusters of active voxels was resolved by presenting the cluster or voxel with the highest intensity value.

It is important to note here that as there was no measure of participant fixation (though a fixation point was present, and subjects were instructed to observe it at all times), it is possible that some spatial representation of disparity and motion may have been lost if they eyes shifted or were incorrectly fixated. That said, over half of the participants were very experienced in long periods of fixation during psychophysical tasks.

Repeatability

In order to ensure that the activation patterns were reliable, and therefore likely to reflect actual underlying functional structures within hMT+, I repeated the third set of scans for motion and disparity for 3 subjects. Analysis of these scans was conducted as for 'Analysis 2: Motion-disparity'. Using custom MATLAB scripts, I calculated the overall percentage of spatial correspondence for voxels above threshold between binarised scans over the whole cortex, and compared that with the same value calculated for the area hMT+, for each contrast. The mean of these percentages was taken. A t-test was performed to assess whether the spatial location of voxels active above threshold within area hMT+ differed significantly between the two scans for each individual.

Functional cluster size

As distances between vertices can be distorted on an inflated surface and undergo different levels of stretch based on location, the scale bars provided in Freesurfer cannot reliably measure the size of structures across the inflated cortex. A cluster was defined as a contiguous region of activation. The size of activation clusters was assessed using a vertex-to-vertex measurement with the Freesurfer tool *mris_pmake*. Measurements were taken at the maximal x and y axes across the cluster. To assess to what extent different stimulus conditions activated area V5/MT, hMT+ and MST, the fslmaths function of FSL was used to output number of voxels activated above threshold within each aforementioned region of interest.

5.3 Results

5.3.1 Disparity Maps

DeAngelis & Newsome (1999) demonstrated that across macaque V5/MT, there are patches of neurons responsive to near and far disparities. As such, we would expect a similar trend in across at least most of human hMT+. The stimulus I used had two disparity conditions ('near' and 'far'), as in macaque V5/MT near and far tuning curves of individual neurons are quite broad (Deangelis & Uka, 2003). The data show patches of contralateral visual hemifield disparity selectivity across hMT+, in concurrence with previous results in the macaque (Figure 5.1). The disparity stimulus also activated area V1 in all subjects, and potentially area V3 (though this was not specifically localised) - areas both associated with disparity sensitivity (Anzai et al, 2011; Okazaki & Fujita, 2010; Cumming et al 1999; Prince et al 2002).

In some instances, the activation within hMT+ also extends outside of the functional definition. This could be the product of increased attention on the part of the participant to the motion-disparity stimulus relative to the hMT+ localiser - attention is known to modulate fMRI signals specifically in the visual cortex (Somers et al, 1999). This increase in signal, potentially as a product of greater blood flow modulated by increased attention, could result in an overestimation of disparity patch size relative to the underlying neuronal grouping. Most participants were not experienced in long periods of central fixation, and eye movements away from fixation could also have produced this effect.

The proportion of voxels active in area hMT+ for either near (negative) or far (positive) contralateral disparities indicate that for the majority of subjects, there is no

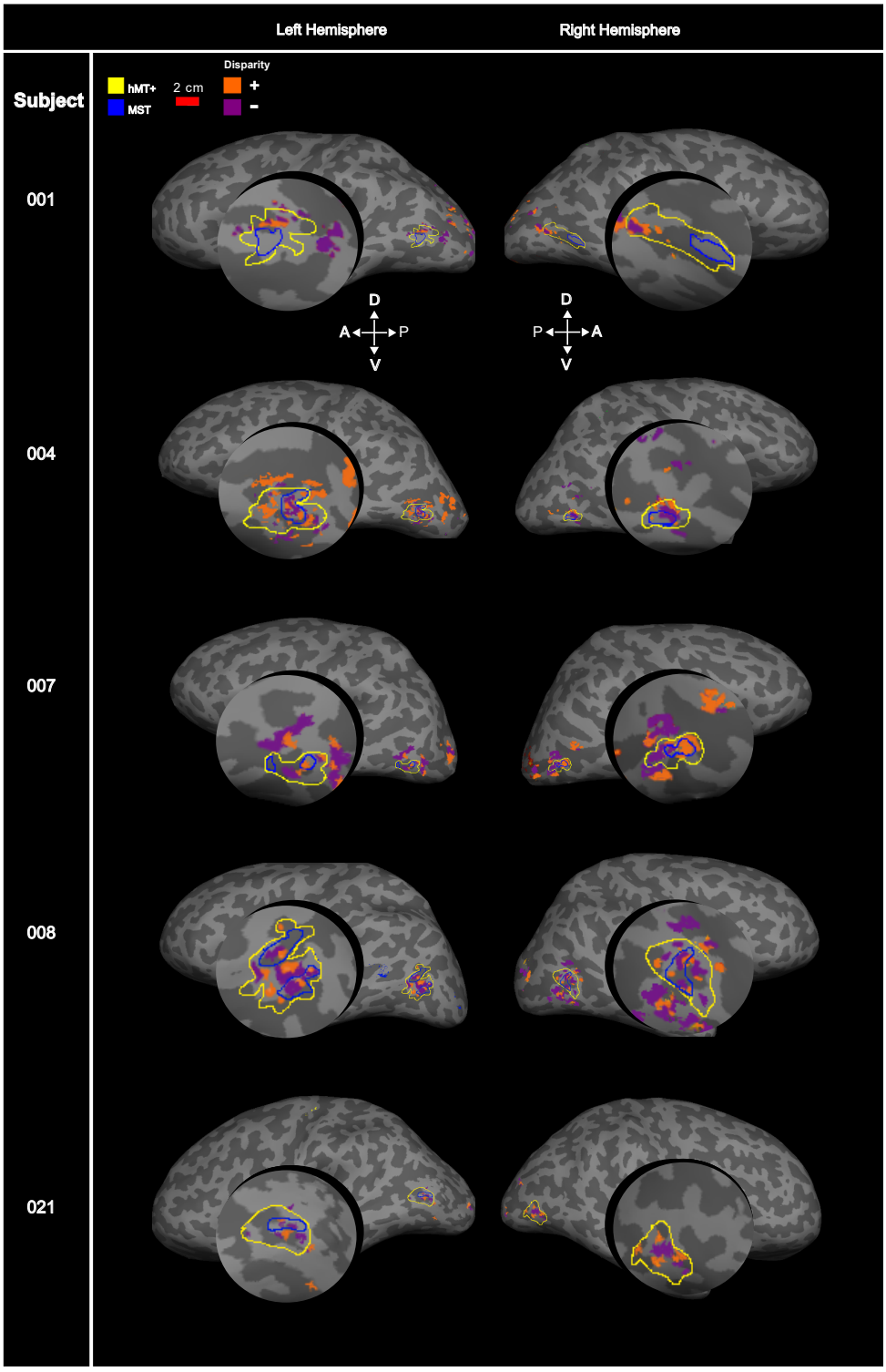

(a)

Figure 5.1: Positive (far) and negative (near) maps across individuals.

Contralateral reponse to far disparity is shown in purple, near disparity in orange, versus response to static full field uncorrelated dots. The functional definition of hMT+ is shown in yellow. The data show a pattern of near and far disparity patches repeating across area hMT+. Orientation crosses are shown for both left and right hemispheres. In cases where clusters overlapped, the cluster with the higher intensity value is shown. Overlap occurred for <0.06 of patches.

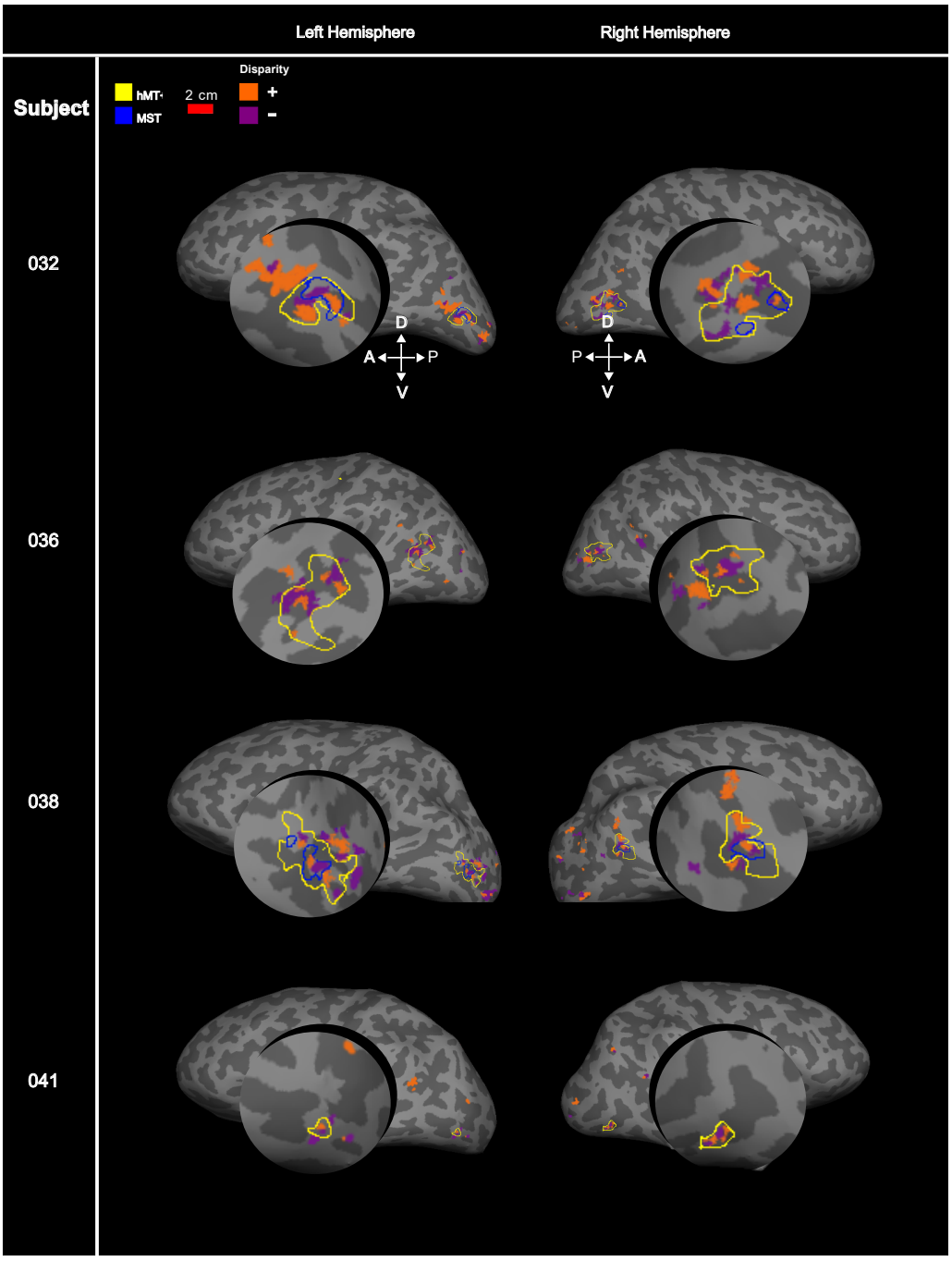

(b)

Figure 5.1: (cont.) Positive (far) and negative (near) maps across individuals
Same convention as in Figure 5.1 (a).

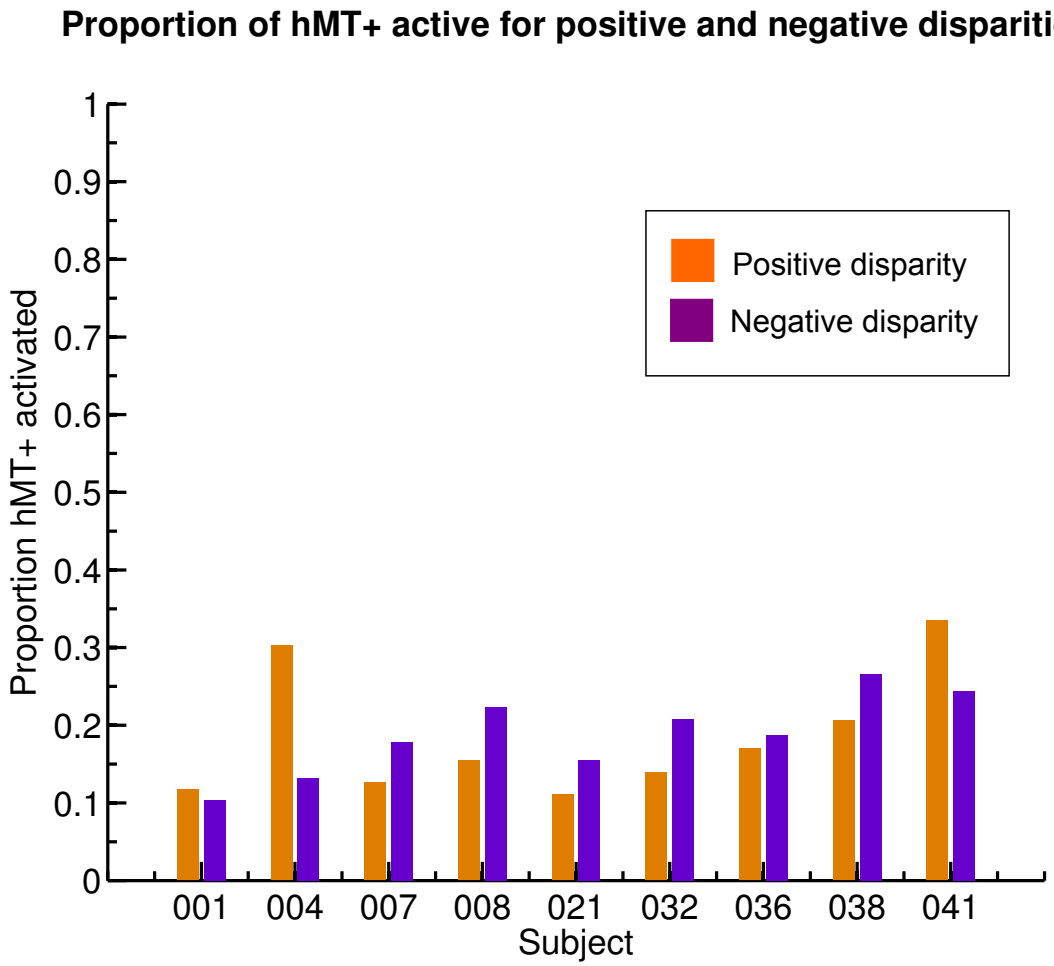

Figure 5.2: **Proportion of voxels in hMT+ active in each subject for far and near disparities of the contralateral visual stimulus**
Data are shown for proportions without adjustment for overlapping regions. Orange bars indicate far (positive) disparities, purple near (negative) disparities. The data show that there is no preference in representation for either disparity, other than for subject 004. Proportion active ranges from 0.1-0.32 of area hMT+.

preference for near or far disparities - other than subject 004, who shows an activation preference for far (positive) disparities (Figure 5.2). Overlapping areas of activity between the two activation patterns were not removed for this analysis. Subregion MST responds to both ipsi and contralateral stimulation (unlike area V5/MT, which does not respond to ipsilateral stimulation, see Huk et al 2002), so it is important to note that some activation within area MST may be assigned the incorrect disparity sign, as activations were contralaterally coded. Up one third of area hMT+ was active for an individual in response to either near or far disparities. Deangelis and Newsome (1999) did find that parts of macaque V5/MT were not responsive to disparity stimulation. The pattern of active and inactive regions could represent a similarity in functional organisation between human and macaque in this regard.

Overall, the data suggest that there might be a patchy organisation of disparity selectivity across hMT+, similar to that found in the macaque (DeAngelis & Newsome, 1999). This suggests that hMT+ might have a columnar organisation specific to disparity, which could be probed further using a gradual step disparity stimulus.

5.3.2 Direction of motion maps at different disparities

Albright (1984) examined the representation of motion in macaque V5/MT using electrophysiology, and showed that each direction of motion activated a column of neurons orthogonal to the cortical layers, with preferred direction changing systematically when moving along a cortical layer parallel to the surface. He found that selectivity for 360° of motion was represented across 1mm of cortical surface. A comparison of similar homologous structures between humans and macaques indicates a hypothetical scale factor of around 2 - ocular dominance columns measure at between 400-700µm in

macaques (Horton et al, 1996) and 800-1400µm in humans (Adams et al, 2007). As such, we could expect to see 360° of motion represented across approximately 2mm of cortex in the human. With a scan resolution of 1 x 1 x 1mm, our data should be sufficiently high-resolution to differentiate between some directions of motion, though not high enough to capture all individual columns.

Figure 5.3 shows that in hMT+, discrete clusters are activated in response to specific directional stimuli, which was the case for all tested subjects. Further to this, in some subjects (001 lh, 004 rh & lh, 008 rh & lh, 036 lh) there are distinct alternating patterns of preference direction that repeat across the surface of hMT+, rather than single regions of activation for each stimulus. The proportion of voxels within hMT+ that responded to specific directions of motion was variable between individuals (from 3 to 35%, Figure 5.4), but generally, each direction activated voxels in hMT+. These results suggest that human hMT+ might have a columnar organisation for specific directions of motion, and that we can detect underlying groups of neurons selective for specific directions of motion - similar to the findings of Albright et al (1984). Larger regions of activity than predicted may have been detected due to the resolution of the scanning protocol.

5.3.3 Disparity-motion activation patterns within area MST

While area V5/MT in the macaque is associated with a direction of motion map that is mostly separable from binocular disparity (DeAngelis & Newsome, 1999; Smolyanskaya et al 2013), neurons in neighbouring region MST are known to reverse their direction preference when disparity is reversed (Roy et al, 1992), showing what disparity-dependent direction selectivity. In the human, areas V5/MT and MST form subregions

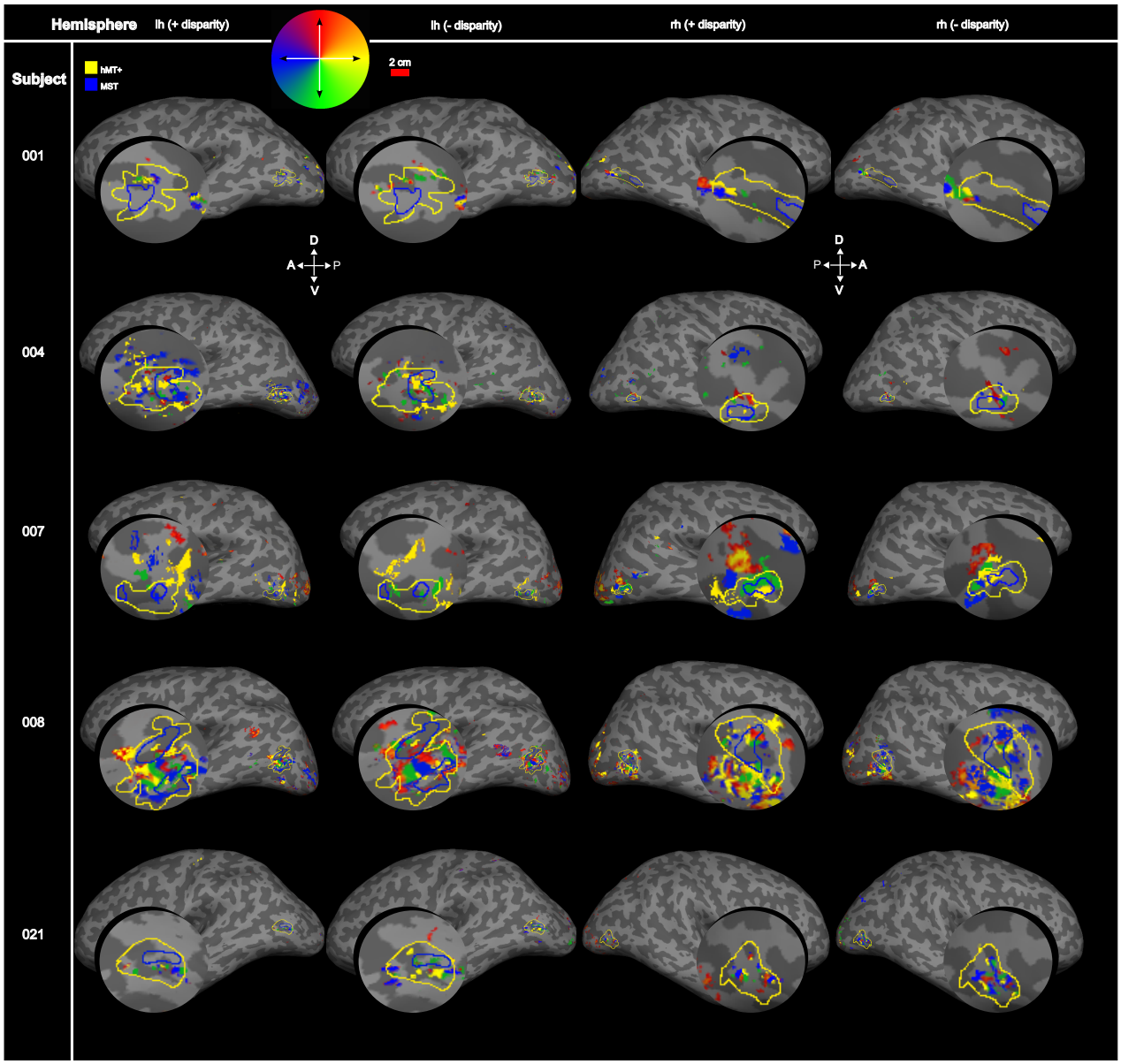

(a)

Figure 5.3: Direction maps at different disparities

The data show discrete clusters of activation in response to 4 different motion directions at two disparities. Visual motion directions are represented on a colour wheel, with hemispheres and disparities shown in separate columns. The data suggest a functional organisation of hMT+ by direction of motion. Area hMT+ is indicated with a yellow outline, and area MST with a blue outline.

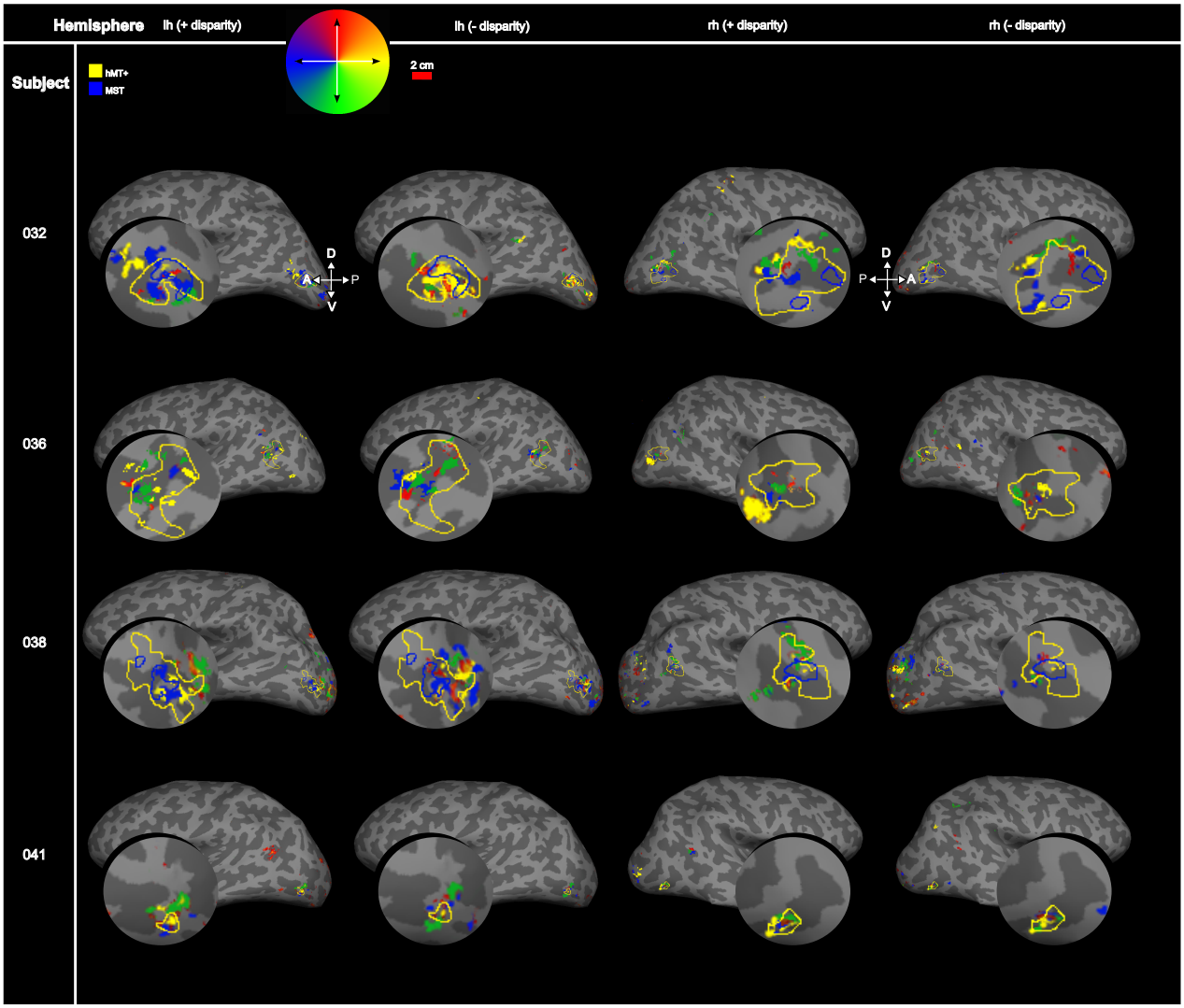

(b)

Figure 5.3: (cont.) Direction maps at different disparities
Same convention as in Figure 5.3 (a)

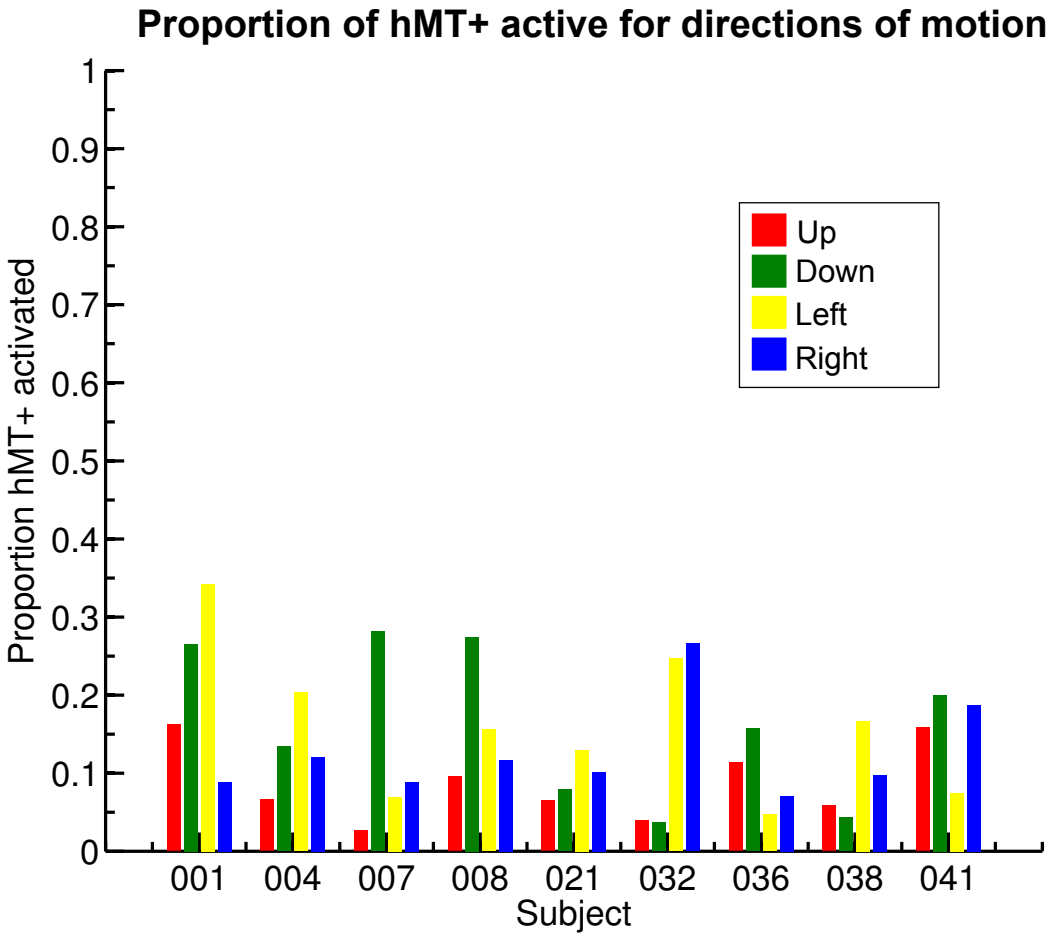

Figure 5.4: **Proportion of voxels hMT+ active for different directions of motion, averaged across near and far disparities of the contralateral visual stimulus**

Red indicates upward motion, green downward, yellow leftward, and blue rightward. The data show activations for all directions, with individual variation in the proportion activated by each direction. Proportion active varies from 0.03 to 0.35.

of area hMT+. From this, we would expect that within functionally defined MST, a reversal of disparity from far to near (or vice versa) would lead to a reversal in motion selectivity. If this theory holds in human MST, activation for a negative (near) disparity upward moving stimulus should overlap with activation for a positive (far) disparity downward moving stimulus within MST.

In order to test this theory in individual subjects, activation for the four directions of motion in the stimulus were combined into two 180 degree motion contrasts (left & up, right & down), each at either positive or negative contralateral disparity (creating 4 contrasts in total). This served the purpose of simplifying the pattern we expected to see across area MST by increasing the size of active patches. Following from the macaque, where each individual's MST was activated by rightward & upward motion at a positive disparity, we would expect it to be activated by leftward & downward motion at a negative disparity - a pattern of reversal that should not be repeated outside of area MST. The activation patterns of these contrasts at positive and negative disparities within and outside of area MST were compared (Figure 5.5). It is important to note that area MST was defined in this study using ipsilateral stimulation (see Methods), though it does respond to both ipsilateral and contralateral stimulation. As the contrasts were coded for by contralateral disparity in this analysis, some activity specific to area MST may be incorrectly defined, or extend out of the borders of this specific ipsilateral definition of MST.

For 11/15 hemispheres, reversing the disparity also reversed the direction of motion selectivity exclusively within area MST, as would be predicted from the macaque data, with relatively consistent spatial activation of reversed motion preference clusters. For the other hemispheres, there are indications of this motion-direction preference reversal,

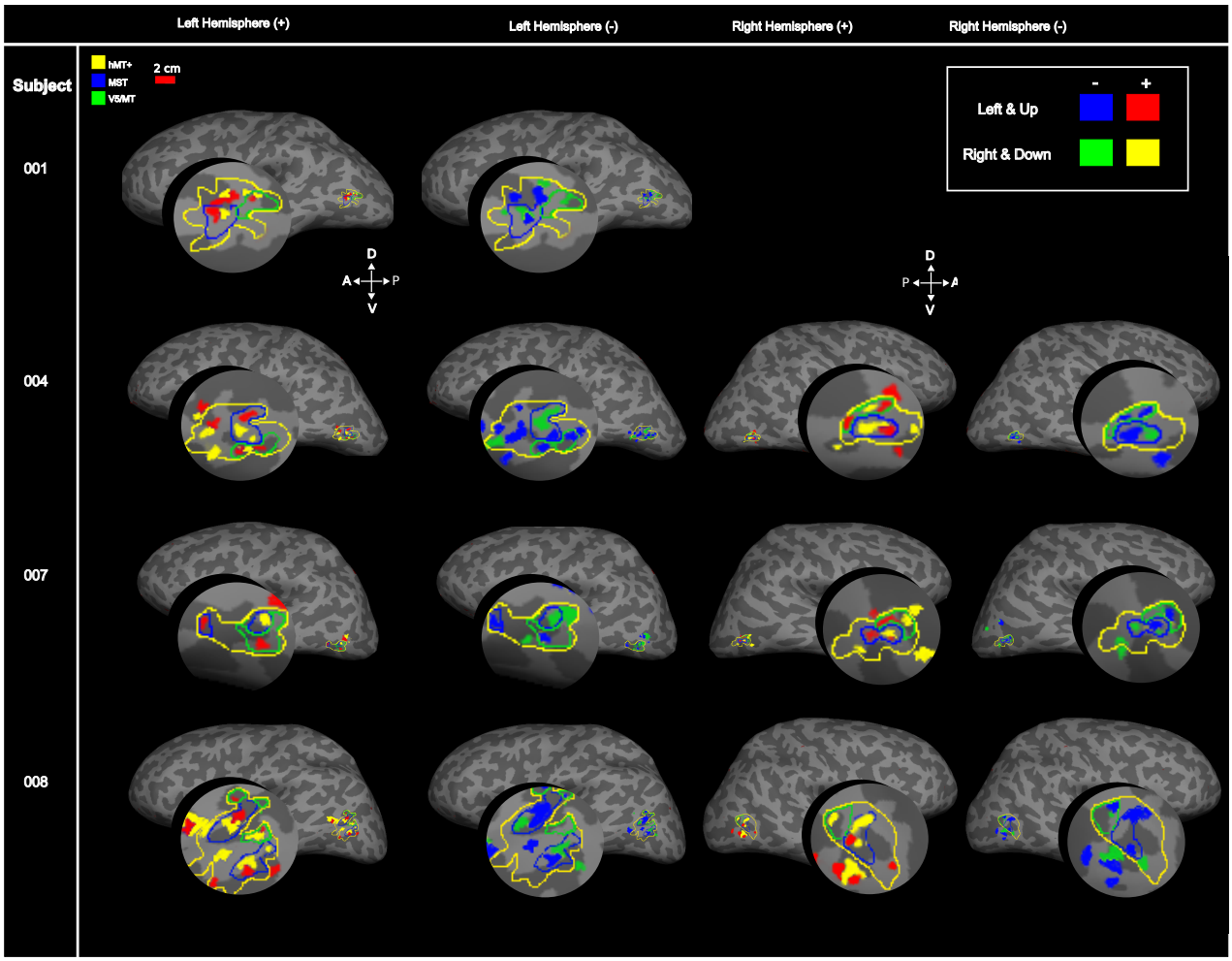

(a)

Figure 5.5: 180 degree motion maps at positive and negative disparities

Area MST is outlined in blue, area V5/MT in green. Four contrasts are presented: activation for leftward + upward motion combined presented at either contralateral negative (blue) or contralateral positive (red) disparity, and activation for rightward + downward motion combined presented at either contralateral negative (green) or positive (yellow) contralateral disparity. For each hemisphere there are two columns, one showing activation at positive (far) and one at negative (near) disparities, contrasting regions that respond to leftward + upward, or rightward + downward motion. The images are not overlaid in order for regions of overlap or reversal at the different disparities to be clear. For one subject (001), the left hemisphere is not included as there was insufficient activation for the combined contrasts.

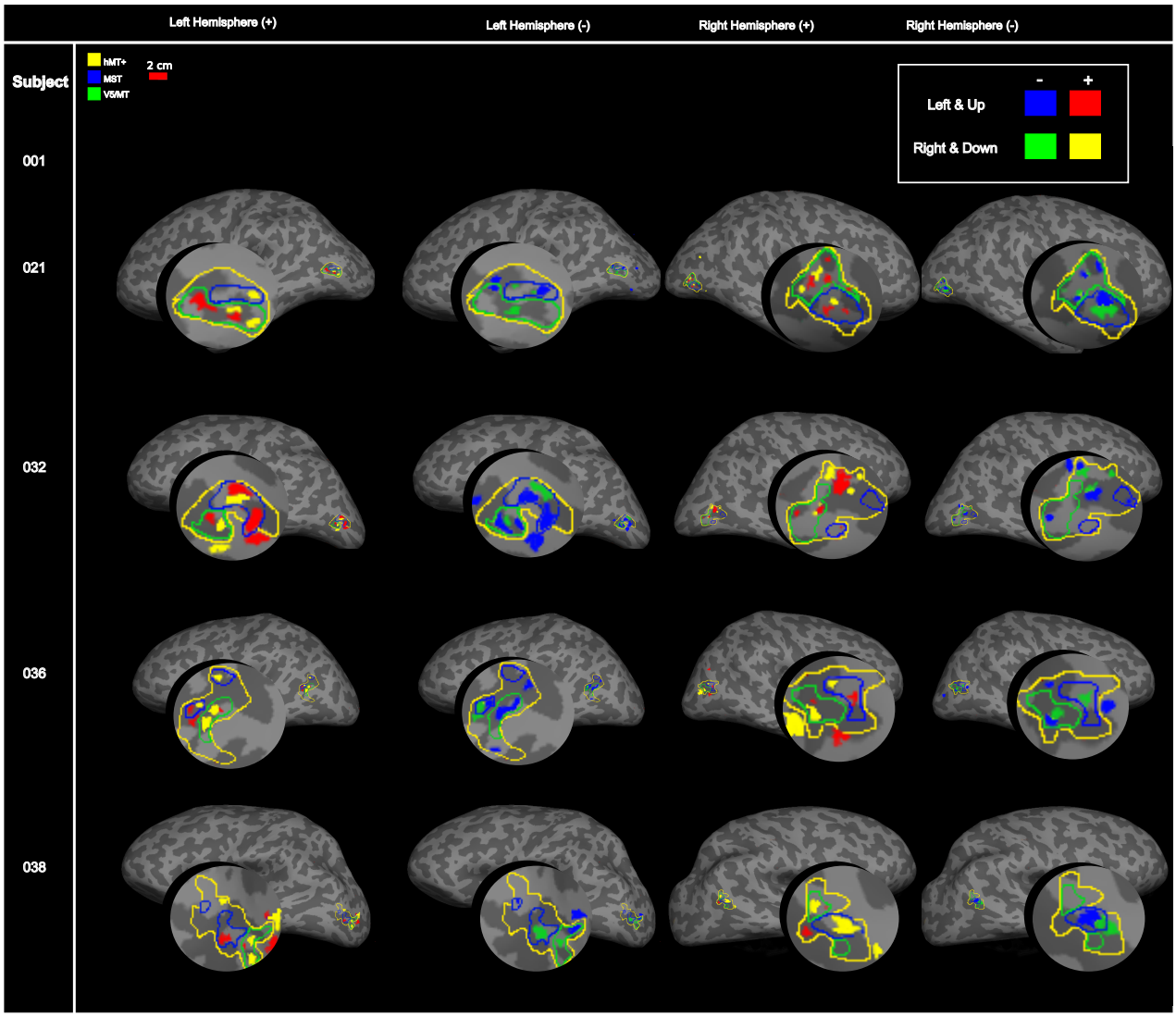

(b)

Figure 5.5: (cont.) 180 degree motion maps at positive and negative disparities
Same convention as in Figure 5.5 (a).

but with imperfect spatial location. Figures 5.2 and 5.4 provide one explanation for the imperfect spatial location match for different directions of motion or disparity in some subjects: in response to specific aspects of the stimulus, the proportion of area hMT+ activated in total is quite variable between individuals. As such, we would not expect the proportion of hMT+ active for rightward & downward versus leftward & upward motion to match, leading in turn to an imperfect spatial match. This also applies to activation cluster sizes for positive versus negative disparity.

Although spatial location of the reversal in direction preference is not perfect for all subjects, there is a general trend for reversal in direction preference when disparity changes from near to far in all hemispheres for all subjects. This supports the idea that human MST may be similarly organised to macaque MST, though the scan resolution may have hindered perfect spatial matching of the reversals observed.

5.3.4 Repeatability of functional scan data

To determine whether the functional scan for columns data were reliable, the motion-disparity scan session was repeated for 3 subjects (001, 021, and 032). Data were thresholded as per the Methods, and binarised such that all data above threshold had a value of 1, and all below a value of 0. They were then analysed on a voxel-by-voxel basis to compare the level of spatial correspondence in above-threshold voxels between the scans. Correspondence across the whole cortex (where we would not expect a high level of replication due to lack of specific activation in response to the stimuli) and correspondence within the region hMT+ (where we would expect replication due to its specific selectivity for the motion and disparity aspects of the stimuli) were taken for each stimulus, and the mean correspondence across all stimuli was calculated (Table

Subject	Mean WCC	Mean lh hMT+ corr.	Mean rh hMT+ corr.	Mean corr. shuff. hMT+
032	4.84%	49.30%	73.24%	5.01%
001	7.06%	51.44%	31.66%	3.27%
021	6.34%	38.37%	46.54%	3.99%

Table 5.2: **Repeatability of functional scan data for 3 subjects who underwent the functional organisation scan twice on separate days**
The first column indicates mean spatial correspondence of active voxels between scans for each stimulus individual motion-disparity stimulus across the whole cortex.WCC = whole cortex correspondence. The third and fourth columns show mean spatial correspondence for activation in response to each individual motion-disparity stimulus within area hMT+ for the left (lh) and right (rh) hemispheres respectively. The last column shows the mean correspondence for scans spatially shuffled (shuff) within hMT+. It is clear from these results that the data have a much higher correspondence than chance within area hMT+.

5.2).

The repeat scan data are shown for each individual in Figure 5.6. Mean correspondence in area hMT+ was consistently higher than whole cortex correspondence (31-73% versus 4-7%), conforming that this area was selective for motion and disparity relative to the rest of the cortex. Higher spatial correspondence in hMT+ relative to whole cortex also suggests that correspondence between scan days within this area was higher than chance. Data within hMT+ were also spatially shuffled in order to assess correspondence against 'chance'. Shuffled datasets showed a correspondence of 3-5% within hMT+, much lower than the correspondence between actual datasets. A visual inspection of the data (Figure 5.6) also shows the reasonable correspondence between scan days of clusters activated by different directions of motion at different disparities. Similar areas for each stimulus are active, albeit with varying spatial sizes - potentially the product of physiological noise or head movement between days and within scans.

Overall, the results suggest that correspondence was higher than chance across area hMT+, and that activation in this area to individual stimuli was not significantly different between scans (Student's t-test, as indicated by the non-significant p-values

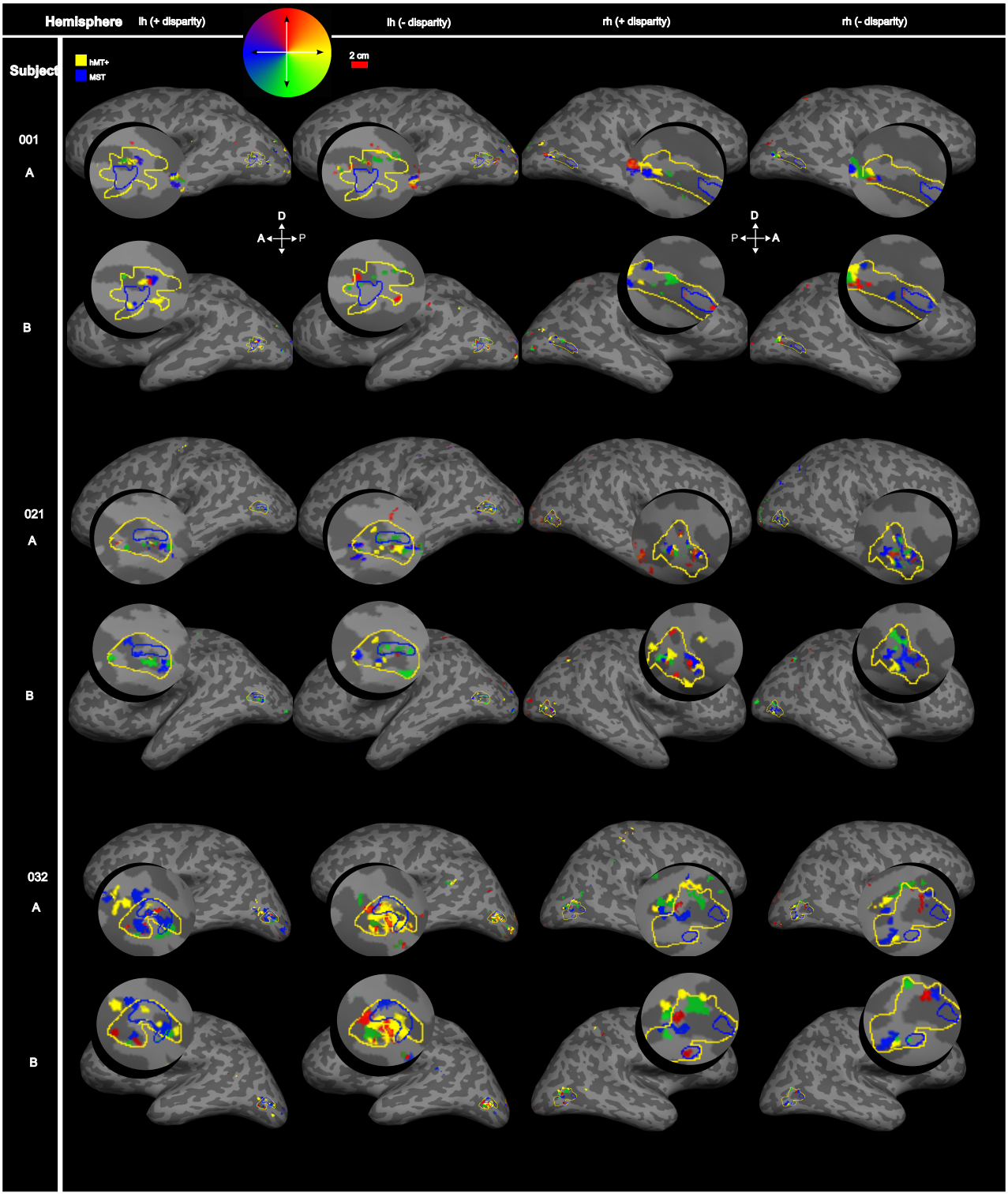

Figure 5.6: **Repeatability of scan data between sessions for three participants**
'A' indicates the first day scan, 'B' indicates the second day scan. Area hMT+ is indicated with a yellow outline, and area MST with a blue outline. The data show that data clusters for specific directions of motion at different disparities are reasonably repeatable between subjects (for percentage repeatability, see Table 5.3). Visual motion directions are represented on a colour wheel, with hemispheres and disparities shown in separate columns. The data suggest a reliable functional organisation of hMT+ by direction of motion.

in all cases). Though the spatial correspondence is not perfect, the data suggest that activation in response to the stimulus arises from the same physically located cluster of neurons, albeit with different haemodynamic spread. This, in conjunction with the low levels of correspondence across the cortex as a whole, suggests that with the motion-disparity stimuli, I could detect neuronal structures selective for specific directions of motion and disparity within hMT+.

5.3.5 Size of functional clusters

In order to assess the activation patterns seen across area hMT+ qualitatively, and whether or not they might be related to the areas defined by electrophysiology in the macaque, preliminary measurements of size and cluster number were taken. One cluster was visually defined as a contiguous region of activation. Cluster size for either direction-responsive activity or disparity-responsive activity was calculated within Freesurfer along the maximal x and y-axes of each cluster (see Figure 5.7 for visual examples, Table 5.3 for results). These are only preliminary measurements, to give an indication of potential activation size along the cortical layers.

Albright et al (1984) showed selectivity for 360 degrees of motion across a milimetre of cortex. Given a putative scale factor of 2, we might expect to see selectivity for 360 degrees across 2mm of cortex, and we might expect that a single direction of motion (representing 90 degrees) would activate 0.5mm of cortex. This scale factor does not hold for our data, with the reported measurements ranging up to 6.22mm for one direction of motion. Likewise, activation cluster sizes for disparity at their largest were orders of magnitude beyond those predicted by electrophysiology. Overall cluster dimensions range from 1.16 to 6.22mm for direction selective clusters, and 5.33 to

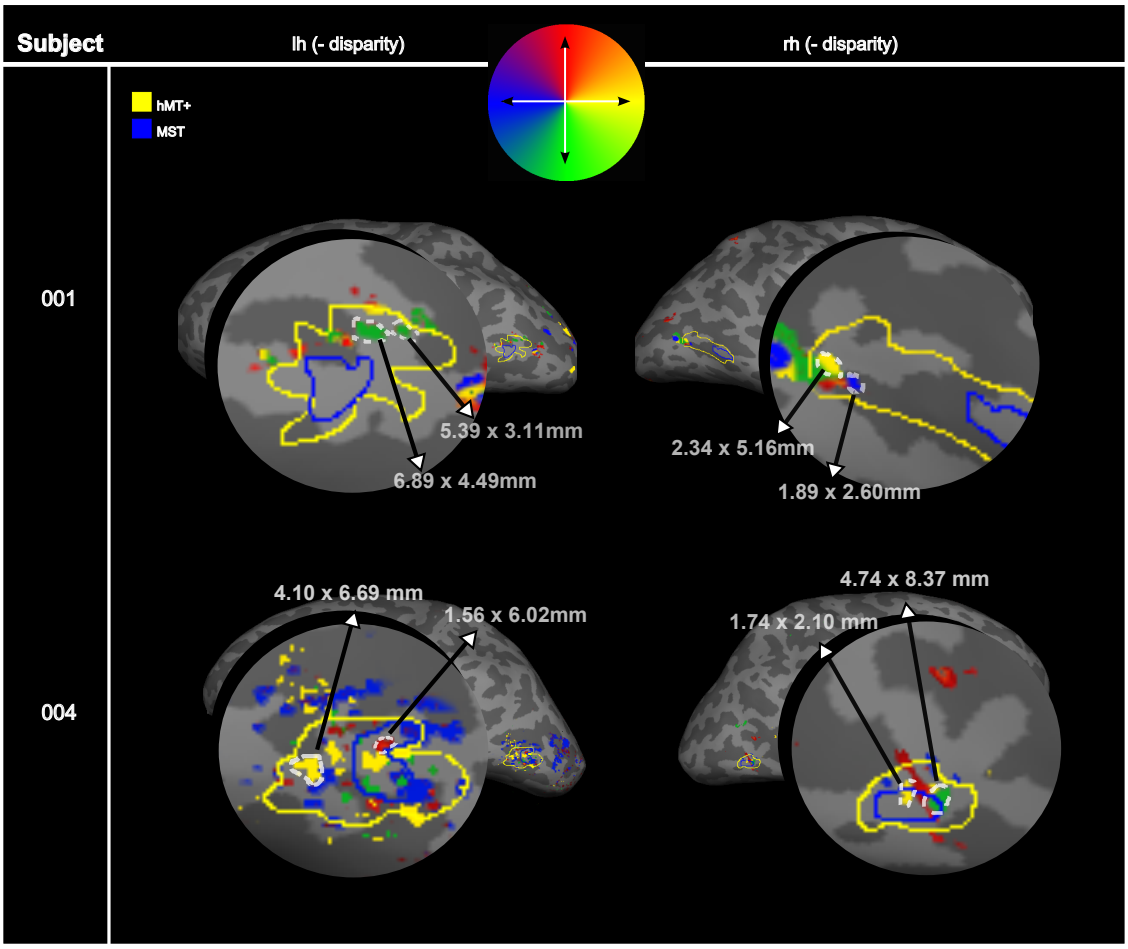

Figure 5.7: **Examples of measurement of activation clusters for direction at negative disparity for two subjects**

Two example subjects are shown. White dashed outlines indicate the cluster whose measurements are indicated by a single arrow. Measurements were taken along the maximal x and y axes using Freesurfer function *mris_pmake* to compensate for the differential stretch places on vertices on an inflated surface misrepresenting distance. The data indicate that regions activated are larger than putative columnar structures (which would be estimated to be 0.5mm for 90 degrees of motion), and as such may represent larger clusters of direction selective columns.

	Direction		Disparity	
Subject	**Avg. dimensions (mm)**	**Mean cluster number (1s.f.)**	**Avg. dimensions (mm)**	**Mean cluster number (1s.f.)**
001	4.33 x 5.32	4	6.82 x 27.29	3
004	2.16 x 1.38	8	15.41 x 6.95	4
007	6.22 x 2.54	3	10.68 x 54.15	2
008	2.45 x 3.18	9	29.45 x 14.11	5
021	1.17 x 1.86	5	9.82 x 7.93	3
032	4.51 x 2.10	5	31.82 x 5.33	3
036	3.36 x 2.92	4	43.81 x 19.21	3
038	3.39 x 1.49	6	12.19 x 9.51	2
041	1.16 x 1.23	3	8.17 x 12.86	2

Table 5.3: **Average dimensions and mean numerical count of activation clusters responding to direction or disparity across all subjects within area hMT** Mean direction cluster number (regardless of specific direction) per subject is shown in the third column. Mean disparity cluster number (regardless of sign) per subject shown in the fifth column. Specific direction and disparity sign were disregarded to compensate for the fact that there were fewer disparity stimulus contrasts relative to direction (two versus four). The data indicate that disparity clusters are fewer in number and greater in size than direction selective clusters. For some subjects (008, 036) disparity clusters are much larger than would be predicted from macaque data, and likely represent multiple clusters that overlap in regions of activation.

54.15mm for disparity selective clusters. Consistent with electrophysiology, however, there were always more direction-selective clusters than disparity-selective (Figure 5.8). That said, I also used more stimulus contrasts for direction than disparity. As such, this requires further investigation.

The data suggest directional cluster sizes sufficiently small enough to potentially encompass groups of neurons selective for one specific direction of motion. Disparity cluster sizes were much larger than would be predicted. This could be the product of less variance in the disparity aspect of the stimulus - supported by the fact that there were fewer disparity clusters on average within hMT+. Although the size of the clusters does not match the previous electrophysiology, the relationship between the number of direction and disparity clusters is potentially supported by the data.

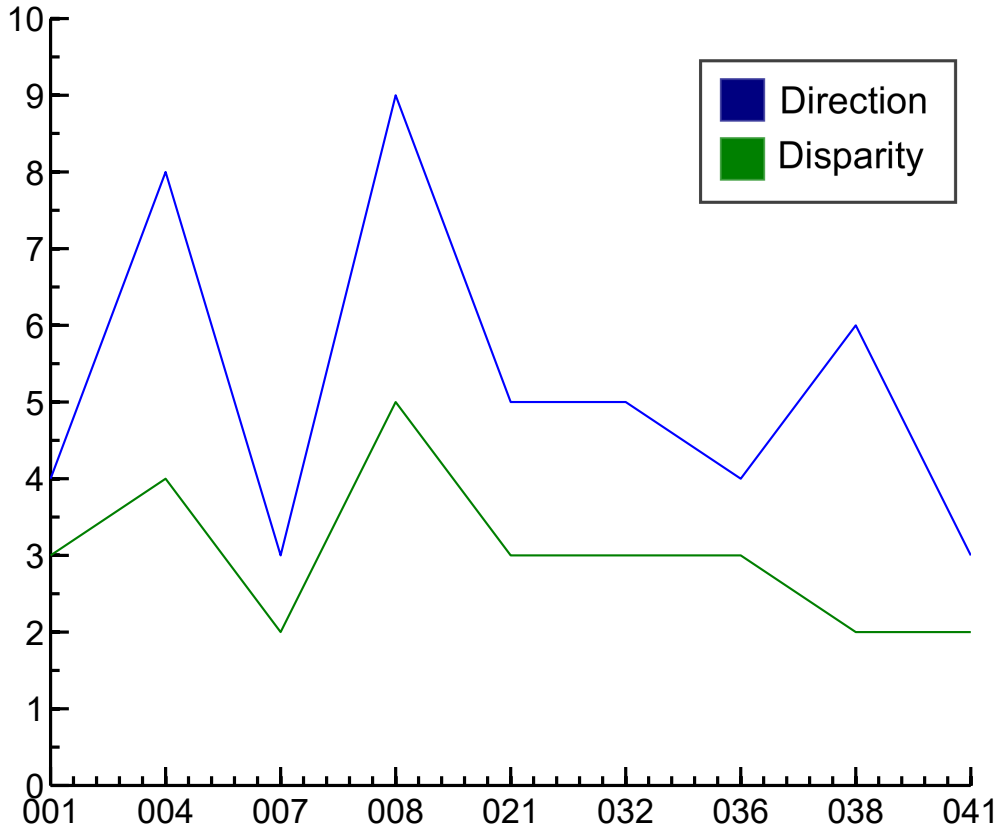

Figure 5.8: **Graph of average cluster number of different participants for direction or disparity**

The data show that there are consistently fewer clusters for disparity. The x-axis indicates subject, the y-axis number of clusters.The blue line shows number of direction clusters, the green line the number of disparity clusters. Specific direction and disparity sign were disregarded when counting clusters, in order to compensate for the fact that there were fewer disparity stimulus contrasts relative to direction (two versus four).

5.3.6 Summary

Overall, the data show plausible evidence for the detection of reliable neuronal clusters selective for both direction and disparity in area hMT+, with a pattern (though not cluster size) comparable to that found in electrophysiology for the macaque. I have found some evidence for a reversal of direction selectivity with disparity reversal in area MST, also predicted from electrophysiology. Though the results are preliminary, and likely hampered by the resolution of the scan protocol, they indicate that it may be possible to detect functional columnar structures in area hMT+ using high field fMRI.

.

5.4 Discussion

My results indicate that there are a number of similarities in the organisation of area hMT+ and macaque area MT. I show distinct repeatable patches of activation for near and far disparity (Figure 5.1), and distinct patches responding to specific directions of motion in a repeating pattern across the surface of area hMT+ (Figure 5.3). There are indications in some subjects that subregion MST represents direction and disparity differently to the rest of area hMT+, with direction preference reversing when disparity moves from near to far. Such work could lay the foundations for future in-scanner psychophysical experiments in which behavioural report could be coupled with sensory and perceptual representation within this region of the visual cortex.

It is important to note that for the majority of analysis, activation in response to stimuli was coded by contralateral stimulation. As each visual hemifield was contralaterally stimulated by one disparity, but ipsilaterally stimulated by the opposite disparity

(with directions of motion remaining constant), some activity in the contralateral brain hemisphere (left for right visual hemifield, right for left visual hemifield) could have potentially been ipsilateral activity in response to an opposite disparity. There may be some implications for this in the data. As hMT+ subdivision V5/MT is considered to be contralaterally activated (Huk & Heeger, 2002; Fischer et al, 2012), we would not expect to see ipsilateral activity represented there. However, some research in humans has indicated that V5/MT has weak ipsilateral responses (Martinez-Trujillo et al, 2007). That said, the study showing this was conducted using MEG, which has a very low spatial resolution relative to fMRI (Nunez, 1981; Hämäläinen et al, 1993). Given the size of area V5/MT, it seems unlikely that such ipsilateral activation was reliably spatially localised using MEG - and was more likely the product of neighbouring subregion MST (which has been shown to have both contralateral and ipsilateral responses, e.g. Huk & Heeger, 2002; Fischer et al 2012). As MST was ipsilaterally defined with the motion localiser, the MST reversal maps should have been driven by ipsilateral rather than contralateral activation. However, the results suggest that the disparity-motion stimulus was not affected by hemifield representation in this way, and that contralateral activation was sufficient to reveal reversal maps in area MST. That said, it is clear that further analysis should be conducted using the hemifield stimuli, in order to establish what drove which activation.

5.4.1 How are direction of motion and disparity represented in area hMT+?

An encouraging aspect of this work is the differentiation in motion representation at different disparities between area MST and the rest of hMT+, including area V5/MT.

While selectivity for direction of motion appears to reverse within MST when disparity changes from near to far, this does not occur external to MST (other than one cluster in area V5/MT for 036 left hemisphere, and 038 left hemisphere, Figure 5.5). This supports the notion of clear homologies for areas between macaques and humans that support direct inferences made about human brain activity in these areas based on data from monkeys.

The reversal of direction preference is not always spatially perfect (e.g. 021, right hemisphere, Figure 5.5) but there is a tendency for overlapping patches to reverse direction preference. The imperfect spatial location may be the product of small head movements or other sources of noise (such as physiological) that occur during scanning. Furthermore, data for the proportion of hMT+ activated in response to specific directions of motion or disparities showed individual variation (Figure 5.2, Figure 5.4), which could also cause an overestimation of cluster size in certain cases. Overall, the results for the MST reversal are encouraging - all individuals showed some degree of motion-direction reversal within this area, while not showing the same trend outside of area MST.

As would be predicted from the macaque data, there was a greater number of patches responsive to direction than disparity across hMT+ (Figure 5.7). However, the average dimensions of active patches extended well beyond the scope predicted by electrophysiological data from the macaque. This might be due to the resolution of the scans, or could reflect differences in the functional organisation between human and macaque. Disparity-selective clusters were consistently larger than direction-selective clusters, though it is apparent from Figures 5.2 and 5.4 that the overall proportions of hMT+ active to disparity relative to direction are similar. This discrepancy is

explained in part by Figure 5.7, which shows that there is a consistently higher number of direction-selective clusters than disparity-selective clusters. Given that our stimulus presented four directions of motion (up, down, left, right) relative to two levels disparity (positive or negative), it is unsurprising that there was a greater number of distinct direction clusters. It may well be that within the areas selective for positive or negative disparity, there exists an organisation responsive to specific gradations of disparity. As such, the disparity patches detected may have represented overlap between multiple clusters of neurons selective for positive or negative disparities. It should also be emphasised that the estimated scaling is based on a different region of the brain, area V1, which may scale up in a different manner than area hMT+. Future research into increasing SNR and improvements in the effective fMRI resolution, with more fine grain stimuli and analysis, may be helpful in resolving this issue.

5.4.2 Is functional activity reliably located spatially?

Replicability of scan data is particularly important if small changes in activation at fine spatial detail are being assessed, in order to distinguish small scale activations from noise fluctuations. Inter-scan reliability for the three participants who underwent the functional motion-disparity scan twice appears to be much greater within area hMT+ than across the cortex as a whole. Due to participant movement in the scanner, subtle differences in registration, and participant attentional differences, we would not expect the location of peak activity in a cluster of voxels at this spatial resolution to be equal between scans. As distortion caused by different head positioning and movement on different scan days can cause the precise location of activity to vary (Qin et al, 2012), smaller patches of activity could be lost overlap analyses.

However, in spite of these impediments, mean correspondence for activity in response to stimuli between scans reached up to 73.24% (Table 5.2) within the are hMT+. When compared to a maximum value of 7.06% across the cortex as a whole, the level of replicability is high. Further to this, statistics indicated that there was no significant difference in activation between the scans for hMT+. Given the reasonable level of replication between scans, I conclude that the functional data were reliable and may be derived from a real underlying functional organisation of neurons into direction and disparity selective groups.

5.4.3 Conclusions

Though macaques have been used as a model for human cognitive experiments requiring invasive techniques for decades, direct links demonstrating that proposed homologous areas are functionally organised in similar ways are hard to come by. These data provide some evidence that visual motion area hMT+ may be organised similarly to the macaque MT-MST complex - in principle, though not scale. Further experiments to compare fMRI responses in the macaque to similar stimuli as used in the human could provide direct links between the electrophysiology and the fMRI, allowing inferences to be made about human process from macaque data with greater confidence.

Excitingly, this dataset in itself provides the basis for potential future perceptual behavioural experiments in the scanner. By mapping an individual's functional organisation in this way, and subsequently conducting behavioural scans using stimuli that combine motion and disparity that are known to activate this region (for example, structure-from-motion cylinders), changes in brain activation patterns in specific columns could be investigated to link sensory activity to behavioural responses to the

stimulus - and therefore to perception. Experiments could be designed akin to neural studies in the macaque (Britten et al, 1996; Dodd et al, 2001). This would allow a non-invasive equivalent of electrophysiology, enabling us to explore the effect of social context (and indeed other contexts, such as reward) not only on behaviour, but also on perceptual representation in the brain.

Chapter 6

Discussion

"There are things known and there are things unknown, and in between are the doors of perception."

- Aldous Huxley, The Doors of Perception

My thesis aimed to explore the way in which contextual social information affects the perceptual decision making process in children, and to begin to lay foundations for examining their potential underlying neural basis. By running behavioural experiments in tandem with computational modelling, I have gained insight into the way in which social information impacts upon decision-making across children's development, and the potential perceptual effects of social influence. Structural and functional MRI have elucidated the organisation of one novel brain region, where the sensory signals for the decisions I studied behaviourally are represented.

Ultimately, the question I wanted to answer was whether one person was capable of changing what another person saw and perceived. Though there is more work to be done, it seems that the answer may be - 'yes'.

6.1 The effect of social influence on perceptual decision-making

As innately social beings, humans have long been interested in the effect of other people on our ability to process information. The effect of social influence on decision-making itself has been the subject of scientific study for more than half a century. However, previous studies have often focused on the way in which normative social influence (peer pressure) affects behaviour, rather than on the effect informational social influence (social information - see Chapters 1 and 2 for further discussion). Normative social influence by definition produces self-aware conformity, in which participants choose to alter their behaviour in order not to contradict a group of confederates, despite that behavioural decision potentially contradicting sensory information. There is a clear adaptive precedent for this behaviour - group integration and co-operation is and has been necessary for individual survival across the course of human evolution. Studies on normative social influence can only really provide insight on how humans respond to social advice at a behavioural level. By contrast, informational social influence acts as additional piece of sensory information - which has the potential to be integrated with other sensory signals (such as those from an experiment stimulus) in the decision-making process. Though there is also an evolutionary precedent for this (further group cohesion), whether or not there was significant enough evolutionary pressure to forge these pathways is unknown. We know that social influence can affect behaviour - what I aimed to discover was whether or not it could affect perception. The very nature of informational social influence provides the opportunity to examine the way in which social advice can affect sensory and perceptual processes, as well as behaviour. By

applying a computational model to behavioural data produced in an informational social influence paradigm, I have gained insight into the processes that underlie potential biases in behaviour.

6.1.1 Social influence across typical development

Previous research has suggested both that children as young as 4 respond to social influence (Haun & Tomasello, 2011), and that the effects of social influence when a stimulus is ambiguous increase with age until 14 (Hamm & Hoving, 1969). It has also shown that conformity effects in line with social influence are greatest when stimulus information is ambiguous (Iscoe et al, 1963). Given that the effects of social influence on behaviour appear to have a developmental course, we might assume that there should equally be a developmental effect on any perceptual effects. This study has expanded on previous work by using informational rather than normative social influence, by comparing the effect of advisor type on response to social advice, and by using a stimulus that can be both ambiguous or unambiguous without participant awareness - all across a critical developmental age range in humans. Furthermore, by using a computational model, it has been possible to study the effect of social influence at a deeper level than behavioural response alone.

The data show a clear change in the effect of social advice on the behaviour of typically-developing children. Regardless of whether the advisor was an adult or an age-matched peer, overall conformity in the direction of social advice increased with age, becoming a significant bias in behaviour (regardless of stimulus ambiguity) from 12 years, though the greatest effect is at the ambiguous level. This ties in well with anecdotal evidence and self-report data that has suggested children become more pre-

occupied with the opinions of other people as they progress through adolescence (Steinberg, 2005). For children between 6 and 8 years, there was no effect of social advice on behaviour, other than when stimulus information was ambiguous - at which point behavioural responses were significantly against the direction of social advice. This effect was slightly smaller when the advisor was an adult. Given that children have been shown to assess advisor expertise from an early age (3 to 6 years; Rakozcy, 2015), the slightly reduced contrarian effect with an adult advisor could be the product of greater perceived reliability. In contrast, although the middle age group, aged between 9 and 11 years, showed no significant effect of social advice on behavioural responses when advised by a peer, there was a significant contrarian response when the stimulus was ambiguous (similar to the youngest group) if they were advised by an adult. This could be the product of the transitional life stages that tend to occur in late childhood - events such as graduating from primary school or getting a mobile phone (69% of children have a mobile phone by the age of 11; Kaiser Family Foundation Survey, 2010) could increase their sense of independence from adults, and desire to form their own opinions - at least when information is ambiguous.

Given the clear behavioural differences in the age groups, it follows to ask what inferences can be made about their underlying causes - were the differences purely behavioural, or did they reflect an underlying perceptual change brought about by social advice? Although anecdotal evidence provides a behavioural explanation for the increase in conformity with age (an increasing preoccupation with other's opinions in adolescence), it does not answer the question of whether social information can affect how visual stimuli are perceived. By applying a drift diffusion model to the reaction time distributions of the behavioural data, specific parameter values can be

used to form hypotheses about mechanisms underlying decisions made in particular contexts (see Chapters 1 and 2 for discussion). Significant changes in drift rate (the rate at which a decision variable drifts towards a decision bound) suggest that responses may have been perceptually biased, while deviations in starting bound (the starting point from which a decision variable drifts) from the midpoint between two decision bounds may indicate judgmental bias. The parameter estimates from fitting the model to behavioural data suggest that the mechanisms underlying behavioural decisions made under social influence change from the age of 12 years. While the starting bound variable significantly deviated from the midpoint for 6-8 and 9-11 year olds, suggesting that their responses were affected by judgmental bias, the starting bound did not significantly deviate from the midpoint in the 12-14 year old group in any condition. However, the drift rate variable consistently increased in the direction of social advice for the oldest group. For the younger two groups, the drift rate variable never significantly changed with advice. Further to this, when drift rate was restricted in the youngest two groups, the model fit the data better - while it had a worse fit for the oldest group. The converse was true for starting bound. This suggests that perceptual bias may have been the underlying cause of behavioural conformity in the oldest age group, but did not affect responses for the younger two groups. It may be that this critical time period for the developmental of social influence integration has an evolutionary basis; pre-modern civilisation, children would typically become more family-independent around this age, and thus rely more strongly on group rather than family unit integration. The capacity to co-operate smoothly with a group outside of one's family unit may have been key to surviving this transitional stage.

These results taken together suggest not only that behavioural responses to social

influence change with the onset of adolescence, but that this change could be the product of a new underlying mechanism of social information integration developing in the brain. It follows to ask where these signals may be integrated. The functional homologue to area hMT+ in macaques (V5/MT) has been shown to play a role in perceptual decisions made about the stimulus used in the behavioural experiment (Krug et al, 2013) as well as showing sensory responses to specific aspects of the stimulus (Albright et al, 1984; DeAngelis & Newsome, 1999; Maunsell & Van Essen 1983; Dodd et al 2001). Changes in the equivalent human region specifically, or in areas connected to it that process social information, could be the physiological basis of this change. As discussed in Chapter 1, there are a number of candidate regions that have been associated with social information processing - the superior temporal sulcus (STS) (e.g. Allison & McCarthy, 2000), the orbitofrontal-amygdala network (e.g. Bachevalier & Loveland, 2006), and the occipital-parietal network (e.g. Berns et al, 2005). Two of these candidate regions share connections with area hMT+, one directly (human STS, Yeo et al, 2011), and one by merit of being part of a loop through the occipital lobe (occipital-parietal network), in which hMT+ is located. Interestingly, homologous area V5/MT in the macaque is located in the STS, and prior research has indicated that social group size directly predicts the amount of grey matter in macaque STS (Sallet et al, 2011), suggesting a link between grey matter development in this region and social interaction. In the same vein, while MRI has shown that grey matter increases up to the age of 12 in the frontal and parietal cortices, then subsequently decreases throughout adolescence (Gied et al, 1999; Sowell et al, 2003; Toga et al, 2006), grey matter in the STS continues to increase up until the age of 16 (Toga et al, 2006). Given that we observe behavioural conformity starting at the age of 12 in the data, this posits

the STS as a strong candidate for a region that may facilitate the integration of social information with sensory information processed in area hMT+. This is particularly the case given other research has suggested that the effects of social influence decline from around 16 years of age (Knoll & Blakemore, 2015) - the point at which grey matter in the STS also starts to decrease. The STS is also linked to numerous other social behaviours, positing it as a candidate social region not only for this particular thesis, but numerous other tasks involving social processing. Though research has not yet been conducted on potential changes in connectivity between the STS and hMT+ across development, it is a plausible neural substrate for the observed behavioural changes and increasing perceptual bias in response to social influence.

6.1.2 Social influence across development in children with ASD

Autism spectrum disorder (ASD) is characterised by deficits in social interaction and behaviour (DSM-V). As is discussed in detail in Chapter 1, children with ASD display unorthodox social interactions, which start in the first year of development (Osterling et al, 2002), and subsequently continue, with abnormal social behaviour and general social disinterest shown at all ages progressing through adolescence (Riby & Hancock 2008; Liebal, 2009; Chevallier et al 2012) and into adulthood (Bowler & Worley 1994; Izuma et al 2011). However, a study on how informational (rather than normative) social influence affects the behaviour of children with ASD across development had not yet been conducted. By conducting such a developmental study with age-matched typical peers I have gained some insight into the development of social influence processing both in typical children, and in those with ASD. While we would expect from previous research that normative social influence would have no effect on the decisions made by

children with ASD (as they tend to have no concept of reputation (Izuma et al 2011) or flattery (Fu & Lee, 2007; Chevallier et al 2012)), it was possible that they might have attended to information delivered in a non-normative context. That said, it has been shown that children with ASD throughout adolescence show inattention towards socially salient aspects of either real or imagined scenes (Klin et al, 1991; Riby & Hancock, 2008), and so one might also hypothesise that informational social influence would have no effect on behaviour, so long as social information was still perceived as socially salient.

Largely, the data fulfilled the prediction that informational social influence does not affect the behaviour of children with ASD, regardless of age. Unlike the typically-developing group (who showed an increase in conformity to advice with age), children with ASD slightly decreased in their behavioural conformity to peer advice as age increased. The youngest two groups (6-8 and 9-11 years) showed weak evidence for behavioural conformity when stimulus information was ambiguous, and this effect was gone by the age of 12. Furthermore, social advice had little effect on task accuracy. Though there are some caveats to the dataset as far as comparison is concerned (the n number of children with ASD at each age group is much lower than for the typical groups) the graphs in Appendix C show that in general, the individuals in each group follow the trend of the average data for the group. As such, group data are a reasonable representation of the individual's behaviour. From this, it is possible to conclude that social advice had little effect on the behaviour of children with ASD across development, and none by the time of adolescence. This behavioural finding is supported by countless other pieces of research that suggest children with ASD do not attend to social elements. Nonetheless, it is interesting to see that the youngest groups respond to social advice

to some degree - this may be the result of behavioural interventions (that encourage children with ASD to conform with their peer group), or a developmental change.

By applying a drift diffusion model to the reaction times from the behavioural data, as was conducted in the typically-developing group, some inferences can be made about the mechanisms underlying perceptual decisions made by the children with ASD. Model parameter estimates were very similar between all age groups, which suggests that there was little, if any, change in underlying mechanisms across development. The estimates for drift rate with advice were consistently low for conforming and non-conforming responses in children with ASD, and in general were strikingly similar to those estimated from data produced by the youngest two typically-developing groups, who showed no behavioural evidence for conformity to advice. In addition, starting bound estimates strongly deviated from the midpoint between the two decisions across all age groups for children with ASD, which suggests that any influence of advice on reaction times was due to judgmental rather than perceptual bias on decision-making. The model results overall suggest that children with ASD were not perceptually biased by social information. As such, we can infer that the small changes in behaviour between age groups were not the product of any developmental or mechanistic change, but simply in how the children chose to behave at different ages. This supports the idea that at younger ages, they may be being encouraged to integrate more with their peer groups by simply conforming.

It follows to ask whether there a is difference in brain development between children with ASD and typically-developing children which could explain their divergence in response to social information - particularly at the oldest age (12-14 years). As discussed in Chapter 1, abnormalities in myelination may be associated with the inci-

dence of ASD (see Deonie et al, 2015) - though Haar et al, 2014 found no difference in myelination between typical and autistic groups. Macaque area V5/MT, known to be activated specifically in response to the stimulus used in this task, is associated with perceptual as well as sensory processing of the stimulus (Dodd et al 2001; Krug et al, 2013), and known to be densely myelinated (Ungerleider et al, 1986). Functionally homologous human hMT+ is also theorised to be densely myelinated (Annese et al, 2005). As shown in Chapter 4, a region of dense myelination does associate with area hMT+ across both individual and average data in adults. Some of the behavioural differences observed could be explained by a reduction in the dense myelination around area hMT+, as this could reduce the speed of signal transmission. That said, area hMT+ is far from the only area involved in perceptual decision-making, even specific to this task - it requires input from a multitude of other regions that may also be implicated in ASD. If they do exist, differences in myelination cannot fully explain the behavioural and perceptual differences observed between the typical and ASD groups. As discussed in the prior section on typically-developing children, the STS is a likely candidate area for the integration of social information with sensory processing. Dakin & Frith (2005) have proposed that abnormalities in the STS exist in children with ASD. As the STS is a socially-associated region of the brain, this could explain why they show a lack of behavioural conformity and perceptual bias in the direction of social information across a broad variety of tasks. This explanation more fully encompass the consistent differences in behaviour during social tasks for people with ASD, and may provide a more satisfying explanation should it be the case.

Differences in myelination of area hMT+ and abnormalities in the development of the STS may together explain differences in sensory and perceptual processing under

social influence between the typical and ASD groups in this task. As with the typically-developing groups, research into connections between areas of the STS and area hMT+ across development in children with ASD could provide grounding evidence for this theory. Furthermore, a developmental study of myelination specific to the occipital lobe and area hMT+ in children with ASD and typically-developing children would give some insight into whether such changes in myelination could be one explanatory factor of the behavioural differences.

6.1.3 Conclusions

Overall, the data show that regardless of advisor, behavioural conformity to social advice increases with age in typically-developing children. These changes may be explained by computational modelling, which indicates that a bias in perception could affect the decisions made by the children above the age of 12. Children with ASD do not show either trend: behavioural conformity decreases with age, and computational modelling gives no suggestion that perceptual bias affects decisions. These differences might be explained by changes in connectivity between the STS and area hMT+, or potentially changes in myelination across development.

6.2 Localising visual perceptual regions

An obvious extension of behavioural work (including that discussed above) is to conduct such tasks in an environment that allows us to measure quantifiable differences in brain activity. Being able to identify accurately the visual regions underlying specific percepts on an individual basis is extremely important for carrying out behavioural experiments

using MRI, which focus on small activations within the identified region. Area hMT+, the region upon which my research has focused, has historically proved difficult to localise consistently in humans. This is likely due to its inconsistent anatomical location, which itself is potentially a product of the extremely variable sulcal patterning of the occipital lobe in humans (Thompson et al, 1996). Area V5/MT in macaque monkeys is a functional homologue of human area hMT+, and is associated with dense myelination (Ungerleider et al, 1986). *Post mortem* analysis of human brains has suggested that hMT+ may likewise be associated with myelin (Annese et al, 2005). Examining myelination density across the cortex posits a good method for consistently localising the areas it is associated with, as it is not tied to sulcal anatomy - but is a product of differences in the cortical cytoarchitecture. Myelin is a fatty tissue, and as such densely myelinated regions are associated with a different tissue water density than areas with less myelin. This means that such patterns may be detected by structural MRI - an imaging method that suffers less from the effects small head movements, physiological noise, and inattention to stimuli can have on functional MRI results.

Developing methods for detecting myelination *in vivo* may also prove invaluable for the numerous neurological disorders associated with abnormal myelination - such as autism. Considering that area hMT+ is associated with perceptual decision-making, and indeed can activate prior to area V1 when visually stimulated (Barbur et al, 1993), it may be that reduced levels of myelin putatively observed in autistic adolescents (Deonie et al, 2015) could be related to a decrease in social signal integration across this region when concerning specific structure-from-motion tasks known to generate choice probabilities within this region. Further to this, developmental changes in myelination in this region could reflect the differences in perceptual social influence integration

observed in typically developing children. I investigated the patterns of myeloarchitecture revealed across cortex in individual and average datasets for two T1-weighted structural scan protocols (MP2RAGE and T1w/T2w, see Chapter 1 for an in-depth discussion of these protocols), and tested how well they matched standard functional localisers in area hMT+.

6.2.1 Matching functional and structural definitions in the visual cortex

For group average data, both scan protocols showed a consistent alignment of dense myelination with functionally localised area hMT+. In the two primary subdivisions of area hMT+, V5/MT and MST, the group average T1w/T2w scan tended towards more myelination in the bordering region between V5/MT and MST, while the mean MP2RAGE showed an exclusive overlap with area V5/MT. While this does mean that two scans ostensibly detecting the same underlying cytoarchitecture were showing slightly different results at a smaller scale, it should be emphasised that neither scan protocol directly detects myelination. Both protocols produce signal intensities that are based on correlates of myelin; as the protocols are different, we should expect some minor differences in the location of regions of high intensity. Large areas known to be densely myelinated in human cortex, such as V1 and the central sulcus, reliably corresponded between scans on a bigger scale, while close inspection revealed local differences in signal intensity between scan protocols. This suggests that average structural data from these protocols may be good for anchoring the location of area hMT+, but not for subdividing it, or localising it independently of functional MRI, for individual subjects. It is possible that the protocols may not have been of suffi-

cient resolution to reliably detect precise patterns across subregions (1 x 1 x 1 mm for T1w/T2w, 0.7 x 0.7 x 0.7 for MP2RAGE), leading to partial voluming effects. Furthermore, the MP2RAGE scan was conducted at 7T, and the T1w/T2w at 3T. Given that 7T fields greatly improve the signal:noise ratio, the scan at 3T could have suffered from greater noise levels relative to the 7T protocol, which may have made areas of high signal intensity appear larger than they were. Given that the T1w/T2w protocol tended to show larger patches of high signal intensity, it seems likely that field strength may have played some role.

Individual myelination maps showed more variability in correspondence with functional localisers than the group average data. While most participants (irrespective of scan protocol) showed a region of dense myelination associated with functionally defined hMT+, there was no consistency in which sub-region it was associated with, or the degree to which the dense myelination overlapped with functional definitions. Given that comparisons of repeat data from a different day using the same scan protocol (MP2RAGE) in three subjects showed almost 100% correspondence in overlapping areas of high signal intensity, it seems plausible to suggest that the data simply reflect the variability of cortical myeloarchitecture at an individual level. The variability across individuals could also be related to the variance in cortical sulcal patterning, which could have affected the sensitivity of the MRI scan in different regions (as is discussed in Chapter 4). hMT+ was almost always functionally localised across a sulcus and gyrus, which could have affected data quality due to partial voluming of differentially orientated voxels (Clare & Bridge, 2005). As with the average data, in individuals the two scan protocols showed reasonable correspondence between areas of high signal intensity, suggesting that the structural scans were detecting changes associated with

real differences in the cytoarchitecture across the cortex when looked at on a broad scale. Finer details of myelination could have been obscured by partial volume effects.

6.2.2 Conclusions

Overall, the data suggest that there is a region of dense myelination associated with area hMT+, but not perfectly aligned with it or any specific subregion. As such, structural MRI may not yet be appropriate for independently localising visual region V5/MT in individuals, though it provides a good anchor for ratifying its functional definitions. This has implications for clinical application, and suggests that further development of structural MRI protocols for myelin detection would benefit studies based on individual participants or patients.

6.3 Exploring the functional organisation of area hMT+

If we are able to harness high field fMRI in order to reliably detect small clusters of activity in response to specific aspects of stimuli, it would be possible to conduct behavioural experiments in the scanner that provide insight into the participant's perceptual and sensory processing relative to their behavioural responses. This would be an ideal way of determining whether the behavioural decisions made by children in Chapters 2 and 3 were the product of perceptual as well as behavioural effects. By presenting a series of motion-disparity stimuli in a high field 7T scanner to participants, I have attempted to map the internal functional organisation of human area hMT+ - a region implicated in the processing of the stimuli used in previous behavioural experiments in this thesis. I have compared the functional organisation to that pre-

viously found using electrophysiological methods in macaque V5/MT (Albright et al, 1984; DeAngelis & Newsome, 1999), in order to strengthen the hypothesised functional homology between these two areas.

6.3.1 Organisation of disparity and direction selectivity

The data suggest that area hMT+ is organised according to both disparity selectivity, and selectivity for specific directions of motion. All individual subjects showed some degree of small repeating stimulus-specific clusters of activation when data were analysed by convolving the haemodynamic response function with the onset of individual stimuli (for 4 directions of motion and 2 disparities). Further to this, when activations to stimuli were collapsed across either positive or negative disparities, larger disparity-specific areas of activation were found in hMT+. Finally, for the majority of subjects, when disparity was reversed, a reversal of direction of motion preference within the same spatial location was observed in subdivision MST, as has been shown in macaque MST (Roy et al, 1992).

For the three subjects who underwent repeat functional scans on separate days, the areas of activation to specific motion-disparity stimuli showed a greater than chance level of correspondence between scans - which suggests that the activations were reflective of an underlying functional architecture. Although the data are promising, they still lack the spatial resolution required to draw definitive conclusions about the functional organisation of area hMT+. Measurements of cluster size for both direction and disparity stimuli are far greater than would be predicted for cortical columns (based on macaque neurophysiology data), and so at best could be argued to represent groups of columns. Overlap between areas of activation to stimuli was observed in some cases,

suggesting that the resolution of 1 x 1 x 1 mm isotropic was not sufficient to fully differentiate between some groups of neurons selective to specific directions or disparities. Part of this was likely related to the stimuli themselves - for example, only two disparities were shown to participants, representing positive (far) and negative (near) - while data from the macaque suggests disparity selectivity has more subtle gradations (DeAngelis & Newsome, 1999). That said, the tuning curve of macaque neurons to disparity is reasonably broad, and as such we might predict the same for human disparity-selective neurons. Generally, there was small overlap between clusters, and a clearly repeating pattern across hMT+, in spite of the coarse stimuli gradation.

The organisation that has been shown by the data does suggest that there is specific selectivity for both disparity and direction of motion in small regions within area hMT+. Further research with higher resolution protocols could refine these maps. This work lays the foundation for potential future behavioural experiments examining the link between behavioural response to specific motion-disparity stimuli and specific sensory activity within small subregions of hMT+.

6.3.2 Does the functional organisation of area hMT+ match organisation in macaque V5/MT-MST?

Although the spatial and temporal resolution of fMRI is no match for single-cell electrophysiology, there are some indications from the data that the functional organisation of area hMT+ may be similar to that in macaque V5/MT and MST. Albright et al (1984) showed that direction-selective neurons in macaque V5/MT were sensitive to 360 degrees of motion across 1mm of cortical surface. While the size estimates of the direction-selective clusters were far greater than this when potential scaling between

species is factored in, the data show specific clusters of voxels sensitive to each of the four directions of motion across area hMT+.

DeAngelis & Newsome (1999) showed macaque V5/MT has an organisation for disparity, with near and far represented in patches intersected with areas of no disparity selectivity. Again, the human data showed cortical patches that were far bigger than would be predicted by scaling, but overall organisation was in specific regions sensitive for near or far disparities, with some regions showing no activation in response to disparity.

Finally, area MST in the macaque has been shown to have disparity-dependent direction selectivity - that is, when disparity is reversed, selectivity for direction is also reversed. To some degree, the human data show this pattern within subdivision MST - in most participants, reversing disparity did reverse the direction a cluster was selective for, though without precise spatial overlap. This lack of perfect overlap was likely the product of small head movements between scans, partial volume effects, and differential activation for specific stimuli (as discussed further in Chapter 5) - particularly as the clusters I found were on the order of milimetres in size. Cluster correspondence between scans could have been improved with the application of spatial smoothing to the data, but in order to preserve the smaller voxel cluster activation that could represent underlying columnar structures, smoothing was only applied at the resolution of the scan (1mm). That said, it is reasonable to say that the data show similarities between hMT+ and macaque V5/MT/MST, albeit in principle rather than scale.

6.3.3 Conclusions

These results suggest that with future improvements to high resolution high field fMRI protocols, it should be possible to map reliably the functional organisation of visual perceptual regions. This would facilitate psychophysical experiments in the scanner that can probe the link between sensory activation on a small scale and behavioural response, such as those conducted with single cell electrophysiology in monkeys (e.g. Britten et al, 1996; Dodd et al, 2001), leading to some insight into the neural basis of a participant's perceptual experience. By conducting such experiments within a social context, it should become possible to match inferences made with computational modelling with those from sensory activation in specific brain regions, using techniques such as multi-voxel pattern analysis (MVPA, e.g. Norman et al 2006).

6.4 Conclusion

Behavioural conformity to social information in typically-developing children increased with age, regardless of advisor type. Computational modelling suggests that this is linked to perceptual bias in the direction of social advice. Conversely, behavioural conformity decreased with age in children with ASD, and may be the product of judgmental rather than perceptual bias. The visual perceptual area (hMT+), linked with decisions made about the stimuli used in the behavioural experiments, is associated with a dense region of myelination - a cytoarchitectonic component that may develop abnormally in children with ASD. This could provide some basis for the differences observed between typical and ASD groups, although a more complete explanation would need to explore connectivity with the STS - a known social region. The functional or-

ganisation of area hMT+ appears to be in principle similar to functionally homologous macaque V5/MT/MST, though current fMRI techniques need to be further developed in order to confirm this. Developing MRI protocols further could allow future research to focus on linking behavioural responses with specific columnar-level activation in visual areas, providing insight into the neural mechanisms for perceptual decisions made under social context.

6.5 Future Directions

At a purely behavioural level, repeating the social psychophysics experiment on the oldest ASD group, with typically-developing controls, using a non-social method of delivering advice could provide further insight into the specific 'rejection' of advice by the ASD group. This method of advice delivery could come from a non-human source (such as a video of a robot), or simply words on a screen. From the data, it is not clear that it is specifically the 'social' aspect of the advice that is causing its lack of integration into the decision making process (although given the literature it seems likely to be the case), and an experiment of this nature could provide some insight.

In order to provide a firm foundation for the inferences from computational modelling of behavioural results, repeating the psychophysical social experiments in the scanner for participants with a detailed functional map of area hMT+ is an obvious goal. A scan protocol with a low TR (ideally around 1s) would be necessary to accurately differentiate between signals from the social stimulus onset, processing, and the sensory and perceptual signals evoked by the task stimulus. A multiband imaging protocol at 7T would be ideal for this, such as that used by Boyacioglu in 2014 on

a Stroop colour-word task. Careful consideration as to the timings of the task would be necessary, in order to account for the temporal limitations of fMRI; while as a behavioural task, each trial can occur quickly in sequence, in the scanner it would be necessary to introduce pauses between trials. By carefully the order of trials, conflation of BOLD signals can be avoided, while the maximal signal for each potential pairing of advice and stimulus (correct, incorrect, neutral) can be achieved. Thought also needs to be given to the analysis methods for this data - multi-voxel pattern analysis (MVPA) conducted via machine learning algorithms is likely to be the best method, as it would facilitate objective groupings of BOLD activation patterns with specific behavioural and perceptual predictions.

In order to measure specific activation in columnar-level structures when advice changes, it is clear that functional MRI scan protocols need to be further developed at high resolution. Although functional scans have been conducted at sub-milimetre levels, they tend to require multiple hours of scanning, repeated over several days, in order to yield reasonable results (e.g. ocular dominance columns by Yacoub et al, 2007). In most cases, this is not practical for the participant, and introduces potential human error in inter-day image alignment. Development of reliable sub-milimetre functional scans, with a high enough SNR to reduce the need for future scan repetitions, would allow more fine-grain functional maps to be produced, which could then be used as the basis for examining responses in behavioural experiments.

Myelination abnormalities are associated with a number of neurological disorders, but most pertinent to this thesis, they are somewhat associated with ASD. While it is clear that structural MRI may not yet perfectly reflect patterns of underlying cortical myelination at a refined scale, this technique could potentially be used to

assess differences in myelination between typical and ASD participants around visual perceptual regions during development. By further refining structural MRI protocols that are sensitive to myelin, and conducting longitudinal studies in individual children with ASD (with matched typical controls), it should be possible to observe the relative levels of myelination in perceptual areas such as hMT+ across development, which may be one contributing factor in the lack of social advice integration observed in their decision-making processes.

Bibliography

Abdollahi, R. O., Kolster, H., Glasser, M. F., Robinson, E. C., Coalson, T. S., Dierker, D., Jenkinson, M., Van Essen, D. C. and Orban, G. A. (2014) 'Correspondences between retinotopic areas and myelin maps in human visual cortex', Neuroimage, 99, pp. 509-24.

Abrahams, B. S. and Geschwind, D. H. (2008) 'Advances in autism genetics: on the threshold of a new neurobiology', Nat Rev Genet, 9(5), pp. 341-55.

Adams, D. L., Sincich, L. C. and Horton, J. C. (2007) 'Complete pattern of ocular dominance columns in human primary visual cortex', J Neurosci, 27(39), pp. 10391-403.

Adams, W. E., Hrisos, S., Richardson, S., Davis, H., Frisby, J. P. and Clarke, M. P. (2005) 'Frisby Davis distance stereoacuity values in visually normal children', Br J Ophthalmol, 89(11), pp. 1438-41.

Ahmed, B., Cordery, P. M., McLelland, D., Bair, W. and Krug, K. (2012) 'Long-range clustered connections within extrastriate visual area V5/MT of the rhesus macaque', Cereb Cortex, 22(1), pp. 60-73.

Albright, T. D. (1984) 'Direction and orientation selectivity of neurons in visual area MT of the macaque', J Neurophysiol, 52(6), pp. 1106-30.

Aldinger, K. A., Plummer, J. T., Qiu, S. and Levitt, P. (2011) 'SnapShot: genetics of autism', Neuron, 72(2), pp. 418-8.e1.

Allison, T., Puce, A. and McCarthy, G. (2000) 'Social perception from visual cues: role of the STS region', Trends Cogn Sci, 4(7), pp. 267-278.

Allman, J. M. and Kaas, J. H. (1976) 'Representation of the visual field on the medial wall of occipital-parietal cortex in the owl monkey', Science, 191(4227), pp. 572-5.

Amano, K., Wandell, B. A. and Dumoulin, S. O. (2009) 'Visual field maps, population receptive field sizes, and visual field coverage in the human MT+ complex', J Neurophysiol, 102(5), pp. 2704-18.

Ameis, S. H. and Szatmari, P. (2012) 'Imaging-genetics in autism spectrum disorder: advances, translational impact, and future directions', Front Psychiatry, 3, pp. 46.

Amodio, D. M. and Frith, C. D. (2006) 'Meeting of minds: the medial frontal cortex

and social cognition', Nat Rev Neurosci, 7(4), pp. 268-77.

Anderson, G. R., Galfin, T., Xu, W., Aoto, J., Malenka, R. C. and Südhof, T. C. (2012) 'Candidate autism gene screen identifies critical role for cell-adhesion molecule CASPR2 in dendritic arborization and spine development', Proc Natl Acad Sci U S A, 109(44), pp. 18120-5.

Annese, J., Gazzaniga, M. S. and Toga, A. W. (2005) 'Localization of the human cortical visual area MT based on computer aided histological analysis', Cereb Cortex, 15(7), pp. 1044-53.

Anzai, A., Chowdhury, S. A. and DeAngelis, G. C. (2011) 'Coding of stereoscopic depth information in visual areas V3 and V3A', J Neurosci, 31(28), pp. 10270-82.

Armstrong, C. L., Traipe, E., Hunter, J. V., Haselgrove, J. C., Ledakis, G. E., Tallent, E. M., Shera, D. and van Buchem, M. A. (2004) 'Age-related, regional, hemispheric, and medial-lateral differences in myelin integrity in vivo in the normal adult brain', AJNR Am J Neuroradiol, 25(6), pp. 977-84.

Asch, S. E. 1951. Effects of group pressure on the modification and distortion of judgments. Groups, leadership and men.

Asch, S. E. 1956. Studies of independence and conformity. A minority of one against a unanimous majority. Psychological Monographs.

Bachevalier, J. and Loveland, K. A. (2006) 'The orbitofrontal-amygdala circuit and self-regulation of social-emotional behavior in autism', Neurosci Biobehav Rev, 30(1), pp. 97-117.

Backus, B. T., Fleet, D. J., Parker, A. J. and Heeger, D. J. (2001) 'Human cortical activity correlates with stereoscopic depth perception', J Neurophysiol, 86(4), pp. 2054-68.

Barbier, E. L., Marrett, S., Danek, A., Vortmeyer, A., van Gelderen, P., Duyn, J., Bandettini, P., Grafman, J. and Koretsky, A. P. (2002) 'Imaging cortical anatomy by high-resolution MR at 3.0T: detection of the stripe of Gennari in visual area 17', Magn Reson Med, 48(4), pp. 735-8.

Barbur, J. L., Watson, J. D., Frackowiak, R. S. and Zeki, S. (1993) 'Conscious visual perception without V1', Brain, 116 (Pt 6), pp. 1293-302.

Barnea-Goraly, N., Kwon, H., Menon, V., Eliez, S., Lotspeich, L. and Reiss, A. L. (2004) 'White matter structure in autism: preliminary evidence from diffusion tensor imaging', Biol Psychiatry, 55(3), pp. 323-6.

Baron-Cohen, S., Joliffe, T., Mortimore, C. and Robertson, M. 1997. Another advanced test of theory of mind: evidence from very high functioning adults with autism or asperger syndrome. J Child Psychol Psychiatry.

Belliveau, J. W., Kwong, K. K., Kennedy, D. N., Baker, J. R., Stern, C. E., Benson, R., Chesler, D. A., Weisskoff, R. M., Cohen, M. S. and Tootell, R. B. (1992) 'Magnetic

resonance imaging mapping of brain function. Human visual cortex', Invest Radiol, 27 Suppl 2, pp. S59-65.

Benson, N. C., Butt, O. H., Brainard, D. H. and Aguirre, G. K. (2014) 'Correction of distortion in flattened representations of the cortical surface allows prediction of V1-V3 functional organization from anatomy', PLoS Comput Biol, 10(3), pp. e1003538.

Berenda, D. R. 1950. The influence of the group on the judgments of children. New York: King's Crown Press.

Berlin, B. and Kay, P. (1969) Basic Color Terms: Their Universality and Evolution. University of California Press.

Berns, G. S., Chappelow, J., Zink, C. F., Pagnoni, G., Martin-Skurski, M. E. and Richards, J. (2005) 'Neurobiological correlates of social conformity and independence during mental rotation', Biol Psychiatry, 58(3), pp. 245-53.

Bertone, A., Hanck, J., Cornish, K. M. and Faubert, J. (2008) 'Development of static and dynamic perception for luminance-defined and texture-defined information', Neuroreport, 19(2), pp. 225-8.

Bertone, A., Mottron, L., Jelenic, P. and Faubert, J. (2003) 'Motion perception in autism: a "complex" issue', J Cogn Neurosci, 15(2), pp. 218-25.

Bhat, H. S. and Kumar, N. 2010. On the derivation of the Bayesian Information Criterion. University of California, Merced.

Bishop, B. R. and Beckman, L. 1971. Developmental Conformity. Developmental Psychology.

Blake, R., Turner, L. M., Smoski, M. J., Pozdol, S. L. and Stone, W. L. (2003) 'Visual recognition of biological motion is impaired in children with autism', Psychol Sci, 14(2), pp. 151-7.

Blakemore, S. J., Burnett, S. and Dahl, R. E. (2010) 'The role of puberty in the developing adolescent brain', Hum Brain Mapp, 31(6), pp. 926-33.

Bland, A. R. and Schaefer, A. (2011) 'Electrophysiological correlates of decision making under varying levels of uncertainty', Brain Res, 1417, pp. 55-66.

Bock, N. A., Hashim, E., Janik, R., Konyer, N. B., Weiss, M., Stanisz, G. J., Turner, R. and Geyer, S. (2013) 'Optimizing T1-weighted imaging of cortical myelin content at 3.0 T', Neuroimage, 65, pp. 1-12.

Bock, N. A., Kocharyan, A., Liu, J. V. and Silva, A. C. (2009) 'Visualizing the entire cortical myelination pattern in marmosets with magnetic resonance imaging', J Neurosci Methods, 185(1), pp. 15-22.

Bonaccio, S. and Dalal, R. Evaluating advisors: A policy-capturing study under conditions of complete and missing information. Journal of Behavioural Decision Making.

Bool, F., Kist, J. R., Locher, J. L. and Wierda, F. 1982. M. C. Escher: His Life

and Complete Graphic Work. New York: Abrams.

Bowler, D. and Worley, K. 1994. Susceptibility to Social Influence in Adults with Asperger's Syndrome. Journal of Child Psychology and Psychiatry.

Brainard, D. H. (1997) 'The Psychophysics Toolbox', Spat Vis, 10(4), pp. 433-6.

Brascamp, J. W., Knapen, T. H., Kanai, R., Noest, A. J., van Ee, R. and van den Berg, A. V. (2008) 'Multi-timescale perceptual history resolves visual ambiguity', PLoS One, 3(1), pp. e1497.

Bridge, H. and Clare, S. (2006) 'High-resolution MRI: in vivo histology?', Philos Trans R Soc Lond B Biol Sci, 361(1465), pp. 137-46.

Bridge, H., Clare, S., Jenkinson, M., Jezzard, P., Parker, A. J. and Matthews, P. M. (2005) 'Independent anatomical and functional measures of the V1/V2 boundary in human visual cortex', J Vis, 5(2), pp. 93-102.

Bridge, H., Clare, S. and Krug, K. (2014) 'Delineating extrastriate visual area MT(V5) using cortical myeloarchitecture', Neuroimage, 93 Pt 2, pp. 231-6.

Bridge, H. and Parker, A. J. (2007) 'Topographical representation of binocular depth in the human visual cortex using fMRI', J Vis, 7(14), pp. 15.1-14.

Britten, K. H., Newsome, W. T., Shadlen, M. N., Celebrini, S. and Movshon, J. A. (1996) 'A relationship between behavioral choice and the visual responses of neurons in macaque MT', Vis Neurosci, 13(1), pp. 87-100.

Britten, K. H., Shadlen, M. N., Newsome, W. T. and Movshon, J. A. (1993) 'Responses of neurons in macaque MT to stochastic motion signals', Vis Neurosci, 10(6), pp. 1157-69.

Britten, K. H. and Van Wezel, R. J. (2002) 'Area MST and heading perception in macaque monkeys', Cereb Cortex, 12(7), pp. 692-701.

Brodmann, K. 1909. Vergleichende Lokalisationslehre der Großhirnrinde in ihren Prinzipien dargestellt auf Grund des Zellenbaues. Barth, Leipzig.

Brouwer, G. J. and van Ee, R. (2007) 'Visual cortex allows prediction of perceptual states during ambiguous structure-from-motion', J Neurosci, 27(5), pp. 1015-23.

Brück, W. (2005) 'The pathology of multiple sclerosis is the result of focal inflammatory demyelination with axonal damage', J Neurol, 252 Suppl 5, pp. v3-9.

Burnett, S., Sebastian, C., Cohen Kadosh, K. and Blakemore, S. J. (2011) 'The social brain in adolescence: evidence from functional magnetic resonance imaging and behavioural studies', Neurosci Biobehav Rev, 35(8), pp. 1654-64.

Calabretta, R. and Parisi, D. 2005a. Evolutionary Connectionism and Mind/Brain Modularity. Modularity.

Calabretta, R. and Parisi, D. 2005b. Modularity. Understanding the development and evolution of complex natural systems Evolutionary Connectionism and Mind/Brain Modularity. Cambridge, MA: MIT Press.

Casey, B. J., Getz, S. and Galvan, A. (2008) 'The adolescent brain', Dev Rev, 28(1), pp. 62-77.

Castelli, F., Frith, C., Happé, F. and Frith, U. (2002) 'Autism, Asperger syndrome and brain mechanisms for the attribution of mental states to animated shapes', Brain, 125(Pt 8), pp. 1839-49.

Chaste, P. and Leboyer, M. (2012) 'Autism risk factors: genes, environment, and gene-environment interactions', Dialogues Clin Neurosci, 14(3), pp. 281-92.

Chavhan, G. B., Babyn, P. S., Thomas, B., Shroff, M. M. and Haacke, E. M. (2009) 'Principles, techniques, and applications of T2*-based MR imaging and its special applications', Radiographics, 29(5), pp. 1433-49.

Chen, Y. P., Lin, C. P., Hsu, Y. C. and Hung, C. P. (2015) 'Network Anisotropy Trumps Noise for Efficient Object Coding in Macaque Inferior Temporal Cortex', J Neurosci, 35(27), pp. 9889-99.

Cheung, M. M., Lau, C., Zhou, I. Y., Chan, K. C., Zhang, J. W., Fan, S. J. and Wu, E. X. (2012) 'High fidelity tonotopic mapping using swept source functional magnetic resonance imaging', Neuroimage, 61(4), pp. 978-86.

Chevallier, C., Molesworth, C. and Happé, F. (2012) 'Diminished social motivation negatively impacts reputation management: autism spectrum disorders as a case in point', PLoS One, 7(1), pp. e31107.

Chubb, C. and Sperling, G. 1988. Second-order motion perception: Space-time separable mechanisms. Washington DC: Proceedings: Workshop on Visual Motion.

Clare, S. and Bridge, H. (2005) 'Methodological issues relating to in vivo cortical myelography using MRI', Hum Brain Mapp, 26(4), pp. 240-50.

Cohen, M. R. and Newsome, W. T. (2004) 'What electrical microstimulation has revealed about the neural basis of cognition', Curr Opin Neurobiol, 14(2), pp. 169-77.

Connor, J. R. and Menzies, S. L. (1996) 'Relationship of iron to oligodendrocytes and myelination', Glia, 17(2), pp. 83-93.

Cottereau, B. R., McKee, S. P., Ales, J. M. and Norcia, A. M. (2011) 'Disparity-tuned population responses from human visual cortex', J Neurosci, 31(3), pp. 954-65.

Coutant, B. E. and Westheimer, G. (1993) 'Population distribution of stereoscopic ability', Ophthalmic Physiol Opt, 13(1), pp. 3-7.

Crutchfield, R. 1955. Conformity and Character. American Psychologist.

Dakin, S. and Frith, U. (2005) 'Vagaries of visual perception in autism', Neuron, 48(3), pp. 497-507.

Dale, A. M., Fischl, B. and Sereno, M. I. (1999) 'Cortical surface-based analysis. I. Segmentation and surface reconstruction', Neuroimage, 9(2), pp. 179-94.

Dale, A. M. and Sereno, M. I. (1993) 'Improved Localizadon of Cortical Activity by Combining EEG and MEG with MRI Cortical Surface Reconstruction: A Linear

Approach', J Cogn Neurosci, 5(2), pp. 162-76.

Davis, K. L., Stewart, D. G., Friedman, J. I., Buchsbaum, M., Harvey, P. D., Hof, P. R., Buxbaum, J. and Haroutunian, V. (2003) 'White matter changes in schizophrenia: evidence for myelin-related dysfunction', Arch Gen Psychiatry, 60(5), pp. 443-56.

De Martino, F., Moerel, M., Xu, J., van de Moortele, P. F., Ugurbil, K., Goebel, R., Yacoub, E. and Formisano, E. (2014) 'High-Resolution Mapping of Myeloarchitecture In Vivo: Localization of Auditory Areas in the Human Brain', Cereb Cortex.

De Valois, R. L., Albrecht, D. G. and Thorell, L. G. (1982) 'Spatial frequency selectivity of cells in macaque visual cortex', Vision Res, 22(5), pp. 545-59.

De Valois, R. L., Morgan, H. and Snodderly, D. M. (1974) 'Psychophysical studies of monkey vision. 3. Spatial luminance contrast sensitivity tests of macaque and human observers', Vision Res, 14(1), pp. 75-81.

DeAngelis, G. C., Cumming, B. G. and Newsome, W. T. (1998) 'Cortical area MT and the perception of stereoscopic depth', Nature, 394(6694), pp. 677-80.

DeAngelis, G. C. and Newsome, W. T. (1999) 'Organization of disparity-selective neurons in macaque area MT', J Neurosci, 19(4), pp. 1398-415.

DeAngelis, G. C. and Uka, T. (2003) 'Coding of horizontal disparity and velocity by MT neurons in the alert macaque', J Neurophysiol, 89(2), pp. 1094-111.

Deistung, A., Schäfer, A., Schweser, F., Biedermann, U., Turner, R. and Reichenbach, J. R. (2013) 'Toward in vivo histology: a comparison of quantitative susceptibility mapping (QSM) with magnitude-, phase-, and R2*-imaging at ultra-high magnetic field strength', Neuroimage, 65, pp. 299-314.

Del Viva, M. M., Igliozzi, R., Tancredi, R. and Brizzolara, D. (2006) 'Spatial and motion integration in children with autism', Vision Res, 46(8-9), pp. 1242-52.

Deoni, S. C., Zinkstok, J. R., Daly, E., Ecker, C., Williams, S. C., Murphy, D. G. and Consortium, M. A. (2015) 'White-matter relaxation time and myelin water fraction differences in young adults with autism', Psychol Med, 45(4), pp. 795-805.

Deutsch, M. and Gerard, H. 1955. A study of normative and informational social influences upon individual judgment. The Journal of Abnormal and Social Psychology.

DeYoe, E. A. and Van Essen, D. C. (1985) 'Segregation of efferent connections and receptive field properties in visual area V2 of the macaque', Nature, 317(6032), pp. 58-61.

Di Martino, A., Yan, C. G., Li, Q., Denio, E., Castellanos, F. X., Alaerts, K., Anderson, J. S., Assaf, M., Bookheimer, S. Y., Dapretto, M., Deen, B., Delmonte, S., Dinstein, I., Ertl-Wagner, B., Fair, D. A., Gallagher, L., Kennedy, D. P., Keown, C. L., Keysers, C., Lainhart, J. E., Lord, C., Luna, B., Menon, V., Minshew, N. J., Monk, C. S., Mueller, S., Müller, R. A., Nebel, M. B., Nigg, J. T., O'Hearn, K., Pelphrey, K. A., Peltier, S. J., Rudie, J. D., Sunaert, S., Thioux, M., Tyszka, J. M., Uddin, L. Q.,

Verhoeven, J. S., Wenderoth, N., Wiggins, J. L., Mostofsky, S. H. and Milham, M. P. (2014) 'The autism brain imaging data exchange: towards a large-scale evaluation of the intrinsic brain architecture in autism', Mol Psychiatry, 19(6), pp. 659-67.

Dick, F., Tierney, A. T., Lutti, A., Josephs, O., Sereno, M. I. and Weiskopf, N. (2012) 'In vivo functional and myeloarchitectonic mapping of human primary auditory areas', J Neurosci, 32(46), pp. 16095-105.

Dinse, J., Waehnert, M., Tardif, C. L., Schäfer, A., Geyer, S., Turner, R. and Bazin, P. L. (2013) 'A histology-based model of quantitative T1 contrast for in-vivo cortical parcellation of high-resolution 7 Tesla brain MR images', Med Image Comput Comput Assist Interv, 16(Pt 2), pp. 51-8.

Ditterich, J., Mazurek, M. E. and Shadlen, M. N. (2003) 'Microstimulation of visual cortex affects the speed of perceptual decisions', Nat Neurosci, 6(8), pp. 891-8.

Dodd, J. V., Krug, K., Cumming, B. G. and Parker, A. J. (2001) 'Perceptually bistable three-dimensional figures evoke high choice probabilities in cortical area MT', J Neurosci, 21(13), pp. 4809-21.

Downs, A. and Smith, T. (2004) 'Emotional understanding, cooperation, and social behavior in high-functioning children with autism', J Autism Dev Disord, 34(6), pp. 625-35.

Dubner, R. and Zeki, S. M. (1971) 'Response properties and receptive fields of cells in an anatomically defined region of the superior temporal sulcus in the monkey', Brain Res, 35(2), pp. 528-32.

Dukelow, S. P., DeSouza, J. F., Culham, J. C., van den Berg, A. V., Menon, R. S. and Vilis, T. (2001) 'Distinguishing subregions of the human MT+ complex using visual fields and pursuit eye movements', J Neurophysiol, 86(4), pp. 1991-2000.

Dumoulin, S. O., Bittar, R. G., Kabani, N. J., Baker, C. L., Le Goualher, G., Bruce Pike, G. and Evans, A. C. (2000) 'A new anatomical landmark for reliable identification of human area V5/MT: a quantitative analysis of sulcal patterning', Cereb Cortex, 10(5), pp. 454-63.

Duong, T. Q., Kim, D. S., Uğurbil, K. and Kim, S. G. (2000) 'Spatiotemporal dynamics of the BOLD fMRI signals: toward mapping submillimeter cortical columns using the early negative response', Magn Reson Med, 44(2), pp. 231-42.

Edwards, A. L. 1965. Measurements of individual differences in ratings of social desirability and in the tendency to give socially desirable responses. Journal of Experimental Research in Personality.

Eickhoff, S. B., Stephan, K. E., Mohlberg, H., Grefkes, C., Fink, G. R., Amunts, K. and Zilles, K. (2005) 'A new SPM toolbox for combining probabilistic cytoarchitectonic maps and functional imaging data', Neuroimage, 25(4), pp. 1325-35.

Engel, S. A., Glover, G. H. and Wandell, B. A. (1997) 'Retinotopic organization in

human visual cortex and the spatial precision of functional MRI', Cereb Cortex, 7(2), pp. 181-92.

Felleman, D. J. and Van Essen, D. C. (1991) 'Distributed hierarchical processing in the primate cerebral cortex', Cereb Cortex, 1(1), pp. 1-47.

Fernald, R. D. (2015) 'Social behaviour: can it change the brain?', Anim Behav, 103, pp. 259-265.

Filipek, P. A., Accardo, P. J., Baranek, G. T., Cook, E. H., Dawson, G., Gordon, B., Gravel, J. S., Johnson, C. P., Kallen, R. J., Levy, S. E., Minshew, N. J., Ozonoff, S., Prizant, B. M., Rapin, I., Rogers, S. J., Stone, W. L., Teplin, S., Tuchman, R. F. and Volkmar, F. R. (1999) 'The screening and diagnosis of autistic spectrum disorders', J Autism Dev Disord, 29(6), pp. 439-84.

Fischer, E., Bülthoff, H. H., Logothetis, N. K. and Bartels, A. (2012) 'Visual motion responses in the posterior cingulate sulcus: a comparison to V5/MT and MST', Cereb Cortex, 22(4), pp. 865-76.

Fischl, B. and Dale, A. M. (2000) 'Measuring the thickness of the human cerebral cortex from magnetic resonance images', Proc Natl Acad Sci U S A, 97(20), pp. 11050-5.

Fischl, B., Sereno, M. I., Tootell, R. B. and Dale, A. M. (1999) 'High-resolution intersubject averaging and a coordinate system for the cortical surface', Hum Brain Mapp, 8(4), pp. 272-84.

Fjær, S., Bø, L., Lundervold, A., Myhr, K. M., Pavlin, T., Torkildsen, O. and Wergeland, S. (2013) 'Deep gray matter demyelination detected by magnetization transfer ratio in the cuprizone model', PLoS One, 8(12), pp. e84162.

Flechsig 1876. Die Leitungsbahnen im Gehirn und Rückenmark des Menschen auf Grund entwicklungsgeschichtlicher Untersuchungen dargestellt

Flechsig, P. 1920. Anatomie des menschichen Gehirns und Ruckenmarks auf Myelogenetischer Grundlage. Leipzig: Thieme.

Flynn, S. W., Lang, D. J., Mackay, A. L., Goghari, V., Vavasour, I. M., Whittall, K. P., Smith, G. N., Arango, V., Mann, J. J., Dwork, A. J., Falkai, P. and Honer, W. G. (2003) 'Abnormalities of myelination in schizophrenia detected in vivo with MRI, and post-mortem with analysis of oligodendrocyte proteins', Mol Psychiatry, 8(9), pp. 811-20.

Frey, H. P., Molholm, S., Lalor, E. C., Russo, N. N. and Foxe, J. J. (2013) 'Atypical cortical representation of peripheral visual space in children with an autism spectrum disorder', Eur J Neurosci, 38(1), pp. 2125-38.

Fu, G., Xu, F., Cameron, C. A., Heyman, G. and Lee, K. 2007. Cross-Cultural Differences in Children's Choices, Categorizations, and Evaluations of Truths and Lies. Dev Psychol.

Gallant, J. L., Shoup, R. E. and Mazer, J. A. (2000) 'A human extrastriate area functionally homologous to macaque V4', Neuron, 27(2), pp. 227-35.

Gallyas, F. (1979) 'Silver staining of myelin by means of physical development', Neurol Res, 1(2), pp. 203-9.

Ganzetti, M., Wenderoth, N. and Mantini, D. (2014) 'Whole brain myelin mapping using T1- and T2-weighted MR imaging data', Front Hum Neurosci, 8, pp. 671.

Gardener, H., Spiegelman, D. and Buka, S. L. (2009) 'Prenatal risk factors for autism: comprehensive meta-analysis', Br J Psychiatry, 195(1), pp. 7-14.

Gennari, F. 1782. De Peculiari Structura Cerebri Nonnulisque Ejus Morbis. Parma Ex Regio Typographeo.

Germar, M., Schlemmer, A., Krug, K., Voss, A. and Mojzisch, A. (2014) 'Social influence and perceptual decision making: a diffusion model analysis', Pers Soc Psychol Bull, 40(2), pp. 217-31.

Gervais, H., Belin, P., Boddaert, N., Leboyer, M., Coez, A., Sfaello, I., Barthélémy, C., Brunelle, F., Samson, Y. and Zilbovicius, M. (2004) 'Abnormal cortical voice processing in autism', Nat Neurosci, 7(8), pp. 801-2.

Glasser, M. F. and Van Essen, D. C. (2011) 'Mapping human cortical areas in vivo based on myelin content as revealed by T1- and T2-weighted MRI', J Neurosci, 31(32), pp. 11597-616.

Gliga, T., Elsabbagh, M., Andravizou, A. and Johnson, M. 2009. Faces Attract Infants' Attention in Complex Displays. Official Journal of the International Society for Infant Studies.

Gold, J. I. and Ding, L. (2013) 'How mechanisms of perceptual decision-making affect the psychometric function', Prog Neurobiol, 103, pp. 98-114.

Gold, J. I. and Shadlen, M. N. (2007) 'The neural basis of decision making', Annu Rev Neurosci, 30, pp. 535-74.

Goldstein, J., Davidoff, J. and Roberson, D. (2009) 'Knowing color terms enhances recognition: further evidence from English and Himba', J Exp Child Psychol, 102(2), pp. 219-38.

Gonzalez, F., Perez, R., Justo, M. S. and Bermudez, M. A. (2001) 'Receptive field organization of disparity-sensitive cells in Macaque medial superior temporal cortex', Eur J Neurosci, 14(1), pp. 167-73.

Gray, C. and Garand, J. 1993. Social Stories: Improving Responses of Students with Autism with Accurate Social Information. Focus on Autism and Other Developmental Disabilities.

Greimel, E., Bartling, J., Dunkel, J., Brückl, M., Deimel, W., Remschmidt, H., Kamp-Becker, I. and Schulte-Körne, G. (2013a) 'The temporal dynamics of coherent motion processing in autism spectrum disorder: evidence for a deficit in the dorsal

pathway', Behav Brain Res, 251, pp. 168-75.

Greimel, E., Nehrkorn, B., Schulte-Rüther, M., Fink, G. R., Nickl-Jockschat, T., Herpertz-Dahlmann, B., Konrad, K. and Eickhoff, S. B. (2013b) 'Changes in grey matter development in autism spectrum disorder', Brain Struct Funct, 218(4), pp. 929-42.

Guleria, S. and Kelly, T. G. (2014) 'Myelin, myelination, and corresponding magnetic resonance imaging changes', Radiol Clin North Am, 52(2), pp. 227-39.

Haar, S., Berman, S., Behrmann, M. and Dinstein, I. (2016) 'Anatomical Abnormalities in Autism?', Cereb Cortex, 26(4), pp. 1440-52.

Hadjikhani, N., Joseph, R. M., Snyder, J. and Tager-Flusberg, H. (2007) 'Abnormal activation of the social brain during face perception in autism', Hum Brain Mapp, 28(5), pp. 441-9.

Hamm, N. H. and Hoving, K. L. (1969) 'Conformity of children in an ambiguous perceptual situation', Child Dev, 40(3), pp. 773-84.

Hanks, T., Kiani, R. and Shadlen, M. N. (2014) 'A neural mechanism of speed-accuracy tradeoff in macaque area LIP', Elife, 3.

Hanks, T. D., Ditterich, J. and Shadlen, M. N. (2006) 'Microstimulation of macaque area LIP affects decision-making in a motion discrimination task', Nat Neurosci, 9(5), pp. 682-9.

Harris, P. L. and Corriveau, K. H. (2011) 'Young children's selective trust in informants', Philos Trans R Soc Lond B Biol Sci, 366(1567), pp. 1179-87.

Haun, D. B. and Tomasello, M. (2011) 'Conformity to peer pressure in preschool children', Child Dev, 82(6), pp. 1759-67.

Haun, D. B., van Leeuwen, E. J. and Edelson, M. G. (2013) 'Majority influence in children and other animals', Dev Cogn Neurosci, 3, pp. 61-71.

Hayakawa, Y., Marumoto, A. and Sawada, Y. (1995) 'Effects of the chaotic noise on the performance of a neural network model for optimization problems', Phys Rev E Stat Phys Plasmas Fluids Relat Interdiscip Topics, 51(4), pp. R2693-R2696.

Heidemann, R. M., Ivanov, D., Trampel, R., Fasano, F., Meyer, H., Pfeuffer, J. and Turner, R. (2012) 'Isotropic submillimeter fMRI in the human brain at 7 T: combining reduced field-of-view imaging and partially parallel acquisitions', Magn Reson Med, 68(5), pp. 1506-16.

Heron, G., Dholakia, S., Collins, D. E. and McLaughlan, H. (1985) 'Stereoscopic threshold in children and adults', Am J Optom Physiol Opt, 62(8), pp. 505-15.

Hertz, U., Romand-Monnier, M., Kyriakopoulou, K. and Bahrami, B. (2016) 'Social influence protects collective decision making from equality bias', J Exp Psychol Hum Percept Perform, 42(2), pp. 164-72.

Hess, R. H., Baker, C. L. and Zihl, J. (1989) 'The "motion-blind" patient: low-level

spatial and temporal filters', J Neurosci, 9(5), pp. 1628-40.

Horton, J. C. and Hocking, D. R. (1996) 'Anatomical demonstration of ocular dominance columns in striate cortex of the squirrel monkey', J Neurosci, 16(17), pp. 5510-22.

Hubbard, E. M., Arman, A. C., Ramachandran, V. S. and Boynton, G. M. (2005) 'Individual differences among grapheme-color synesthetes: brain-behavior correlations', Neuron, 45(6), pp. 975-85.

Hubel, D. H. and Wiesel, T. N. (1968) 'Receptive fields and functional architecture of monkey striate cortex', J Physiol, 195(1), pp. 215-43.

Hughes, C., Jaffee, S. R., Happé, F., Taylor, A., Caspi, A. and Moffitt, T. E. (2005) 'Origins of individual differences in theory of mind: from nature to nurture?', Child Dev, 76(2), pp. 356-70.

Huk, A. C., Dougherty, R. F. and Heeger, D. J. (2002) 'Retinotopy and functional subdivision of human areas MT and MST', J Neurosci, 22(16), pp. 7195-205.

Hämäläinen, M., Hari, R., Ilmoniemi, R., Knuutila, J. and Lounasmaa, O. 1993. Magnetoencephalography—theory, instrumentation, and applications to noninvasive studies of the working human brain. Rev. Mod. Phys.

Inaba, N. and Kawano, K. (2014) 'Neurons in cortical area MST remap the memory trace of visual motion across saccadic eye movements', Proc Natl Acad Sci U S A, 111(21), pp. 7825-30.

Iscoe, I., Williams, M. and Harvey, J. 1963. Modification of children's judgments by a simulated group technique: A normative developmental study.: Child Development.

Izuma, K., Matsumoto, K., Camerer, C. F. and Adolphs, R. (2011) 'Insensitivity to social reputation in autism', Proc Natl Acad Sci U S A, 108(42), pp. 17302-7.

Jellema, T., Baker, C. I., Wicker, B. and Perrett, D. I. (2000) 'Neural representation for the perception of the intentionality of actions', Brain Cogn, 44(2), pp. 280-302.

Jeness, A. 1932. The role of discussion in changing opinion regarding a matter of fact.: The Journal of Abnormal and Social Psychology.

Jenkinson, M., Beckmann, C. F., Behrens, T. E., Woolrich, M. W. and Smith, S. M. 2012. FSL. NeuroImage.

JN, G., J, B., N, J., FX, C., H, L., A, Z., T, P., AC, E. and JL., R. 1999. Brain development during childhood and adolescence: a longitudinal MRI study. Nature Neuroscience.

Johnson, C. P., Myers, S. M. and Disabilities, A. A. o. P. C. o. C. W. (2007) 'Identification and evaluation of children with autism spectrum disorders', Pediatrics, 120(5), pp. 1183-215.

Kaiser, M. D. and Shiffrar, M. (2009) 'The visual perception of motion by observers with autism spectrum disorders: a review and synthesis', Psychon Bull Rev, 16(5), pp.

761-77.

Kanner, L. 1943. Autistic Disturbances of Affective Contact. Pathology.

Kaplan, M., Rimland, B. and Edelson, S. 1999. Strabismus in Autism Spectrum Disorder.

Kasari, C., Rotheram-Fuller, E., Locke, J. and Gulsrud, A. (2012) 'Making the connection: randomized controlled trial of social skills at school for children with autism spectrum disorders', J Child Psychol Psychiatry, 53(4), pp. 431-9.

Kim, H. R., Angelaki, D. E. and DeAngelis, G. C. (2015) 'A functional link between MT neurons and depth perception based on motion parallax', J Neurosci, 35(6), pp. 2766-77.

Kiselev, S., Espy, K. A. and Sheffield, T. (2009) 'Age-related differences in reaction time task performance in young children', J Exp Child Psychol, 102(2), pp. 150-66.

Klaver, P., Lichtensteiger, J., Bucher, K., Dietrich, T., Loenneker, T. and Martin, E. (2008) 'Dorsal stream development in motion and structure-from-motion perception', Neuroimage, 39(4), pp. 1815-23.

Klin, A. 1991. Young autistic children's listening preferences in regard to speech.: Journal of autism and developmental disorders.

Klink, P. C., van Wezel, R. J. and van Ee, R. (2012) 'United we sense, divided we fail: context-driven perception of ambiguous visual stimuli', Philos Trans R Soc Lond B Biol Sci, 367(1591), pp. 932-41.

Knoll, L. J., Magis-Weinberg, L., Speekenbrink, M. and Blakemore, S. J. (2015) 'Social influence on risk perception during adolescence', Psychol Sci, 26(5), pp. 583-92.

Koldewyn, K., Whitney, D. and Rivera, S. M. (2011) 'Neural correlates of coherent and biological motion perception in autism', Dev Sci, 14(5), pp. 1075-88.

Kolster, H., Peeters, R. and Orban, G. A. (2010) 'The retinotopic organization of the human middle temporal area MT/V5 and its cortical neighbors', J Neurosci, 30(29), pp. 9801-20.

Kornmeier, J. and Bach, M. (2004) 'Early neural activity in Necker-cube reversal: evidence for low-level processing of a gestalt phenomenon', Psychophysiology, 41(1), pp. 1-8.

Kornmeier, J. and Bach, M. (2005) 'The Necker cube–an ambiguous figure disambiguated in early visual processing', Vision Res, 45(8), pp. 955-60.

Kourtzi, Z. and Kanwisher, N. (2000) 'Activation in human MT/MST by static images with implied motion', J Cogn Neurosci, 12(1), pp. 48-55.

Krug, K., Cicmil, N., Parker, A. J. and Cumming, B. G. (2013) 'A causal role for V5/MT neurons coding motion-disparity conjunctions in resolving perceptual ambiguity', Curr Biol, 23(15), pp. 1454-9.

Lee, L., Frederick, S. and Ariely, D. (2006) 'Try it, you'll like it: the influence of

expectation, consumption, and revelation on preferences for beer', Psychol Sci, 17(12), pp. 1054-8.

Lefebvre, A., Beggiato, A., Bourgeron, T. and Toro, R. (2015) 'Neuroanatomical Diversity of Corpus Callosum and Brain Volume in Autism: Meta-analysis, Analysis of the Autism Brain Imaging Data Exchange Project, and Simulation', Biol Psychiatry, 78(2), pp. 126-34.

Leon, M. I. and Shadlen, M. N. (1999) 'Effect of expected reward magnitude on the response of neurons in the dorsolateral prefrontal cortex of the macaque', Neuron, 24(2), pp. 415-25.

Lewis, J. W. and Van Essen, D. C. (2000) 'Mapping of architectonic subdivisions in the macaque monkey, with emphasis on parieto-occipital cortex', J Comp Neurol, 428(1), pp. 79-111.

Li, M., Liu, F., Juusola, M. and Tang, S. (2014) 'Perceptual color map in macaque visual area V4', J Neurosci, 34(1), pp. 202-17.

Liebal, K., Behne, T., Carpenter, M. and Tomasello, M. (2009) 'Infants use shared experience to interpret pointing gestures', Dev Sci, 12(2), pp. 264-71.

Link, S. W. and Heath, R. A. 1975. A Sequential Theory of Psychological Discrimination. Psychometrika.

Lutti, A., Dick, F., Sereno, M. I. and Weiskopf, N. (2014) 'Using high-resolution quantitative mapping of R1 as an index of cortical myelination', Neuroimage, 93 Pt 2, pp. 176-88.

Malikovic, A., Amunts, K., Schleicher, A., Mohlberg, H., Eickhoff, S. B., Wilms, M., Palomero-Gallagher, N., Armstrong, E. and Zilles, K. (2007) 'Cytoarchitectonic analysis of the human extrastriate cortex in the region of V5/MT+: a probabilistic, stereotaxic map of area hOc5', Cereb Cortex, 17(3), pp. 562-74.

Marques, J. P. and Gruetter, R. (2013) 'New developments and applications of the MP2RAGE sequence–focusing the contrast and high spatial resolution R1 mapping', PLoS One, 8(7), pp. e69294.

Mars, R. B., Sallet, J., Neubert, F. X. and Rushworth, M. F. (2013) 'Connectivity profiles reveal the relationship between brain areas for social cognition in human and monkey temporoparietal cortex', Proc Natl Acad Sci U S A, 110(26), pp. 10806-11.

Maunsell, J. H. and van Essen, D. C. (1983) 'The connections of the middle temporal visual area (MT) and their relationship to a cortical hierarchy in the macaque monkey', J Neurosci, 3(12), pp. 2563-86.

McGuire, K., London, K. and Wright, D. B. (2011) 'Peer influence on event reports among adolescents and young adults', Memory, 19(6), pp. 674-83.

Menzies, L., Goddings, A. L., Whitaker, K. J., Blakemore, S. J. and Viner, R. M. (2015) 'The effects of puberty on white matter development in boys', Dev Cogn

Neurosci, 11, pp. 116-28.

Miles, J. H. (2011) 'Autism spectrum disorders–a genetics review', Genet Med, 13(4), pp. 278-94.

Moscovici, S. and Personnaz, B. 1980. Minority Influence and Conversion Behaviour in a Perceptual Task. Journal of Experimental Social Psychology.

Murray, L. and Andrews, A. (2005) The Social Baby: Understanding Babies' Communication from Birth.

Naidich, T. P., Blum, J. T. and Firestone, M. I. (2001) 'The parasagittal line: an anatomic landmark for axial imaging', AJNR Am J Neuroradiol, 22(5), pp. 885-95.

Nawrot, M. and Blake, R. (1993) 'On the perceptual identity of dynamic stereopsis and kinetic depth', Vision Res, 33(11), pp. 1561-71.

Neath, A. and Cavanaugh, J. 2012. The Bayesian information criterion: background, derivation, and applications. Wiley Interdisciplinary Reviews: Computational Statistics.

Neri, P., Bridge, H. and Heeger, D. J. (2004) 'Stereoscopic processing of absolute and relative disparity in human visual cortex', J Neurophysiol, 92(3), pp. 1880-91.

Newschaffer, C. J., Croen, L. A., Daniels, J., Giarelli, E., Grether, J. K., Levy, S. E., Mandell, D. S., Miller, L. A., Pinto-Martin, J., Reaven, J., Reynolds, A. M., Rice, C. E., Schendel, D. and Windham, G. C. (2007) 'The epidemiology of autism spectrum disorders', Annu Rev Public Health, 28, pp. 235-58.

Norman, K. A., Polyn, S. M., Detre, G. J. and Haxby, J. V. (2006) 'Beyond mind-reading: multi-voxel pattern analysis of fMRI data', Trends Cogn Sci, 10(9), pp. 424-30.

Noterdaeme, M., Wriedt, E. and Hohne, C. 2010. Asperger's syndrome and high-functioning autism: language, motor and cognitive profiles. Eur Child Adolesc Psychiatry.

Noterdaeme, M. A. and Wriedt, E. (2010) '[Comorbidity in autism spectrum disorders - I. Mental retardation and psychiatric comorbidity]', Z Kinder Jugendpsychiatr Psychother, 38(4), pp. 257-66.

Nunez, P. 1981. Electric Fields of the Brain. New York: Oxford University Press.

Nuñez, J. L., Huppenbauer, C. B., McAbee, M. D., Juraska, J. M. and DonCarlos, L. L. (2003) 'Androgen receptor expression in the developing male and female rat visual and prefrontal cortex', J Neurobiol, 56(3), pp. 293-302.

O'Brien, J., Spencer, J., Girges, C., Johnston, A. and Hill, H. (2014) 'Impaired perception of facial motion in autism spectrum disorder', PLoS One, 9(7), pp. e102173.

Okazaki, Y. and Fujita, I. 2010. Responses of disparity-sensitive V3/V3A neurons to anti-correlated random-dot stereograms. Journal of Vision.

Olesen, P. J., Nagy, Z., Westerberg, H. and Klingberg, T. (2003) 'Combined analysis

of DTI and fMRI data reveals a joint maturation of white and grey matter in a fronto-parietal network', Brain Res Cogn Brain Res, 18(1), pp. 48-57.

Ono, Kubick and Abernathey Atlas of the Cerebral Sulci. Thieme Medical Publishers.

Orban, G. A., Fize, D., Peuskens, H., Denys, K., Nelissen, K., Sunaert, S., Todd, J. and Vanduffel, W. (2003) 'Similarities and differences in motion processing between the human and macaque brain: evidence from fMRI', Neuropsychologia, 41(13), pp. 1757-68.

Orban, G. A., Van Essen, D. and Vanduffel, W. (2004) 'Comparative mapping of higher visual areas in monkeys and humans', Trends Cogn Sci, 8(7), pp. 315-24.

Osterling, J. A., Dawson, G. and Munson, J. A. (2002) 'Early recognition of 1-year-old infants with autism spectrum disorder versus mental retardation', Dev Psychopathol, 14(2), pp. 239-51.

Palmer, S. E. (1980) ' What makes triangles point: Local and global effects in configurations of ambiguous triangles', 12, pp. 85-305 Available: Cognitive Psychology.

Parker, A. J. and Newsome, W. T. (1998) 'Sense and the single neuron: probing the physiology of perception', Annu Rev Neurosci, 21, pp. 227-77.

Patton, G. C. and Viner, R. (2007) 'Pubertal transitions in health', Lancet, 369(9567), pp. 1130-9.

Pellicano, E. and Burr, D. (2012) 'When the world becomes 'too real': a Bayesian explanation of autistic perception', Trends Cogn Sci, 16(10), pp. 504-10.

Pelphrey, K. A., Morris, J. P. and McCarthy, G. (2005) 'Neural basis of eye gaze processing deficits in autism', Brain, 128(Pt 5), pp. 1038-48.

Pike, A. R. (1966). "Stochastic Models of Choice Behaviour: Response Probabilities and Latencies of Finite Markov Chain Systems". British Journal of Mathematical and Statistical Psychology 19 (1): 15–32.

Phillips, M. L., Drevets, W. C., Rauch, S. L. and Lane, R. (2003) 'Neurobiology of emotion perception I: The neural basis of normal emotion perception', Biol Psychiatry, 54(5), pp. 504-14.

Powell, J., Lewis, P. A., Roberts, N., García-Fiñana, M. and Dunbar, R. I. (2012) 'Orbital prefrontal cortex volume predicts social network size: an imaging study of individual differences in humans', Proc Biol Sci, 279(1736), pp. 2157-62.

Powell, J. L., Lewis, P. A., Dunbar, R. I., García-Fiñana, M. and Roberts, N. (2010) 'Orbital prefrontal cortex volume correlates with social cognitive competence', Neuropsychologia, 48(12), pp. 3554-62.

Prince, S. J., Pointon, A. D., Cumming, B. G. and Parker, A. J. (2002) 'Quantitative analysis of the responses of V1 neurons to horizontal disparity in dynamic random-dot stereograms', J Neurophysiol, 87(1), pp. 191-208.

Qin, L., van Gelderen, P., Derbyshire, J. A., Jin, F., Lee, J., de Zwart, J. A., Tao, Y. and Duyn, J. H. (2009) 'Prospective head-movement correction for high-resolution MRI using an in-bore optical tracking system', Magn Reson Med, 62(4), pp. 924-34.

Rakoczy, H., Ehrling, C., Harris, P. L. and Schultze, T. (2015) 'Young children heed advice selectively', J Exp Child Psychol, 138, pp. 71-87.

Ratcliff, R. and McKoon, G. (2008) 'The diffusion decision model: theory and data for two-choice decision tasks', Neural Comput, 20(4), pp. 873-922.

Ratcliff, R., Philiastides, M. G. and Sajda, P. (2009) 'Quality of evidence for perceptual decision making is indexed by trial-to-trial variability of the EEG', Proc Natl Acad Sci U S A, 106(16), pp. 6539-44.

Redcay, E. (2008) 'The superior temporal sulcus performs a common function for social and speech perception: implications for the emergence of autism', Neurosci Biobehav Rev, 32(1), pp. 123-42.

Rees, G., Friston, K. and Koch, C. (2000) 'A direct quantitative relationship between the functional properties of human and macaque V5', Nat Neurosci, 3(7), pp. 716-23.

Reuter, M., Schmansky, N. J., Rosas, H. D. and Fischl, B. (2012) 'Within-subject template estimation for unbiased longitudinal image analysis', Neuroimage, 61(4), pp. 1402-18.

Riby, D. M. and Hancock, P. J. (2008) 'Viewing it differently: social scene perception in Williams syndrome and autism', Neuropsychologia, 46(11), pp. 2855-60.

Robertson, C. E., Thomas, C., Kravitz, D. J., Wallace, G. L., Baron-Cohen, S., Martin, A. and Baker, C. I. (2014) 'Global motion perception deficits in autism are reflected as early as primary visual cortex', Brain, 137(Pt 9), pp. 2588-99.

Rokers, B., Cormack, L. and Huk, A. 2009. isparity- and velocity-based signals for three-dimensional motion perception in human MT+. Nature Neuroscience.

Roy, J. P., Komatsu, H. and Wurtz, R. H. (1992) 'Disparity sensitivity of neurons in monkey extrastriate area MST', J Neurosci, 12(7), pp. 2478-92.

Rudolph, K. and Pasternak, T. (1999) 'Transient and permanent deficits in motion perception after lesions of cortical areas MT and MST in the macaque monkey', Cereb Cortex, 9(1), pp. 90-100.

Rushworth, M. F., Mars, R. B. and Sallet, J. (2013) 'Are there specialized circuits for social cognition and are they unique to humans?', Curr Opin Neurobiol, 23(3), pp. 436-42.

Rutherford, M. D. and Troje, N. F. (2012) 'IQ predicts biological motion perception in autism spectrum disorders', J Autism Dev Disord, 42(4), pp. 557-65.

S, F., L, B., K, M., Ø, T. and S, W. 2015. Magnetization transfer ratio does not correlate to myelin content in the brain in the MOG-EAE mouse model. Neurochem

Int.

Sally, D. and Hill, E. 2006. The development of interpersonal strategy: Autism, theory-of-mind, cooperation and fairness. Journal of Economic Psychology.

Salzman, C. D., Britten, K. H. and Newsome, W. T. (1990) 'Cortical microstimulation influences perceptual judgements of motion direction', Nature, 346(6280), pp. 174-7.

Schmierer, K., Scaravilli, F., Altmann, D. R., Barker, G. J. and Miller, D. H. (2004) 'Magnetization transfer ratio and myelin in postmortem multiple sclerosis brain', Ann Neurol, 56(3), pp. 407-15.

Schultz, R. T. (2005) 'Developmental deficits in social perception in autism: the role of the amygdala and fusiform face area', Int J Dev Neurosci, 23(2-3), pp. 125-41.

Scott, S. and Bruce, R. 1995. Decision-making style: The development and assessment of a new measure. Educational and Psychological Measurement.

Sereno, M. I., Lutti, A., Weiskopf, N. and Dick, F. (2013) 'Mapping the human cortical surface by combining quantitative T(1) with retinotopy', Cereb Cortex, 23(9), pp. 2261-8.

Serletis, D., Zalay, O. C., Valiante, T. A., Bardakjian, B. L. and Carlen, P. L. (2011) 'Complexity in neuronal noise depends on network interconnectivity', Ann Biomed Eng, 39(6), pp. 1768-78.

Shah, A. and Frith, U. (1993) 'Why do autistic individuals show superior performance on the block design task?', J Child Psychol Psychiatry, 34(8), pp. 1351-64.

Shen, X., Nguyen, T. D., Gauthier, S. A. and Raj, A. (2013) 'Robust myelin quantitative imaging from multi-echo T2 MRI using edge preserving spatial priors', Med Image Comput Comput Assist Interv, 16(Pt 1), pp. 622-30.

Sherif, M. 1935. A study of some social factors in perception. Archives of Psychology.

Shutts, K., Banaji, M. R. and Spelke, E. S. (2010) 'Social categories guide young children's preferences for novel objects', Dev Sci, 13(4), pp. 599-610.

Sincich, L. C. and Horton, J. C. (2003) 'Independent projection streams from macaque striate cortex to the second visual area and middle temporal area', J Neurosci, 23(13), pp. 5684-92.

Smith, A. T., Greenlee, M. W., Singh, K. D., Kraemer, F. M. and Hennig, J. (1998) 'The processing of first- and second-order motion in human visual cortex assessed by functional magnetic resonance imaging (fMRI)', J Neurosci, 18(10), pp. 3816-30.

Smith, S. M. 2002. Fast robust automated brain extraction. Human Brain Mapping.

Smolyanskaya, A., Ruff, D. A. and Born, R. T. (2013) 'Joint tuning for direction of motion and binocular disparity in macaque MT is largely separable', J Neurophysiol, 110(12), pp. 2806-16.

Sniezek, J. A. and Buckley, T. 1995. Cueing and cognitive conflict in judge–advisor decision making.: Organizational Behavior and Human Decision Processes.

Sniezek, J. A. and Van Swol, L. M. (2001) 'Trust, Confidence, and Expertise in a Judge-Advisor System', Organ Behav Hum Decis Process, 84(2), pp. 288-307.

Somers, D. C., Dale, A. M., Seiffert, A. E. and Tootell, R. B. (1999) 'Functional MRI reveals spatially specific attentional modulation in human primary visual cortex', Proc Natl Acad Sci U S A, 96(4), pp. 1663-8.

Sowell, E. R., Trauner, D. A., Gamst, A. and Jernigan, T. L. (2002) 'Development of cortical and subcortical brain structures in childhood and adolescence: a structural MRI study', Dev Med Child Neurol, 44(1), pp. 4-16.

Spencer, J., O'Brien, J., Riggs, K., Braddick, O., Atkinson, J. and Wattam-Bell, J. (2000) 'Motion processing in autism: evidence for a dorsal stream deficiency', Neuroreport, 11(12), pp. 2765-7.

Steinberg, L. and Monahan, K. C. (2007) 'Age differences in resistance to peer influence', Dev Psychol, 43(6), pp. 1531-43.

Stevens, M. C., Pearlson, G. D. and Calhoun, V. D. (2009) 'Changes in the interaction of resting-state neural networks from adolescence to adulthood', Hum Brain Mapp, 30(8), pp. 2356-66.

Strassberg, D. and Wiggen, E. 1972. Conformity as a Function of Age in Preadolescents. The Journal of Social Psychology.

Stüber, C., Morawski, M., Schäfer, A., Labadie, C., Wähnert, M., Leuze, C., Streicher, M., Barapatre, N., Reimann, K., Geyer, S., Spemann, D. and Turner, R. (2014) 'Myelin and iron concentration in the human brain: a quantitative study of MRI contrast', Neuroimage, 93 Pt 1, pp. 95-106.

Summerfield, C. and Koechlin, E. (2010) 'Economic value biases uncertain perceptual choices in the parietal and prefrontal cortices', Front Hum Neurosci, 4, pp. 208.

Sumter, S. R., Bokhorst, C. L., Steinberg, L. and Westenberg, P. M. (2009) 'The developmental pattern of resistance to peer influence in adolescence: will the teenager ever be able to resist?', J Adolesc, 32(4), pp. 1009-21.

Sykes, N. H. and Lamb, J. A. (2007) 'Autism: the quest for the genes', Expert Rev Mol Med, 9(24), pp. 1-15.

Sánchez-Panchuelo, R. M., Francis, S. T., Schluppeck, D. and Bowtell, R. W. (2012) 'Correspondence of human visual areas identified using functional and anatomical MRI in vivo at 7 T', J Magn Reson Imaging, 35(2), pp. 287-99.

Tallantyre, E. C., Morgan, P. S., Dixon, J. E., Al-Radaideh, A., Brookes, M. J., Evangelou, N. and Morris, P. G. (2009) 'A comparison of 3T and 7T in the detection of small parenchymal veins within MS lesions', Invest Radiol, 44(9), pp. 491-4.

Taylor, J. L. and Seltzer, M. M. (2010) 'Changes in the autism behavioral phenotype during the transition to adulthood', J Autism Dev Disord, 40(12), pp. 1431-46.

Thompson, P. M., Schwartz, C., Lin, R. T., Khan, A. A. and Toga, A. W. (1996) 'Three-dimensional statistical analysis of sulcal variability in the human brain', J Neurosci, 16(13), pp. 4261-74.

Toga, A. W., Thompson, P. M. and Sowell, E. R. (2006) 'Mapping brain maturation', Trends Neurosci, 29(3), pp. 148-59.

Tremblay, L. and Schultz, W. (2000) 'Modifications of reward expectation-related neuronal activity during learning in primate orbitofrontal cortex', J Neurophysiol, 83(4), pp. 1877-85.

Triantafyllou, C., Hoge, R. D., Krueger, G., Wiggins, C. J., Potthast, A., Wiggins, G. C. and Wald, L. L. (2005) 'Comparison of physiological noise at 1.5 T, 3 T and 7 T and optimization of fMRI acquisition parameters', Neuroimage, 26(1), pp. 243-50.

Turner, R. and Geyer, S. (2014a) 'Comparing like with like: the power of knowing where you are', Brain Connect, 4(7), pp. 547-57.

Turner, R. and Geyer, S. (2014b) 'Introduction to the NeuroImage special issue: "In vivo Brodmann mapping of the human brain"', Neuroimage, 93 Pt 2, pp. 155-6.

Usher, M.; J. L McClelland (2001). "The time course of perceptual choice: the leaky, competing accumulator model.". Psychological Review 108 (3): 550–592

Valeiras, B., Rosato Siri, M. V., Codagnone, M., Reinés, A. and Pasquini, J. M. (2014) 'Gender influence on schizophrenia-relevant abnormalities in a cuprizone demyelination model', Glia, 62(10), pp. 1629-44.

Van Essen, D. C., Glasser, M. F., Dierker, D. L. and Harwell, J. (2012) 'Cortical parcellations of the macaque monkey analyzed on surface-based atlases', Cereb Cortex, 22(10), pp. 2227-40.

Van Essen, D. C., Maunsell, J. H. and Bixby, J. L. (1981) 'The middle temporal visual area in the macaque: myeloarchitecture, connections, functional properties and topographic organization', J Comp Neurol, 199(3), pp. 293-326.

Vargas, D. L., Nascimbene, C., Krishnan, C., Zimmerman, A. W. and Pardo, C. A. (2005) 'Neuroglial activation and neuroinflammation in the brain of patients with autism', Ann Neurol, 57(1), pp. 67-81.

Vaughan, J. T., Garwood, M., Collins, C. M., Liu, W., DelaBarre, L., Adriany, G., Andersen, P., Merkle, H., Goebel, R., Smith, M. B. and Ugurbil, K. (2001) '7T vs. 4T: RF power, homogeneity, and signal-to-noise comparison in head images', Magn Reson Med, 46(1), pp. 24-30.

Wang, S. S., Kloth, A. D. and Badura, A. (2014) 'The cerebellum, sensitive periods, and autism', Neuron, 83(3), pp. 518-32.

Ward, A. J. (1990) 'A comparison and analysis of the presence of family problems

during pregnancy of mothers of "autistic" children and mothers of normal children', Child Psychiatry Hum Dev, 20(4), pp. 279-88.

Ward, L. M., Porac, C., Coren, S. and Girgus, J. S. (1977) 'The case for misapplied constancy scaling: depth associations elicited by illusion configurations', Am J Psychol, 90(4), pp. 609-20.

Wong-Riley, M. (1979) 'Changes in the visual system of monocularly sutured or enucleated cats demonstrable with cytochrome oxidase histochemistry', Brain Res, 171(1), pp. 11-28.

Woolsey, T. A. and Van der Loos, H. (1970) 'The structural organization of layer IV in the somatosensory region (SI) of mouse cerebral cortex. The description of a cortical field composed of discrete cytoarchitectonic units', Brain Res, 17(2), pp. 205-42.

Xin, F. and Lei, X. (2015) 'Competition between frontoparietal control and default networks supports social working memory and empathy', Soc Cogn Affect Neurosci.

Yacoub, E., Shmuel, A., Logothetis, N. and Uğurbil, K. (2007) 'Robust detection of ocular dominance columns in humans using Hahn Spin Echo BOLD functional MRI at 7 Tesla', Neuroimage, 37(4), pp. 1161-77.

Yaniv, I. and Kleinberger, E. (2000) 'Advice Taking in Decision Making: Egocentric Discounting and Reputation Formation', Organ Behav Hum Decis Process, 83(2), pp. 260-281.

Yeo, B. T., Krienen, F. M., Sepulcre, J., Sabuncu, M. R., Lashkari, D., Hollinshead, M., Roffman, J. L., Smoller, J. W., Zöllei, L., Polimeni, J. R., Fischl, B., Liu, H. and Buckner, R. L. (2011) 'The organization of the human cerebral cortex estimated by intrinsic functional connectivity', J Neurophysiol, 106(3), pp. 1125-65.

Yoshiura, T., Higano, S., Rubio, A., Shrier, D. A., Kwok, W. E., Iwanaga, S. and Numaguchi, Y. (2000) 'Heschl and superior temporal gyri: low signal intensity of the cortex on T2-weighted MR images of the normal brain', Radiology, 214(1), pp. 217-21.

Zeki, S. M. (1974) 'Functional organization of a visual area in the posterior bank of the superior temporal sulcus of the rhesus monkey', J Physiol, 236(3), pp. 549-73.

Zhang, Y., Brady, M. and Smith, S. 2001. Segmentation of brain MR images through a hidden Markov random field model and the expectation-maximization algorithm. IEEE Trans Med Imag.

Zilbovicius, M., Meresse, I., Chabane, N., Brunelle, F., Samson, Y. and Boddaert, N. (2006) 'Autism, the superior temporal sulcus and social perception', Trends Neurosci, 29(7), pp. 359-66.

Zimmermann, J., Goebel, R., De Martino, F., van de Moortele, P. F., Feinberg, D., Adriany, G., Chaimow, D., Shmuel, A., Uğurbil, K. and Yacoub, E. (2011) 'Mapping the organization of axis of motion selective features in human area MT using high-field fMRI', PLoS One, 6(12), pp. e28716.

Appendix A

1. Your co-pilot can not see which way the black holes are spinning.

2. You need to help out your co-pilot by telling them which way the black holes are spinning!

3. First, focus on the white square in the middle of the screen.

4. Tell your co-pilot when you are ready to start.

5. Keep looking at the white square! A black hole is about to appear.

6. When the black hole is gone, touch the screen to show which way you saw it spinning.

7. You can press 'LEFT' or 'RIGHT'.

8. Stay on your toes! When you have pressed which way the black hole is spinning, another will appear!

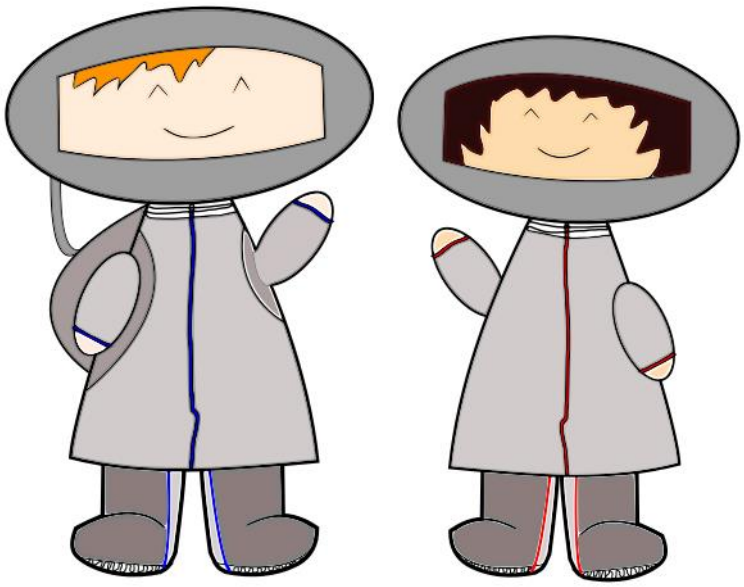

Figure 1: **Information sheet used for the social experiment**

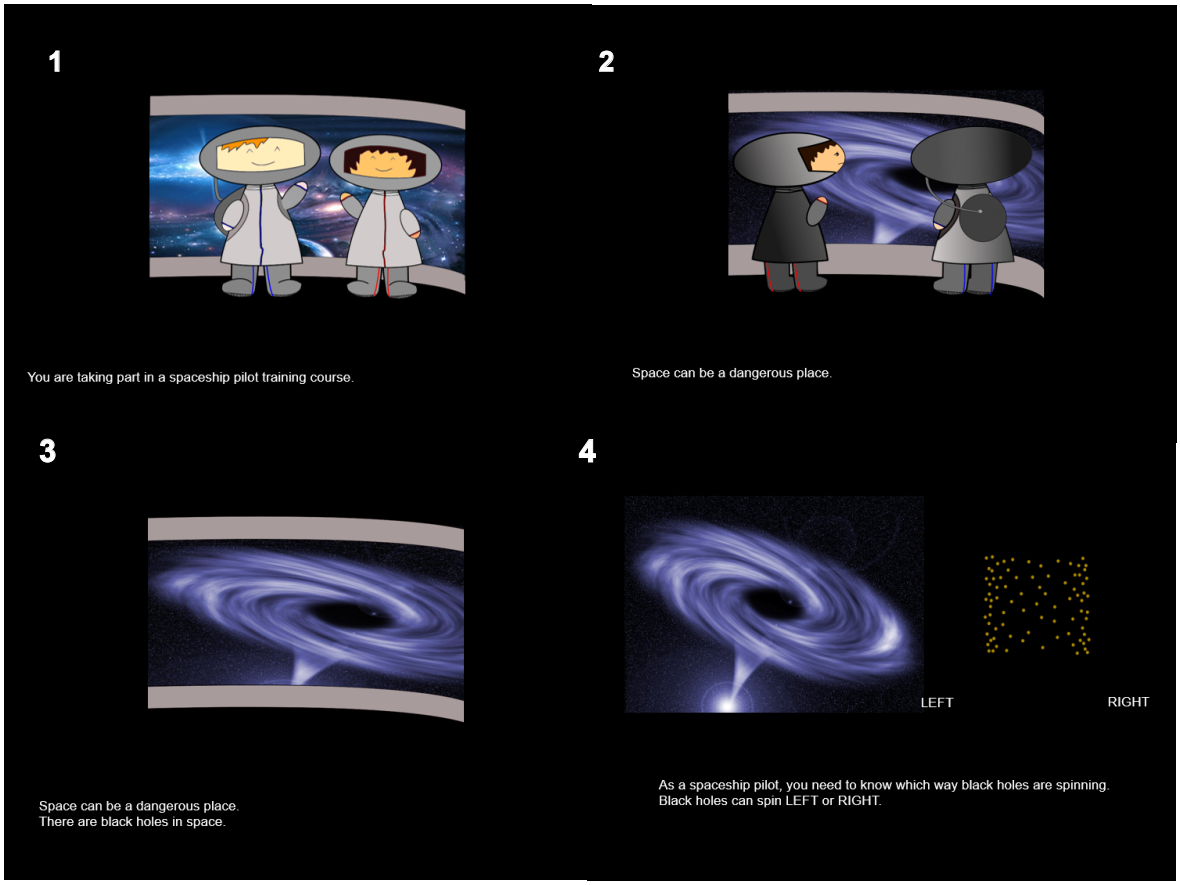

(a)

Figure 2: Slides 1-4/8 of the presentation used to introduce the threshold experiment

Slides presented to the participants prior to participation in the experiment. The children read the slides aloud to the researcher collecting data. Text reads: 1) You are taking part in a spaceship pilot training course. 2) Space can be a dangerous place. 3) There are black holes in space. 4) As a spaceship pilot, you need to know which way black holes are spinning. Black holes can spin LEFT or RIGHT.

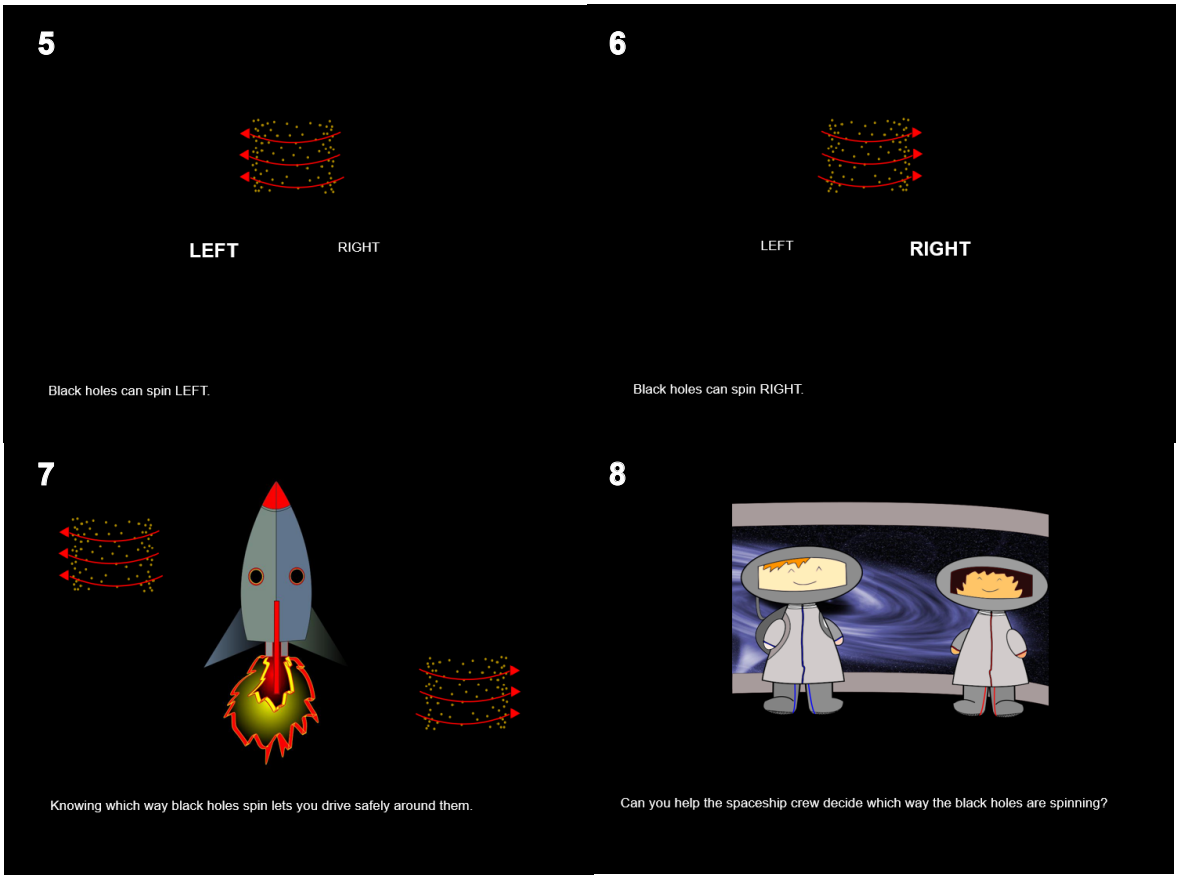

(b)

Figure 2: (cont.)Slides 4-8/8 of the presentation used to introduce the threshold experiment

Text reads: 5) Black holes can spin LEFT. 6) Black holes can spin RIGHT. 7) Knowing which way black holes spin lets you drive safely around them. 8) Can you help the spaceship crew decide which way the black holes are spinning?

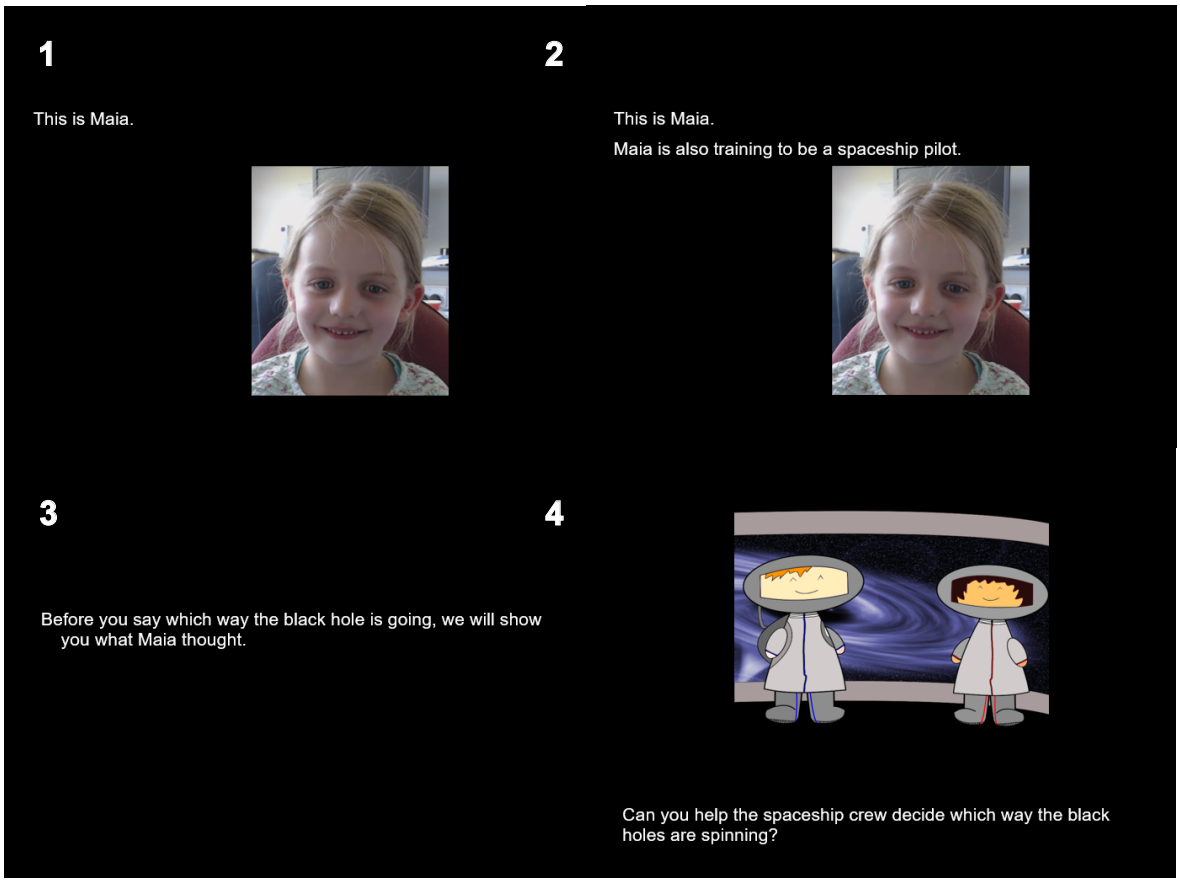

(c)

Figure 2: (cont.)Extension presentation used to introduce the social experiment (with example advisor)

Text reads: 1) This is Maia. 2) Maia is also training to be a spaceship pilot. 3) Before you say which way the black hole is going, we will show you what Maia thought. 4) Can you help the spaceship crew decide which way the black holes are spinning?

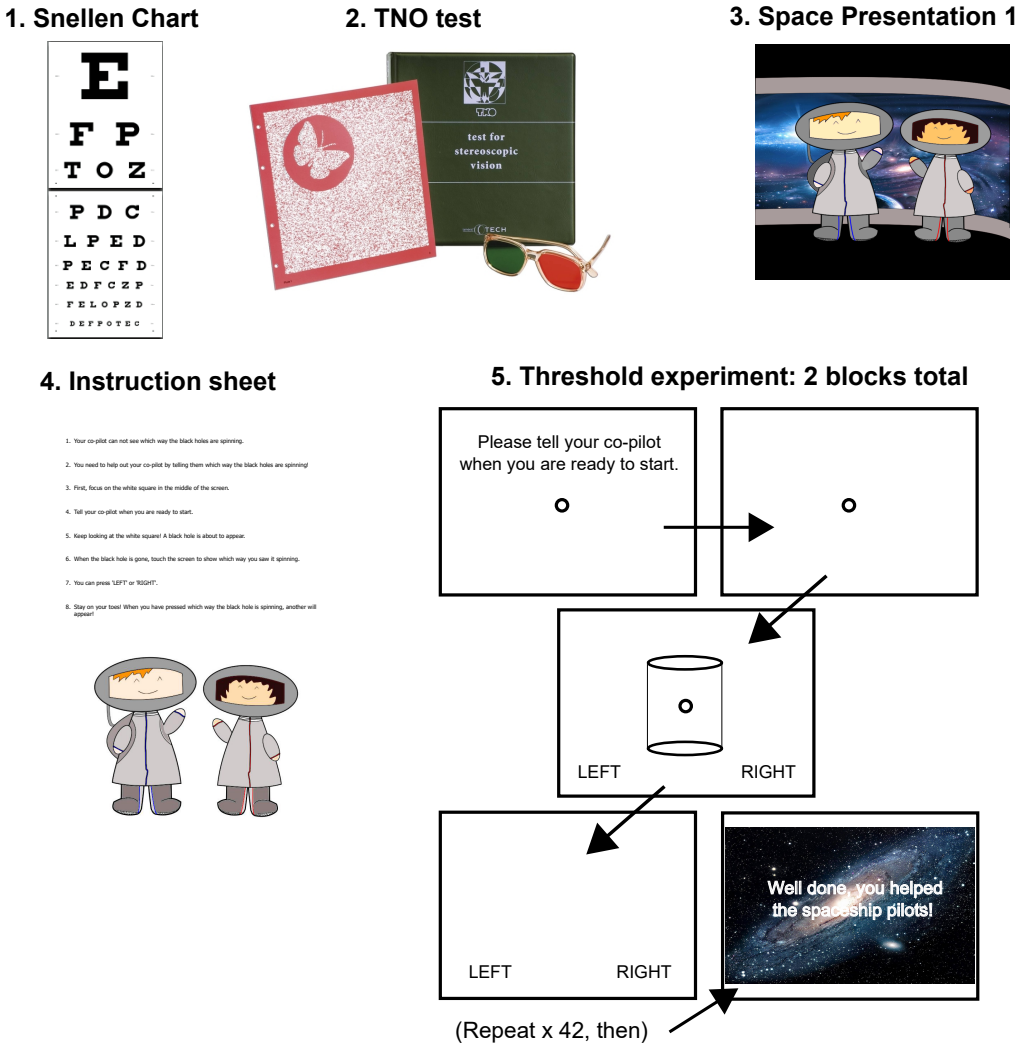

Figure 3: **Order of events for behavioural experiment**

Appendix B

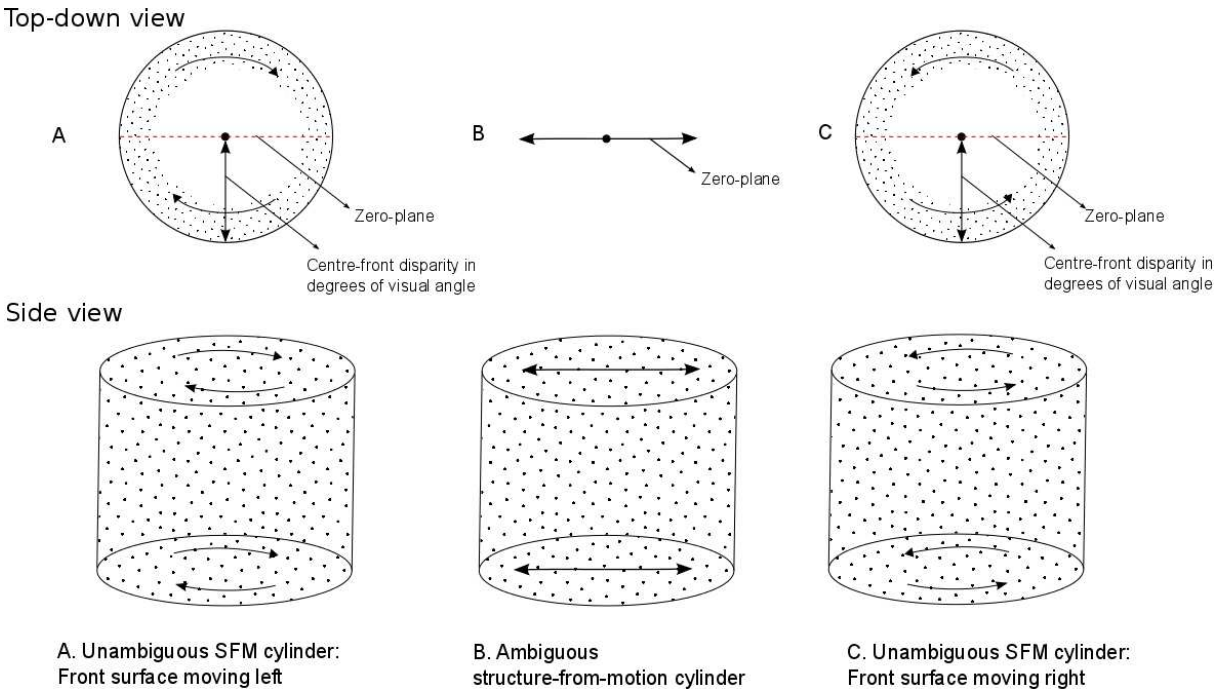

Figure 4: **Structure-from-motion stimuli**
Randomly plotted dots form two fields of sinusoidal velocity oppositional motion. In A and C, binocular disparity differentiates the front and back surfaces (applied with a sinusoidal profile, such that the closest and furthest dots are in the centre of the field). In B, dots move left and right along the zero plane as two fields, and the 3D percept arises solely from the sinusoidal velocity of the dots.

Appendix C

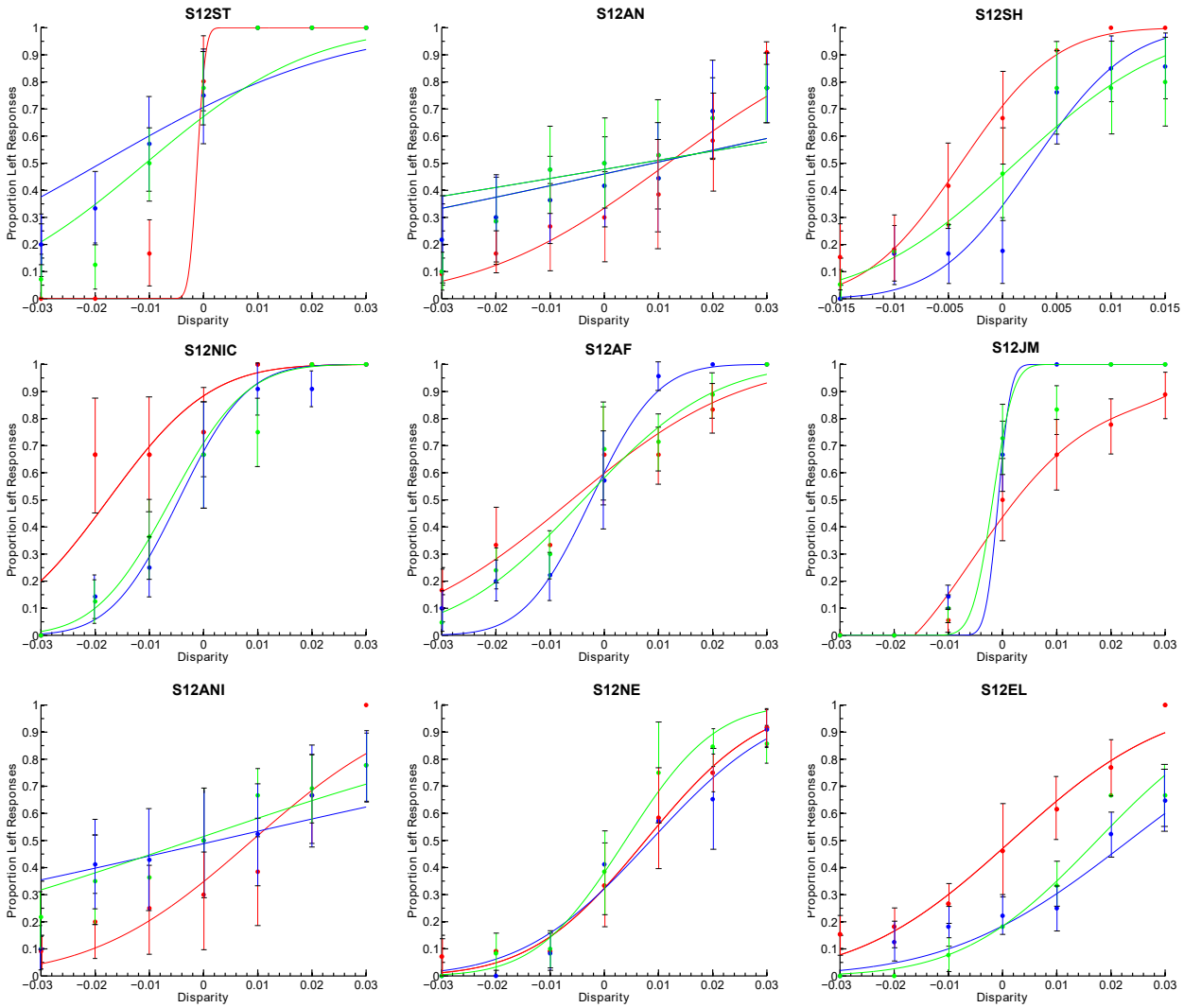

(a)

Figure 5: Individual graphs - typically developing, peer-advised, 6-8 year olds.

Graphs show the average psychometric functions from children aged 6-8 years with social advice from an age-matched peer. Behavioural responses were plotted against normalised binocular disparities and were fitted with two cumulative Gaussians, separately for advice 'left' (blue) and advice 'right' (green). Red points and lines where applicable represent the participant's performance in a stereoacuity experiment prior to the social experiment. Error bars = standard error of the mean (SEM).

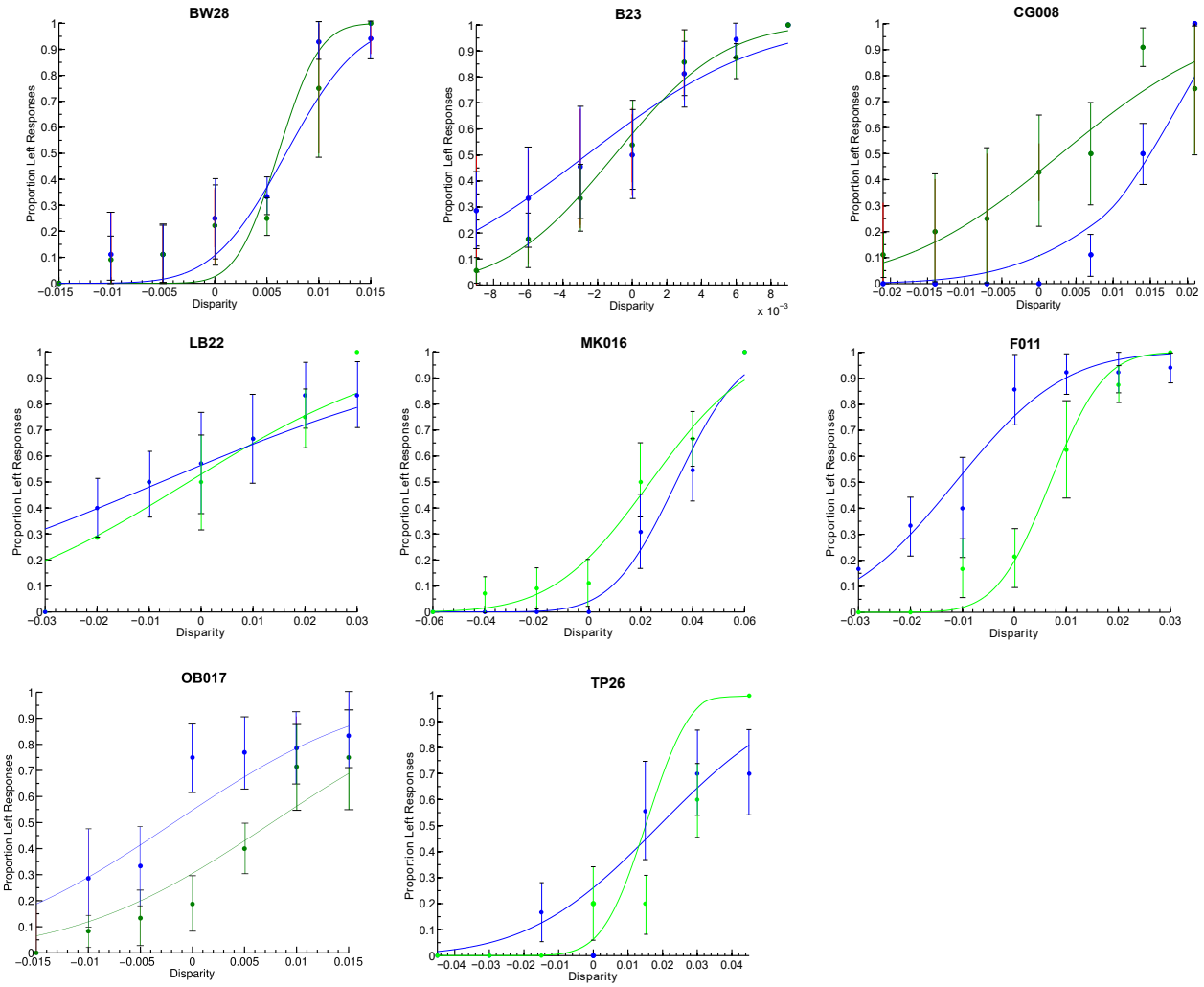

(b)

Figure 5: (cont.) Individual graphs - typically developing, peer-advised, 6-8 year olds.

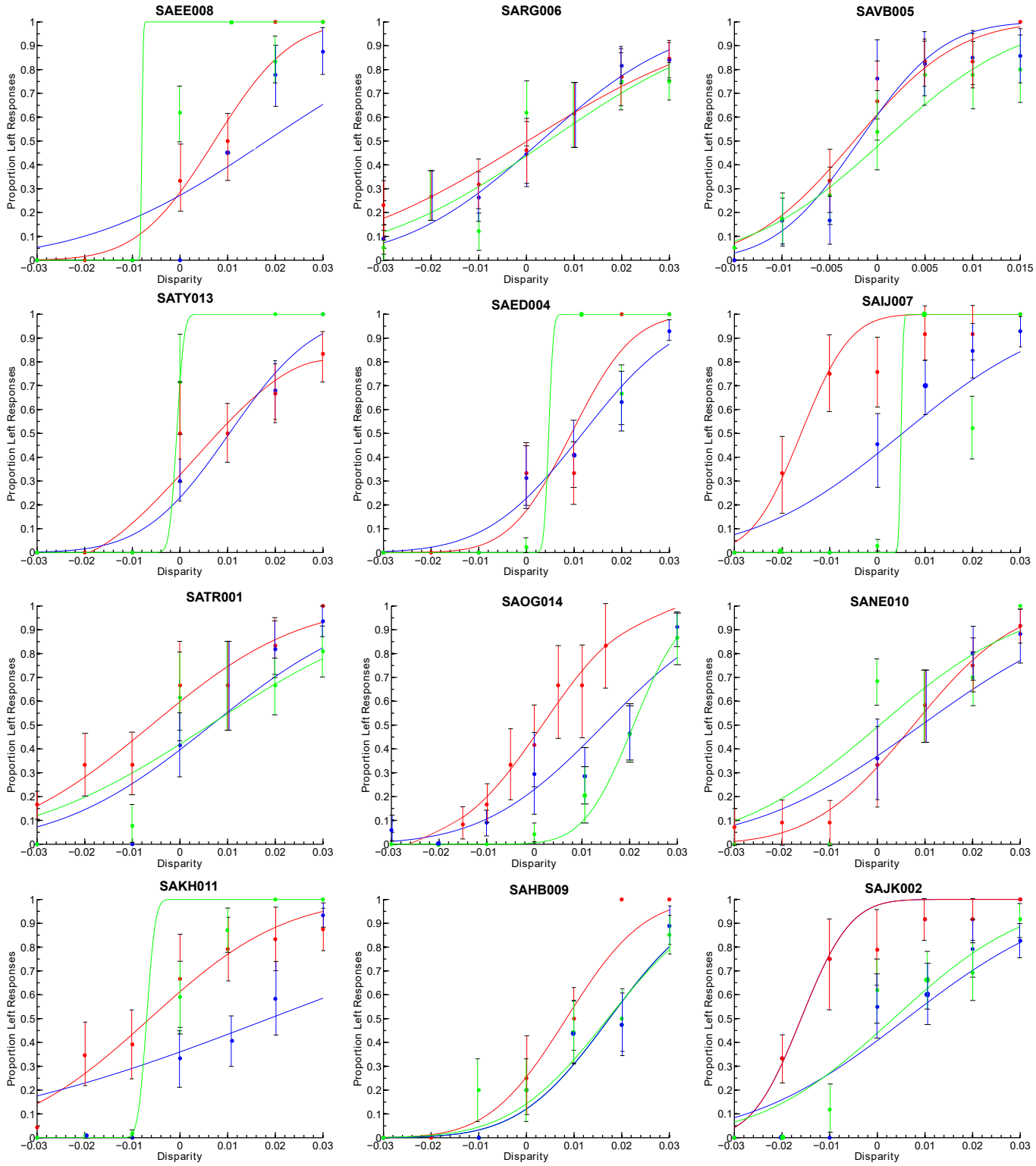

(a)

Figure 6: Individual graphs - typically developing, peer-advised, 9-11 year olds.

Graphs show the average psychometric functions from children aged 9-11 years with social advice from an age-matched peer. Behavioural responses were plotted against normalised binocular disparities and were fitted with two cumulative Gaussians, separately for advice 'left' (blue) and advice 'right' (green). Red points and lines where applicable represent the participant's performance in a stereoacuity experiment prior to the social experiment. Error bars = standard error of the mean (SEM).

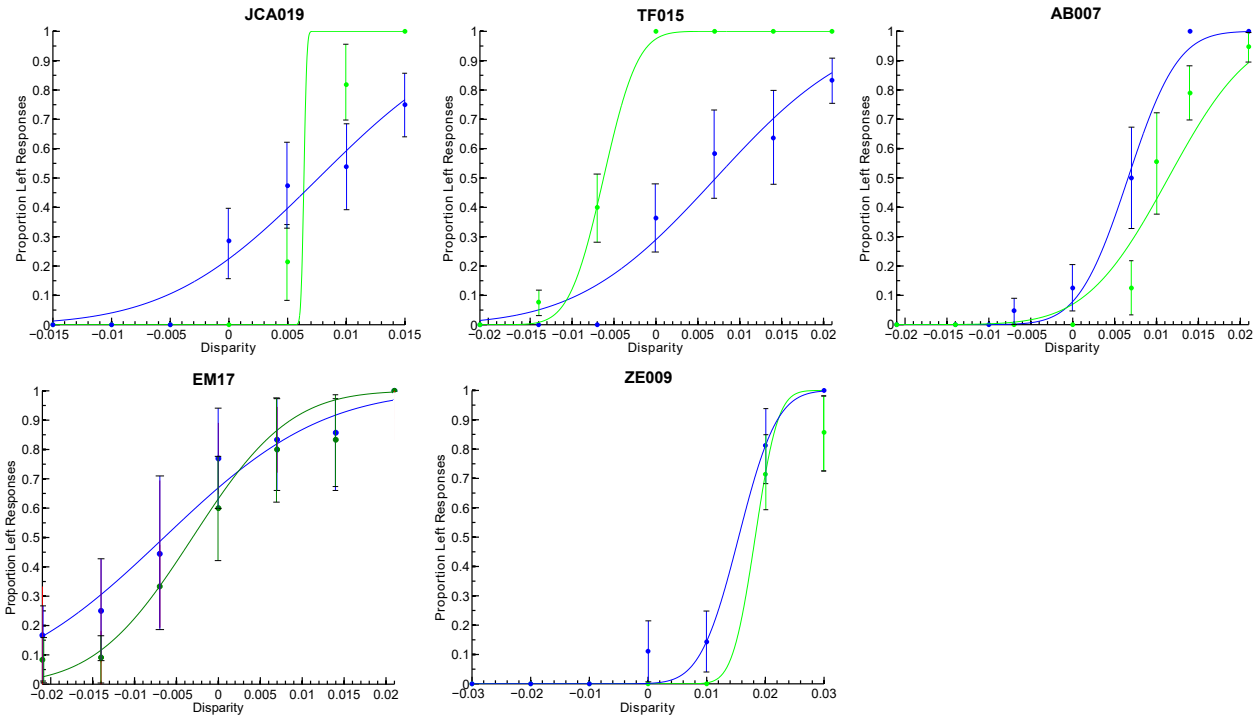

(b)

Figure 6: (cont.) Individual graphs - typically developing, peer-advised, 9-11 year olds.

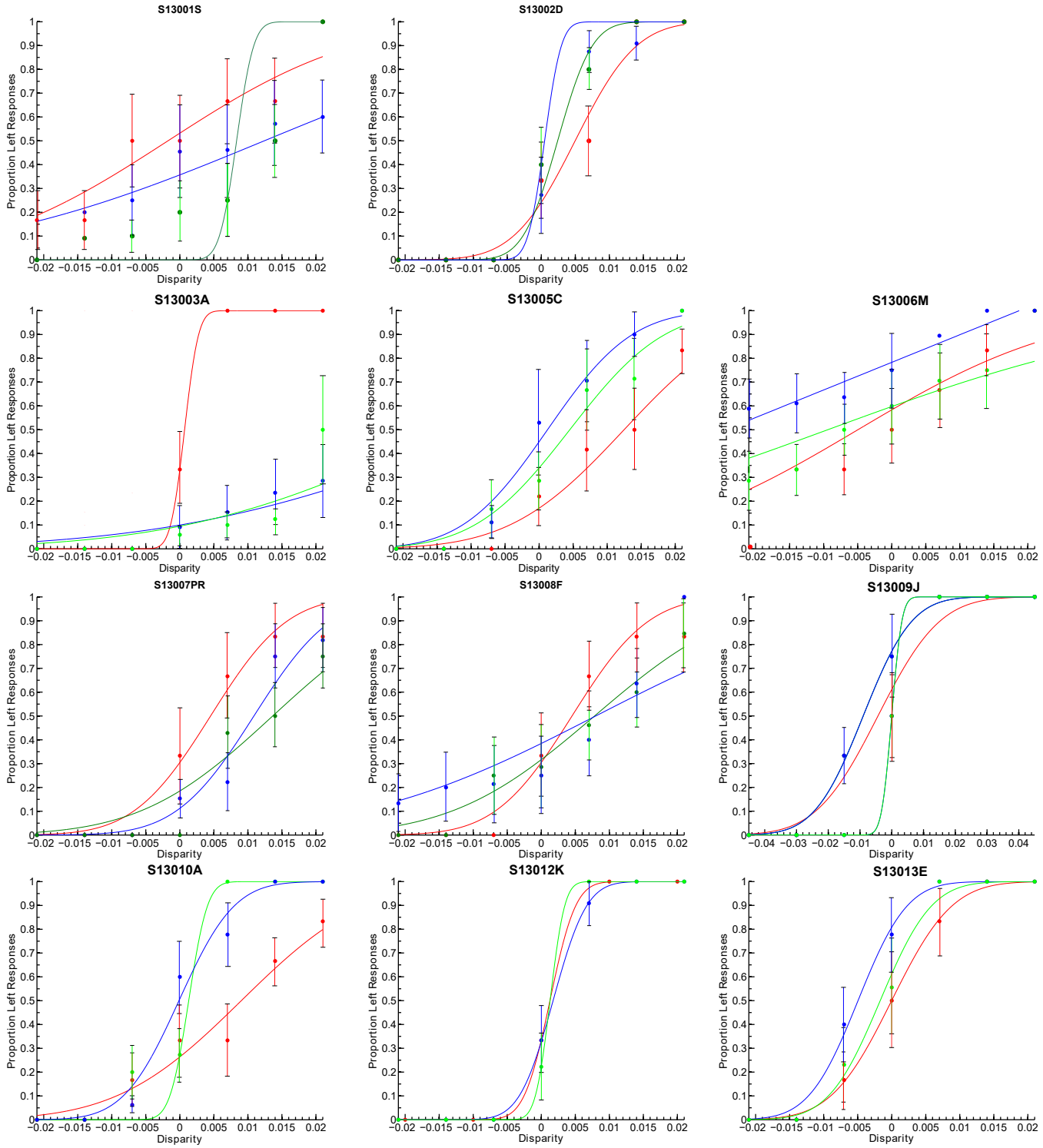

(a)

Figure 7: Individual graphs - typically developing, peer-advised, 12-14 year olds.

Graphs show the average psychometric functions from children aged 12-14 years with social advice from an age-matched peer. Behavioural responses were plotted against normalised binocular disparities and were fitted with two cumulative Gaussians, separately for advice 'left' (blue) and advice 'right' (green). Red points and lines where applicable represent the participant's performance in a stereoacuity experiment prior to the social experiment. Error bars = standard error of the mean (SEM).

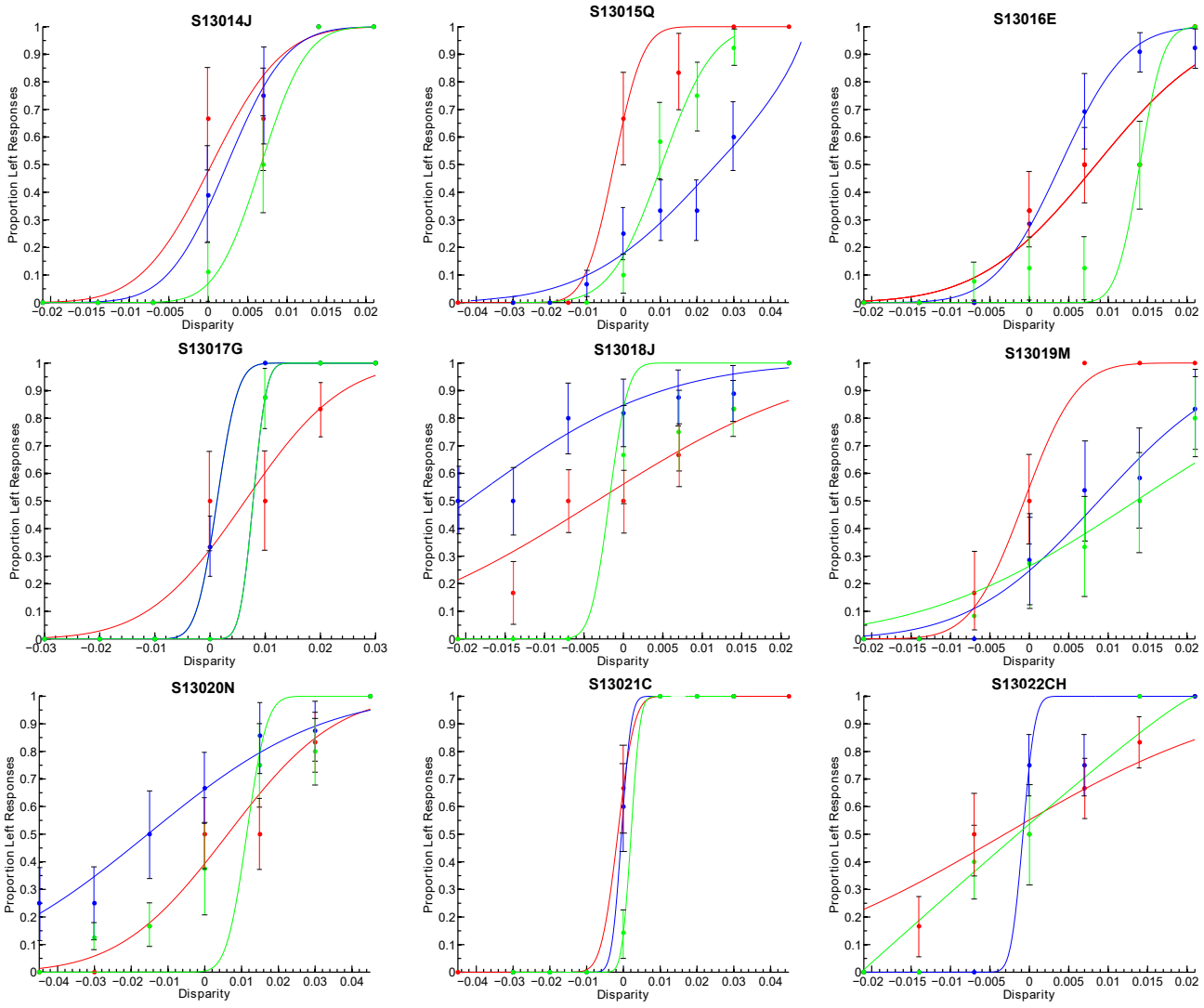

(b)

Figure 7: (cont.) Individual graphs - typically developing, peer-advised, 12-14 year olds.

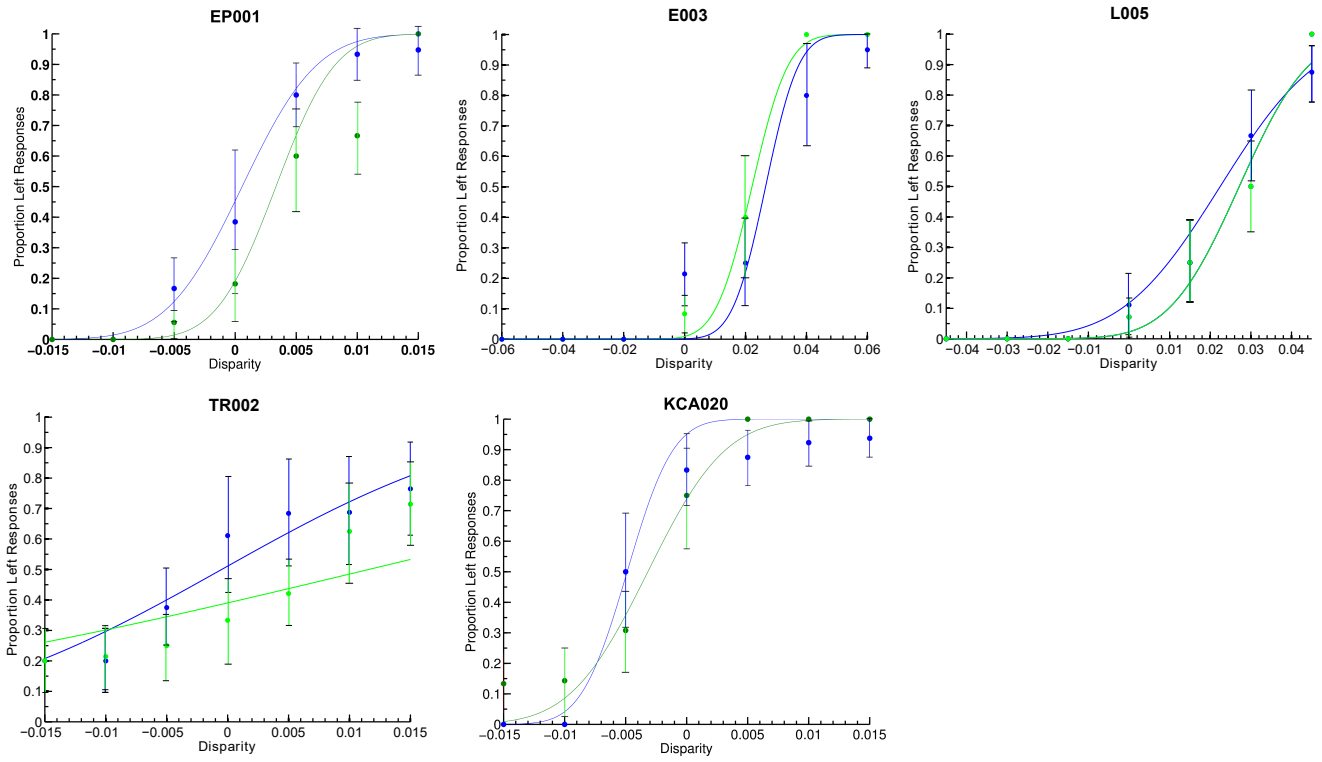

(c)

Figure 7: (cont.) Individual graphs - typically developing, peer-advised, 12-14 year olds.

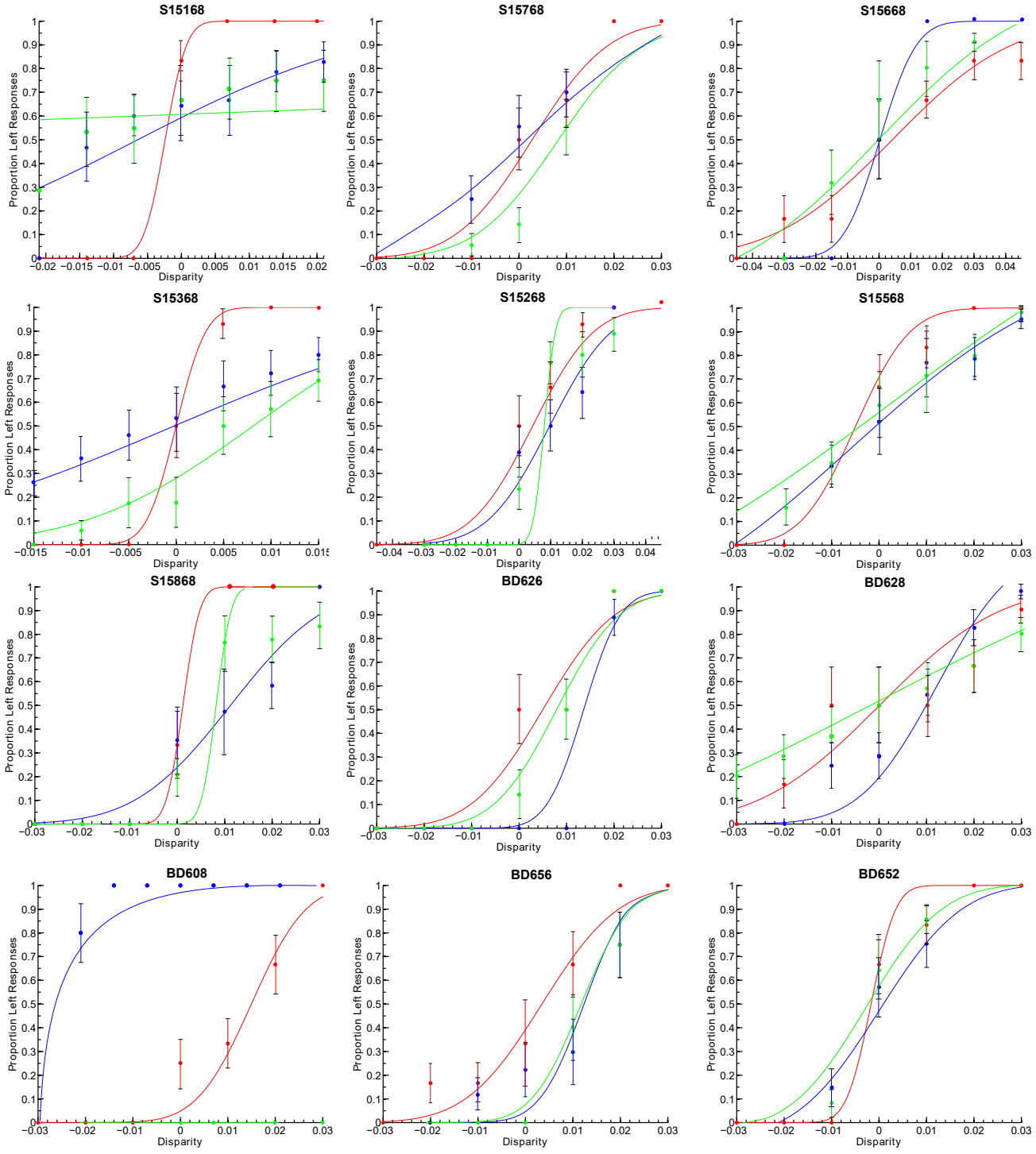

(a)

Figure 8: Individual graphs - typically developing, adult-advised, 6-8 year olds.

Graphs show the average psychometric functions from children aged 6-8 years with social advice from an adult. Behavioural responses were plotted against normalised binocular disparities and were fitted with two cumulative Gaussians, separately for advice 'left' (blue) and advice 'right' (green). Red points and lines where applicable represent the participant's performance in a stereoacuity experiment prior to the social experiment. Error bars = standard error of the mean (SEM).

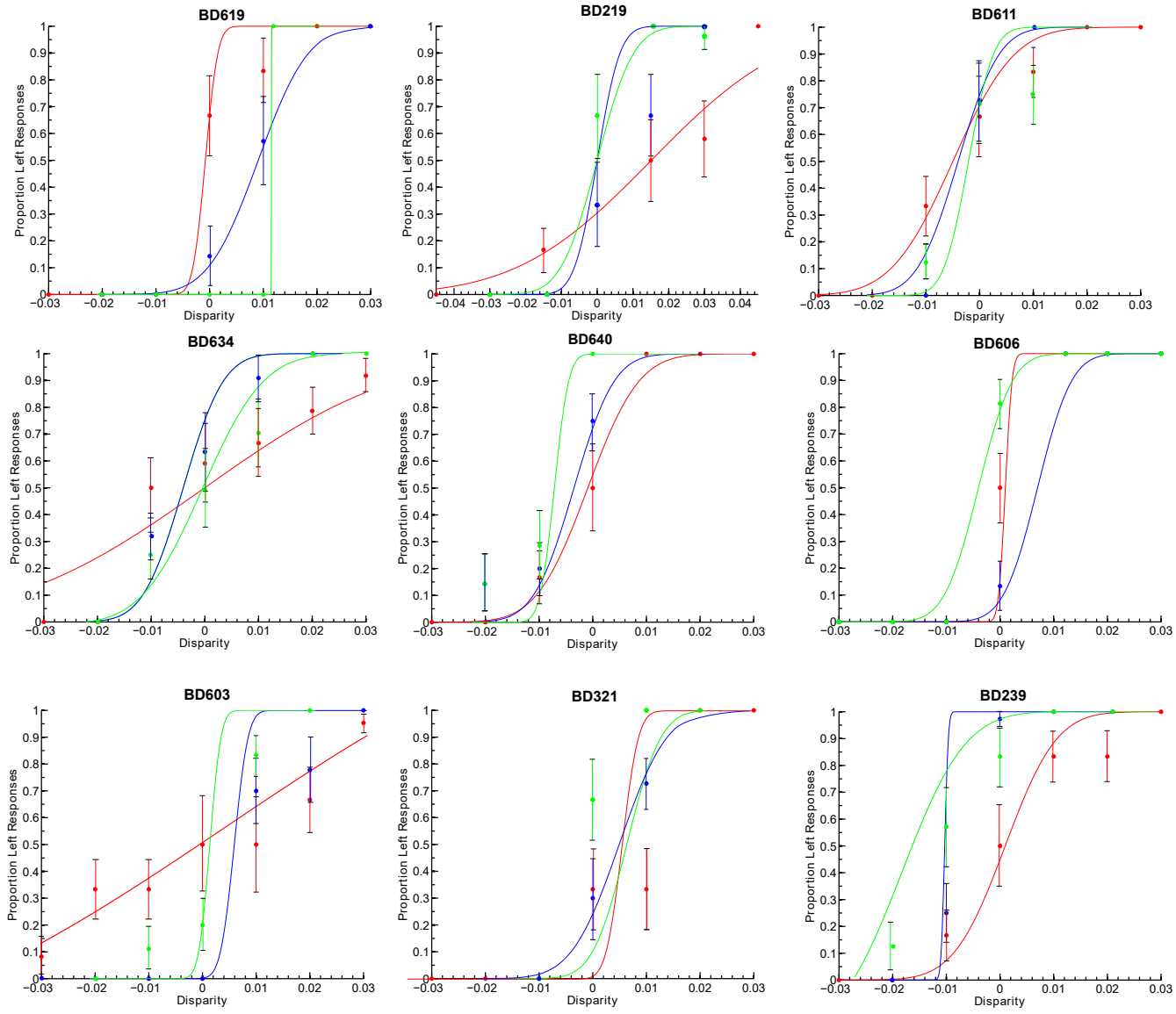

(b)

Figure 8: (cont.) Individual graphs - typically developing, adult-advised, 6-8 year olds.

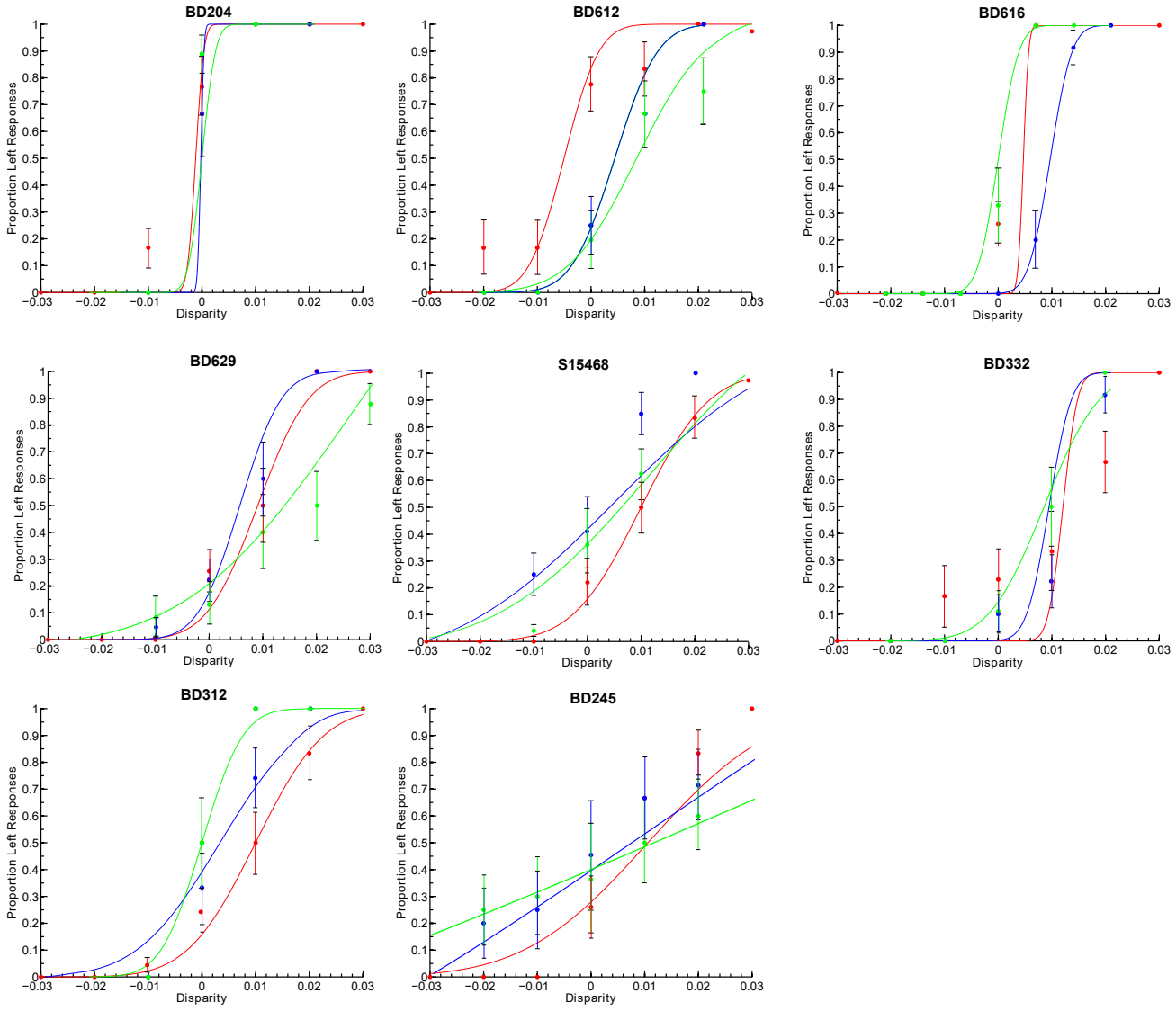

(c)

Figure 8: (cont.) Individual graphs - typically developing, adult-advised, 6-8 year olds.

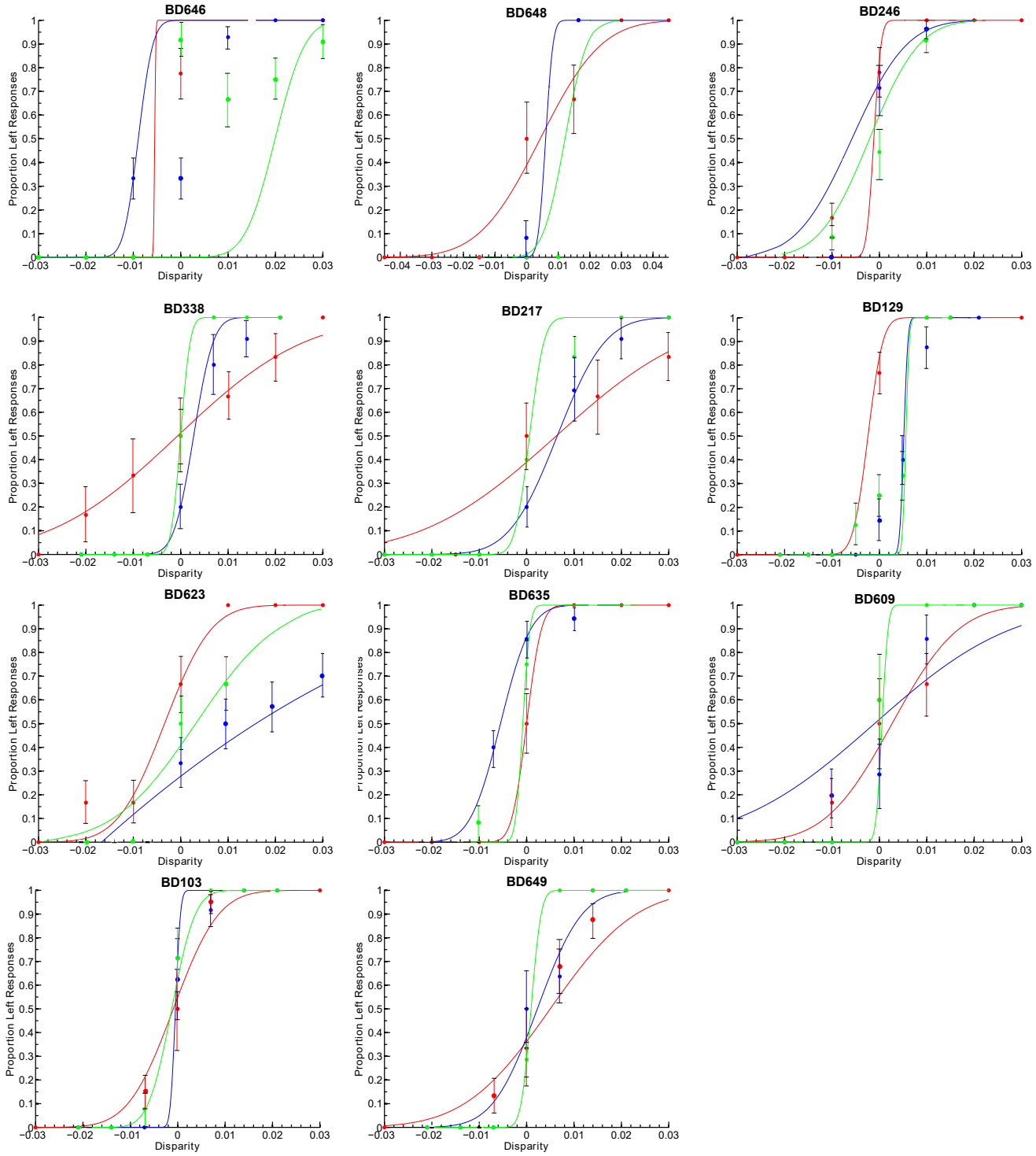

(a)

Figure 9: Individual graphs - typically developing, adult-advised, 9-11 year olds.

Graphs show the average psychometric functions from children aged 9-11 years with social advice from an adult. Behavioural responses were plotted against normalised binocular disparities and were fitted with two cumulative Gaussians, separately for advice 'left' (blue) and advice 'right' (green). Red points and lines where applicable represent the participant's performance in a stereoacuity experiment prior to the social experiment. Error bars = standard error of the mean (SEM).

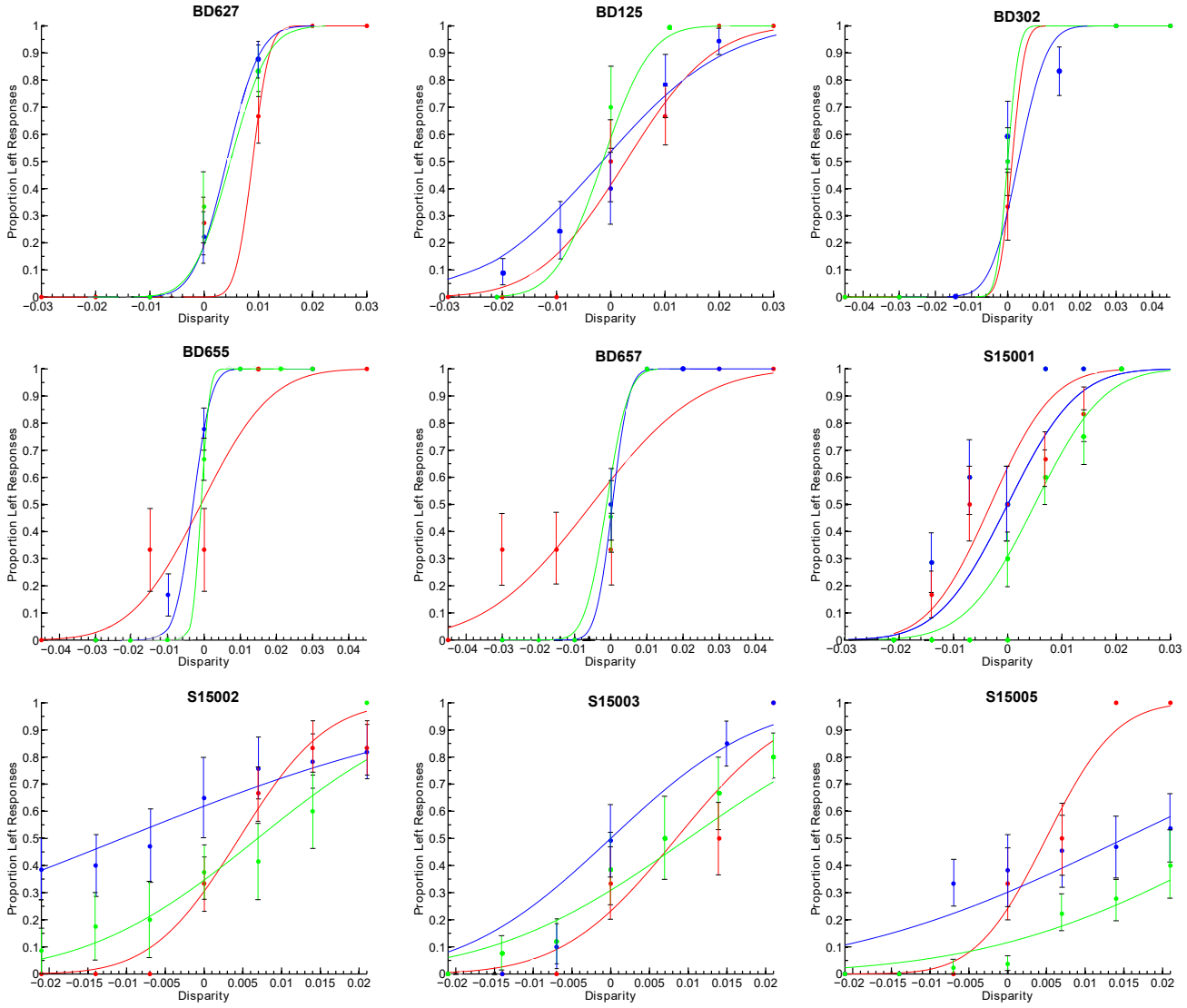

(a)

Figure 10: Individual graphs - typically developing, adult-advised, 12-14 year olds.

Graphs show the average psychometric functions from children aged 12-14 years with social advice from an adult. Behavioural responses were plotted against normalised binocular disparities and were fitted with two cumulative Gaussians, separately for advice 'left' (blue) and advice 'right' (green). Red points and lines where applicable represent the participant's performance in a stereoacuity experiment prior to the social experiment. Error bars = standard error of the mean (SEM).

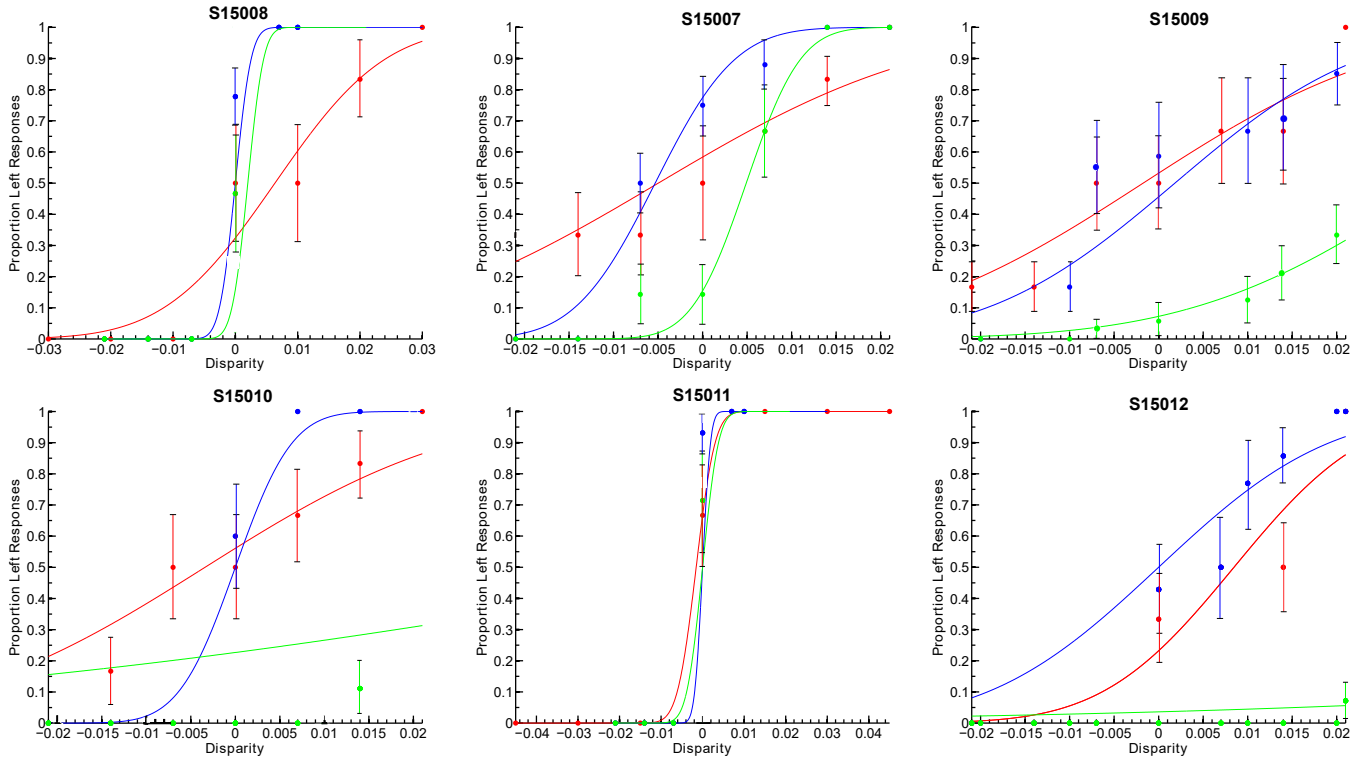

(b)

Figure 10: (cont.) Individual graphs - typically developing, adult-advised, 12-14 year olds.

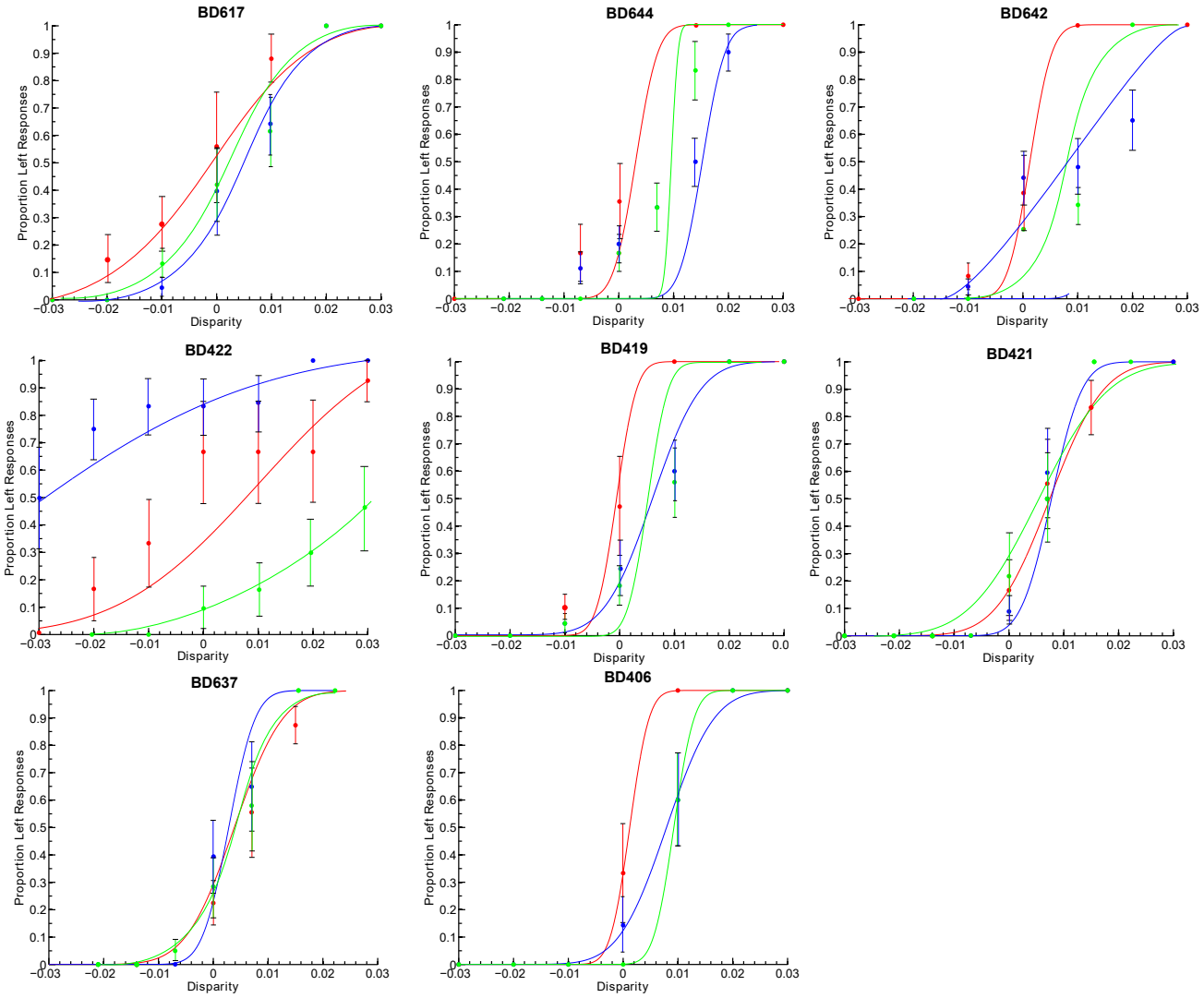

(a)

Figure 11: Individual graphs - ASD group, peer-advised, 6-8 year olds.

Graphs show the average psychometric functions from children with ASD by age group, with social advice from an age-matched peer. Behavioural responses were plotted against normalised binocular disparities and were fitted with two cumulative Gaussians, separately for advice 'left' (blue) and advice 'right' (green). Red points and lines where applicable represent the participant's performance in a stereoacuity experiment prior to the social experiment. Error bars = standard error of the mean (SEM).

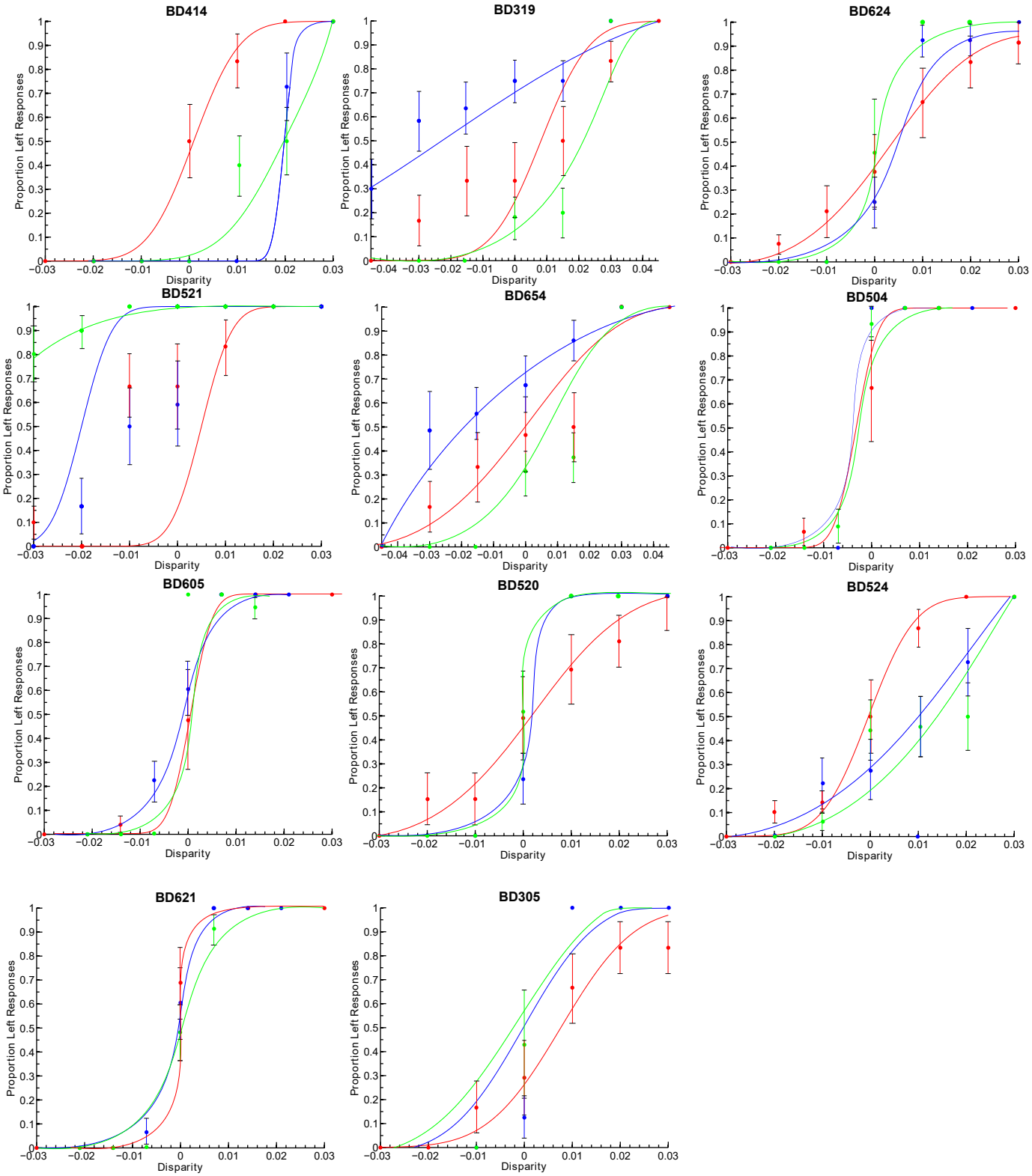

(b)

Figure 11: (cont.) Individual graphs - ASD group, peer-advised, 9-11 year olds.

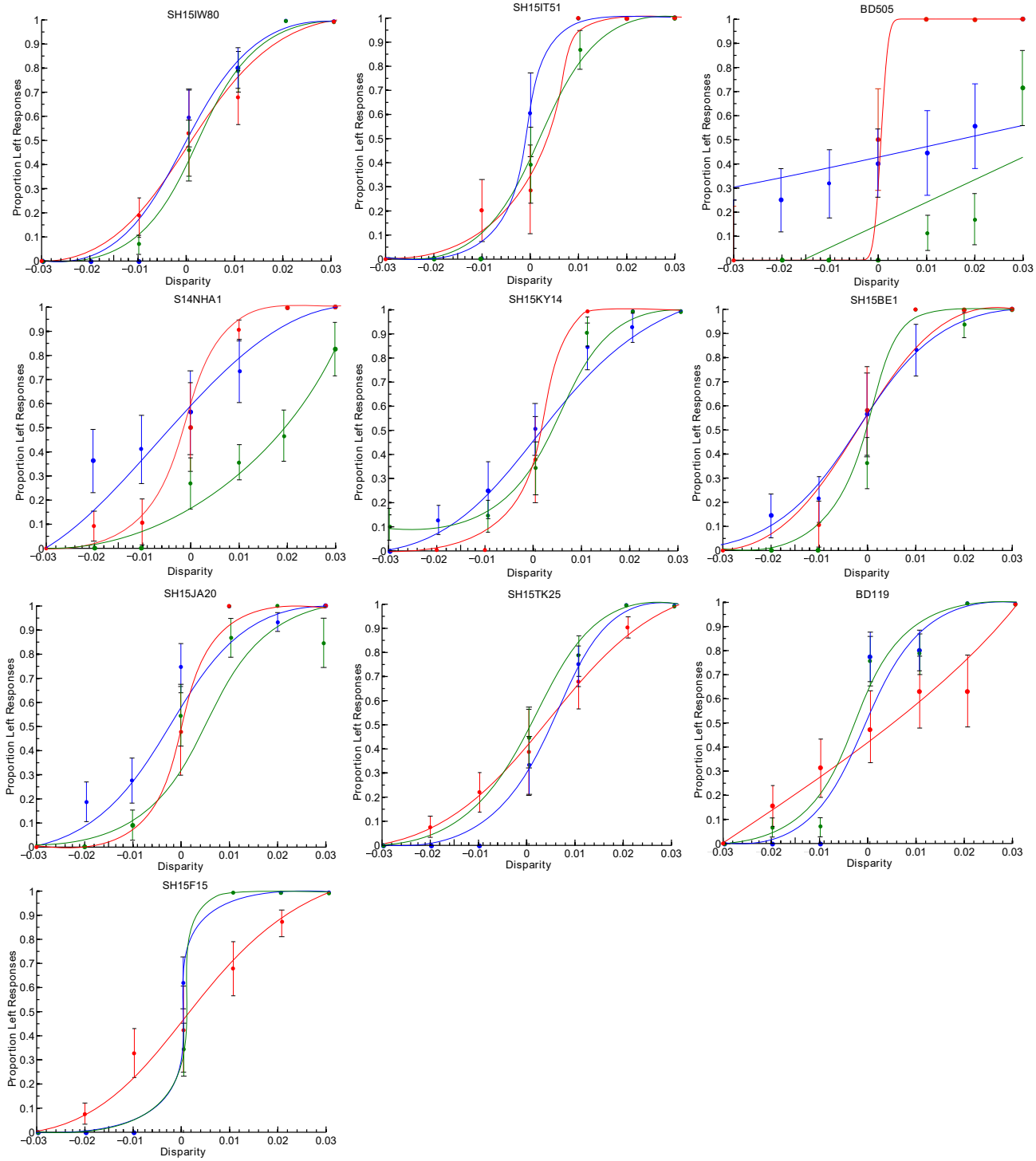

(c)

Figure 11: (cont.) Individual graphs - ASD group, peer-advised, 12-14 year olds.

Appendix D

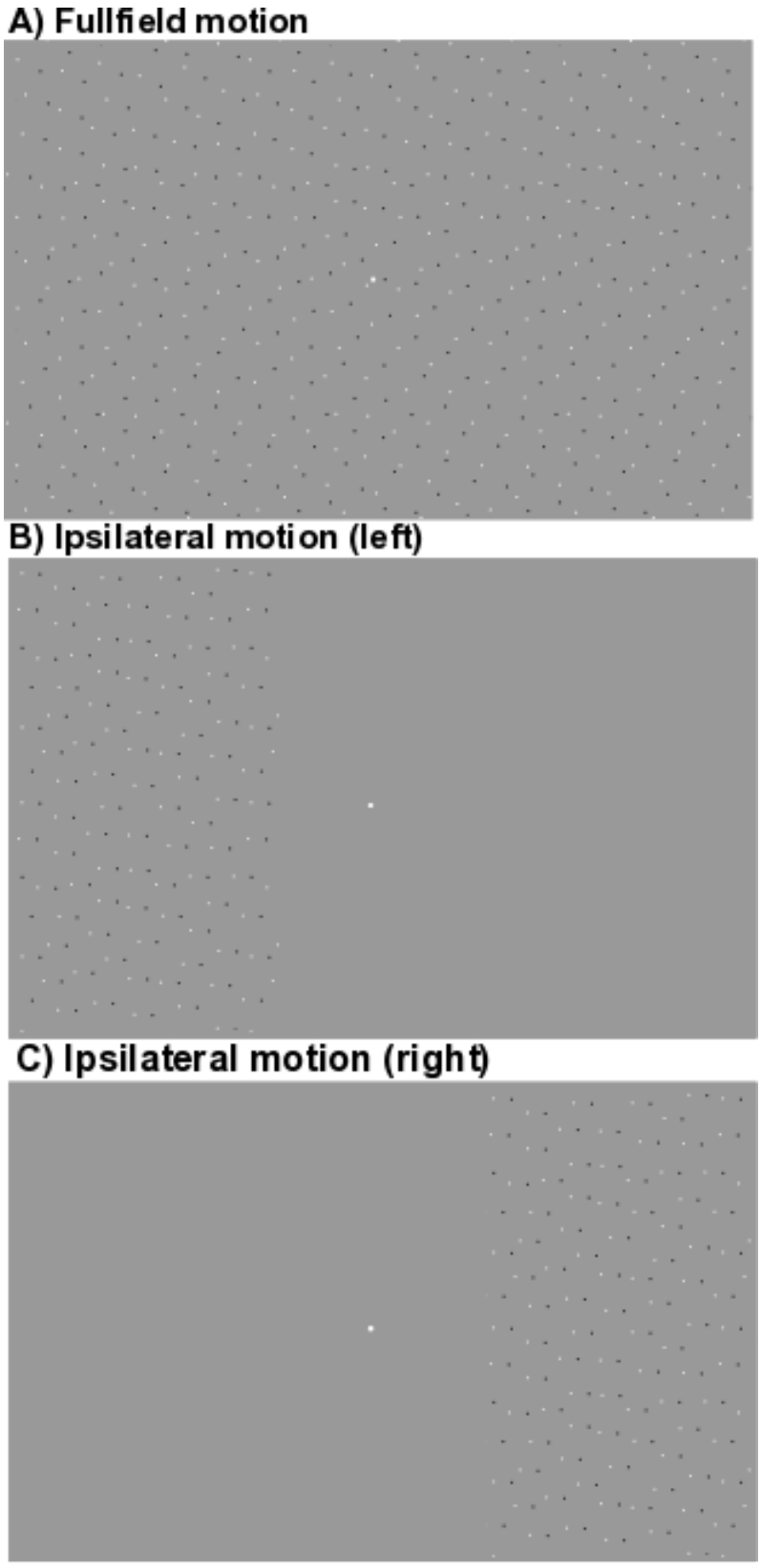

Figure 12: **Motion Localiser Stimulus**
The dots were constantly in random motion. For more detail. See Chapter 4 and 5 methods.

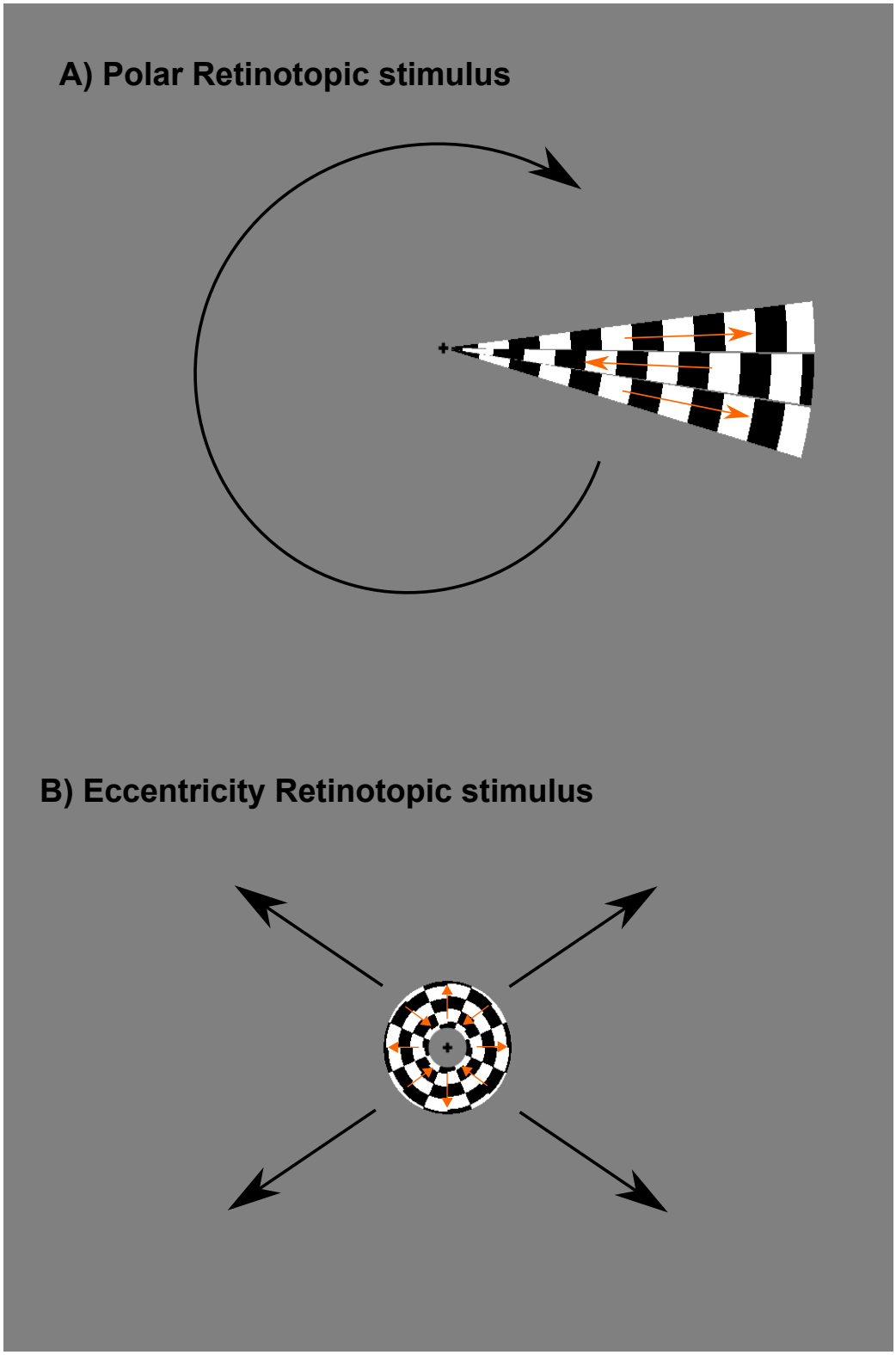

Figure 13: **Retinotopy Stimulus**
Black arrows indicate overall stimulus motion direction. Orange arrows indicate motion of the stimulus 'spokes'. For more detail, see Chapter 4 and 5 methods.

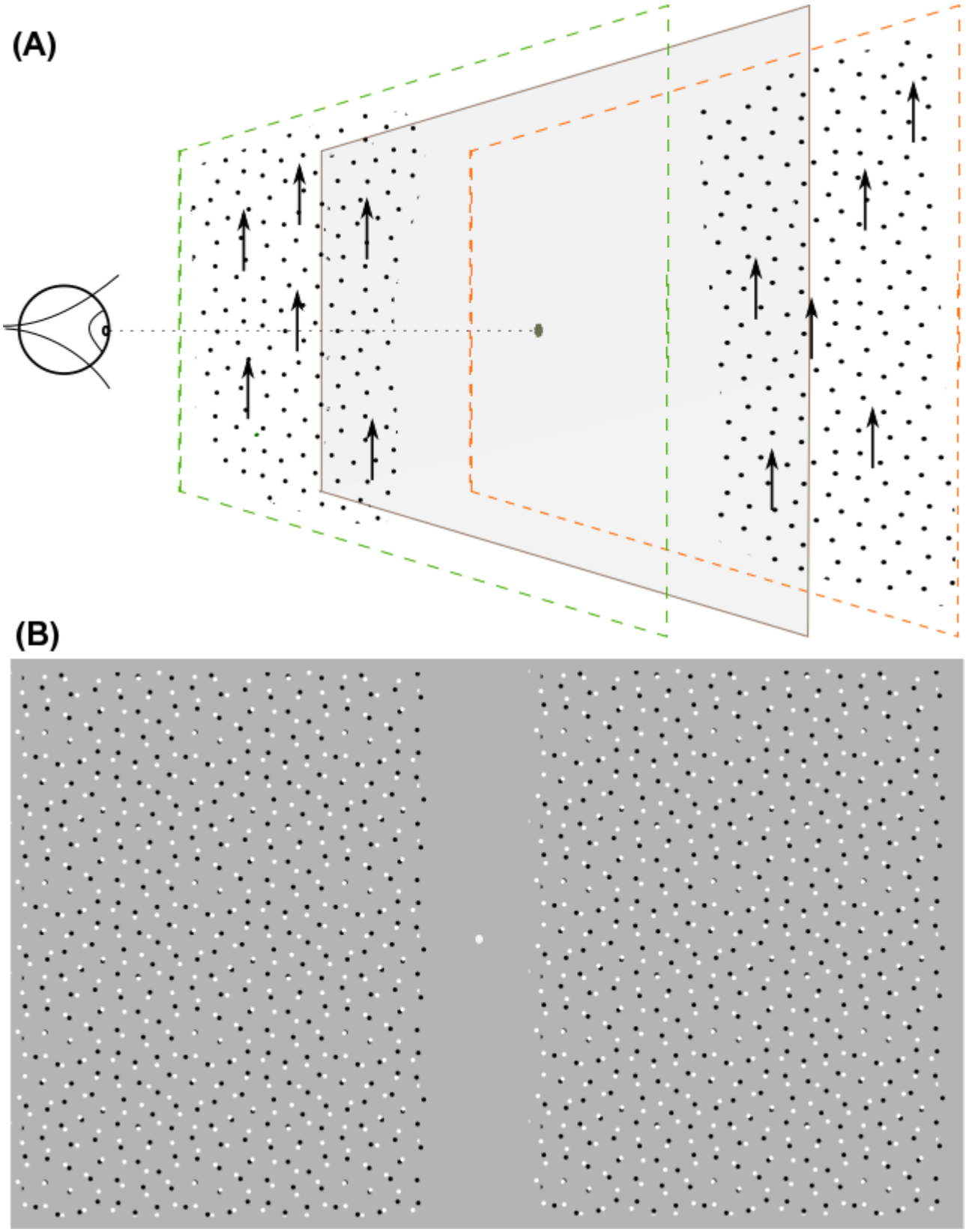

Figure 14: **Motion-disparity Stimulus**
The dots were constantly in random motion. A) is a schematic of how the participant would see the stimulus - grey represents the 0 disparity plane. B) is a diagram of the stimulus. For more detail, see Chapter 5 methods.

Appendix E

Subject	MP2RAGE	T1/T2	hMT+ Localiser	Retinotopy	hMT+ Columns
001	Y		Y	Y	Y
002	Y		Y		
003	Y		Y	Y	Y
004	Y	Y	Y	Y	Y
007	Y	Y	Y	Y	Y
008	Y	Y	Y	Y	Y
011	Y		Y		
021	Y		Y	Y	Y
022	Y		Y	Y	Y
032	Y		Y	Y	Y
036	Y		Y	Y	Y
038	Y		Y	Y	Y
041	Y		Y	Y	Y

Table 1: **List of MRI Scan Participants**
The first column gives the subject code. Subsequent columns indicate potential scans. The first two scans are the structural images pertinent in Chapter 4 - either the 7T MP2RAGE, or the 3T T1/T2, both putatively detecting myelin density. The last 3 scans are functional, with columns 4 and 5 indicating standard localisers (for hMT+, MST, and retinotopic V5/MT), and column 6 the motion-disparity functional organisation data pertinent in Chapter 5.